



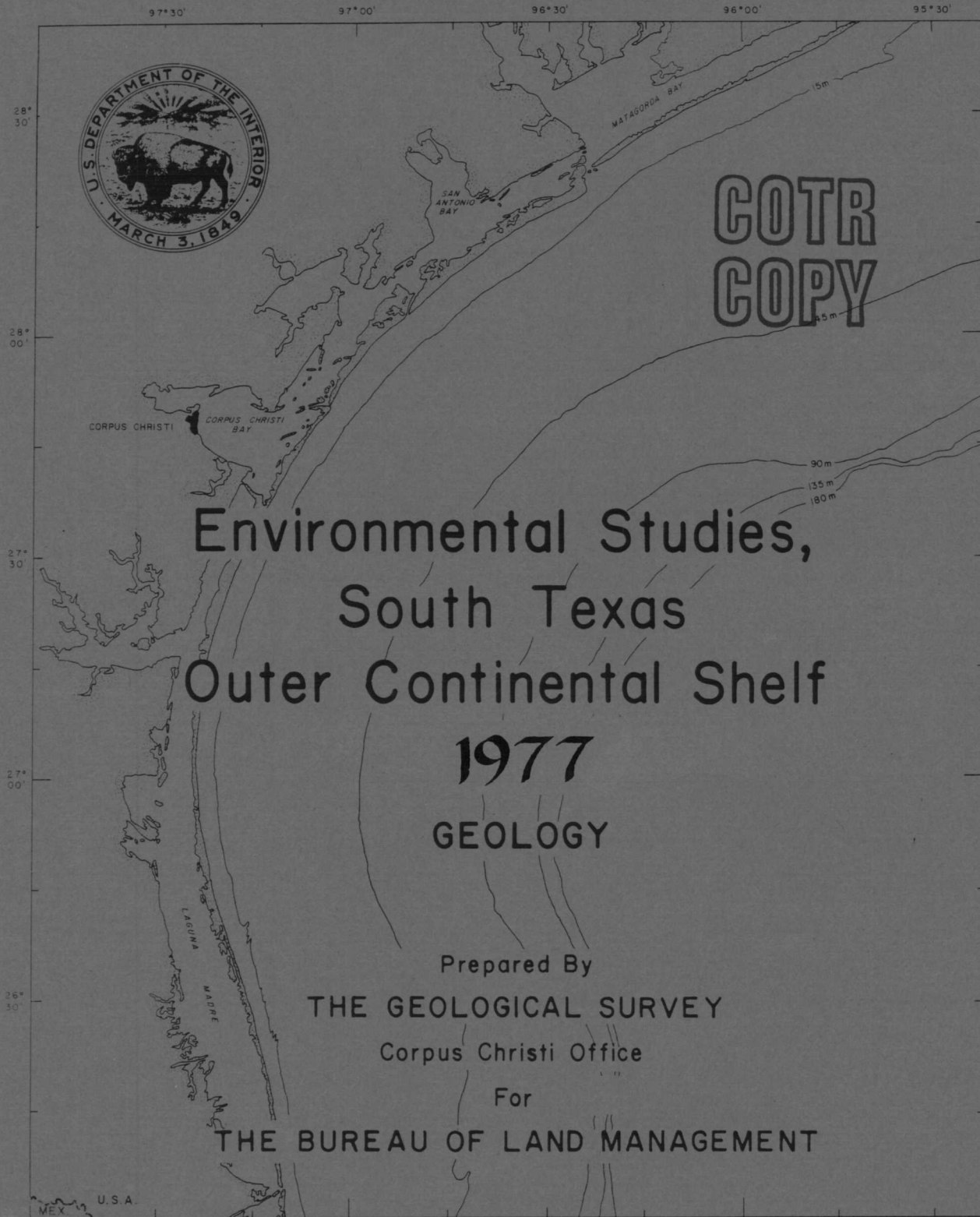
COTR
COPY

Environmental Studies,
South Texas
Outer Continental Shelf
1977

GEOLOGY

Prepared By
THE GEOLOGICAL SURVEY
Corpus Christi Office

For
THE BUREAU OF LAND MANAGEMENT



U.S.A.
MEX

ENVIRONMENTAL STUDIES, SOUTH TEXAS OUTER CONTINENTAL SHELF

1977

GEOLOGY

Element Leader and Editor
Henry L. Berryhill, Jr.

Assisted by Anita R. Trippet

Scientific Contributors:

Henry L. Berryhill, Jr.
Gerald L. Shideler
Steven S. Barnes
Cynthia A. Rice
Charles W. Holmes
E. Ann Martin

A report to the Bureau of Land Management in fulfillment
of contractual agreement AA550-MU7-27 for the period
October 1976 to October 1977

Prepared by
U.S. Geological Survey

This report has been reviewed by the Bureau of Land Management and approved for publication. Approval does not signify that the contents necessarily reflect the views and policies of the Bureau, nor does mention of trade names or commercial products constitute endorsement or recommendation for use.

TABLE OF CONTENTS

	<u>Page</u>
INTRODUCTION -----	1
Study plan -----	1
Objectives and rationale -----	4
Field investigations -----	6
Inventory of field data -----	7
Principal investigators -----	8
 SUSPENDED SEDIMENTS -----	 10
Physical Characteristics -----	10
Methods -----	10
Field techniques -----	10
Laboratory techniques -----	13
Patterns of movement for the surface drifters -----	15
October-November 1976 cruise -----	16
March 1977 cruise -----	18
May 1977 cruise -----	20
Water turbidity patterns -----	20
Transmissivity and temperature -----	22
Surface patterns -----	22
Vertical transmissivity/temperature gradients -----	28
Summary -----	51
Particle concentrations -----	52
October-November 1976 -----	52
March 1977 -----	55
May 1977 -----	57
Summary -----	60
Textural patterns -----	60
October-November 1976 -----	61
General composition -----	61
Mean grain size -----	61
Sorting characteristics -----	64
March 1977 -----	66
General composition -----	66
Mean grain size -----	68
Sorting characteristics -----	68
May 1977 -----	71
General composition -----	71
Mean grain size -----	73
Sorting characteristics -----	73
Summary -----	76
Chemical characteristics - trace metal content -----	77
Methods -----	77
Results and conclusions -----	81
 CLAY MINERALOGY, SUSPENDED AND SEA-FLOOR SEDIMENTS -----	 98
Method of study -----	99
Suspended sediment -----	99
Sea-floor sediment -----	102
Results -----	102
Discussion -----	103
Suspended sediment -----	103

	<u>Page</u>
CLAY MINERALOGY, SUSPENDED AND SEA-FLOOR SEDIMENTS--Continued	
Discussion--Continued	
Suspended sediment--Continued	
Sediment concentration -----	123
Organic carbon -----	123
Mineralogy -----	124
Sea-floor sediment -----	125
Mineralogy of suspended sediment versus sea-floor sediment -----	125
SEA-FLOOR SEDIMENTS -----	128
Physical characteristics -----	128
Seasonal variability of texture -----	128
Methods -----	128
Sand/mud ratio variability -----	135
Silt/clay ratio variability -----	137
Mean diameter variability -----	140
Standard deviation variability -----	142
Summary -----	144
Origin of discrete sand layers and mobility of sea-floor sediments -----	145
Introduction -----	145
Grain size distribution in sand layers -----	146
Depositional structures -----	155
Conclusions -----	164
Chemical characteristics -----	170
Surface sediments - seasonal variability in trace metals content -----	170
Introduction -----	170
Methods -----	173
Results -----	177
Discussion -----	178
Areal variation -----	178
Seasonal variability -----	178
Trace metal content -----	193
Geochemical anomaly along the 27° parallel -----	195
Methods -----	195
Results -----	200
Discussion -----	201
CONCLUSIONS AND INTERRELATIONSHIPS -----	205
REFERENCES CITED -----	219
APPENDIXES -----	222

LIST OF ILLUSTRATIONS

		<u>Page</u>
Figure 1.	Map showing location of study area -----	2
Figure 2.	Map showing geographic limits, physiography, and bathymetry of the South Texas OCS -----	3
Figure 3.	Map showing sampling station locations for suspended sediments -----	11
Figure 4.	Map showing results of surface drifter releases, October-November cruise -----	17
Figure 5.	Map showing results of surface drifter releases, March cruise -----	19
Figure 6.	Map showing results of surface drifter releases, May cruise -----	21
Figure 7.	Map showing surface water transmissivity, October-November cruise -----	23
Figure 8.	Map showing surface water transmissivity, March cruise -----	25
Figure 9.	Map showing surface water transmissivity, May cruise -----	27
Figure 10.	Graphs showing transmissivity/temperature profiles, Matagorda Bay inlet stations -----	29
Figure 11.	Graphs showing transmissivity/temperature profiles, stations 3 and 4 -----	31
Figure 12.	Graphs showing transmissivity/temperature profiles, station 5 -----	33
Figure 13.	Graphs showing transmissivity/temperature profiles, station 6 -----	34
Figure 14.	Graphs showing transmissivity/temperature profiles, stations 7 and 8 -----	35
Figure 15.	Graphs showing transmissivity/temperature profiles, Aransas Pass inlet stations -----	37
Figure 16.	Graphs showing transmissivity/temperature profiles, stations 10 and 11 -----	39
Figure 17.	Graphs showing transmissivity/temperature profiles, station 12 -----	40

	<u>Page</u>
Figure 18. Graphs showing transmissivity/temperature profiles, stations 13 and 14 -----	42
Figure 19. Graphs showing transmissivity/temperature profiles, stations 16 and 17 -----	44
Figure 20. Graphs showing transmissivity/temperature profiles, station 18 -----	45
Figure 21. Graphs showing transmissivity/temperature profiles, station 19 -----	47
Figure 22. Graphs showing transmissivity/temperature profiles, stations 20, 21, and 22 -----	48
Figure 23. Graphs showing transmissivity/temperature profiles, Rio Grande-Brazos Santiago inlet stations -----	50
Figure 24. Maps showing distribution of suspended sediments, October-November 1976 cruise -----	53
Figure 25. Maps showing distribution of suspended sediments, March cruise -----	56
Figure 26. Maps showing distribution of suspended sediments, May cruise -----	58
Figure 27. Maps showing silt/clay ratios for suspended sediments, October-November cruise -----	62
Figure 28. Maps showing mean diameters for suspended sediments, October-November cruise -----	63
Figure 29. Maps showing standard deviations for suspended sediments, October-November cruise -----	65
Figure 30. Maps showing silt/clay ratios for suspended sediments, March cruise -----	67
Figure 31. Maps showing mean diameters for suspended sediments, March cruise -----	69
Figure 32. Maps showing standard deviation for suspended sediments, March cruise -----	70
Figure 33. Maps showing silt/clay ratios for suspended sediments, May cruise -----	72
Figure 34. Maps showing mean diameters for suspended sediments, May cruise -----	74

	<u>Page</u>
Figure 35. Maps showing standard deviations for suspended sediments, May cruise -----	75
Figure 36. Map showing location of stations sampled for trace metal content of suspended sediments -----	78
Figure 37. Maps showing amounts of suspended sediment -----	88
Figure 38. Maps showing total particulate carbon in suspended sediments -----	89
Figure 39. Maps showing amounts of cadmium in suspended sediments -----	90
Figure 40. Maps showing amounts of chromium in suspended sediments -----	91
Figure 41. Maps showing amounts of copper in suspended sediments -----	92
Figure 42. Maps showing amounts of manganese in suspended sediments -----	93
Figure 43. Maps showing amounts of nickel and zinc in suspended sediments -----	94
Figure 44. Maps showing amounts of lead in suspended sediments -----	95
Figure 45. Maps showing amounts of vanadium in suspended sediments -----	96
Figure 46. Maps showing amounts of iron in suspended sediments -----	97
Figure 47. Maps showing locations of sample stations for clay mineralogy, total mass, and total organic carbon in suspended sediments -----	100
Figure 48. Maps showing amounts of suspended sediment, November 1974-May 1976 -----	105
Figure 49. Maps showing amounts of suspended sediment, November 1976-May 1977 -----	106
Figure 50. Maps showing percentage total particulate carbon in suspended sediments, November 1975-November 1976 -----	107
Figure 51. Maps showing percentage total particulate carbon in suspended sediments, March 1977-May 1977 -----	108

	<u>Page</u>
Figure 52. Map showing percentage of clay minerals in suspended sediments, November 1975, one m below the air-water interface -----	109
Figure 53. Map showing percentage of clay minerals in suspended sediments, November 1975, one m above the sea-floor surface -----	110
Figure 54. Map showing percentage of clay minerals in suspended sediments, May 1976, one m below the air-water interface -----	111
Figure 55. Map showing percentage of clay minerals in suspended sediments, May 1976, one m above the sea-floor surface -----	112
Figure 56. Map showing percentage of clay minerals in suspended sediments, November 1976, one m below the air-water interface -----	113
Figure 57. Map showing percentage of clay minerals in suspended sediments, November 1976, mid depth -----	114
Figure 58. Map showing percentage of clay minerals in suspended sediments, November 1976, one m above the sea-floor surface -----	115
Figure 59. Map showing percentage of clay minerals in suspended sediments, March 1977, one m below the air-water interface -----	116
Figure 60. Map showing percentage of clay minerals in suspended sediments, March 1977, mid depth -----	117
Figure 61. Map showing percentage of clay minerals in suspended sediments, March 1977, one m above the sea-floor surface -----	118
Figure 62. Map showing percentage of clay minerals in suspended sediments, May 1977, one m below the air-water interface -----	119
Figure 63. Map showing percentage of clay minerals in suspended sediments, May 1977, mid depth -----	120
Figure 64. Map showing percentage of clay minerals in suspended sediments, May 1977, one m above the sea-floor surface -----	121

	<u>Page</u>
Figure 65. Map showing distribution of suspended material on the Texas continental shelf based on Landsat imagery -----	122
Figure 66. Map showing percent expandable clay in bottom sediments -----	126
Figure 67. Map showing location of bottom stations for seasonal sampling -----	129
Figure 68. Graphs showing sand/mud ratios for benthic sediments -----	136
Figure 69. Graphs showing silt/clay ratios for benthic sediments -----	139
Figure 70. Graphs showing mean diameters for benthic sediments -----	141
Figure 71. Graphs showing standard deviations for benthic sediments -----	143
Figure 72. Map showing location of sample stations for cores used to study the shallow subsurface sediments -----	147
Figure 73. Diagrams showing core 0A -----	149
Figure 74. Diagrams showing core 1A -----	151
Figure 75. Diagrams showing core 23 -----	152
Figure 76. Diagrams showing core 28A -----	153
Figure 77. Diagrams showing core 28B -----	154
Figure 78. Diagrams showing core 45 -----	156
Figure 79. Diagrams showing core 68 -----	157
Figure 80. Map showing location of cores that contain sedimentary structures indicating transport and deposition of sediments by flowing bottom water -----	161
Figure 81. Map showing location of cores in which bottom scour and small-scale slumping of sediments is indicated -----	162
Figure 82. Map showing distribution of a discrete sand layer at a subsurface depth of 90 cm -----	163

	<u>Page</u>
Figure 83. Photograph of core from South Baker Reef -----	168
Figure 84. Map showing biologic infaunal stations from which subsamples were taken for trace metal analysis -----	171
Figure 85. Graph showing variations in barium concentrations in benthic sediments -----	179
Figure 86. Graph showing variations in cadmium concentrations in benthic sediments -----	180
Figure 87. Graph showing variations in chromium concentrations in benthic sediments -----	181
Figure 88. Graph showing variations in copper concentrations in benthic sediments -----	182
Figure 89. Graph showing variations in iron concentrations in benthic sediments -----	183
Figure 90. Graph showing variations in lead concentrations in benthic sediments -----	184
Figure 91. Graph showing variations in manganese concentrations in benthic sediments -----	185
Figure 92. Graph showing variations in nickel concentrations in benthic sediments -----	186
Figure 93. Graph showing variations in vanadium concentrations in benthic sediments -----	187
Figure 94. Graph showing variations in zinc concentrations in benthic sediments -----	188
Figure 95. Graphs of dispersion indices for barium, cadmium, chromium, and copper -----	190
Figure 96. Graphs of dispersion indices for iron, lead, manganese, and nickel -----	191
Figure 97. Graphs of dispersion indices for vanadium and zinc -----	192
Figure 98. Map showing manganese distribution from 1974 grab samples -----	196
Figure 99. Map showing nickel distribution from 1974 grab samples -----	197

	<u>Page</u>
Figure 100. Map showing copper distribution from 1974 grab samples -----	198
Figure 101. Map showing rates of sedimentation estimated from ²¹⁰ Pb content -----	203
Figure 102. Maps showing patterns of distribution for various aspects of the suspended sediments, surface water, October 29 to November 3, 1976 -----	206
Figure 103. Maps showing patterns of distribution for various aspects of the suspended sedi- ments, bottom water, October 29 through November 3, 1976 -----	207
Figure 104. Maps showing patterns of distribution for various aspects of the suspended sedi- ments, surface water, March 17 through 21, 1977 -----	210
Figure 105. Maps showing patterns of distribution for various aspects of the suspended sedi- ments, bottom water, March 17 through 21, 1977 -----	211
Figure 106. Maps showing patterns of distribution for various aspects of the suspended sedi- ments, surface water, May 19 through 23, 1977 -----	212
Figure 107. Maps showing patterns of distribution for various aspects of the suspended sedi- ments, bottom water, May 19 through 23, 1977 -----	213
Figure 108. Maps showing patterns of distribution for various aspects of the suspended sedi- ments, surface water, November 21 to 26, 1975 -----	214
Figure 109. Maps showing patterns of distribution for various aspects of the suspended sedi- ments, bottom water, November 21 to 26, 1975 -----	215
Figure 110. Maps showing patterns of distribution for various aspects of the suspended sedi- ments, surface water, May 21 to 26, 1976 -----	216

	<u>Page</u>
Figure 111. Maps showing patterns of distribution for various aspects of the suspended sediments, bottom water, May 21 to 26, 1976 -----	217
Figure 112. Maps showing patterns of distribution for various aspects of the benthic sediments as determined during the first year of study in 1975 -----	218

LIST OF TABLES

	<u>Page</u>
Table 1. Replicate analyses, November 1976 -----	82
Table 2. Averages of the amounts of trace metals in suspended sediments -----	84
Table 3. Summary of total suspended sediment and of total particulate carbon in suspended sediments -----	104
Table 4. Results of t-statistic tests for seasonal comparison of textural parameters -----	138
Table 5. Location of stations used for studying the seasonal variability of trace metals in benthic sediments -----	172
Table 6. Intercalibration samples (ppm) -----	174
Table 7. Instrument parameters and mode of analysis -----	175
Table 8. Results of reanalysis of 1976 seasonal samples -----	194
Table 9. Rates of sedimentation - 1977 study -----	199

INTRODUCTION

The geologic studies of the South Texas Outer Continental Shelf made during 1977 were a continuation of the investigations started in late 1974, as a part of the National Outer Continental Shelf Environmental Studies Program sponsored by the Bureau of Land Management. The results of the previous two years of studies were reported by Berryhill and others, 1976 and Berryhill, 1977. The initial investigations were keyed primarily to establishing baselines prior to the first petroleum lease sale for the South Texas OCS held in early 1975. The nature of the initial field investigations, the density of the data collected, and the scheduling of the field sampling were by necessity scaled to the few months of time available prior to the lease sale. The investigations for 1977 are based primarily on the results obtained during the first two years. The study plan for the third year provides data coverage for seasonal monitoring of parameters; it also provides further details and quantification of those sedimentary processes operative on the South Texas OCS.

STUDY PLAN

The geographic limits of field operations during the third year remained the same as for the first two years, which was the South Texas OCS lease area as defined by the Department of the Interior. The geographical delineation of the area in which the studies were conducted is shown by two figures: figure 1, which shows the location of the South Texas OCS regionally within the Gulf of Mexico; and figure 2, of a larger scale, which shows the geographic limits, physiography, and bathymetry of the South Texas OCS lease area.

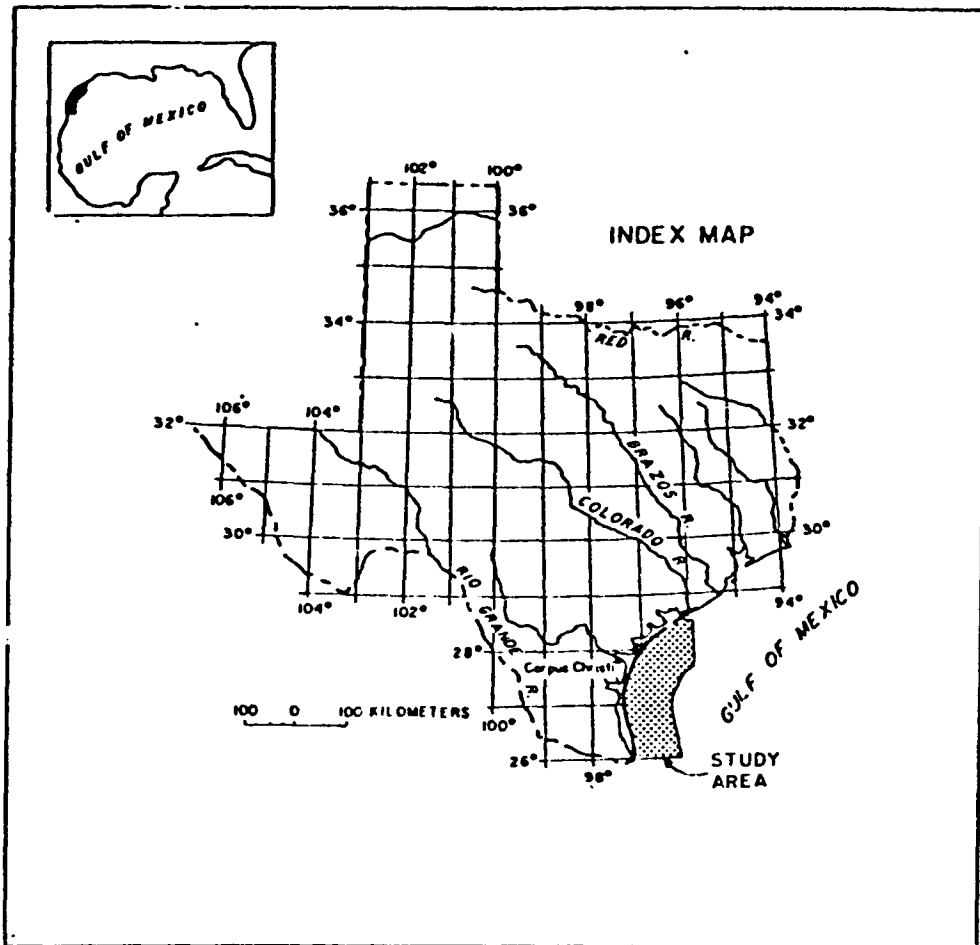


Figure 1. Location of the study area.

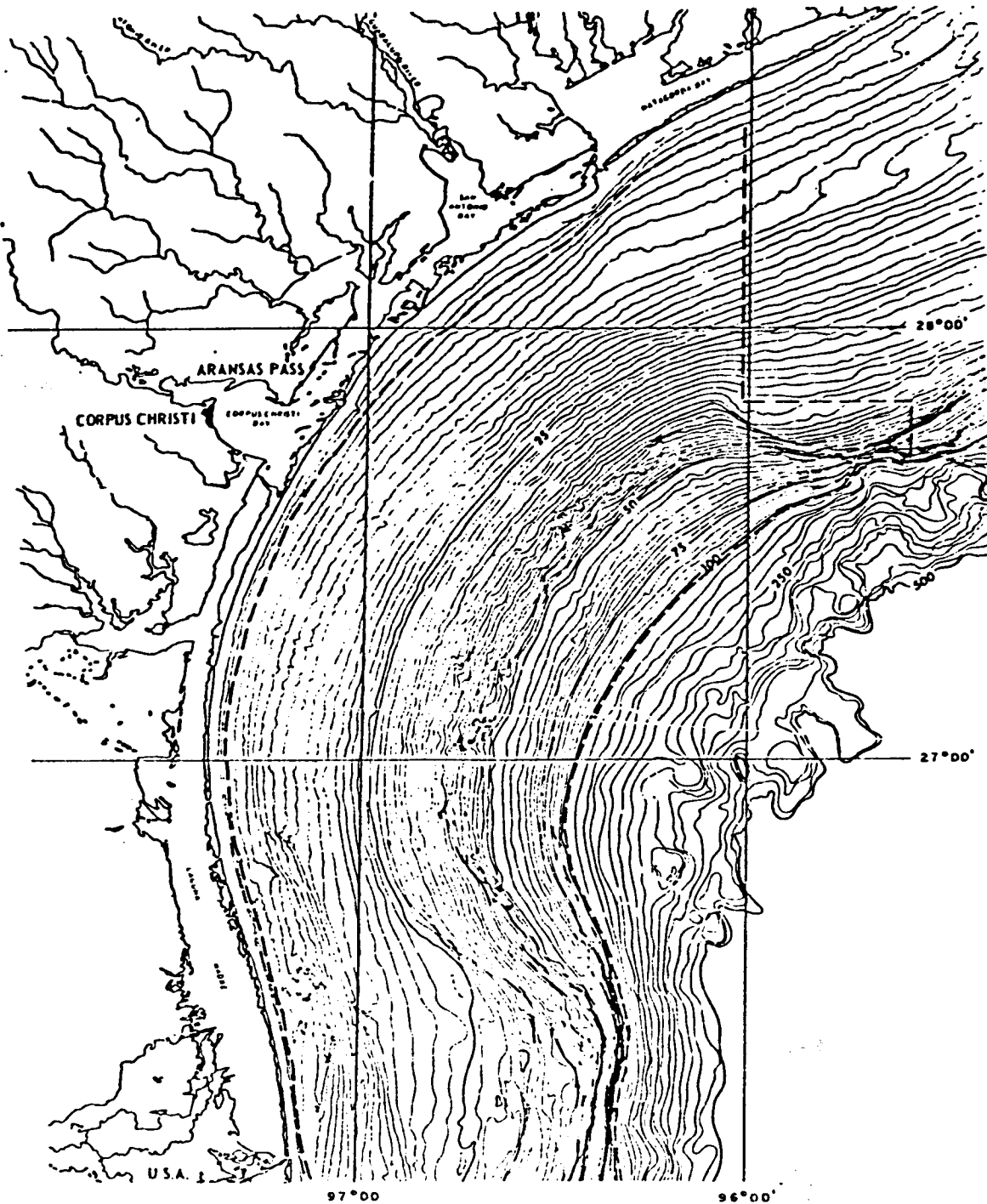


Figure 2. Geographic limits (heavy dashed line), physiography and bathymetry of the South Texas Outer Continental Shelf (depth in fathoms). From Berryhill and others, 1976, Part 1, figure 3.

OBJECTIVES AND RATIONALE

The elements of study were selected to provide qualitative data relative to defining the environmental character of the South Texas OCS, as pertinent to the mission of the BLM. Sample location maps for each element are included within each chapter. The topics studied and the rationale for their selection are as follows:

1. The amounts, composition, sources, and dispersal patterns for inorganic particulate matter suspended in the water column -- In 1976 samples for the suspended sediments were collected on a seasonal basis and a composite net of 26 sample stations was covered during each period of seasonal sampling in the shortest time span possible. In no case did a seasonal cruise exceed 4 1/2 days. Also, the sampling from three levels in the water was supplemented by transmissometry, which gave a turbidity profile from surface to bottom at each station. The same format of study was continued during 1977 to: 1) acquire adequate time-series data for a seasonal (synoptic) evaluation of movement patterns; 2) evaluate more fully the diurnal tidal contributions from inlet sources; 3) build a bank of synoptic data extending over a minimum of 2 years for predicting the probable patterns of movement for pollution locally within the region; 4) develop a regional sediment dispersal model for large-scale prediction relative to water mass movement.

As a part of the suspended sediments studies, analysis of the trace metals content also was continued during 1977 following the same plan of sampling and procedures used previously.

2. Textural stratigraphy and sedimentary structures, shallow subbottom

sediments -- The vertical variations in grain size from fine to coarse at a specific locality indicate the temporal ranges in transporting energy at that place through time; the lateral variations from one place to another indicate the degree to which energy conditions have varied geographically over the region. The gross textural stratigraphy of the shallow bottom sediments over the region, as indicated by the vertical alteration of very fine grained sediments and layers of discrete sand plus the nature of the depositional structures implanted during deposition, records the prevalent directions of sediment dispersal and deposition with time and indicates the persistence of these patterns during the recent past. Consequently, data derived from the shallow subsurface sediments supplement those from both suspended sediments and oceanography in providing the means for predicting both the likely dispersal patterns and the effect of high-energy conditions in spreading sediments over the area. Study of the internal stratification of sand and fine-grained sediments and the regional nature of depositional structures in cores was continued in 1977 to provide additional detail for recognizing the deposits possibly laid down during and in the aftermath of hurricanes. The work entailed closer internal study and analysis than time permitted during the first and second years' studies. The objective for the work in 1977 was to document the depositional structures typical of the various grain-size components represented across the shelf with the intent of establishing regional criteria for distinguishing storm deposits from the normal weather deposits. Sample material was the 175 cores collected during the 1975 and 1976 investigations.

3. Geochemistry of benthic sediments along the 27° north latitude anomaly — The regional patterns of distribution for concentrations of trace metals in benthic sediments, as revealed by the analyses for the 1975 effort, indicated that for several elements the levels of concentration are higher over the southern part of the South Texas OCS than over the northern part. Those metals that have this pattern in notable amounts are Cu, Mn, and Ni. The "boundary" between these regional background levels roughly approximates the 27° north latitude line. Interestingly, the regional "boundary" between infaunal types and concentrations seems to lie roughly along the same parallel. Additional closely spaced sampling and analyses across the "boundary" were carried out to define the physiochemical reasons for the boundary.

FIELD INVESTIGATIONS

The vessels used for the field investigations were the R/V IDA GREEN, made available by the University of Texas Marine Science Institute, Galveston, and the R/V DECCA PROFILER, leased from Decca Surveys, Incorporated.

The first of the three cruises made to gather seasonal synoptic samples for the suspended sediments studies was made from October 29 through November 3, 1976 using the IDA GREEN. The chief scientist for the cruise was Gerald Shideler and the sampling consisted of three water-column samples at each of 26 stations and vertical transmittance-temperature profiles also at each station. In addition a total of 36 drifter bottles were released, 13 at each sampling station.

The second cruise, March 17 through March 21, 1977 and the third cruise, May 24 through May 27, 1977, were made aboard the DECCA PROFILER. The sampling

plan for the second and third cruises was the same as that used for the first cruise. Gerald Shideler acted as chief scientist on both cruises.

A fourth cruise, May 28 through June 5, 1977, was devoted to collecting a series of short cores along the 27° north latitude "boundary" to study the geochemical anomalies. Chief scientist for the cruise was Charles Holmes. Navigation for all four used a combination of radar and LORAN-A: radar was used for positioning at the coastal inlet stations that were near shore; LORAN A was used for all other stations.

INVENTORY OF FIELD DATA

Two types of samples were collected under the work plan for 1977: cores of benthic sediments; and samples of water at three depths, near surface, mid depth, and near bottom, for extraction of suspended particulate matter. During the sampling for the suspended sediment studies by NISKIN casts, the following subsamples were prepared: particulate grain size at all three levels for three seasons; and trace metals content and clay mineralogy at surface and near bottom for the winter and spring seasons for 12 of the 26 stations. The turbidity through the water from surface to bottom was measured with the same MARTEK transmissometer used in 1976.

A summary listing of the samples collected by category follows. In part A of the table, column 1 lists the number of samples specified in the work plan; column 2 lists the number of samples actually collected; and column 3 indicates the deviations from the numbers specified. In all cases, where a larger number of samples were collected than were specified, the work was done at no extra cost to the BLM.

A. Summary listing of samples by type and number:

	<u>1</u>	<u>2</u>	<u>3</u>
<u>Suspended sediments:</u>			
1. Textural analysis- - - - -	234	234	0
2. Transmissivity/temperature profiles- - -	78	78	0
3. Trace metals content - - - - -	72	66	-6 ^{1/}
4. Clay mineralogy- - - - -	234	216	-18 ^{1/}
5. Surface drifters - - - - -	<u>2/</u>	983 ^{3/}	
<u>Benthic sediments cores for trace metal analysis-</u>	20	22	+2
(Supplemented by 44 cores collected in 1976) - - - - -			+66 ^{4/}
<u>Clay mineralogy, benthic sediments-</u>	195	251	+56
(Completion of 195 grab samples collected in 1975)			

- ^{1/}Samples from one station lost
- ^{2/}No number specified in the contract
- ^{3/}Drifters supplied by USGS at no cost to the BLM
- ^{4/}Total number analyzed

B. Summary listing of samples collected by the University of Texas as a part of the biological monitoring studies and submitted to USGS for analysis:

1. Subsamples collected at biological stations for textural analysis	- - - - - 159
2. Subsamples collected at biological stations for trace metals analysis	- - - - - 195

PRINCIPAL INVESTIGATORS

Element leader for the geologic investigations was Henry Berryhill, Jr., who also assembled and edited the geologic report for 1977. Assistance in the editing and report preparation was provided by Anita Trippet.

Principal investigators delegated responsibility for carrying out the

laboratory analysis, interpretation, compilation and reporting of data for specific topics of the geologic investigations were:

Suspended sediments, texture, and transmissometry- - - -	Gerald Shideler
Suspended sediments, clay mineralogy - - - - -	Charles Holmes
Suspended sediments, trace metals- - - - -	Steven Barnes and Cynthia Rice
Benthic sediments, texture - - - - -	Gerald Shideler
Benthic sediments, sedimentary structures and origin of sand layers - - - - -	Henry Berryhill, Jr.
Benthic sediments, trace metals- - - - -	Ann Martin and Charles Holmes
Benthic sediments, trace metals "boundary" - - - - -	Charles Holmes and Ann Martin
Benthic sediments, clay mineralogy - - - - -	Charles Holmes

SUSPENDED SEDIMENTS

PHYSICAL CHARACTERISTICS

by

Gerald L. Shideler

This report presents the third-year results of continuing studies designed to evaluate the physical characteristics of suspended sediment within the South Texas OCS region in order to develop a conceptual model for sediment transport that could contribute to effective environmental management. The physical characteristics of the suspended particulate system, in terms of both turbidity and texture, were evaluated to determine the seasonal variability of regional distribution patterns and to gain insight into the regional sediment transport system.

Methods

Field Techniques

The seasonal variability of regional suspended sediment patterns was determined on the basis of both turbidity and textural measurements at 26 monitoring stations during the October-November, March, and May cruises (see fig. 3 for station locations). The 26 stations were located to provide optimum geographic coverage of the region and to provide concentrated coverage of three coastal inlets that serve as major sources of sediment (Matagorda Bay inlet, Aransas Pass, Rio Grande-Brazos Santiago channel). The inlet stations were located along 3.2 km radii from the center of the respective inlets and were occupied during ebb tides at the approximate time of maximum current flow. Water column measurements for each cruise

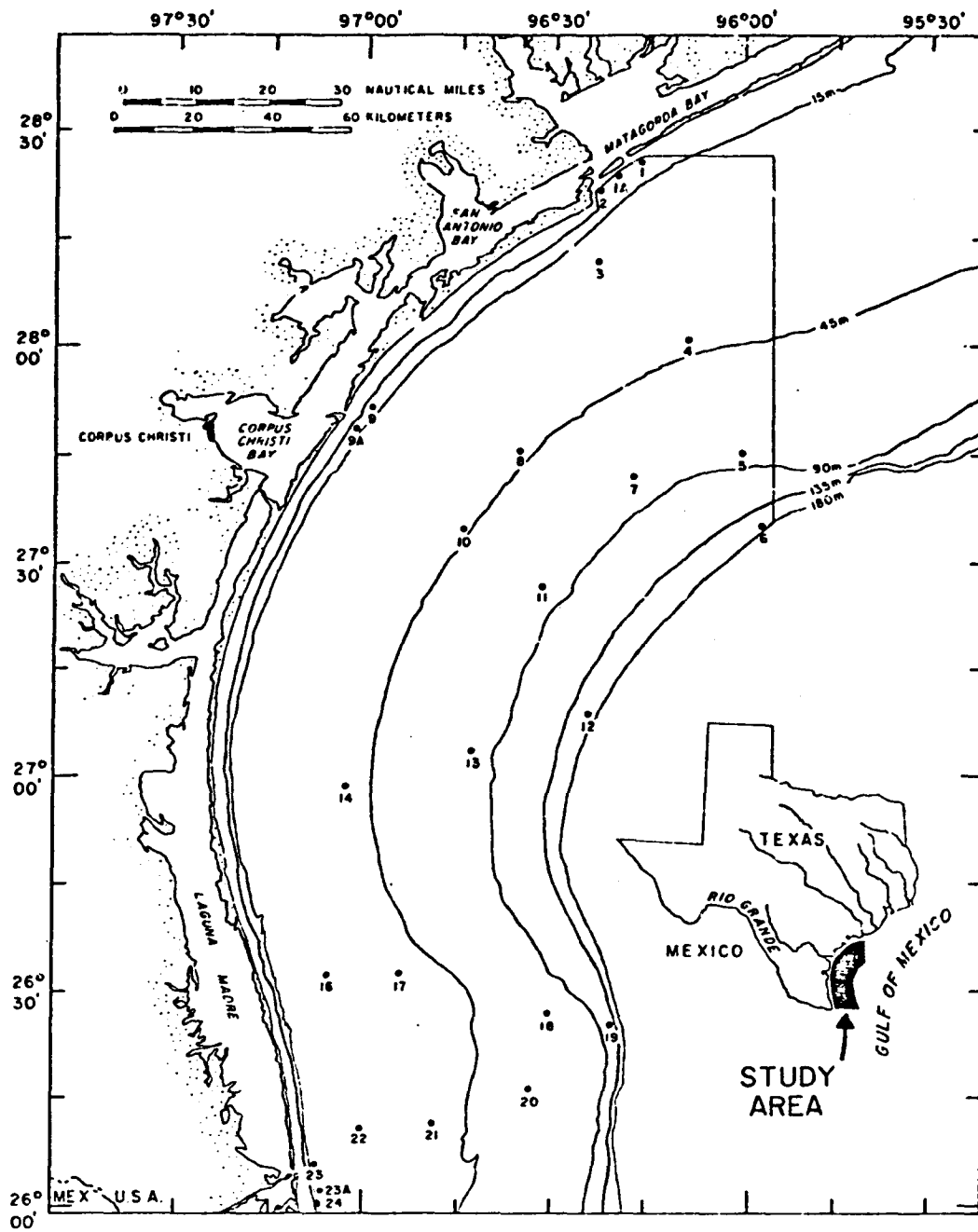


Figure 3. Locations of stations sampled for suspended sediments.

were obtained over a maximum period of 5 days, thus providing quasi-synoptic regional coverage. Radar navigation was used for inlet station positioning; deeper stations were located and repositioned by LORAN-A.

During each of the three cruises, regional wind conditions and surface drift patterns were recorded. Daily wind speed and azimuth data compiled by the National Weather Service at Corpus Christi were considered to be representative of the OCS region, although wind velocity can vary from offshore to onshore. The wind data were added vectorially over a 15 day interval that was centered on the cruise period, in order to determine the resultant wind directions during each cruise. Quasi-synoptic surface drift patterns were determined by releasing ballasted surface drifter bottles at each station during the cruise. Only drifters recovered within 30 days of the release date were used to determine net drifter trajectories between release and recovery points. Drifters recovered within 15 days from the date of release also were used to calculate net minimum drift velocities, based on straight-line trajectory distances and the corresponding elapsed time intervals.

Vertical in situ transmissivity/temperature profiles were recorded at each station. Processing of the profiles consisted of manually digitizing the field analog recordings at selected depth intervals, tabulating the corresponding transmittance and temperature values, and reducing the profiles to a common scale. The recorded transmittance values (percent T per 25 cm optical path) were converted to values corresponding to a 1 m optical path, a more commonly used mode of comparison. Time-sequence profiles from the 3 cruises were then prepared for each of the 26 monitoring stations to document the transmissivity and temperature variability

within the water column. The transmissivity and temperature values are tabulated in appendix 1.

At each of the 26 stations, water samples were obtained at three levels: top, mid depth, and approximately 2 m above the bottom. Water samples were collected in 30 liter NISKIN bottles and were immediately transferred to particle-free amber polypropylene storage bottles. As a means of inhibiting organic growth, a sufficient quantity of formalin was added to the storage bottles to result in a 5 percent concentration. The sediment dispersal patterns derived from the data are based on the textural and turbidity gradients observed at the 26 monitoring stations.

Laboratory Techniques

The suspended sediment from the 234 water samples collected during the 3 cruises was analyzed for both texture and total particle concentrations using the following procedures:

Textural analyses

1. The field samples were brought to room temperature and thoroughly agitated; a representative split was taken.
2. The work sample was then filtered through a 125 μm sieve to remove particles capable of blocking the COULTER COUNTER 200 μm tube aperture.
3. Grain-size distributions were determined at a 0.5 ϕ interval electronically, employing a 16-channel model TA COULTER COUNTER.

Duplicate analyses were conducted with 200 μm and 30 μm tube apertures, providing an effective analytical range from 0.63 to 81 μm . All COULTER analyses were conducted using the following standard procedures:

- a. The sample concentrations were maintained at a level sufficiently low to produce less than 5 percent coincidence error. If dilution was required, a particle-free sea water diluent, passed through a 0.2 μm filter, was used.
 - b. The 200 μm tube analysis was conducted first to determine the coarser half of the size distribution; the sample was agitated during analysis at a standard speed.
 - c. The residual sample from the 200 μm tube analysis was passed through a clean 20 μm sieve and was analyzed with the 30 μm tube to determine the finer half of the size distribution. No agitation was used during the 30 μm tube analysis.
 - d. The results from both 200 μm and 30 μm tube analyses were combined to obtain the total size distribution, using standard two-tube overlap techniques.
4. The textural data were processed by computer to derive statistical grain-size parameters over a 3.5-11.0 ϕ analytical range. Derived parameters include the silt/clay ratios and the four moment measures (mean diameter, standard deviation, skewness, and kurtosis). These parameters are tabulated in appendix 1.
 5. The regional variability of selected size parameters (silt/clay ratio, mean diameter, standard deviation) was then mapped for both surface and bottom water sediments.

Particle concentration analyses

Suspended sediment particle concentrations within the size range of 0.63 to 81 μm also were determined for each water sample. The particle concentrations (counts/cc), as determined by COULTER COUNTER,

were used as an index of relative water turbidity. Particle counts were made using the following procedures:

1. The water sample was brought to room temperature and thoroughly agitated.
2. Counts were made first with the 200 μm tube, running the sample full strength after passing it through a 125 μm sieve. A standard 150 ml sample volume was agitated at a standard speed. Duplicate counts were made; if they agreed within ± 10 percent, the average value was used. If the deviation was greater than ± 10 percent, additional counts were run until the value spread was within the ± 10 percent limits. The 200 μm tube analysis counted particles within the size range of 12.7 to 81 μm .
3. The residual sample from the 200 μm tube analysis was passed through a 20 μm sieve and then used for the 30 μm tube analysis to obtain the particle count within the size range of 0.63 to 12.7 μm . The sample was diluted to produce less than 3 percent coincidence error. The particle count was determined and adjusted by the dilution factor. Duplicate counts were made using a ± 10 percent value spread, as described in the 200 μm analyses.
4. Particle counts from both the 200 μm and 30 μm tube analyses were arithmetically combined to provide total particle counts/cc. Particle count data are tabulated in appendix 1. The regional variability of total particle counts was then mapped for both surface and bottom water sediments.

Patterns of Movement for the Surface Drifters

The patterns of surface drifter movement and associated wind vectors

were determined for each of the three cruise periods (figs. 4-6) to gain insight into the trajectories and minimal velocities of surface currents, which are important dispersing agents of suspended sediments.

October-November 1976 Cruise

During the October 29-November 3 cruise period, the composite wind vector was oriented southward and daily wind speeds were within the 2-19 km/hr range (fig. 4). The period preceding the cruise (October 25-28) was characterized by a composite wind vector toward the southwest, with relatively high daily wind speeds within the 13-40 km/hr range. Following the cruise (November 4-8), the composite wind vector was toward the west, with relatively low daily speeds within the 3-15 km/hr range. The resultant wind vector for the entire 15 day period was oriented toward the southwest (213°).

A total of 336 surface drifters were released during the cruise, but only 4 percent were recovered within 30 days: 3 percent within the 0-15 day interval and 1 percent within the 16-30 day interval. The regional pattern of surface drift was to the south/southwest (fig. 4). Net minimum drift velocities based on the 0-15 day recoveries ranged from 9-23 km/day, with an overall mean velocity of 16 km/day. The southward regional drift appeared to reflect a wind-drift pattern largely generated in response to the southwest-oriented 15 day resultant wind vector. Most of the drifters recovered were from release sites along the inner shelf (<45 m depth); recoveries from outer shelf sites were conspicuously absent except for station 19. The pattern suggests that drifters from the outer shelf sites may have been transported to relatively remote Mexican beaches farther to the

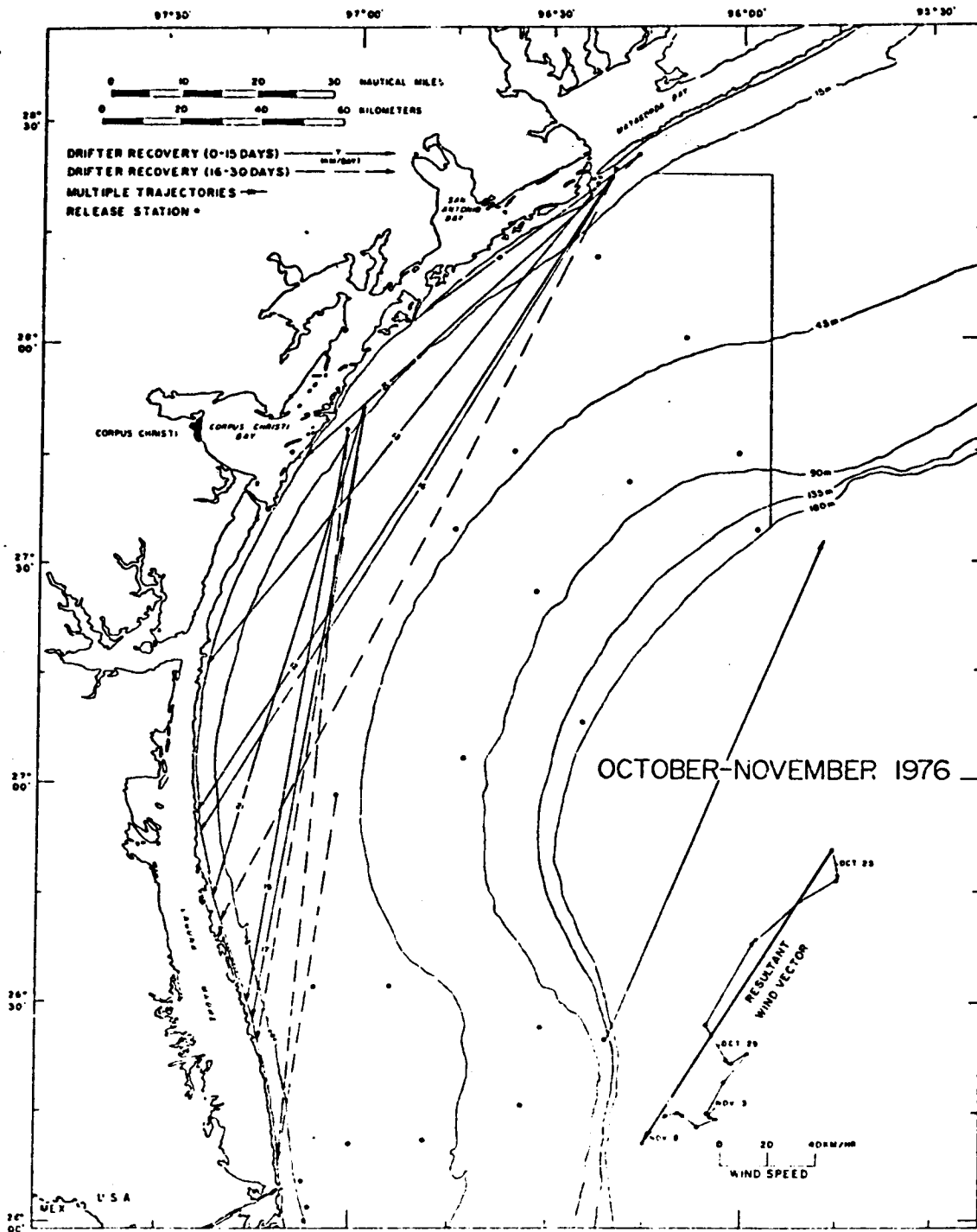


Figure 4. Results of surface drifter releases, October-November cruise .

south, with little chance of recovery. Alternatively, they may have been transported either northward or farther out into the Gulf by an outer shelf countercurrent; this possibility is suggested by the northeastward orientation of the station 19 trajectory, which had the highest average velocity (23 km/day) within the drifter pattern.

March 1977 Cruise

Daily winds during the March 17-21 cruise period were variable, but the composite vector was oriented toward the west (fig. 5). Daily wind speeds were within the 7-26 km/hr range. Preceding the cruise (March 12-16), the composite wind vector was toward the northwest, with daily speeds within the 4-21 km/hr range. Following the cruise (March 22-26), the composite wind vector was toward the west, with daily wind speeds within the 8-27 km/hr range. The resultant wind vector for the entire 15 day period was westward (277°).

A total of 312 drifters were released, and 22 percent were recovered within 30 days: 20 percent within the 0-15 day interval, and 2 percent within 16-30 day interval. The regional surface drift was toward the south/southwest. Net minimum drift velocities were within the 2-40 km/day range, with a mean velocity of 15 km/day. The regional pattern was similar to that in October-November except for a substantially higher percentage of recovery, including several returns from outer shelf (>45 m depth) release sites. The greater recovery from outer-shelf stations could reflect the stronger onshore component of the March resultant wind vector. The regional drift pattern is not in agreement with the prevailing winds during most of the cruise period; the reason is unknown but possible explanations are: 1) the drift pattern is

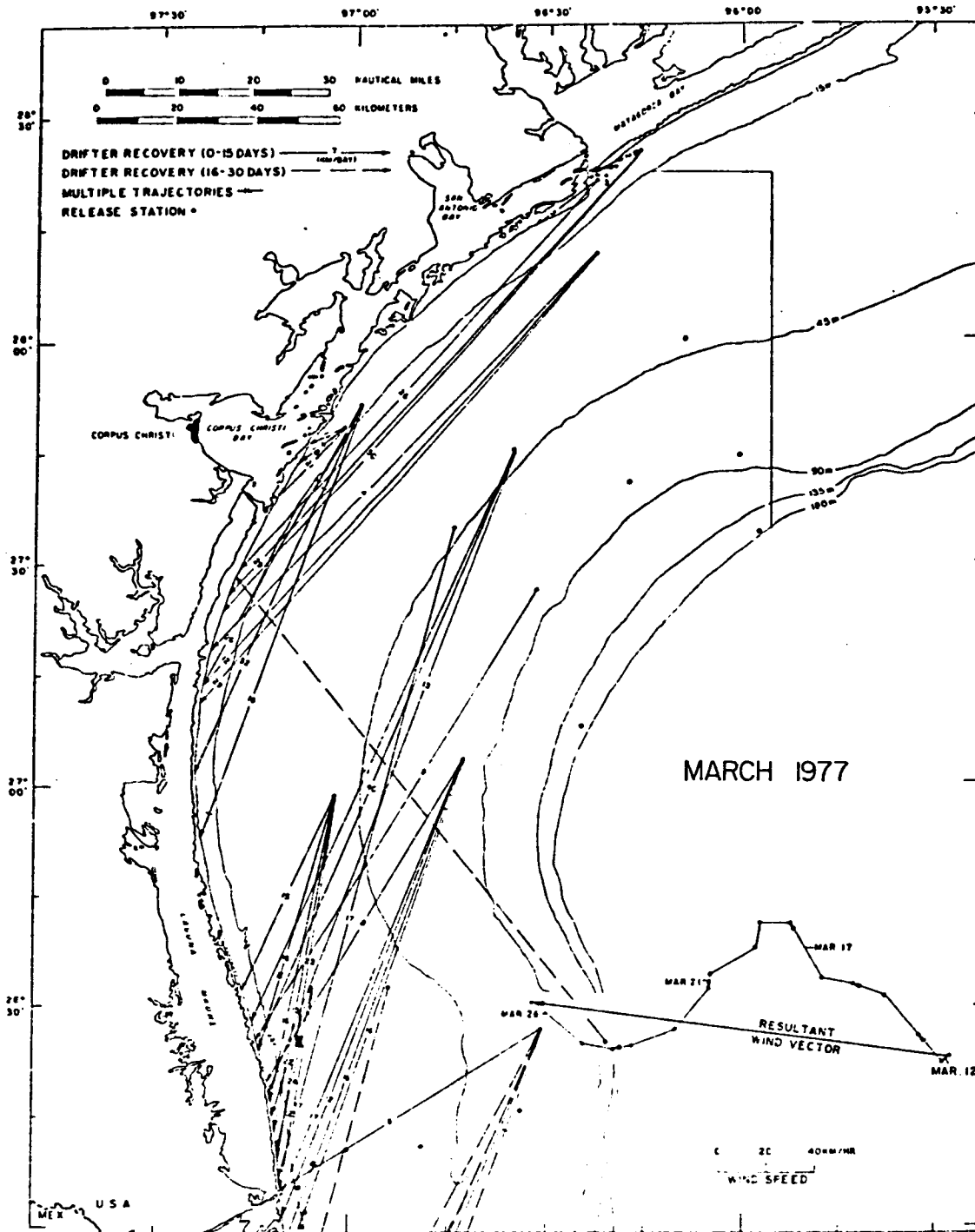


Figure 5. Results of surface drifter releases, March cruise.

a response to late-cruise/post-cruise winds, or 2) the drift was not wind-driven but was a density-related pattern.

May 1977 Cruise

Winds during the May 24-27 cruise period had a composite vector oriented toward the northwest, with daily wind speeds within the 13-18 km/hr range (fig. 6). Preceding the cruise (May 19-23), the composite wind vector was toward the northwest, and the relatively high daily speeds were within the 18-29 km/hr range. Following the cruise (May 28-June 2), the composite wind vector also was toward the northwest, and daily wind speeds were within the 4-19 km/hr range. The winds during the entire 15 day period were relatively uniform in direction, and the resultant wind vector was oriented toward the northwest (315°).

A total of 336 drifters were released, and 29 percent were recovered within 30 days: 16 percent within the 0-15 day interval, and 13 percent within the 16-30 day interval. The regional surface drift was predominantly toward the north in the southern half of the OCS, changing to predominantly northeastward within the northern sector. Net minimum drift velocities were within the 2-54 km/day range, with a mean velocity of 16 km/day. The regional pattern appeared to reflect wind-drift currents generated by persistent southeasterly winds; the change in trajectory orientation toward the north probably reflects coastal curvature. The drifter pattern for May is in notable contrast to the south/southwesterly drift during the October-November and March cruises.

Water Turbidity Patterns

In an effort to evaluate the suspended sediment transport system, regional turbidity gradients were compared for the three cruises. Both

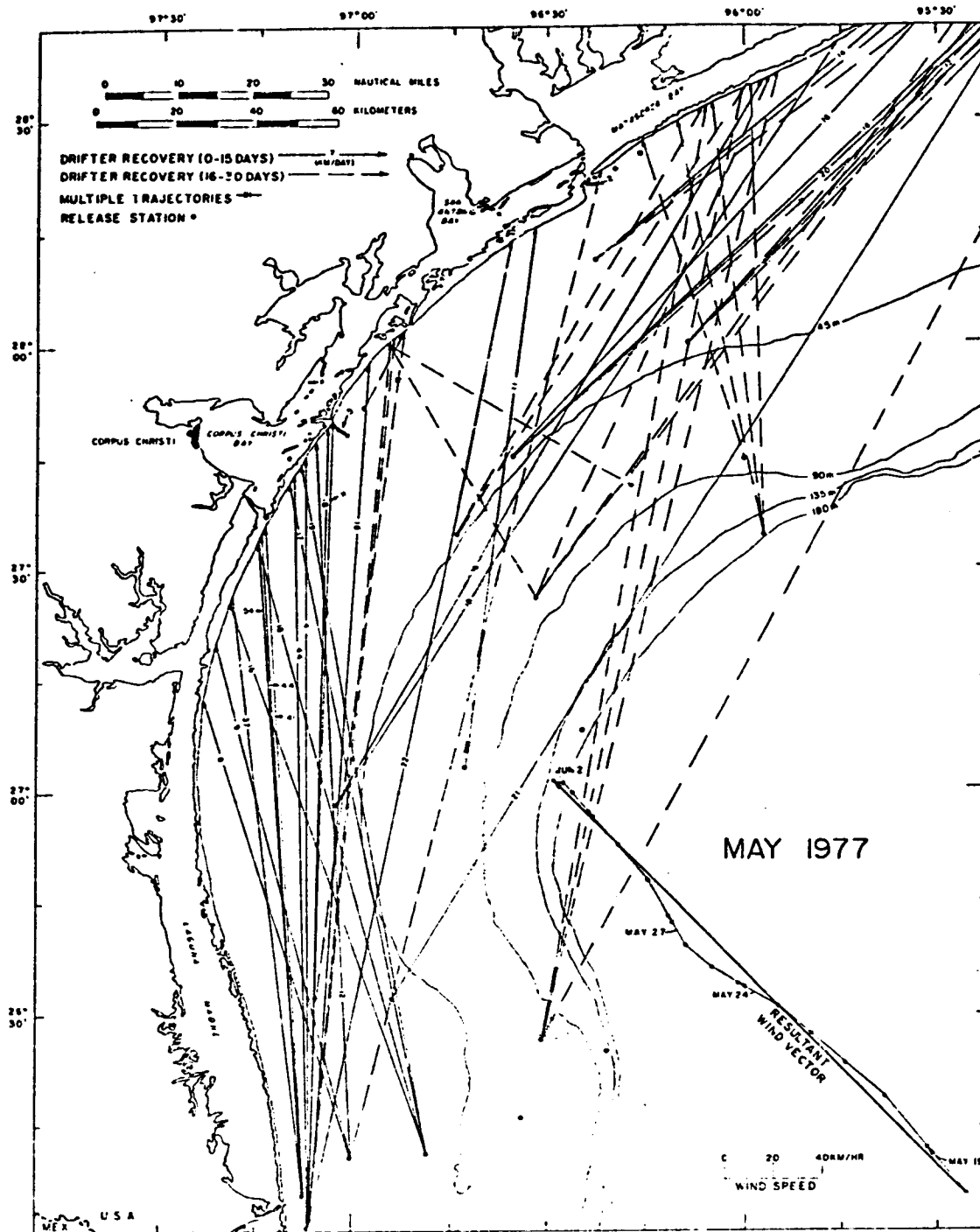


Figure 6. Results of surface drifter releases, May cruise.

lateral and vertical turbidity gradients were determined, using measurements of water transmissivity and particle concentrations. Vertical temperature gradients also were measured to relate vertical variations in turbidity to the thermostructure of the water column.

Transmissivity and Temperature

Measurements of water transmissivity (percent T/m) using a light-beam transmissometer system are influenced by a number of variables that affect the optical properties of seawater (Jerlov, 1968; Gibbs, 1974). The most influential variable is the concentration of sediment in suspension at a given time and place. Consequently, in situ transmissivity measurements can be used as approximations of the relative degree of turbidity. Transmissometer measurements were used to determine the seasonal variability of turbidity gradients. For descriptive purposes, an arbitrary verbal scale of relative turbidity based on water transmissivity values was defined as follows: 1) highly turbid (opaque) = <5 percent T/m; 2) turbid = 5-30 percent T/m; 3) moderately turbid = 30-70 percent T/m; 4) nonturbid (transparent) = >70 percent T/m.

Surface patterns

October-November 1976 pattern (fig. 7)--Transmissivity values of surface waters during the October-November cruise ranged from opaque (0 percent) at some inlet stations, to highly transparent (96 percent) at the northern shelf edge (station 6). The regional trend was a general, shoreward increase in turbidity, with most of the inner shelf (<45 m depth) characterized by turbid conditions (<30 percent). This trend probably

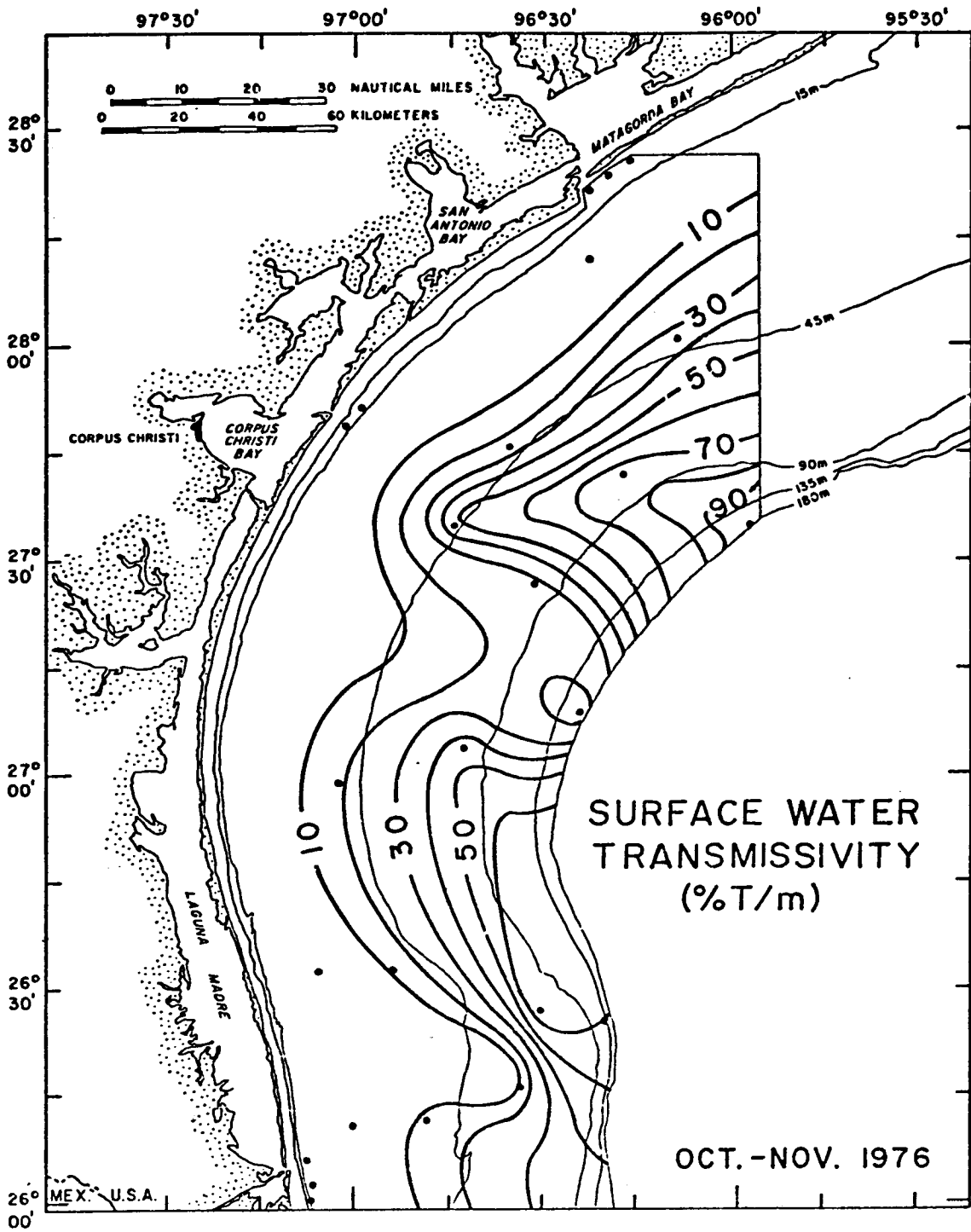


Figure 7. Surface water transmissivity, October-November cruise.

reflects both increasing proximity to coastal sediment sources, as well as a progressive shoreward increase in wave surge intensity that maintains sediment in suspension. Two seaward-trending turbid water salients centered near latitude $26^{\circ} 20'$ N. in the southern sector and near latitude $27^{\circ} 15'$ N. in the central sector were discordant with the bathymetry and appeared to reflect the offshore transport of turbid inner shelf water masses; the southern salient further suggested the presence of a southward transport component, which would be compatible with the ambient wind conditions and regional surface drift pattern. The turbid salients are separated by prominent shoreward-trending reentrants of relatively nonturbid outer shelf water masses.

March 1977 pattern (fig. 8)-- Surface water transmissivity during the March cruise ranged from opaque (0 percent) at some inlet stations, to transparent (89 percent) at the northern shelf edge (station 6). The regional trend was a general shoreward increase in turbidity, and gradients were relatively high and concordant to water depth along the inner shelf. The gradients were lower and largely discordant to water depth over the outer shelf. The amount and distribution of turbidity were different from that during the October-November cruise. The water over the inner shelf was substantially less turbid. Additionally, the gradient indicated a single broad seaward-trending turbid salient that suggested both offshore and southward transport of turbid inner shelf waters. The transparent waters (>70 percent) to the north and south of the salient were more extensive than in October-November. The transparent water possibly reflected the simultaneous shelfward incursion of relatively nonturbid deep Gulf waters, which may have been more extensive in March because of a more substantial onshore component of the

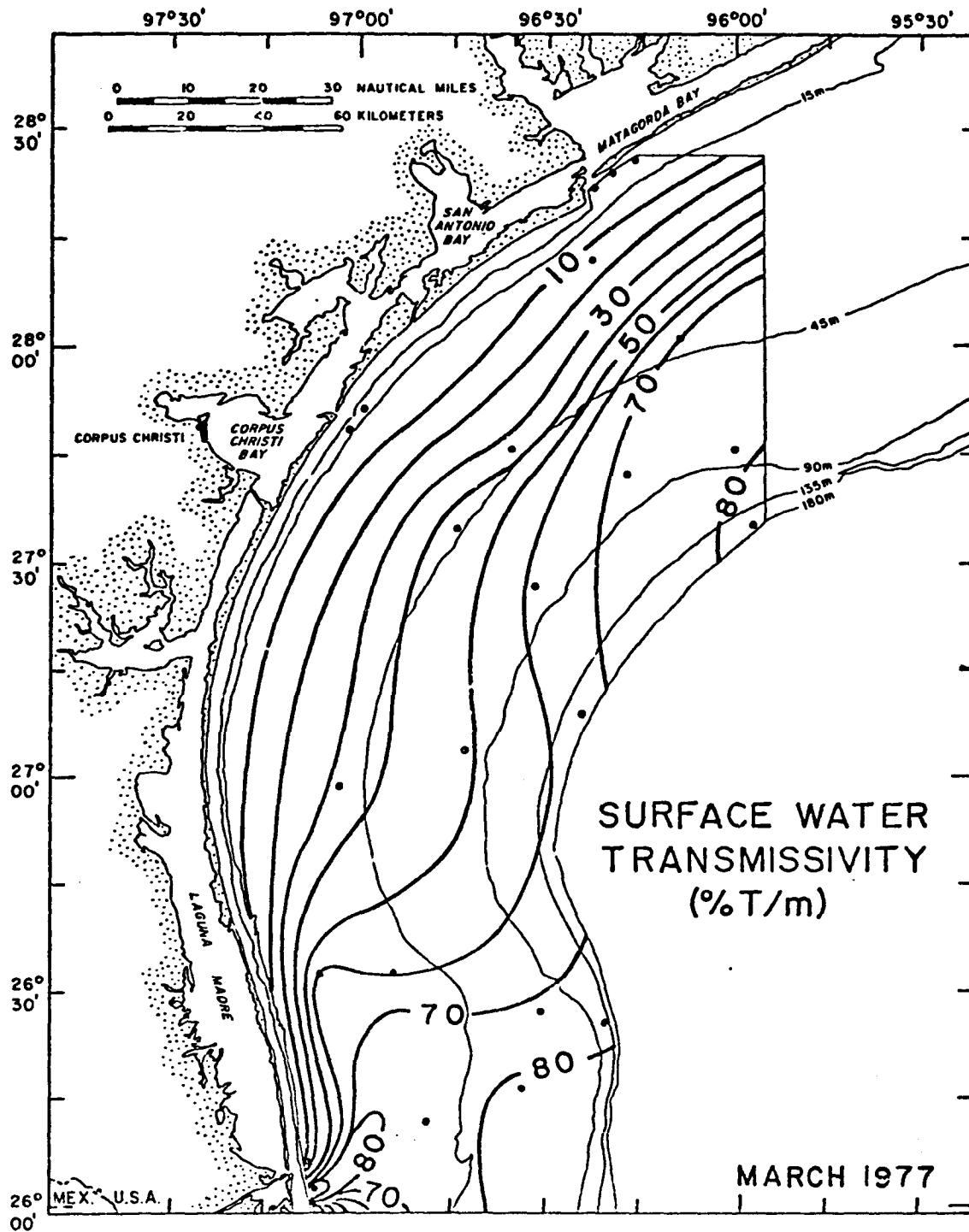


Figure 8. Surface water transmissivity, March cruise.

ambient wind and associated surface-drift pattern. The Rio Grande-Brazos Santiago inlet area was nonturbid.

May 1977 pattern (fig. 9)-- The transmissivity of surface waters during the May cruise ranged from 0 percent at some inlet stations, to a maximum of 75 percent along parts of the outer shelf (stations 5, 11). The pattern showed a regional shoreward increase in turbidity. The turbidity gradients were relatively steep and largely concordant to bathymetry along the inner shelf, but were less steep and largely discordant to water depth over the outer shelf. The relatively transparent waters (percent T >70) occurred within shoreward-directed reentrants, the most extensive one being in the southern sector; these reentrants appeared to represent shoreward incursions of deep open Gulf waters. The incursion of open Gulf waters in May would have been facilitated by the strong onshore component of the ambient wind and associated surface-drift pattern. The component of sediment transport parallel to the coast during May was northward, as indicated by the surface-drift pattern.

The time-sequence profiles of surface water transmissivity from the three cruises indicate substantial variability in regional turbidity patterns. Variations in sediment dispersal patterns are tentatively interpreted as a result of the opposing movements of two discrete water masses: 1) a relatively turbid, inner shelf water mass that exhibits both offshore movement and either northward or southward movement parallel to the coast; and 2) a relatively transparent outer shelf water mass moving onshore, which results from the shelfward incursion of deep Gulf waters. The exchange between these two opposing water masses appears to largely determine the regional turbidity patterns. Although this shelf-water exchange process is

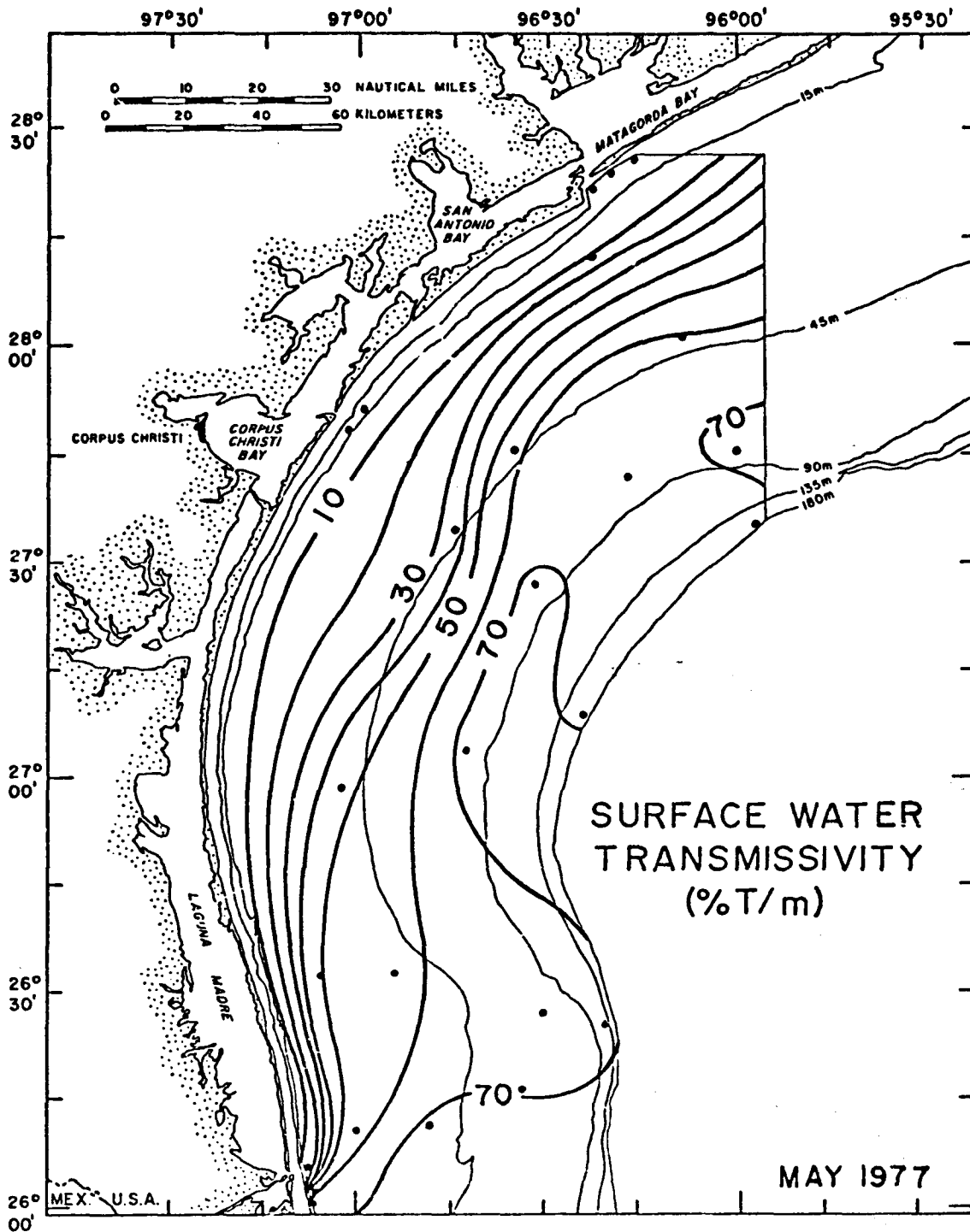


Figure 9. Surface water transmissivity, May cruise.

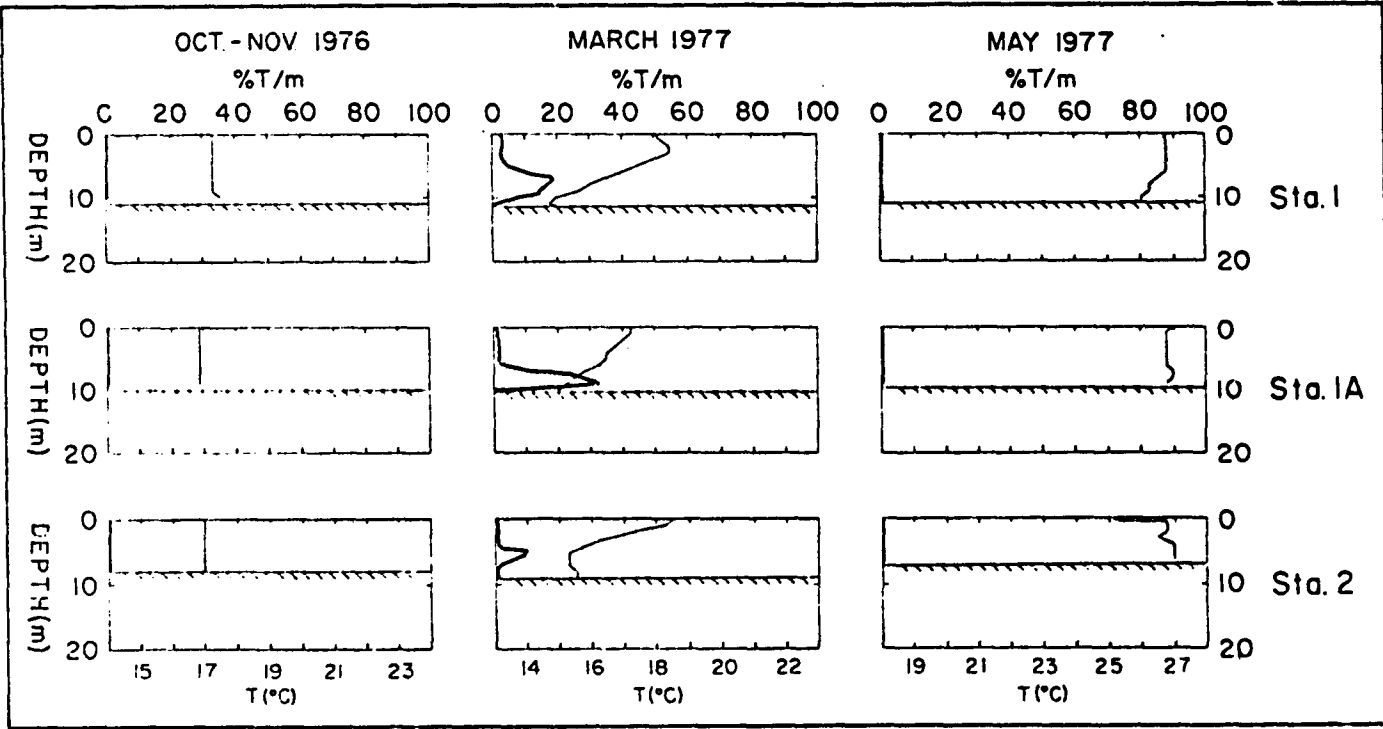
a tentative interpretation, it is supported by hydrographic data presently being compiled by the writer for the FY 78 program. Additionally, the incursion of deeper Gulf waters into the OCS environment is further supported by microzooplankton studies (Casey, 1976, 1977).

Vertical transmissivity/temperature gradients

Vertical transmissivity/temperature profiles of the water column for the 26 OCS monitoring stations are illustrated by figures 10 to 23. Transmissivity (percent T/m) is indicated by the relatively broad graph line; temperature (C°) is indicated by the thin line. The sea-floor surface is represented by the hachured surface. Precision limitations of the navigation system made it impossible to occupy the identical spot for each station on each cruise. Therefore, water depth varied among the three profiles for some stations.

Matagorda Bay Inlet; Stations 1, 1A, 2 (fig. 10)-- These three stations monitored the sediment dispersion associated with Matagorda Bay inlet. During the October-November cruise all three stations exhibited a uniform water column characterized by highly turbid, isothermal conditions, indicating a high degree of water mixing. During March, all three stations showed some degree of turbidity stratification and generally negative temperature gradients. Surface waters were relatively warmer and more turbid than deep waters. This pattern apparently reflected an ebb-tidal sediment plume that had maintained its identity as a discrete, low density surface flow, indicating an absence of significant coastal water mixing. During May, the water column at all three stations was uniformly highly turbid with only minor temperature variations, indicating a moderate degree of mixing. The varying

Figure 10. Transmissivity/temperature profiles, Matagorda Bay inlet stations.

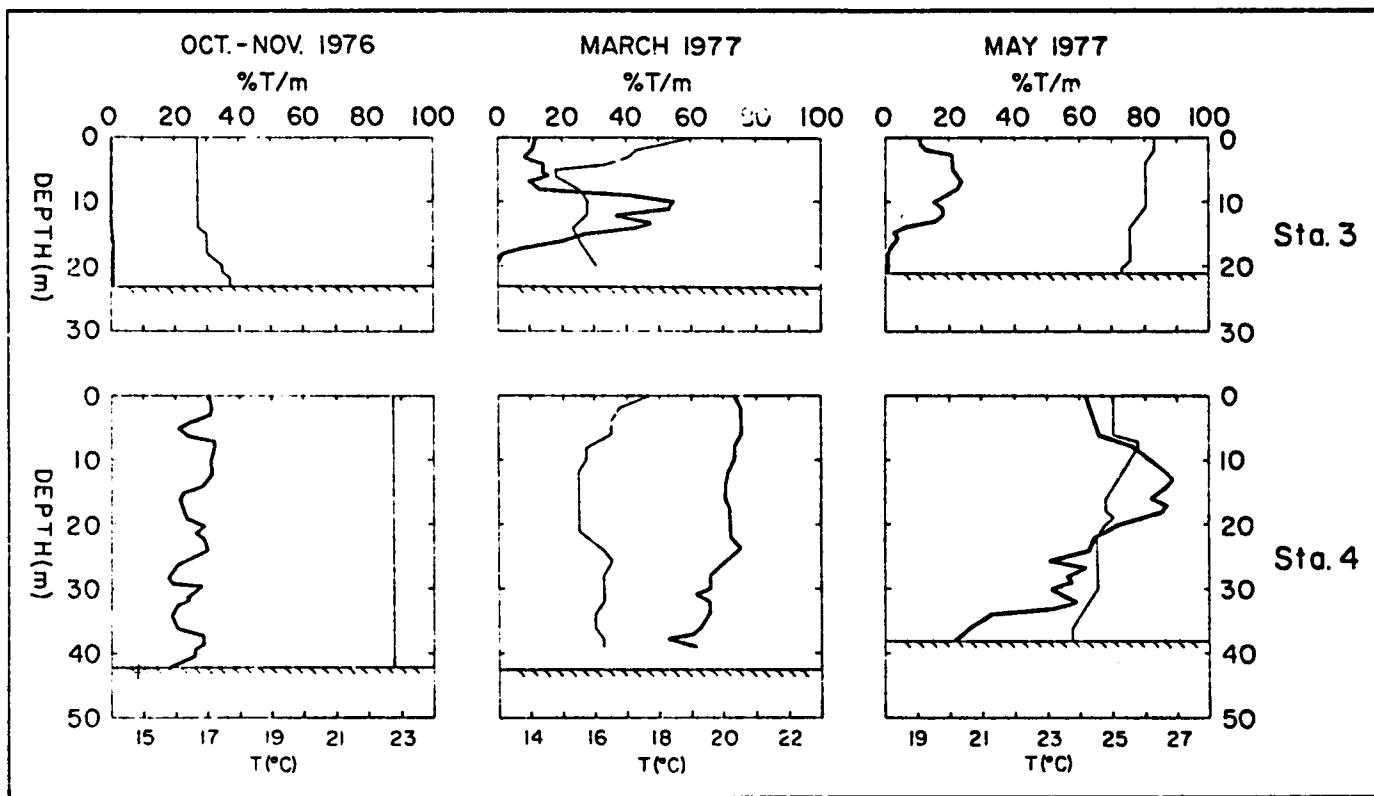


degrees of coastal water homogenization indicated by the time-sequence profiles probably reflect variations in hydraulic conditions.

Station 3 (fig. 11)-- The water column at this inner shelf station during the October-November cruise was uniformly turbid with an isothermal layer overlying waters with a positive temperature gradient. In March, a three-layer turbidity structure included a nepheloid layer 10 m thick; the March thermostructure consisted of a negative temperature gradient above a gradient reversal. Some correlation is possible between turbidity and thermostructure. In May, the water column had a two-layer turbidity structure with a nepheloid layer 8 m thick; the thermostructure consisted of a negative temperature gradient. The time-sequence profiles indicate substantial seasonal variability in turbidity/thermal structures. The water was both most turbid and most homogeneous during October-November, indicating maximum mixing effects, and was most stratified during March, indicating minimal mixing effects.

Station 4 (fig. 11)-- The October-November water column at this inner shelf station showed essentially homogeneous temperature and transmissivity values. In March, the column had a slightly increasing turbidity gradient with depth and variable temperature gradients. During May, a three-layered turbidity structure was evident, including a nepheloid layer approximately 17 m thick; the May thermostructure consisted of a generally negative temperature gradient. The time-sequence profiles indicated changing thermostructure associated with a progressive transition in water column turbidity structure from essentially homogeneous conditions in October-November to stratified conditions in May, with the progressive development of a nepheloid layer.

Figure 11. Transmissivity/temperature profiles, stations 3 and 4.

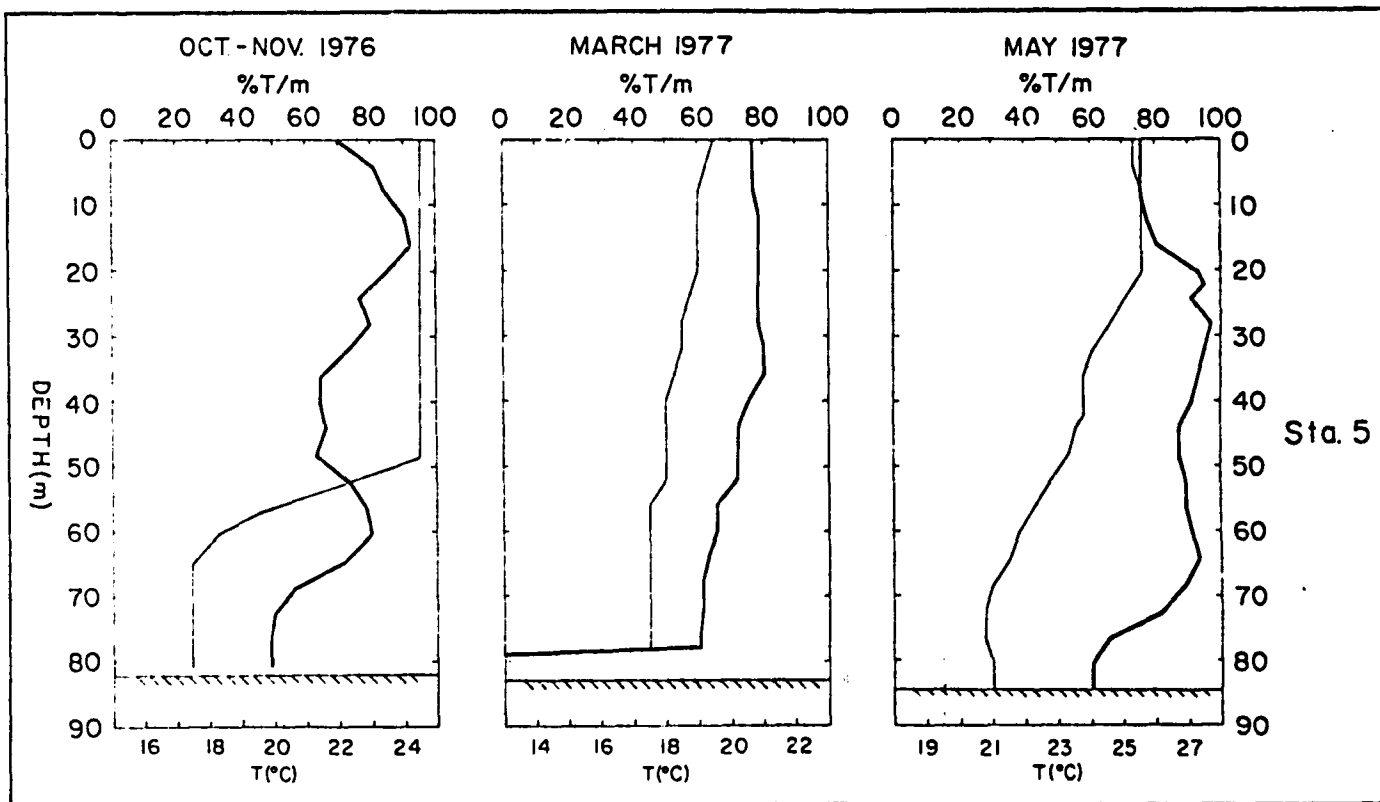


Station 5 (fig. 12)--An increasing turbidity gradient with depth was indicated during October-November, with no apparent stratification. The October-November thermostructure consisted of a prominent thermocline at the 50-65 m depth interval, with warm water above and cool water below. In March, a two-layer turbidity structure developed, producing a nepheloid layer 5 m thick associated with a negative temperature gradient. The May turbidity profile suggested a poorly developed, three-layer structure, with a possible rudimentary nepheloid layer. The May thermostructure consisted of isothermal waters overlying waters with a generally negative temperature gradient; some correlation is suggested between turbidity and thermostructure. The time-sequence profiles indicate substantial seasonal variability in the turbidity/temperature structures, with turbidity stratification best developed during March.

Station 6 (fig. 13)--The water column at this shelf-edge station during October-November was essentially nonturbid; water with a negative temperature gradient was overlain by an isothermal water layer. The March profile was incomplete because of strong currents but indicated homogeneously nonturbid waters with a negative temperature gradient. During May, the water column showed a slightly decreasing turbidity gradient and a negative temperature gradient with depth. The time-sequence profiles indicate general conditions of homogeneously nonturbid shelf-edge waters and a negative temperature gradient, with no indication of a shelf-edge nepheloid layer.

Station 7 (fig. 14)--This outer shelf station during October-November exhibited uniformly nonturbid, isothermal conditions. In March, a four-layer turbidity structure developed, which included a nepheloid layer 5 m thick associated with a slightly negative temperature gradient. In May, the

Figure 12. Transmissivity/temperature profiles, station 5.



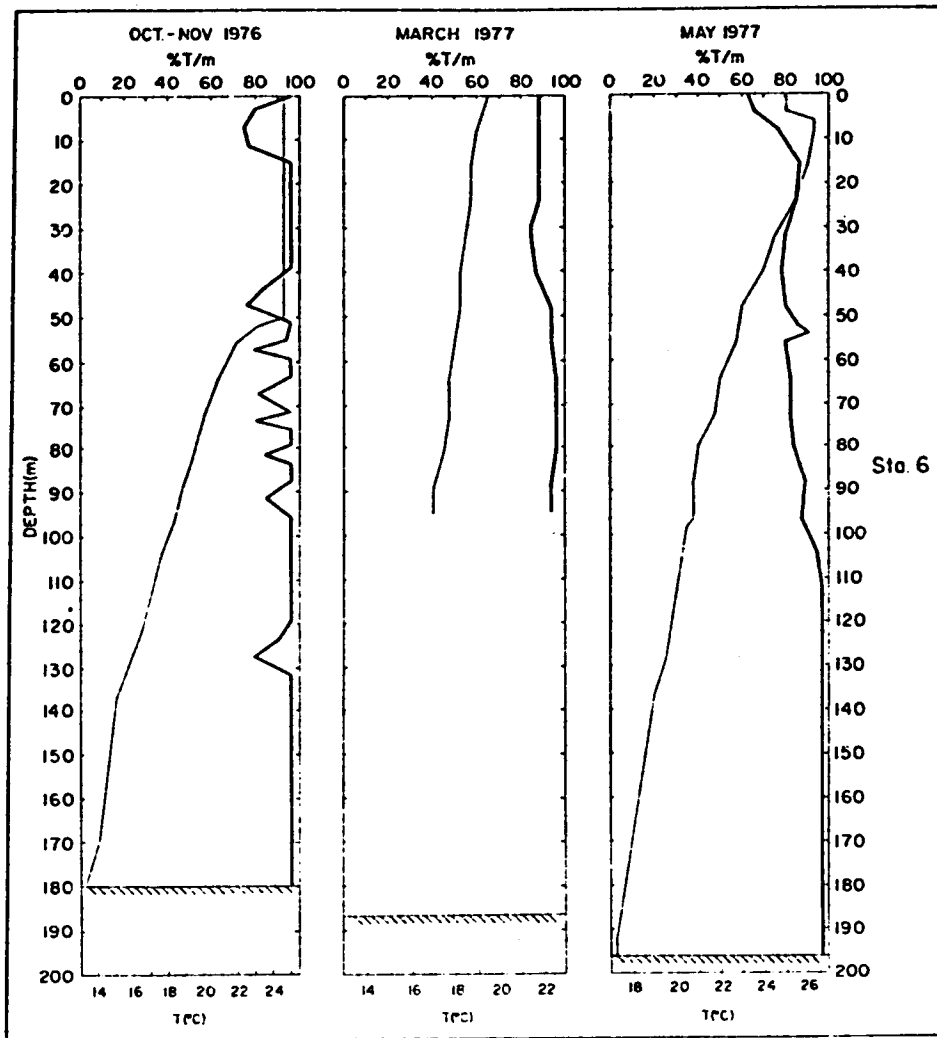
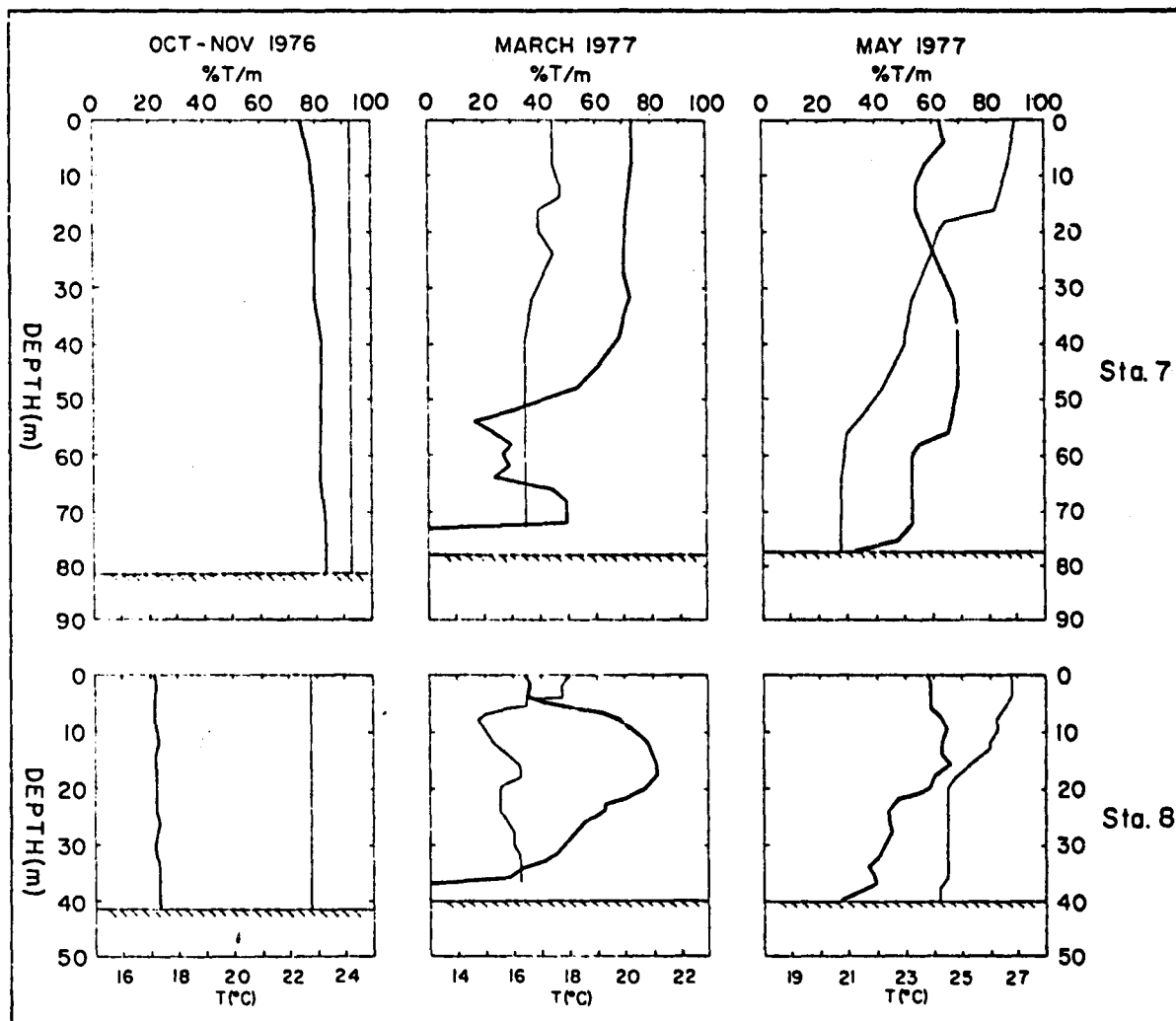


Figure 13. Transmissivity/temperature profiles, station 6.

Figure 14. Transmissivity/temperature profiles, stations 7 and 8.

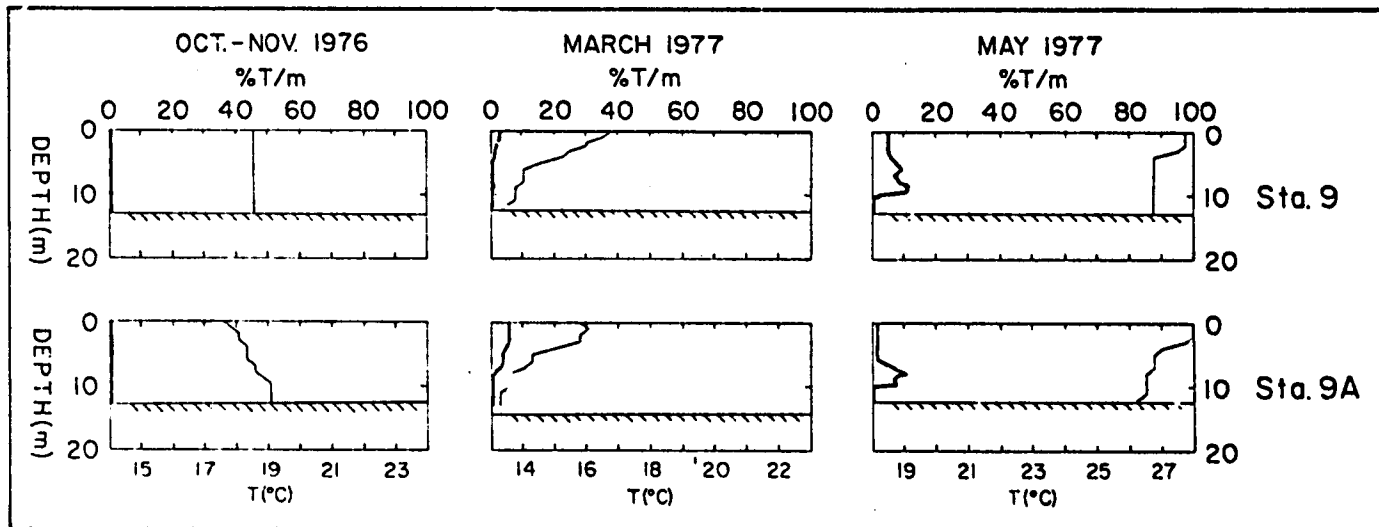


turbidity stratification diminished and more uniform conditions developed in association with a pronounced negative temperature gradient. The time-sequence profiles indicate substantial seasonal changes in turbidity/thermal structures; the turbidity structure was most homogeneous in October-November and most highly stratified in March.

Station 8 (fig. 14)-- In October-November the water column at this inner shelf station was uniformly turbid and isothermal. During March, a three-layer turbidity structure with variable temperatures developed, including a nepheloid layer about 18 m thick. In May a poorly defined nepheloid layer was present. The May thermostructure exhibited a minor thermocline in the 15-20 m depth interval; some correlation existed between turbidity and thermostructure. The time-sequence profiles indicate substantial variability in turbidity/temperature structures, with turbidity most homogeneous in October-November and most highly stratified in March.

Aransas Pass Inlet: Stations 9, 9A (fig. 15)-- These stations reflect sediment dispersion associated with Aransas Pass. During October-November, the water column at both stations had uniformly high turbidity; waters were isothermal at station 9 and had a positive temperature gradient at station 9A. In March, both stations were highly turbid with slightly increasing turbidity and negative temperature gradients; some correlation existed between turbidity and thermostructure. In May, both stations were highly turbid, with the weak development of a three-layer structure. The relatively turbid upper layer probably reflected the ebb-tidal sediment plume, whereas the bottom layer may have reflected sea-floor sediment resuspension by wave surge. In May both stations showed a near-surface thermocline. The time-sequence profiles suggest that mixing of coastal waters was maximum in October-November and minimum in May.

Figure 15. Transmissivity/temperature profiles, Aransas Pass inlet stations.

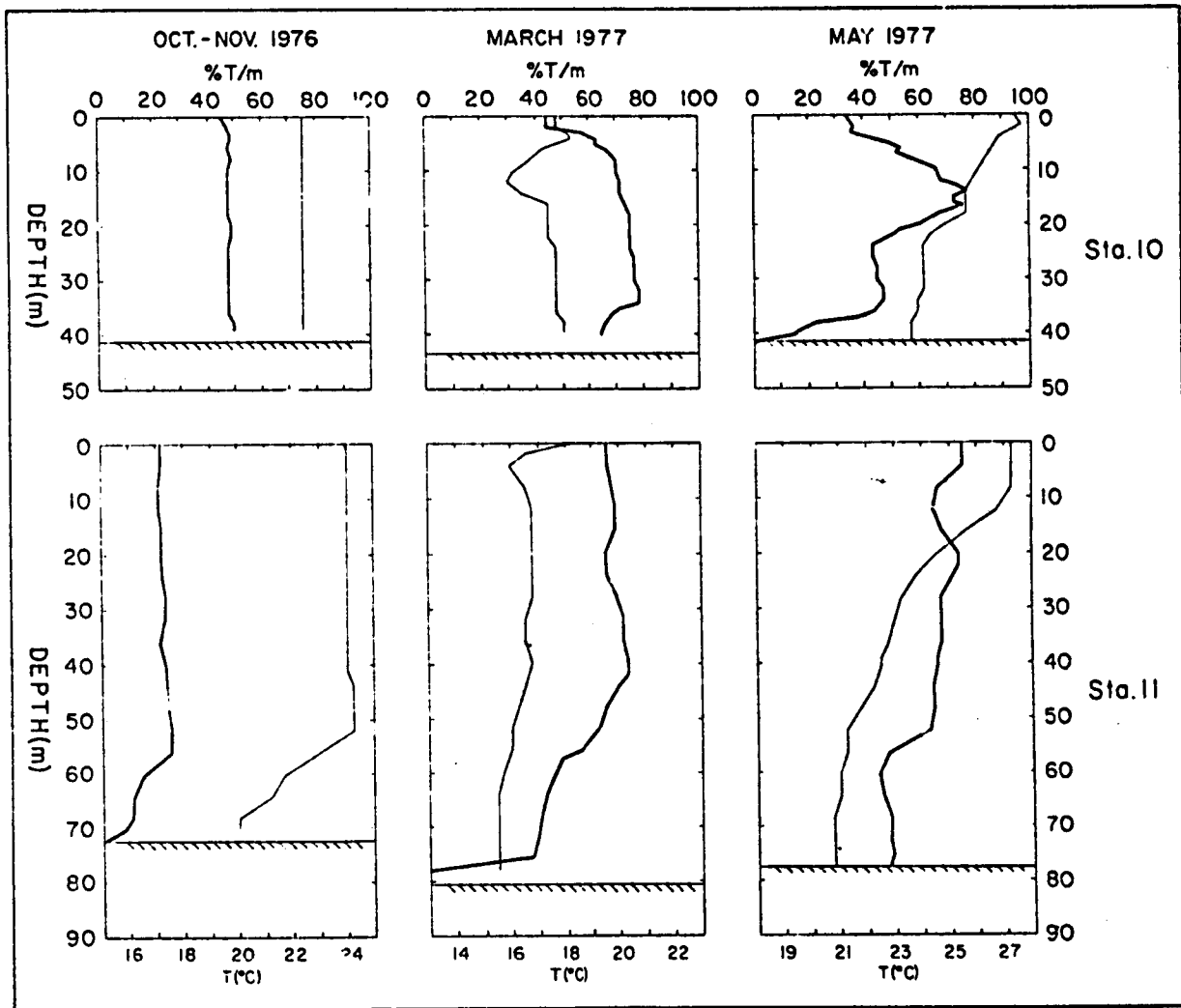


Station 10 (fig. 16)--During October-November, this inner shelf station showed moderately turbid and isothermal conditions. In March a poorly defined, three-layer turbidity structure with a 6 m nepheloid layer was developed; the temperature gradient was variable. During May, the degree of turbidity stratification had increased, resulting in a multilayered structure with a nepheloid layer approximately 23 m thick, associated with a negative temperature gradient. The sequence of profiles indicates substantial seasonal variability in turbidity/temperature structures, with turbidity most homogeneous in October-November and most highly stratified in May.

Station 11 (fig. 16)--During October-November this station had a two-layer turbidity structure including a nepheloid layer approximately 15 m thick. The nepheloid layer exhibited a negative temperature gradient and the overlying water column was essentially isothermal. During March, the nepheloid layer had increased in thickness to approximately 35 m and was associated with a negative temperature gradient. In May, a poorly defined two-layer turbidity structure was present with an apparent nepheloid layer approximately 25 m thick; the May thermostructure consisted of isothermal surface waters overlying waters with a negative temperature gradient. The time-sequence profiles indicate a variable thermostructure and a persistent, two-layer turbidity structure with a nepheloid layer of variable thickness.

Station 12 (fig. 17)--The three profiles of this shelf-edge station were incomplete because of strong currents. In every season, essentially uniform turbidity was indicated to the extent measured. The turbid water column ($T/m = 12\%$) in October-November indicates that the central salient outlined by the surface water transmissivity pattern (fig. 7) was not

Figure 16. Transmissivity/temperature profiles, stations 10 and 11.



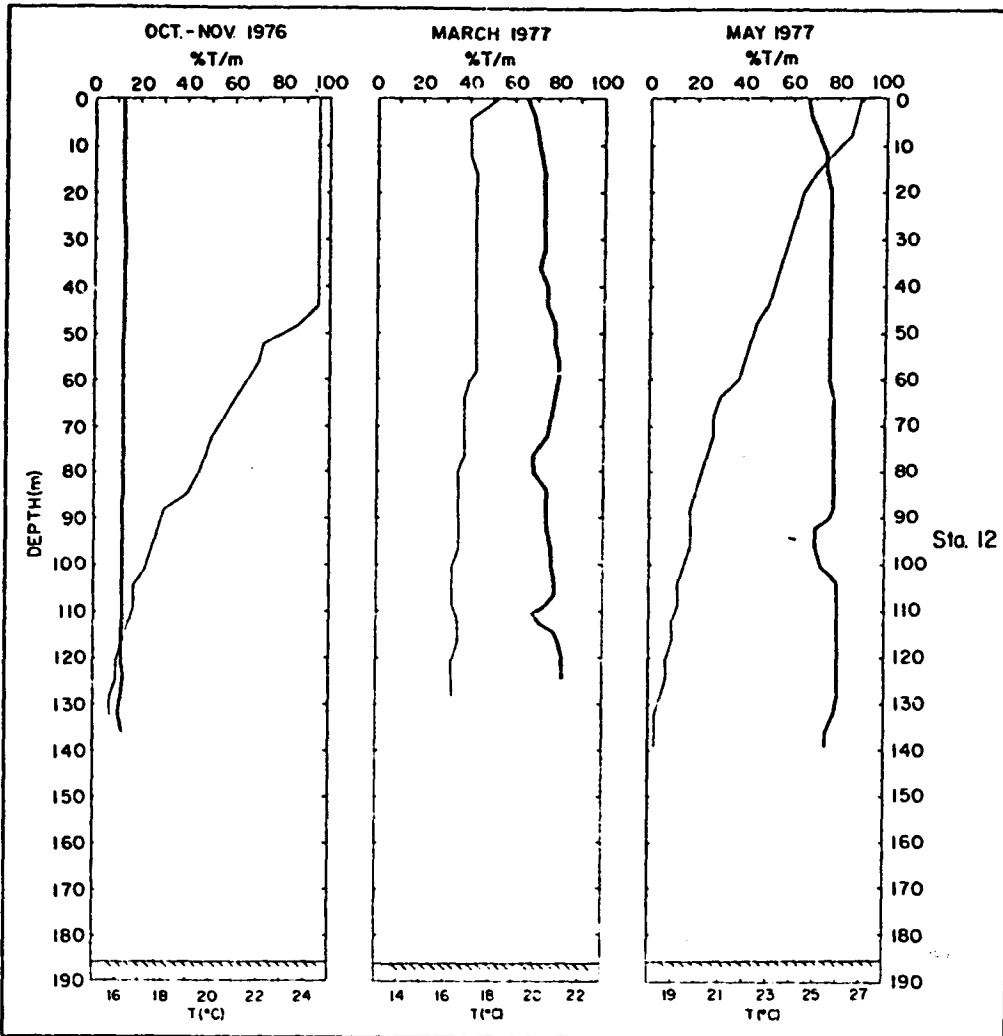


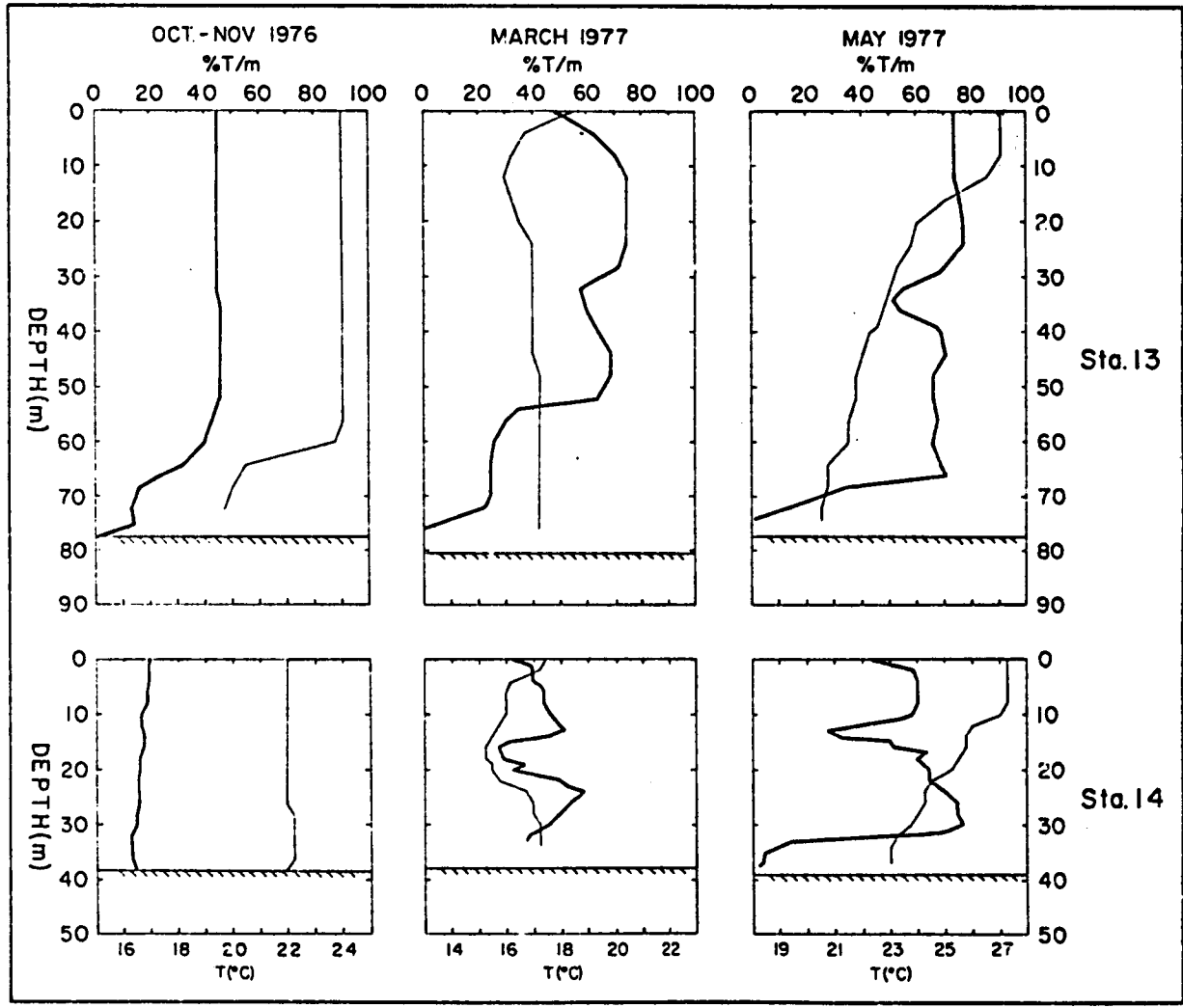
Figure 17. Transmissivity/temperature profiles, station 12.

simply a surface phenomenon. Water thermostructure was variable during the three cruises and showed no apparent correlation with turbidity.

Station 13 (fig. 18)-- During October-November, this outer shelf station had a two-layer turbidity structure that included a nepheloid layer approximately 20 m thick. A good correlation existed with thermostructure: the nepheloid layer occurred at a thermocline and the overlying water column was essentially isothermal. During March, a multilayer turbidity structure was present, including a prominent nepheloid layer about 30 m thick. The March thermostructure consisted of a gradient reversal above largely isothermal waters. In May, a multilayer turbidity structure was present, including a nepheloid layer 10 m thick. The May thermostructure consisted of a shallow thermocline (10-20 m depth) separating isothermal surface waters from waters having a negative temperature gradient. The time-sequence profiles indicate seasonally variable turbidity/thermal structures. The turbidity structure was persistently stratified; the nepheloid layer was thickest in March.

Station 14 (fig. 18)-- During October-November, this inner shelf station was essentially both isothermal and turbid, with only a slight increase in turbidity with depth. A multilayer turbidity structure with variable temperature gradients developed in March. During May, a well-defined, multilayered turbidity structure and a nepheloid layer about 7 m thick were indicated. The May thermostructure consisted of a minor thermocline (10 m depth) separating isothermal surface waters from waters having a negative temperature gradient. The sequence of profiles indicates variable turbidity/thermal structures; the turbidity structure was homogeneous in fall and stratified during the spring.

Figure 18. Transmissivity/temperature profiles, stations 13 and 14.



Station 16 (fig. 19)--The water during October-November had homogeneously high turbidity; the thermostructure consisted of isothermal waters overlying waters with a positive temperature gradient. In March, a multilayer turbidity structure with a 10 m nepheloid layer developed. The March thermostructure included a near-surface thermocline which appeared to be associated with a turbidity interface. Conditions in May were similar to those in March, except that the nepheloid layer had increased in thickness to about 18 m. The seasonal profiles indicated a progressive increase in turbidity stratification and nepheloid layer development from late fall to late spring, associated with the development of a thermocline.

Station 17 (fig. 19)---The water column turbidity and thermostructure relationships at this inner shelf station are similar to those of adjacent station 16. The time-sequence profiles indicate a transition from homogeneously turbid conditions during late fall, to stratified conditions and a nepheloid layer (15 m thick) during the early and late spring; a prominent thermocline also developed during this transition.

Station 18 (fig. 20)--During October-November this outer shelf station exhibited a well-defined, two-layer turbidity structure, with a nepheloid layer 21 m thick. Turbidity and thermostructure correlated in general: the nepheloid layer contained a prominent thermocline, while the overlying column was isothermal. In March, the two-layer turbidity structure was still present, but the nepheloid layer had decreased to 10 m in thickness. The March thermostructure showed a negative temperature gradient. In May, the degree of turbidity stratification had diminished, and a prominent mid-depth thermocline had developed. A correlation existed between turbidity and thermostructure, with the water showing a negative temperature gradient and variable turbidity below the thermocline; essentially uniform temperature

Figure 19. Transmissivity/temperature profiles, stations 16 and 17.

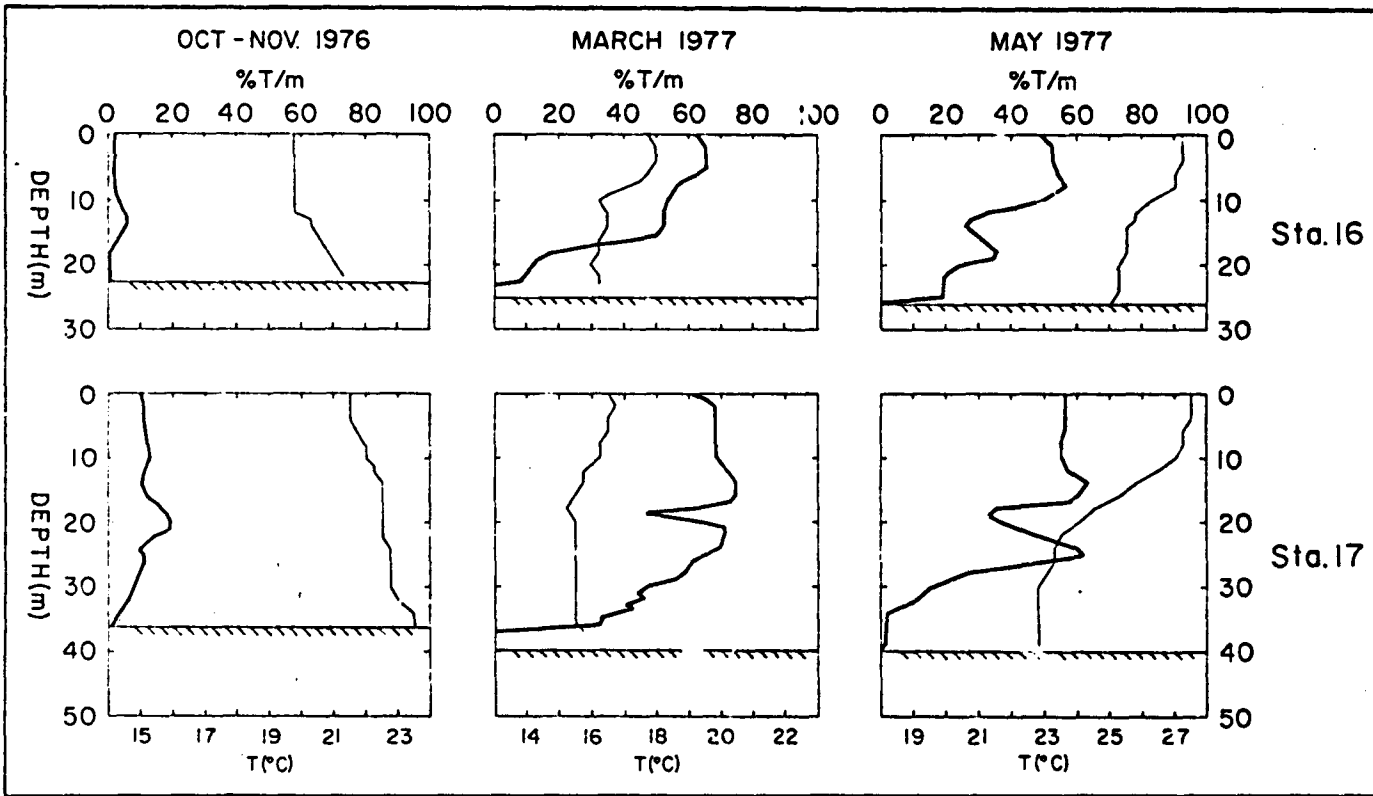
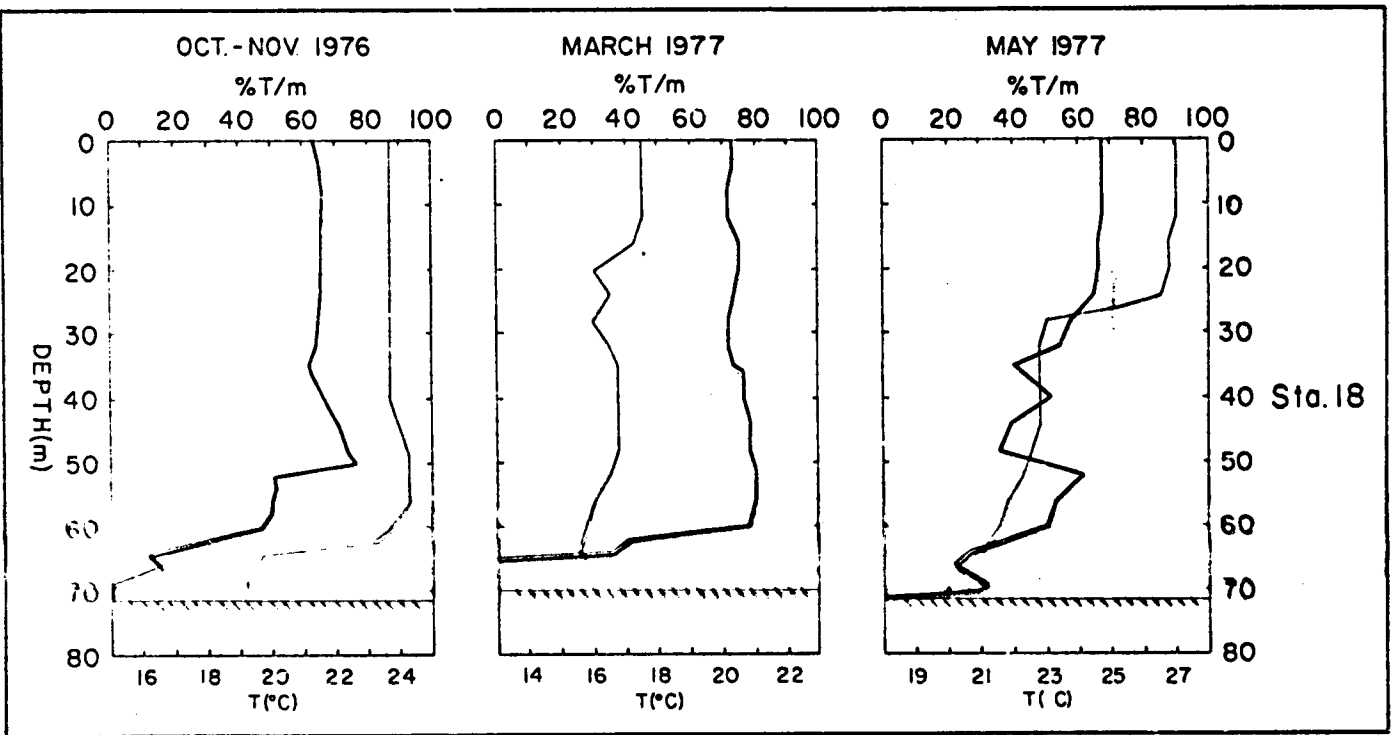


Figure 20. Transmissivity/temperature profiles, station 18.



and turbidity were indicated above the thermocline. The time-sequence profiles indicate seasonal variations in the degree of turbidity stratification and in thermostructure.

Station 19 (fig. 21)-- At this shelf-edge station, complete profiles were not obtainable during October-November and March because of strong currents that kept the transmissometer from reaching bottom. The October-November profile showed a three-layer turbidity structure with a very thick nepheloid layer (29 m); the turbidity structure showed excellent correlation with thermostructure, with the top of the nepheloid layer occurring at a major thermocline. In March, the nepheloid layer increased in thickness to 32 m, the column changed into a two-layer turbidity structure, the prominent thermocline disappeared, and a weak negative temperature gradient was indicated. In May, the degree of stratification had diminished, but a nepheloid layer (30 m thick) was still discernible. The May thermostructure consisted of a shallow thermocline (10-20 m depth) above a relatively strong negative temperature gradient. The profiles show that in spite of prominent seasonal changes in thermostructure, a thick nepheloid layer persisted. The nepheloid layer at this station was the thickest observed within the STOCS region.

Station 20 (fig. 22)-- The water column of this outer shelf station during October-November showed a turbidity gradient reversal and a positive temperature gradient. In March, a two-layer turbidity structure developed with an 18 m nepheloid layer; a negative temperature gradient characterized the March thermostructure. During May, a well-defined, two-layer turbidity structure included a nepheloid layer 16 m thick; above a prominent thermocline the water was isothermal. When compared, the profiles indicate

Figure 21. Transmissivity/temperature profiles, station 19.

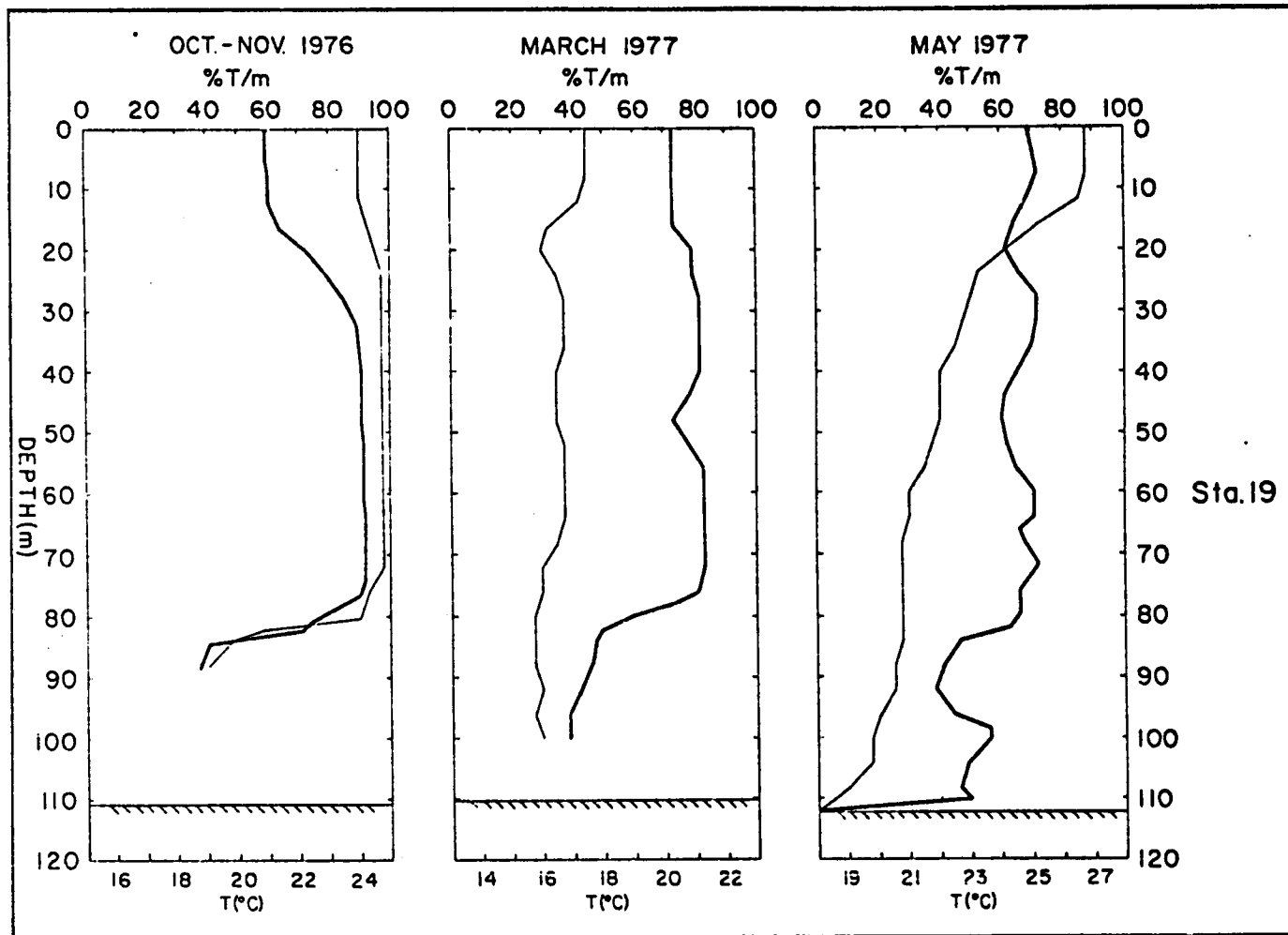
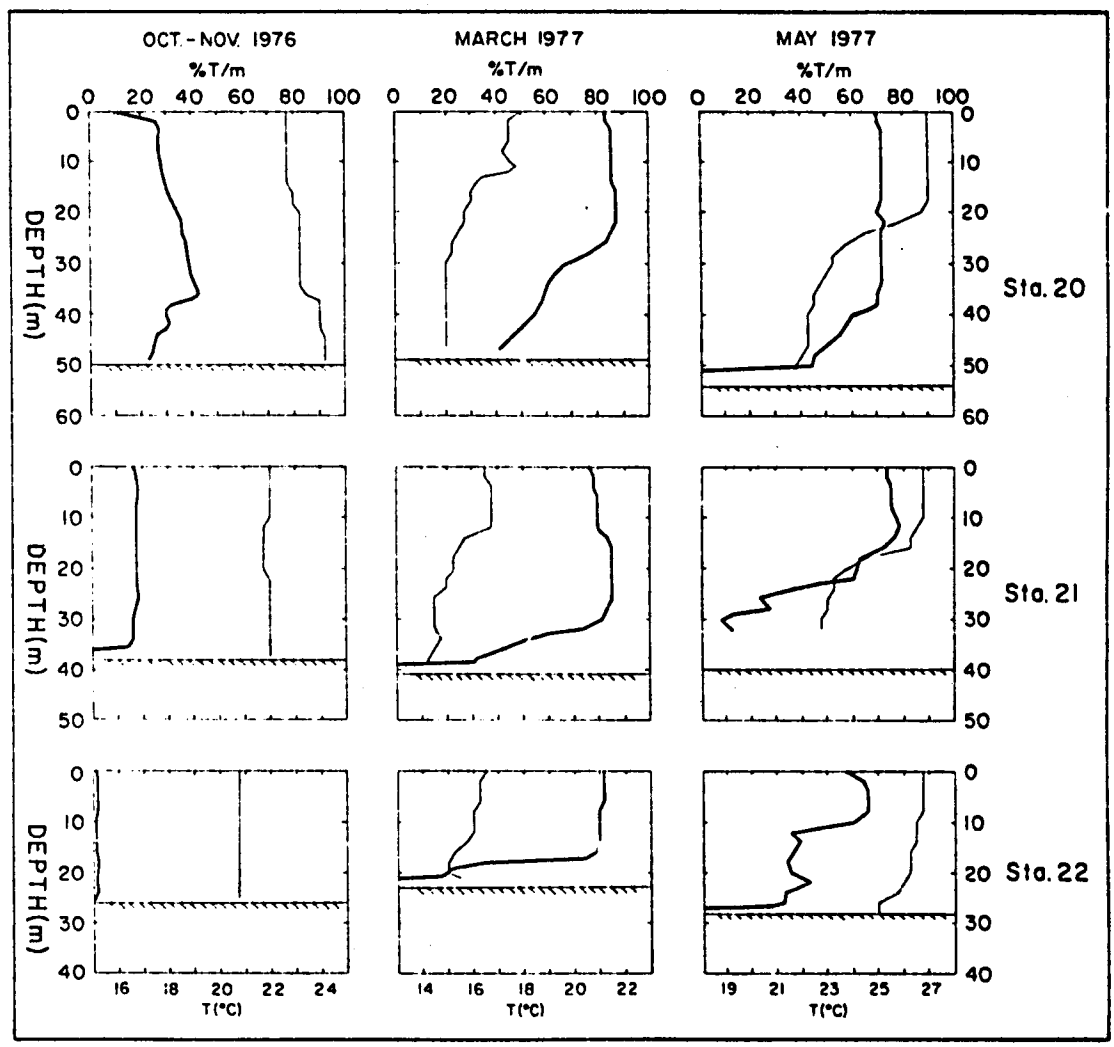


Figure 22. Transmissivity/temperature profiles, stations 20, 21, and 22.



substantial variability of turbidity/thermal structures, with turbidity stratification best developed in May in association with a major thermocline.

Station 21 (fig. 22)--This inner shelf station had a two-layer turbidity structure during all three cruises but showed a progressive increase in nepheloid layer development from fall to late spring. The nepheloid layer was thinnest during October-November (3 m) when the water was isothermal, and thickest during May (25 m) in the presence of a prominent thermocline; March was characterized by an intermediate nepheloid layer thickness (9 m) and a negative temperature gradient. Nepheloid layer development appeared to increase with the progressive development of a major thermocline.

Station 22 (fig. 22)--The water column at this inner shelf station was homogeneously turbid and isothermal during October-November. In March, a negative temperature gradient developed along with a two-layer turbidity structure which included a nepheloid layer 5 m thick. In May, the negative temperature gradient and two-layer turbidity structure persisted, but the thickness of the nepheloid layer increased (18 m). The time-sequence profiles indicate an intermittent nepheloid layer, which developed when the water column showed a negative temperature gradient during the spring.

Rio Grande-Brazos Santiago Inlet: Stations 23, 23A, 24 (fig. 23)--These stations reflect sediment dispersion associated with a major inlet. During the October-November cruise, the water column at all three stations was uniformly turbid and essentially isothermal, indicating substantial mixing of coastal waters. In March, all three stations showed a three-layer turbidity structure and a negative temperature gradient with a minor mid-depth thermocline. The March profiles indicated insignificant coastal water

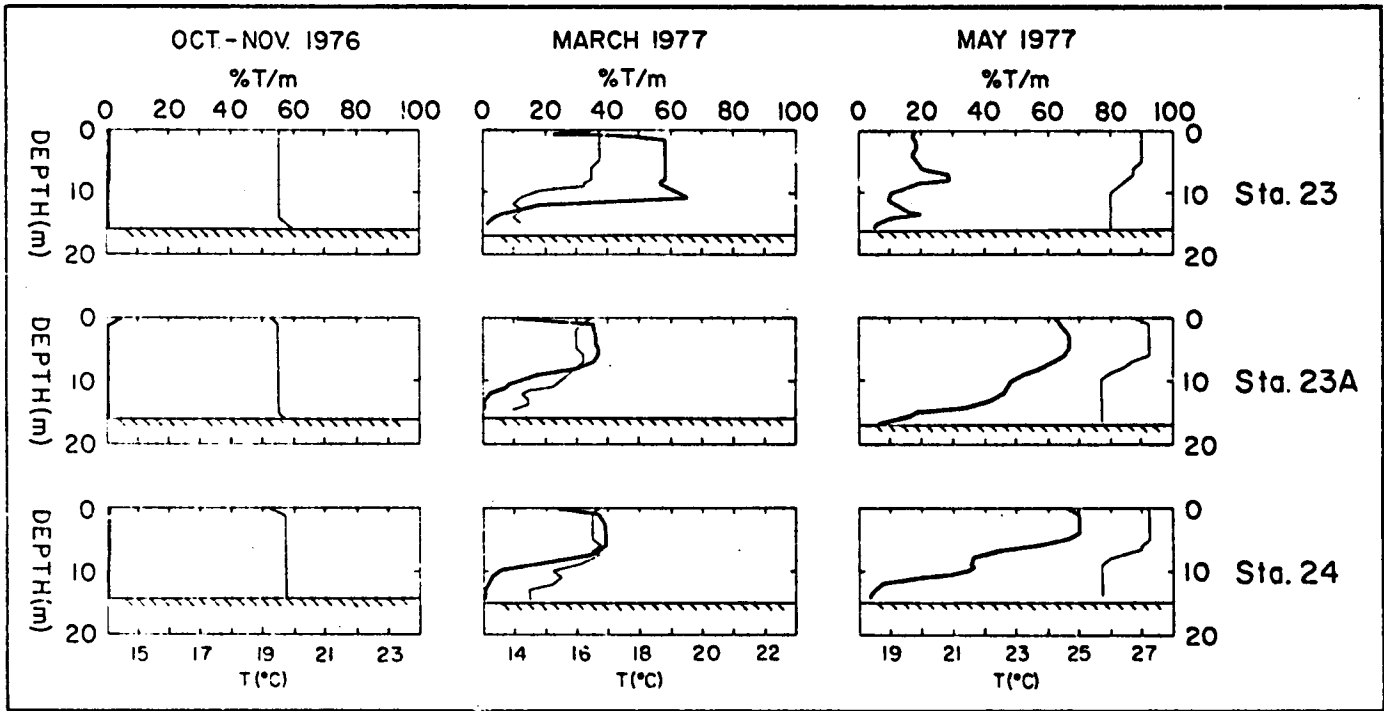


Figure 23. Transmissivity/temperature profiles, Rio Grande-Brazos Santiago inlet stations.

mixing. The relatively turbid bottom water probably reflected the wave-surge resuspension of benthic sediments; whereas, the thin surface layer of turbidity probably reflected an ebb-tidal sediment plume that maintained its identity as a surface flow. Surface sediment dispersion apparently was uniform among the three stations. In May, the water column at all three stations had a mid-depth thermocline and an increasing turbidity gradient with depth. The turbidity gradient was least at station 23, where surface waters were most turbid. The May inlet pattern reflected the northward movement of an ebb-tidal plume. The time-sequence profiles indicate that both overall inlet turbidity and coastal water mixing were greatest during the October-November cruise.

Summary

The vertical turbidity/temperature gradients of the water column at the 26 OCS monitoring stations exhibit substantial spatial and seasonal variability. The gradients at inlet stations largely reflect the degree of mixing of inlet tidal waters with nearshore waters, as determined by ambient wave and long-shore current conditions. Inlet station conditions ranged from well-mixed, homogeneous water columns to relatively unmixed, stratified columns. The only apparent seasonal trend among the inlet stations is that the degree of water-column homogenization tended to be greatest during the October-November cruise.

The turbidity/temperature gradients at the inner and outer shelf stations showed substantial temporal variability. In general, transitions from relatively homogeneous turbidity structures during the fall to stratified structures during the spring were most common. Under stratified conditions, a variable nepheloid layer was generally present. The thickest nepheloid layer occurred at the southern shelf edge (station 19).

The relation of turbidity structure to thermostructure is complex. Variations in turbidity are closely associated with temperature variations at some stations; conversely, the two parameters are independent at other stations. On the basis of the observations, no direct cause-and-effect relationship between temperature and turbidity is apparent. The observed turbidity/temperature associations may simply reflect the ability to distinguish discrete water masses on the basis of a distinct combination of turbidity and temperature characteristics.

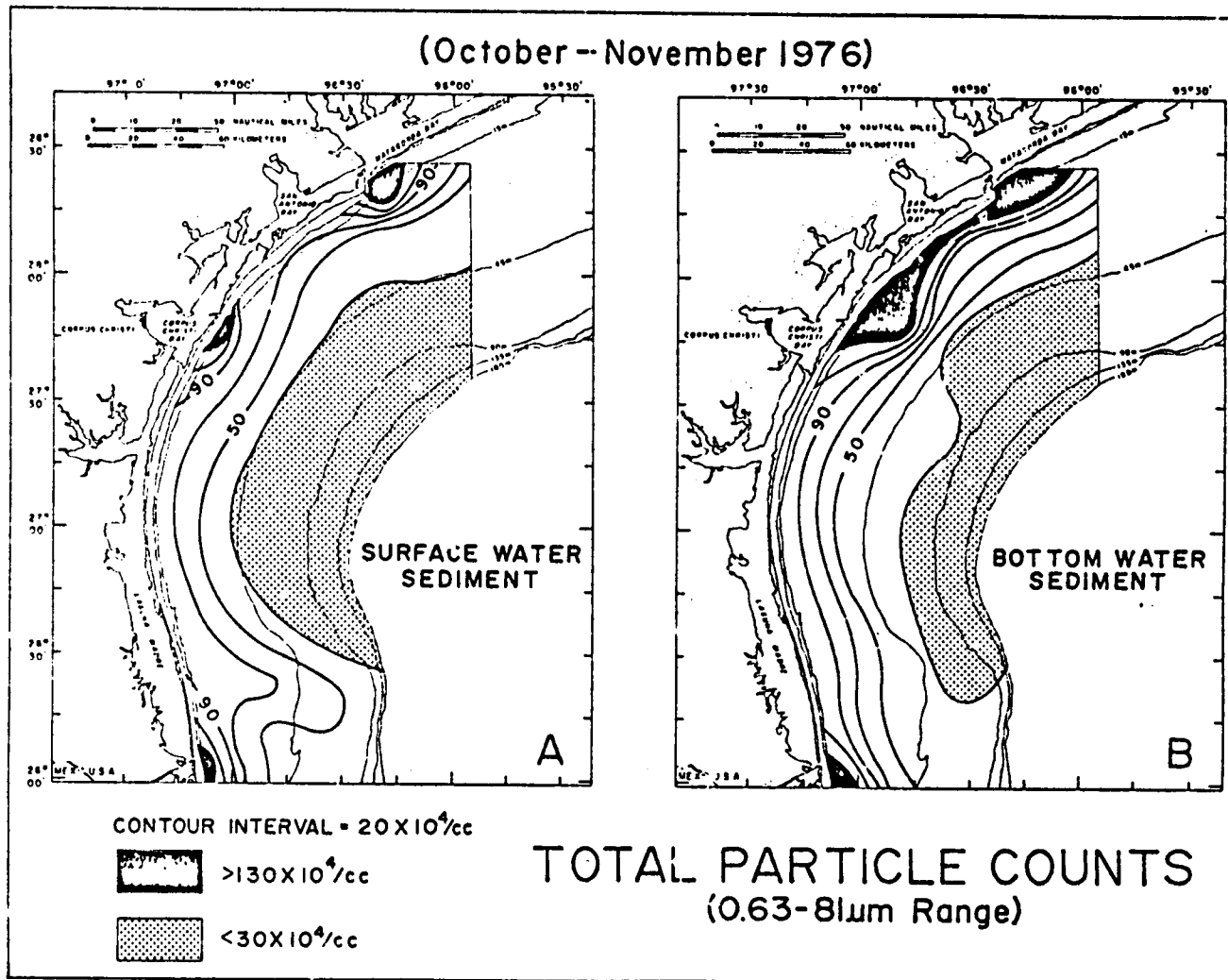
Particle Concentrations

Measurements of suspended sediment particle concentrations were made on the quasi-synoptic water samples to show regional variations for both surface and bottom waters for each of the three cruises. Particle concentrations within the 0.63 to 81 μm size range, in terms of total particle counts/cc of water sample, were analyzed by COULTER COUNTER. These data formed the basis for determining relative turbidity patterns.

October-November 1976

Surface water (fig. 24A)--Particle concentrations in surface waters ranged from a minimum of 12×10^4 at station 7 in the northern outer shelf sector, to a maximum of 433×10^4 at Maragorda Bay inlet (station 1A). The highest concentrations of suspended material ($>130 \times 10^4$) were at the three major coastal inlets: Matagorda Bay inlet, Aransas Pass, and the Rio Grande-Brazos Santiago inlet. Relative particle concentrations at the Matagorda Bay inlet stations (241×10^4 at station 1, 433×10^4 at station 1A, and 166×10^4 at station 2) suggested a predominantly southward-trending ebb-sediment plume from the Matagorda ship channel, a more prolific sediment source than the natural Pass Cavallo. Relative concentrations at Aransas Pass

Figure 24. Distribution of suspended sediments based on numbers of particles, October-November 1976 cruise.



(93×10^4 at station 9 and 154×10^4 at station 9A) also suggested predominantly southward plume dispersion. Relative concentrations at the Rio Grande-Brazos Santiago inlet (158×10^4 at station 23, 167×10^4 at station 23A, and 135×10^4 at station 24) suggested a predominantly radial plume pattern from the Brazos Santiago channel, with a small southward component parallel to the coast. This channel appeared somewhat more prolific than the Rio Grande as a sediment source.

The regional pattern of particle concentrations showed a general shoreward increase in turbidity throughout the OCS, with the highest concentrations and gradients occurring at the three coastal inlets which served as prominent sediment sources. Matagorda inlet appeared to be the most prolific source. The concentration isopleths along the inner shelf were largely subparallel to the isobaths, except for a seaward-trending salient of relatively turbid water centered near latitude $26^{\circ}20'N.$, suggesting a southward transport component. A broad reentrant of relatively nonturbid water ($<30 \times 10^4$) occupied the northern two-thirds of the area. The regional concentration pattern correlated reasonably well with the surface transmissivity pattern (fig. 7), with lowest concentrations generally in areas of highest transmissivity.

Bottom water (fig. 24B)--Particle concentrations in bottom waters ranged from a minimum of 9×10^4 at station 6 near the northern shelf edge to a maximum of 621×10^4 at Matagorda Bay inlet (station 1A). Highest concentrations ($>130 \times 10^4$) occurred at the three inlets and along the coastal sector between Matagorda Bay and Corpus Christi Bay. Lowest concentrations ($<30 \times 10^4$) occurred in a broad shoreward-directed reentrant along the outer shelf.

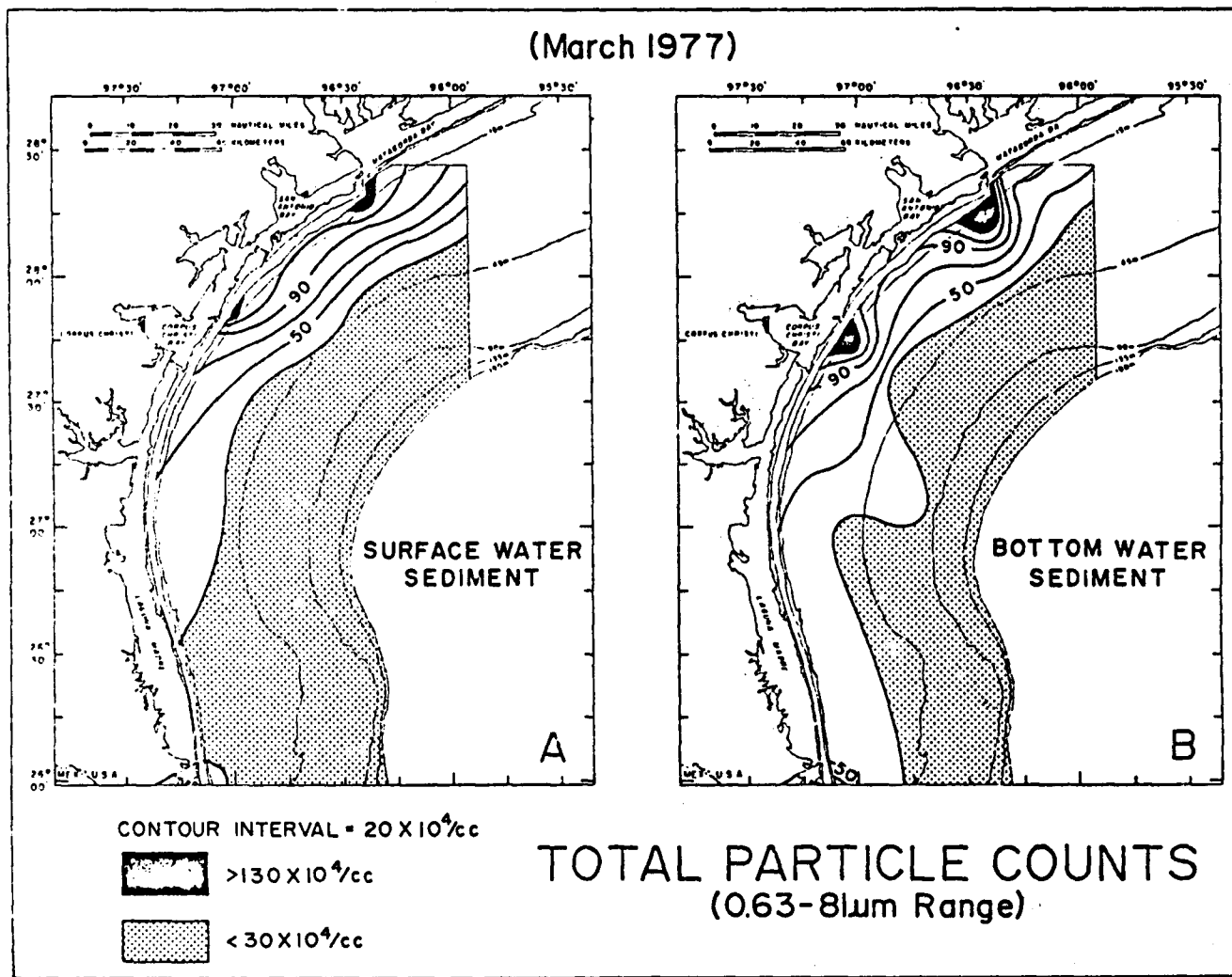
As in the surface water pattern, there was a regional trend of increasing turbidity shoreward. There were some differences between the two patterns,

however, suggesting possible differences in dispersal mechanisms. On the inner shelf, bottom water was more turbid than surface water, possibly reflecting an additional source of sediment through the resuspension of sea-floor deposits by wave surge, whereas surface water sediment may have been derived mainly from inlet tidal waters. The high concentration pattern in the Matagorda Bay inlet area further suggested that, in addition to inlet tidal waters, southward-flowing currents parallel to the coast may have introduced substantial sediment derived from coastal areas north of the OCS region. The turbid surface water salient in the southern sector was absent from the bottom water, suggesting the absence of southward transport at depth; the transport of bottom water sediment may have been essentially in a coast-normal direction.

March 1977

Surface water (fig. 25A)--Concentrations of particles in surface waters ranged from a minimum of 13×10^4 at station 22 on the southern inner shelf, to a maximum of 177×10^4 at Matagorda Bay inlet (station 2). Highest concentrations of sediment ($>130 \times 10^4$) were at Matagorda Bay inlet and Aransas Pass. Concentrations at the Matagorda Bay inlet stations (128×10^4 at station 1, 128×10^4 at station 1A, and 177×10^4 at station 2) suggested a seaward-trending ebb-sediment plume derived primarily from Pass Cavallo and secondarily from the Matagorda ship channel. Concentrations at Aransas Pass (135×10^4 at station 9 and 92×10^4 at station 9A) suggested a predominantly northward-trending plume; the pattern at the Rio Grande-Brazos Santiago inlet (18×10^4 at station 23, 44×10^4 at station 23A, and 43×10^4 at station 24) was inconclusive.

Figure 25. Distribution of suspended sediments based on numbers of particles, March cruise.



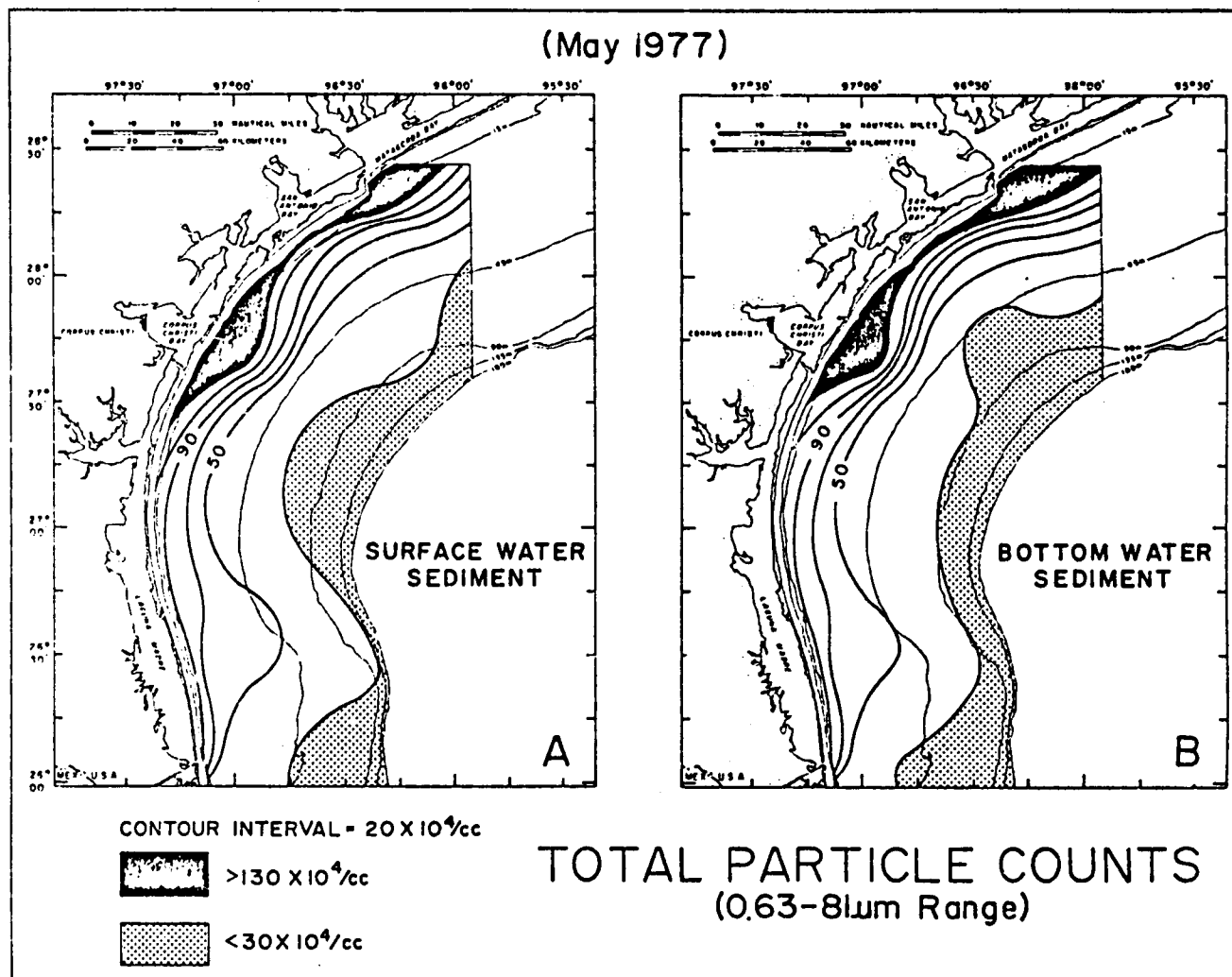
The regional pattern showed a general increase in turbidity shoreward, with the highest gradients in the vicinity of Aransas Pass and Matagorda Bay inlet, the principal sediment sources. The Rio Grande-Brazos Santiago inlet had no substantial influence on the regional pattern. Concentration isopleths were largely subparallel to isobaths, except south of Corpus Christi Bay where they suggested a southward transport component. The entire outer shelf (>45 m depth) and most of the southern inner shelf had relatively nonturbid waters (<30x10⁴). A general correlation existed between areas of low particle concentrations and areas of relatively high transmissivity.

Bottom water (fig. 25B)--Concentrations of particles in bottom waters ranged from a minimum of 5x10⁴ at station 6 along the northern shelf edge, to a maximum of 157x10⁴ near Pass Cavallo (station 3). Highest concentrations of sediment (>130x10⁴) were at Aransas Pass and Matagorda Bay inlet. An area of relatively nonturbid bottom waters (<30x10⁴) extended over the entire outer shelf (depth >45 m) and deeper portions of the inner shelf. The regional trend was a general shoreward increase in turbidity with highest gradients at Matagorda Bay inlet and Aransas Pass, which were the main sources of sediment. Regionally, the nonturbid bottom waters were somewhat more restricted than nonturbid surface waters. In addition, the bottom water gradients better illustrated the effects of Aransas Pass and Matagorda Bay inlet; the gradients south of Corpus Christi Bay also suggest a southward transport component.

May 1977

Surface water (fig. 26A)--Particle concentrations in surface water ranged from a minimum of 19x10⁴ at station 6 along the northeastern shelf

Figure 26. Distribution of suspended sediments based on numbers of particles, May cruise.



edge to a maximum of 374×10^4 at Matagorda Bay inlet (station 1A). Relative concentrations at the Matagorda Bay inlet stations (256×10^4 at station 1, 374×10^4 at station 1A, and 317×10^4 at station 2) suggested some southward movement of an ebb-sediment plume; concentrations at Aransas Pass stations (177×10^4 at station 9 and 220×10^4 at station 9A) also indicated some southward plume dispersion. The concentrations at the Rio Grande-Brazos Santiago inlet (81×10^4 at station 23, 41×10^4 at station 23A, 47×10^4 at station 24) suggested predominantly northward plume movement, with the Brazos Santiago ship channel being a more prolific sediment source than the Rio Grande.

The regional pattern of particle concentrations indicated a general shoreward increase in turbidity. Highest concentrations and gradients were near the Aransas Pass and Matagorda Bay inlets, which were the main sources for surface sediments in May; Matagorda Bay inlet and possible coastal areas farther north appeared to have been the dominant sources of sediment. The effects from the Rio Grande-Brazos Santiago inlet appeared to have been minimal. Relatively nonturbid waters ($<30 \times 10^4$) covered approximately half of the outer shelf (depth >45 m), showing a general correlation with areas of high surface water transmissivity (compare with fig. 9).

Bottom water (fig. 26B)---Particle concentrations ranged from a minimum of 8×10^4 at station 12 along the central shelf edge, to a maximum of 309×10^4 at Matagorda Bay inlet (station 2). The regional pattern was very similar to the surface water pattern, showing a general shoreward increase in turbidity with highest concentrations and gradients near Matagorda Bay inlet and Aransas Pass. The only apparent difference was minor variations in the distribution of the nonturbid ($<30 \times 10^4$) water, which was localized along the outer shelf.

Summary

The regional turbidity patterns based on particle concentrations by seasons indicate substantial variability. Both surface and bottom water were least turbid during the March cruise, which may reflect a period of maximum shelfward incursion by relatively nonturbid deep Gulf waters and of minimum seaward dispersion of turbid coastal waters. Regional turbidity patterns during the October-November and May cruises were approximately the same. During all three cruises, both surface and bottom waters exhibited regional gradients of increasing turbidity shoreward, apparently reflecting proximity to sediment source areas and a shoreward increase in wave surge that maintains sediment in suspension. Superimposed on this regional gradient were local gradients established near the coastal inlets, which served as the main sources of suspended sediment. The Matagorda Bay inlet appears to have been the most prolific source during all three cruises. In general, bottom waters were somewhat more turbid than surface waters, except during May when sediment concentrations were very similar. All seasonal patterns indicate net offshore transport. In addition, both the October-November and March patterns suggested a southward transport component.

Textural Patterns

Textural patterns in both surface and bottom suspended sediments were determined for each of the three cruises. The textural parameters investigated include: silt/clay ratios, which provide a general overview of suspended sediment composition; mean grain size (first moment), which provides an indication of dispersion gradients; and standard deviation (second moment), which provides an indication of sediment sorting or uniformity. All size

terminology is in accordance with the Udden-Wentworth grade scale and is expressed in terms of Krumbein's (1934) phi transformation.

October-November 1976

General composition

The general textural composition of suspended sediments in surface waters is shown by the silt/clay ratio isopleth map (fig. 27A). The ratios ranged from a maximum of 1.66 at station 5 to a minimum of 0.48 at station 23A. The regional ratio pattern indicated that clay-size sediment (ratios <1.0) was somewhat more widely distributed than silt-size sediment (ratios >1.0). The silt occurred in isolated areas within the northeastern, central, and southern sectors. Ratios indicated predominantly clay distribution from both Aransas Pass and the Rio Grande-Brazos Santiago inlet.

The suspended sediment in bottom waters showed a substantially different textural pattern (fig. 27B). Ratios ranged from a maximum of 2.01 at station 5 to a minimum of 0.51 at station 23. Silt and clay were nearly equally distributed, with silt predominating in the northern half of the OCS, and clay predominating in the southern half. The regional trend was a general reduction in grain size toward the south; the coarsest sediment occurred in the northeastern corner of the OCS. Except near inlets, the bottom sediments generally tended to be slightly more silty (coarser) than the surface sediments.

Mean grain size

The regional distribution of suspended sediments by mean diameter (first moment) in surface waters (fig. 28A) might provide a more sensitive indication of dispersion than the more general silt/clay ratios provide.

Figure 27. Silt/clay ratios for suspended sediments, October-November cruise.

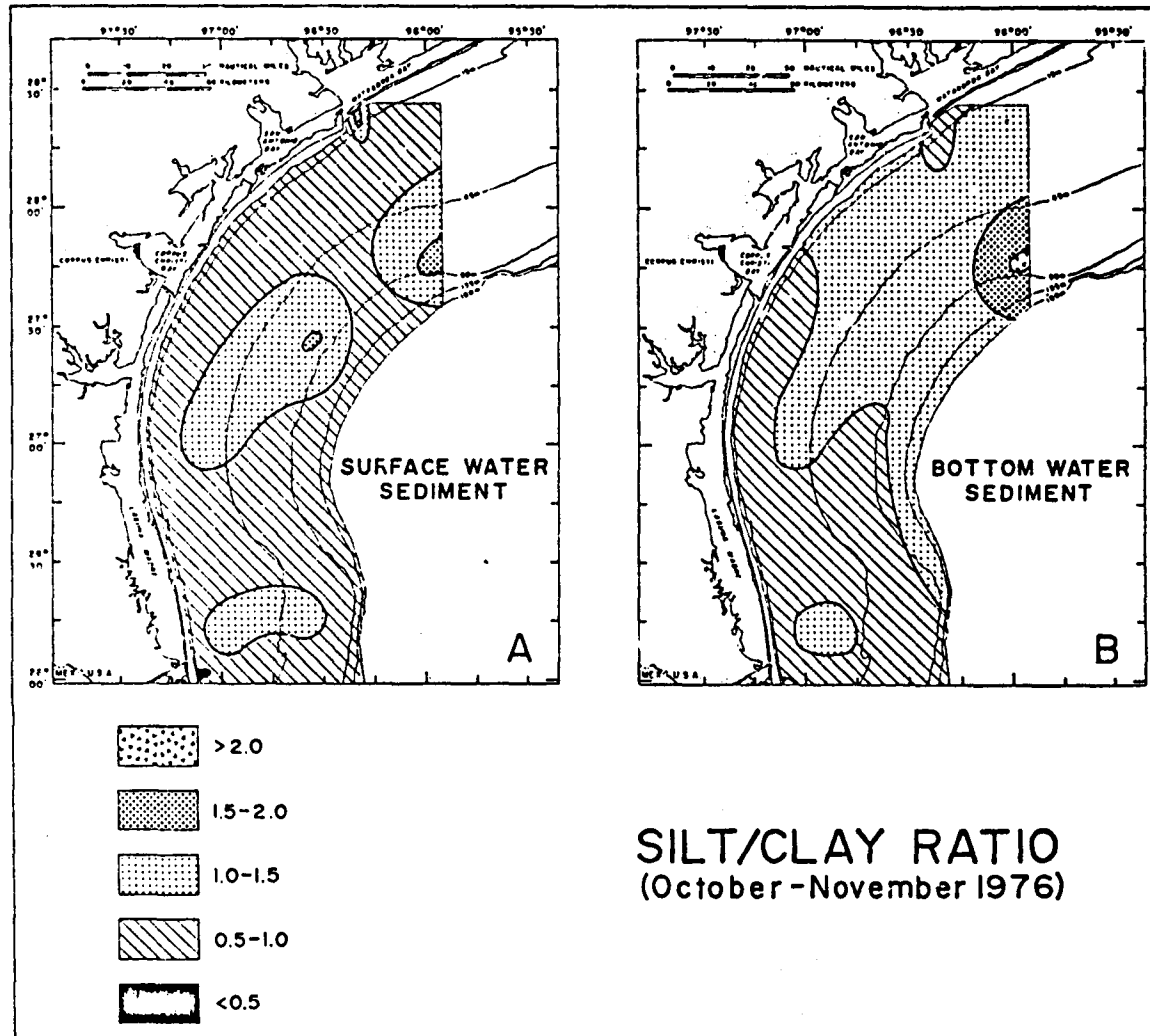
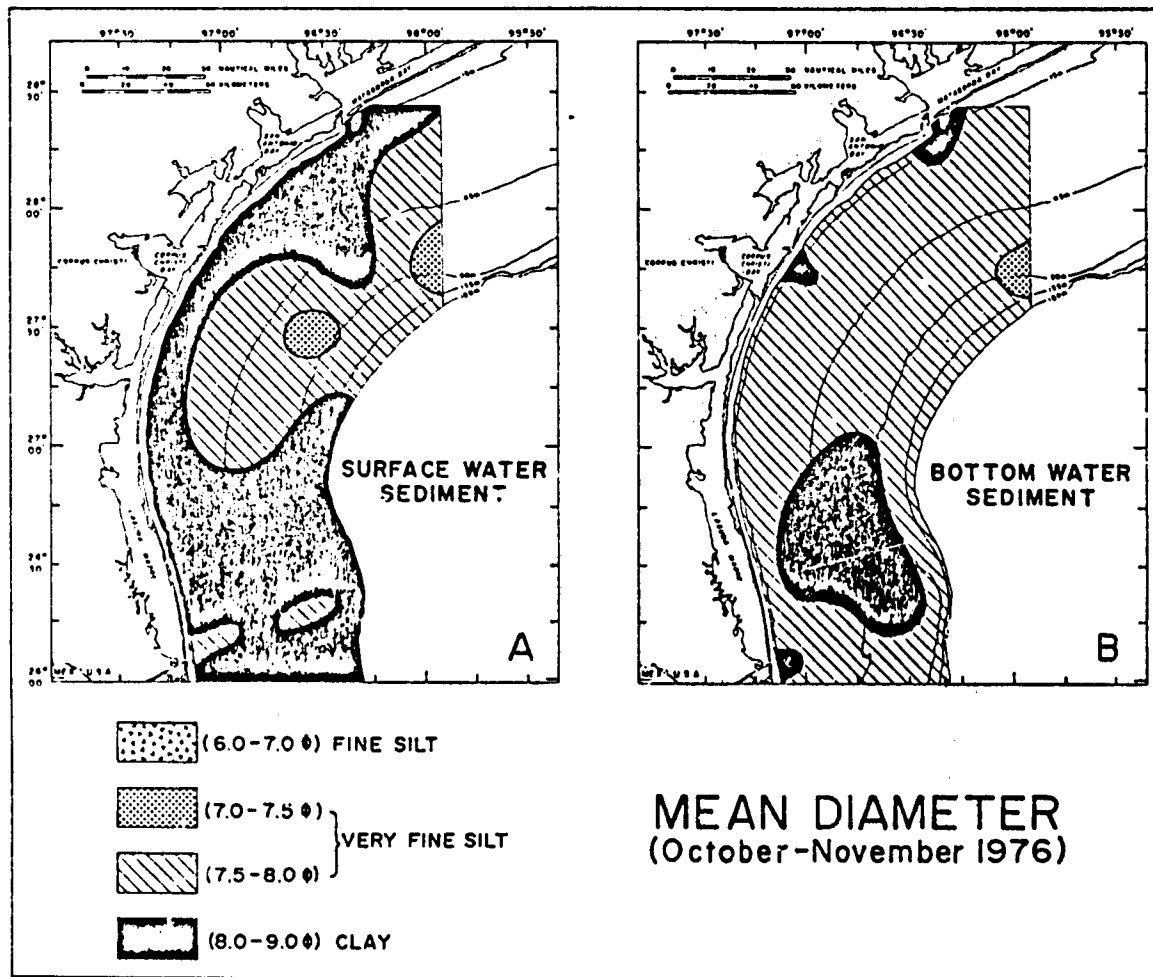


Figure 28. Mean diameters for suspended sediments, October-November cruise.



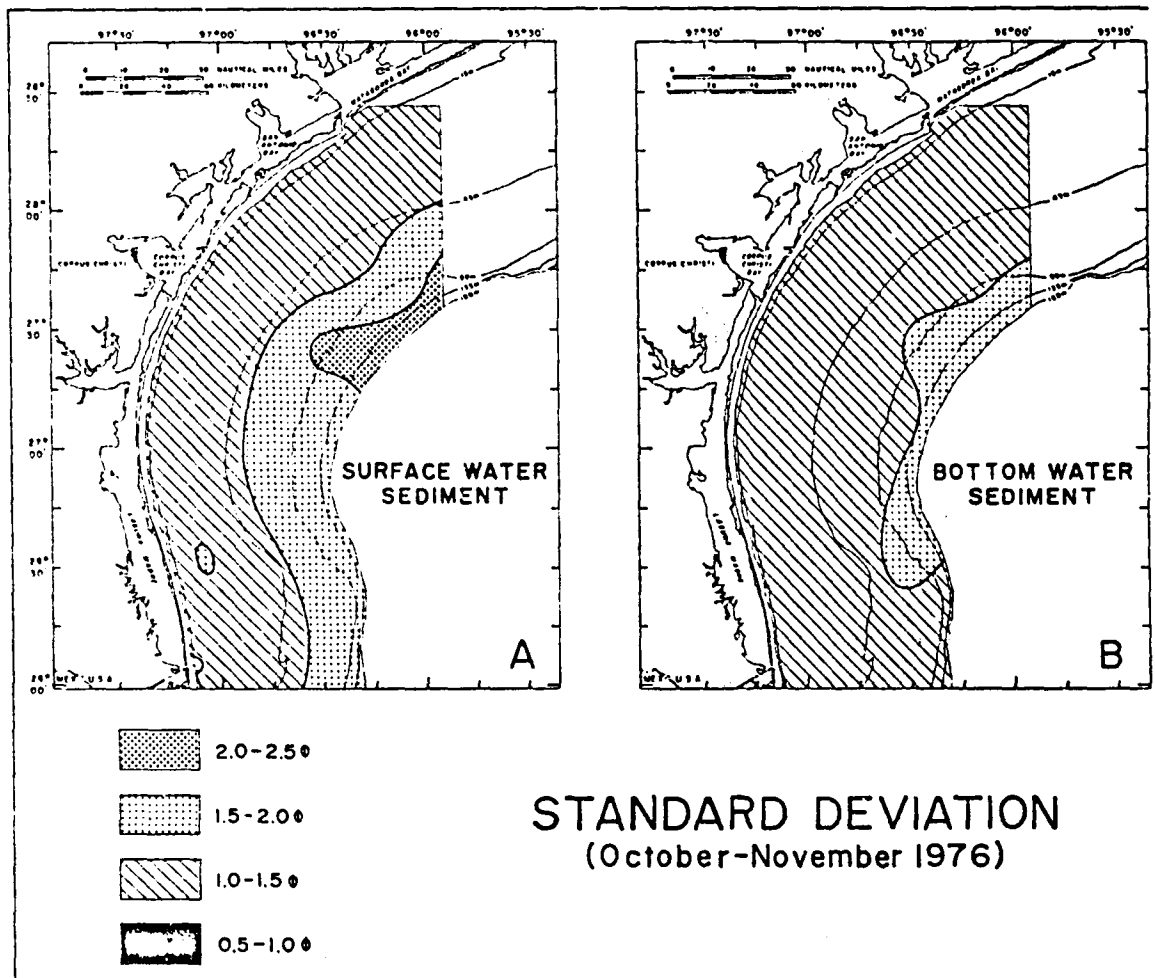
Mean diameters ranged from 8.36 ϕ (clay) at station 16 to 7.20 ϕ (very fine silt) at station 5. Clay was the most widely distributed type of surface sediment. The regional pattern showed a trend of increasing coarseness toward the northeastern sector, which might reflect the shoreward incursion of relatively coarse, open-ocean biogenic particulates.

The regional distribution pattern for mean diameters of bottom water sediments was substantially different from the surface pattern (fig. 28B). The mean diameters ranged from 8.37 ϕ (clay) at station 16 to 7.41 ϕ (very fine silt) at station 5. Very fine silt was the most widely distributed sediment type. Clay was present within the south central sector and in salients extending from the three inlets. In general, bottom water sediments were somewhat coarser than surface water sediments.

Sorting characteristics

The standard deviation isopleth map (fig. 29A) provides an indication of the textural uniformity (sorting) of surface water sediments. Using Folk's (1965) sorting classification, the standard deviation (second moment) values of surface water sediments ranged from 1.09 ϕ (poorly sorted) at station 24 to 2.20 ϕ (very poorly sorted) at station 6. Regionally the sediments were poorly sorted and showed a general seaward reduction in sorting (increasing standard deviations). The most poorly sorted sediments were along the outer shelf of the northeastern sector within a relatively coarse-grained area, suggesting a relationship between sorting and grain size. The mixing of different sizes of biogenic and inorganic sediment subpopulations could produce the observed textural characteristics.

Figure 29. Standard deviations for suspended sediments, October-November cruise.



The standard deviation values of bottom water sediments ranged from 1.06 ϕ at station 23 to 1.75 ϕ at station 6 (fig. 29B). All bottom water sediments were poorly sorted and showed a general seaward reduction in sorting toward the central outer shelf. In comparison with surface water sediments, the bottom water sediments tended to be better sorted and were more regionally uniform.

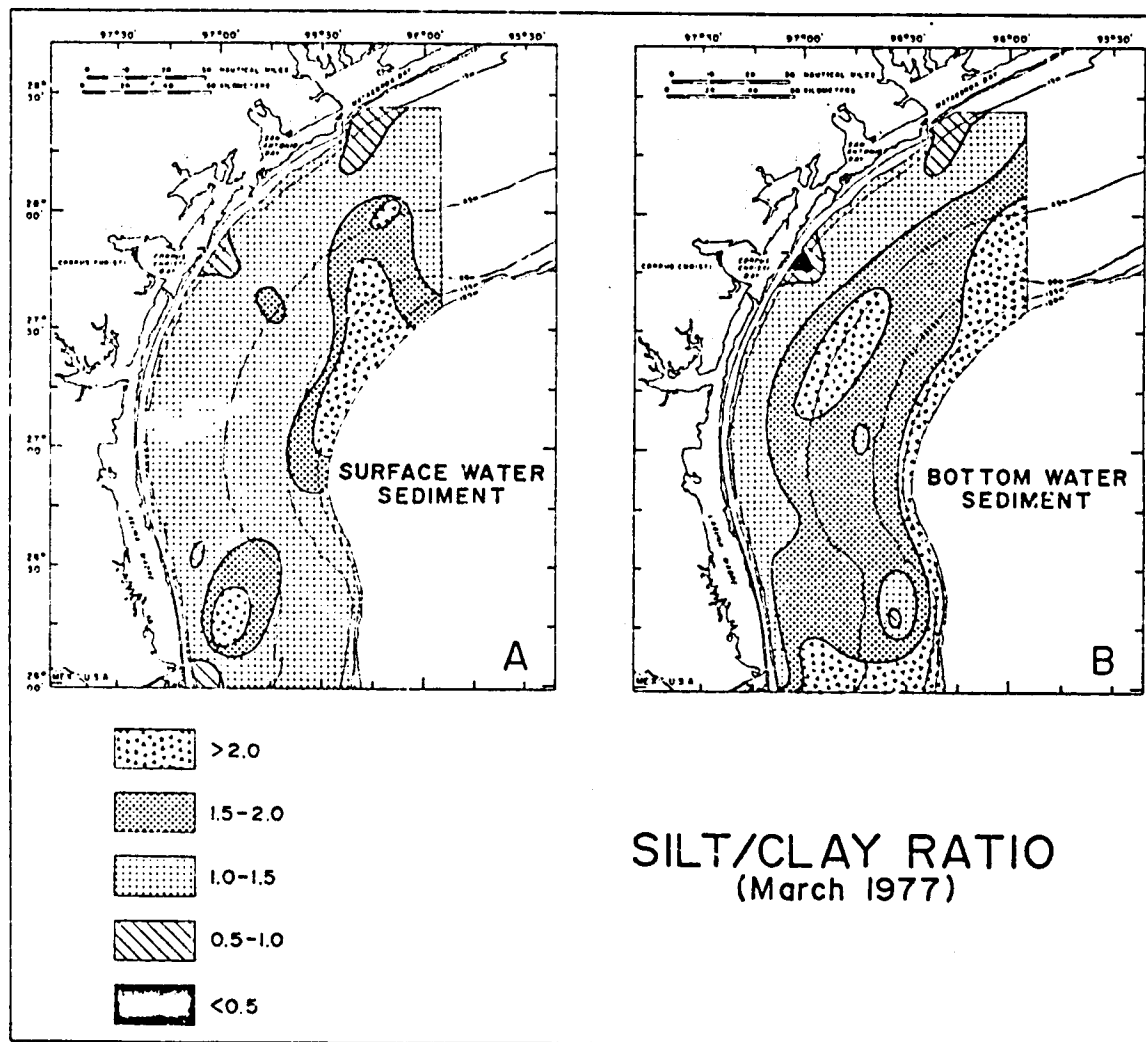
March 1977

General composition

The general composition of surface water sediments is shown by the silt/clay ratio isopleth map (fig. 30A). Ratio values ranged from a maximum of 4.74 at station 22 to a minimum of 0.50 at station 3. The regional pattern indicated that silt was highly predominant; clay was localized mainly in salients associated with the three coastal inlets. The regional trend was a general increase in silt content (coarseness) toward the northern outer shelf.

The sediments in bottom waters showed a different pattern of silt/clay ratios (fig. 30B). Values ranged from a maximum of 5.50 at station 10 to a minimum of 0.46 at station 9A. Silt was regionally predominant; clay was mainly localized in salients associated with Aransas Pass and Matagorda Bay inlet. Regionally, silt content (coarseness) increased both seaward and southward. Compared to surface water sediments, the bottom water sediments were generally somewhat coarser and showed a better defined regional size zonation. The seaward increase in coarseness may have reflected a progressive seaward increase in the amount of silt-size biogenic admixtures, both phytoplankton and zooplankton.

Figure 30. Silt/clay ratios for suspended sediments, March cruise.



Mean grain size

Variations in the mean grain size of surface water sediments are illustrated by figure 31A. Mean diameters ranged from 8.36 ϕ (clay) at station 3 to 6.40 ϕ (fine silt) at station 22. The predominant sediment type was very fine silt. The regional trend was a general increase in coarseness both seaward and southward, but the coarsest sediments were near the northern outer shelf, correlating with the area of highest silt/clay ratios. The finest grained sediments were associated with the three coastal inlets.

The mean grain size of bottom water sediments (fig. 31B) ranged from 8.37 ϕ (clay) at station 9 to 6.18 ϕ (fine silt) at station 10. As in the surface water sediment pattern, the dominant sediment type was very fine silt, and the regional trend was a general seaward increase in coarseness. The coarsest area occurred along the northeastern outer shelf; the finest sediments were associated with Aransas Pass and Matagorda Bay inlet. The bottom and surface water sediment patterns do show local differences, but they were regionally similar.

Sorting characteristics

The standard deviation values of surface water sediments (fig. 32A) ranged from 1.34 ϕ (poorly sorted) to 2.30 ϕ (very poorly sorted) at station 5; poorly sorted sediments were the predominant type. Sorting generally decreased seaward, and the most poorly sorted sediments occurred along the outer shelf. The best sorted sediments were at Aransas Pass and Matagorda Bay inlet. The seaward reduction in sorting may have reflected increasing biogenic admixtures.

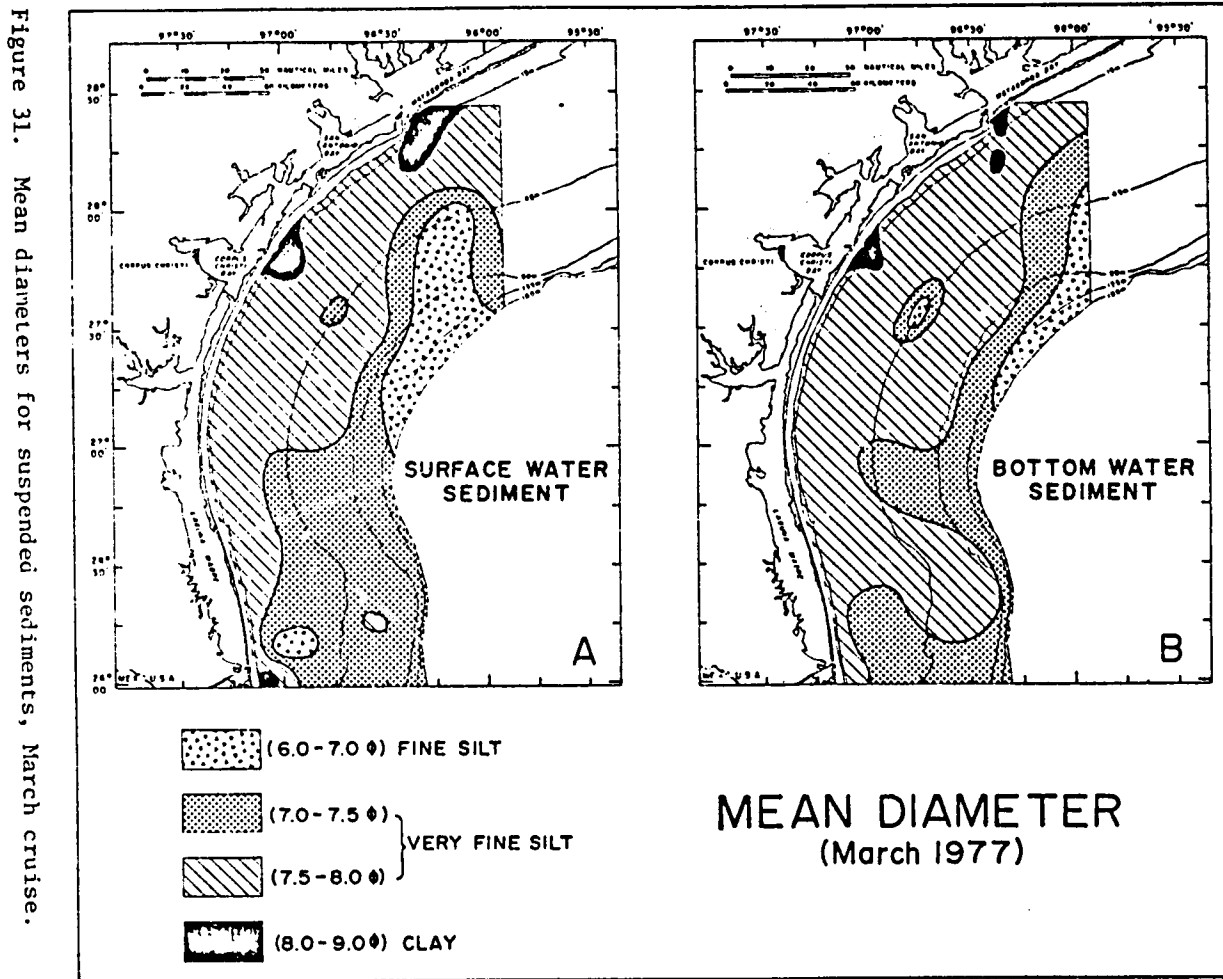
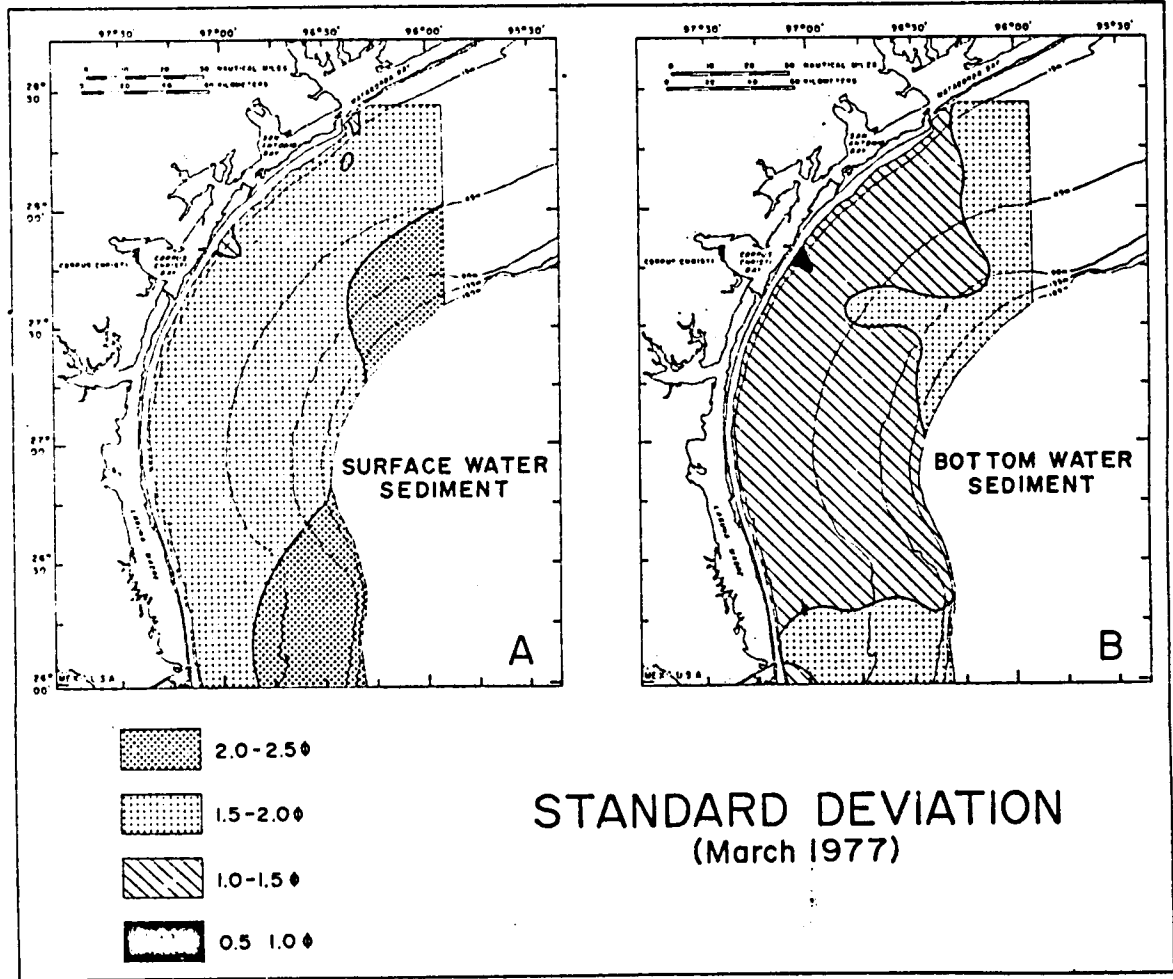


Figure 32. Standard deviations for suspended sediments, March cruise.



The standard deviations of bottom water sediments (fig. 32B) ranged from 0.99 ϕ (moderately sorted) at station 9A to 1.88 ϕ (poorly sorted) at station 6; poorly sorted sediments were the predominant type. A poorly defined regional trend consisted of a reduction in sorting away from the central sector. In comparison with surface water sediments, the bottom water sediments exhibited a somewhat different regional sorting pattern and were generally better sorted.

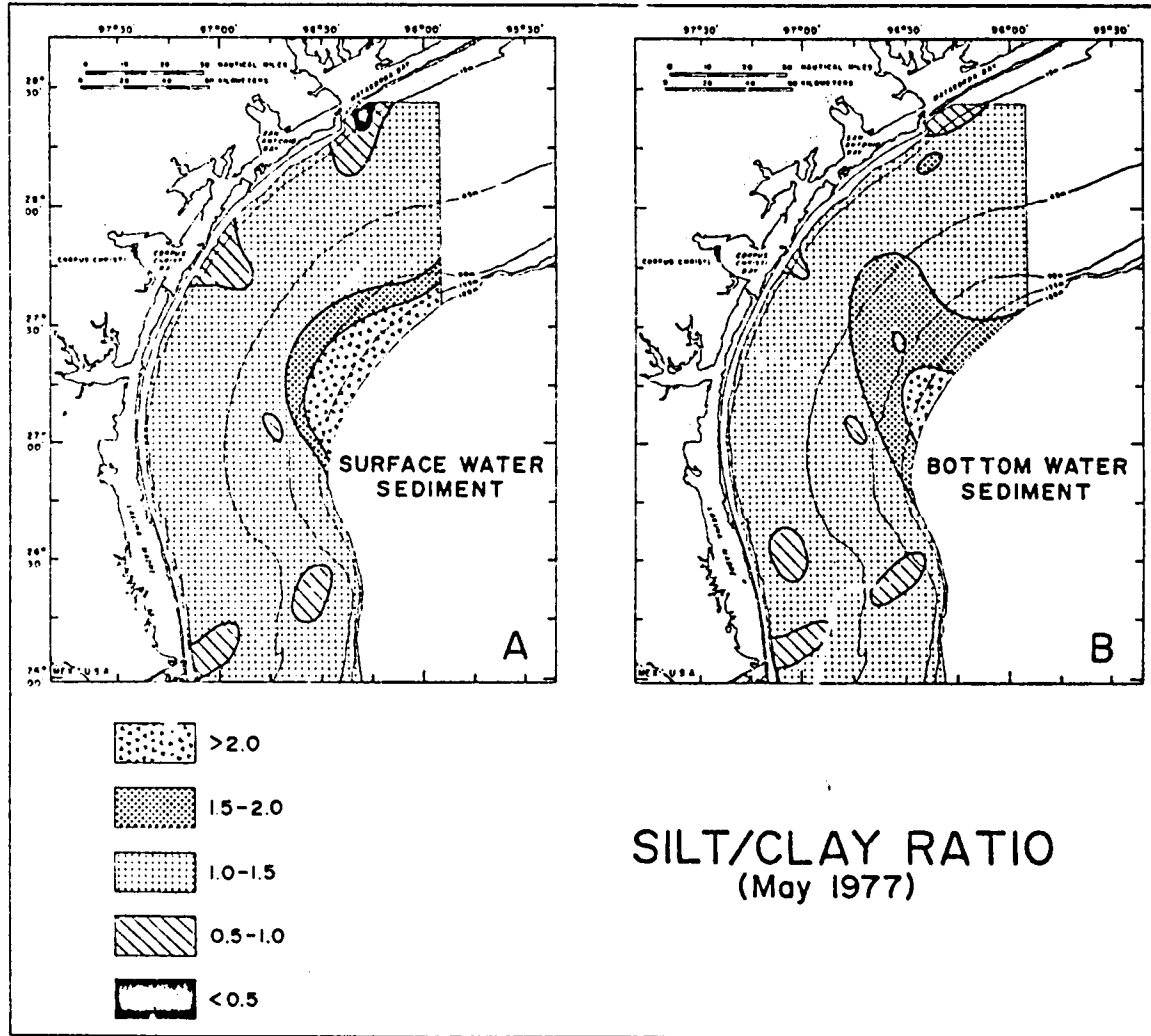
May 1977

General composition

The general composition of surface water suspended sediments is illustrated by the silt/clay ratio isopleth map (fig. 33A). Ratios varied from a maximum of 6.51 at station 12 to a minimum of 0.46 at station 1. The regional pattern indicated that silt was highly predominant; clay was largely localized in salients associated with the three coastal inlets. Silt content generally increased toward the northern outer shelf, as in both the October-November and March surface water sediment trends.

The regional trend for bottom water was similar to that for surface water sediments (fig. 33B). Ratios ranged from a maximum of 2.44 at station 12, to a minimum of 0.57 at station 1. Silt was predominant; clay was localized at the three inlets and in a few isolated pockets. Similar bottom and surface water sediment trends illustrated a high degree of textural homogeneity within the May water column, as opposed to the October-November and March patterns which indicated significant size differences between surface and bottom water sediments.

Figure 33. Silt/clay ratios for suspended sediments, May cruise.



Mean grain size

The mean diameter of surface water sediments (fig. 34A) ranged from 8.42 ϕ (clay) at station 1A to 6.09 ϕ (fine silt) at station 12. The predominant sediment type was a very fine silt, and coarseness increased seaward. The coarsest sediment was along the outer shelf, and the finest was associated with the three coastal inlets.

The mean grain size of bottom water sediments (fig. 34B) ranged from 8.25 ϕ (clay) at station 1 to 7.06 ϕ (very fine silt) at station 12. The dominant sediment type was very fine silt. The regional trend for both surface and bottom water sediment was a general seaward increase in coarseness, possibly reflecting a seaward increase in biogenic components.

Sorting characteristics

The standard deviation values of surface water sediments (fig. 35A) ranged from 1.00 ϕ (poorly sorted) at station 1A to 2.32 ϕ (very poorly sorted) at station 22; poorly sorted and very poorly sorted sediments were nearly equally distributed. The regional trend consisted of a general reduction in sorting toward the longitudinal axis of the CCS region. The significance of the trend was not readily apparent, but could have been related to the northward transport of surface water sediment during May.

In bottom water sediments (fig. 35B), the standard deviation values ranged from 2.25 ϕ (poorly sorted) at station 13 to 2.25 ϕ (very poorly sorted) at station 23A; poorly sorted sediments were the predominant sediment type. The regional trend showed a general southward reduction in sorting.

Figure 34. Mean diameters for suspended sediments, May cruise.

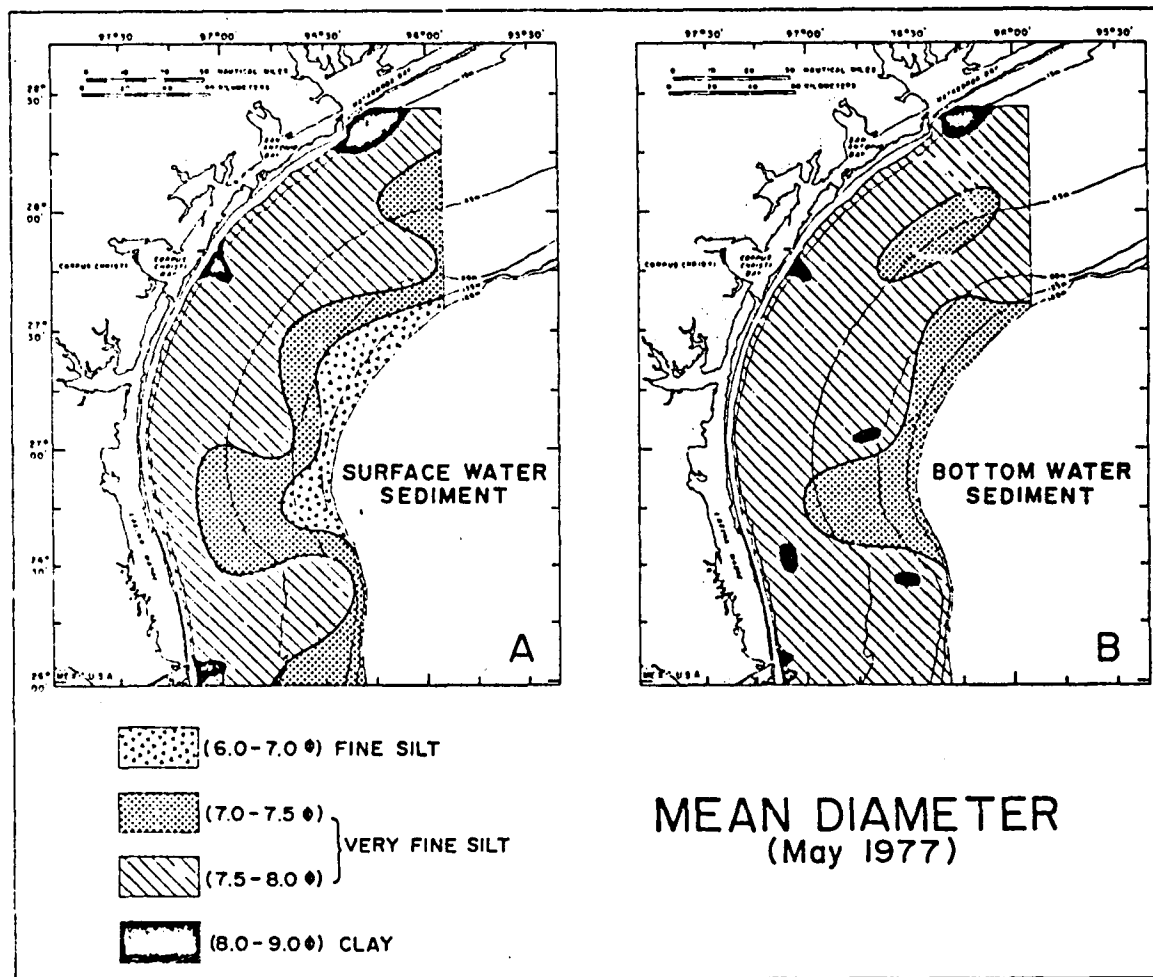
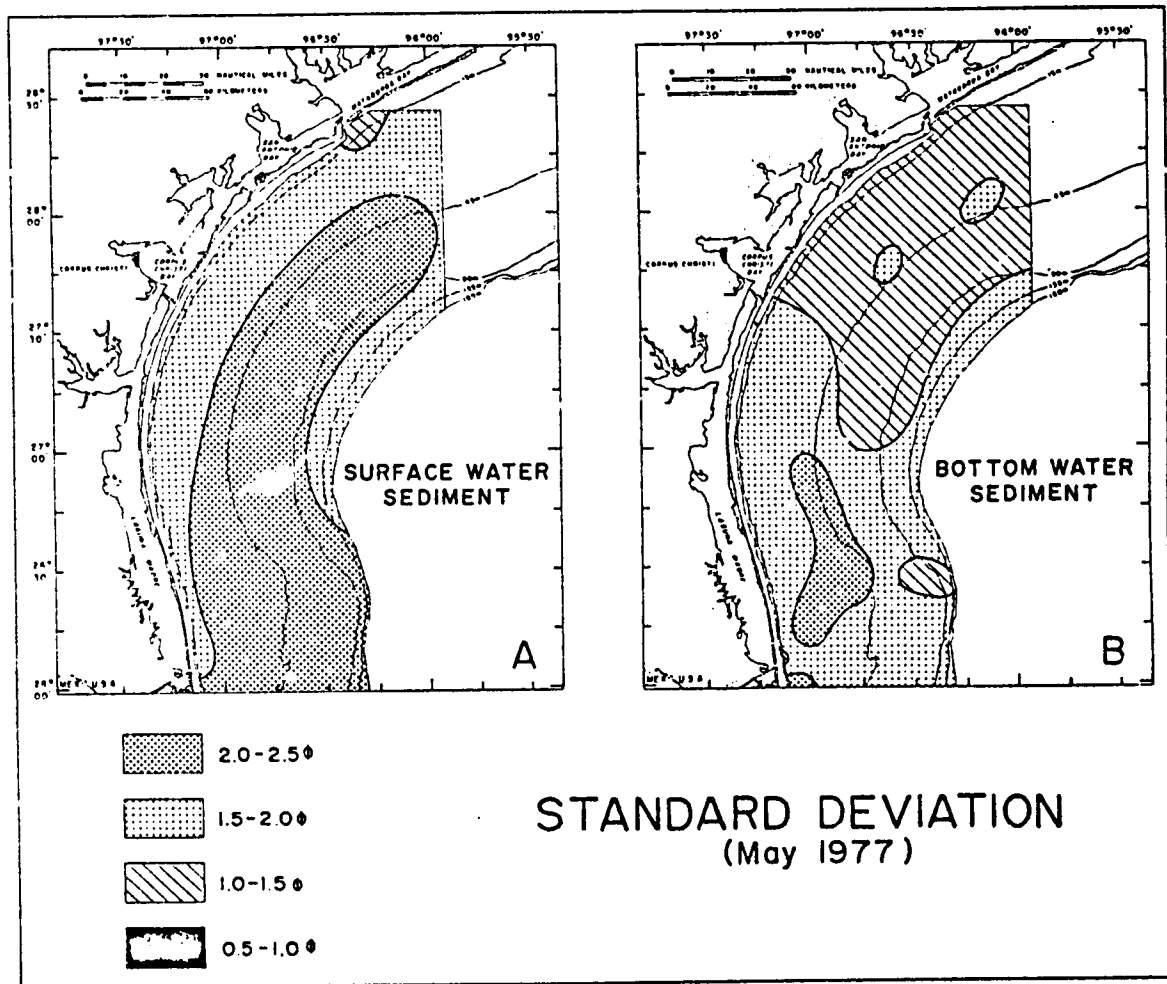


Figure 35. Standard deviations for suspended sediments, May cruise.



Summary

The textural gradients of suspended sediments in both surface and bottom waters are highly variable. In terms of grain size, very fine silt is generally the dominant sediment type within the OCS region. The sediment was finest grained and had the highest clay content during October-November. The differences between surface and bottom grain-size patterns may reflect either hydraulic fractionation within the water column or differences in surface and bottom dispersal mechanisms. Sediment grain size throughout the water column was most uniform in May. The most prevalent regional grain-size trend is a seaward increase in sediment coarseness, possibly indicating a progressive seaward increase in relatively large biogenic particulates.

In terms of textural uniformity, both surface and bottom water sediment is generally poorly to very poorly sorted. The poor sorting apparently reflects the multicomponent nature of the suspended particulate system, which consists of various sizes of phytoplankton, zooplankton, and inorganic subpopulations. Sediments in bottom waters tend to be somewhat more uniform than those in surface waters, possibly reflecting a lower concentration of size-variable organic constituents. The most prevalent regional sorting trend is a general seaward reduction in sediment uniformity, possibly reflecting a progressive size difference between the inorganic and organic fractions.

CHEMICAL CHARACTERISTICS - TRACE METAL CONTENT

by

Steven S. Barnes and Cynthia A. Rice

Methods

During 1977 an additional sampling period in March was added, and sampling in November and May was repeated as in the previous year. The addition was made to check further the seasonal variations noted during the first two years of this study. The locations of the 11 stations sampled are shown by figure 36.

No significant changes were made in shipboard or laboratory procedures. Whenever possible, all filtrations were done on board ship as soon as the samples were taken. When this was not possible, samples were frozen in acid prewashed polyethylene bottles and returned to the laboratory.

On board ship, the filtration was accomplished by an adaptation of the in situ filters of Davey and Soper (1975). The filters were made by heating 0.4 μ m NUCLEPORE filter material to make bags 3.5 cm in diameter by 7 cm in length. The filter bags were encapsulated in polyethylene vials with entrance and exit tubes sealed at each end. The inline filter capsules were washed with 1 to 1 nitric acid and deionized water before use. The filters were attached to the polyethylene bottles containing the sample water to be filtered by means of polyethylene fittings sealed to the bottle caps. Ten liters of seawater were then passed through the filter. Once filtration was completed, the encapsulated filters were sealed in polyethylene bags for transfer to the laboratory. The March samples were stored until the May samples were collected and returned to the laboratory, then both sets of samples were analyzed at the same time.

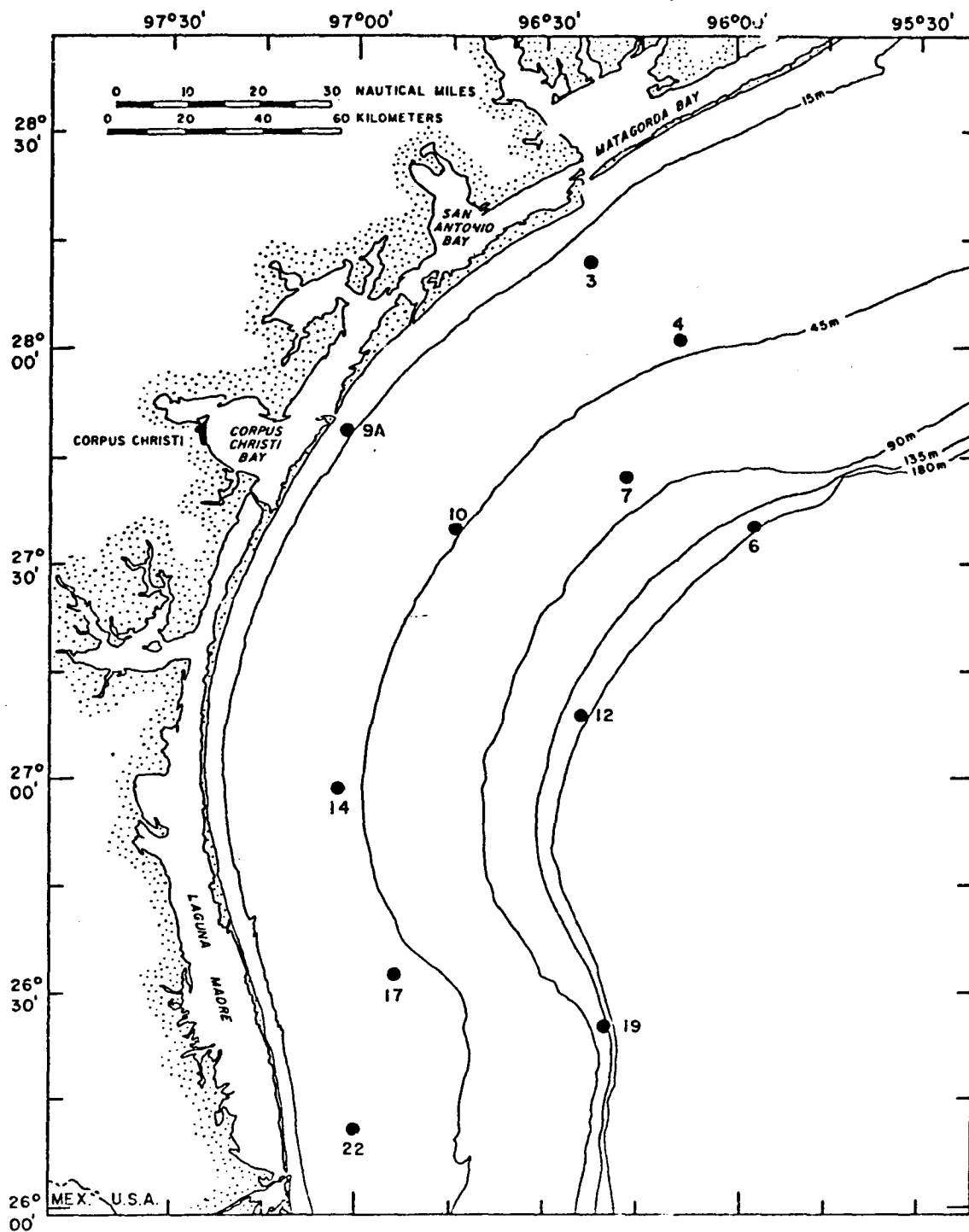


Figure 36. Location of stations sampled for trace metal content of suspended sediments, 1975-1977.

In the laboratory, all analytical preparation was performed in an ENVIRCO clean bench which utilized a filtered air flow to isolate the interior of the bench from the remainder of the laboratory. The samples were thawed, the filter capsules opened and the bags removed. A jet of deionized water was directed onto the exposed filter surface. The water and dislodged particulate material were collected in a 100 ml beaker; 70 to 100 ml of deionized water was used in this step. This suspension was then filtered under vacuum on a 25 mm diameter, 0.4 μm pore-size NUCLEPORE filter which had been acid washed, dried over anhydrous magnesium perchlorate and weighed. The filters with sample material were then placed in a desiccator over anhydrous magnesium perchlorate for 24 hours and reweighed. All weighings were made on a PERKIN ELMER AD-2 autobalance (readable to 1.0 μg) placed in the clean bench. Only deionized water and redistilled nitric acid were used in the analytical preparation. All labware was washed with 1 to 1 nitric acid and deionized water before use.

After reweighing, the filter and sample were placed in a 50 ml teflon beaker. Two ml of concentrated nitric acid were added and the samples were dried under infrared lamps at a temperature of 30°C . One ml of concentrated nitric acid was then pipetted onto the dry sample. The sample and acid were allowed to equilibrate for half an hour and this solution was used for analysis by atomic absorption spectroscopy. All analyses were made by a PERKIN ELMER model 303 atomic absorption spectrophotometer using a model 2100 HGA graphite furnace. For all metals the amounts were determined in the deionized water and the redistilled nitric acid. A procedural blank was then determined by taking one of the original acid-washed filter capsules through the entire procedure as if it were a sample. Four blanks were run. The blank value thus determined was used in all calculations.

The sample size, 0.1 to 15 mg total weight, made contamination a problem in analysis. Every effort was made to control all possible types of contamination, including analysis of ship's paint, use of clean bench, use of carefully selected reagents, and careful washing of all labware in 1 to 1 nitric acid.

As for the first two years of study, total carbon analysis was performed by a commercial laboratory (Galbraith Laboratories, Inc., Knoxville, Tenn.) on glass-fiber filter samples. These filter samples were prepared in the following manner. GELMAN type A-E glass-fiber filters with a nominal pore size of 0.6 μm (Feely, 1975) were ashed in a muffle furnace for 2 hours at 400°C. Two of these filters were placed one on top of the other in a vacuum filtering apparatus. Between 1.5 and 2.0 liters of seawater were then filtered. The sample was followed by 100 ml distilled water to remove salt. The filters were dried over magnesium perchlorate dessicant, placed in petri dishes and sealed in polyethylene bags to be shipped to the analytical laboratory for analysis. Particulate carbon was taken as the difference between the carbon values for the two filters, as the top filter should retain the particulate carbon plus some dissolved carbon adsorbed on the glass fibers, and the bottom filter should only contain adsorbed dissolved carbon (Feely, 1975).

Mass determinations were made by filtering a known amount of sea water through a prewashed, dried, and weighed 0.4 μm NUCLEPORE filter. Deionized water was forced through the filter behind the sample to remove salt. The sample was then dried over magnesium perchlorate dessicant and reweighed. All weighings were made on the PERKIN-ELMER AD-2 autobalance.

Results and Conclusions

For the March and May samples, the blank values for zinc were two to three orders of magnitude higher than previous sample values, making the zinc data useless. The March nickel blank was high and variable, making the nickel results also suspect. The May values for nickel ranged from a low of not detected to a high of 3200 ppm with a mean of 910 ppm. Data from previous years contain some individual high values, but the values were not as consistently high as in 1977. Manheim (1975) also reported nickel in amounts up to 3609 ppm for suspended sediment in the Gulf of Mexico. Whether the high degree of variability in the nickel results for 1977 is real or an artifact of sample processing is difficult to determine.

Sample material collected during the November 1976 cruise was sufficient in a number of cases for replicate analysis. This was done by taking the material from an individual filtration, splitting it into subsamples, and then taking each of these subsamples independently through the remainder of the analytical procedure. The results of the replicate analyses are given by station in table 1. Mean values for each element at each station were calculated, and percent deviations from the mean were determined. The average of the relative percent deviations was then taken for each element over all samples (table 1). The results of the replicate analyses indicate that the overall procedure is satisfactory because of the low percent deviation values (5-14) of the elements not subject to contamination or to instrumental analysis problems. The results also quantitatively point out the elements that are the most difficult to analyze in suspended sediment samples. The average values ranged from a low of 5 percent for manganese and iron to a high of 37 percent for cadmium. The intermediate values for the other metals

Table 1. Replicate Analyses, November 1976

Sample Number	Mn	Fe	Zn	Cu	Ni	Cr	Cd	Pb	V
3T	739	0.75	224	13.4	12	-	0.54	83.2	4.9
	455	0.92	172	11.9	16	-	0.30	109.1	44.7
								85.0	6.8
3B	575	1.0	61	13.0	12	13.0	0.92	53.1	9.5
	526	0.91	147	14.7	11	-	0.35	40.4	10.0
								52.1	26.3
17B	908	1.0	261	20.6	20	2.8	11.21	35.3	9.2
	986	1.1	144	20.7	15	6.3	5.93	42.0	10.7
22T	602	1.0	114	14.3	9	-	3.41	50.0	7.4
	610	0.94	169	16.1	11	-	0.36	47.1	9.7
	650	0.92	151	14.1	17	2.6	0.15	54.9	12.5
								48.8	16.5
22B	544	0.74	107	7.1	12	-	6.46	18.7	6.0
	569	0.77	503	9.7	11	-	4.26	27.5	7.2
	588	0.80	238	11.6	11	1.1	4.99	26.8	11.6
								27.3	19.2
4B	733	1.0	678	114.8	15	-	1.19	263.8	3.2
	769	1.1	1070	97.8	21	7.9	0.89	248.9	8.9
9AB	582	0.98	298	25.4	15	12.0	2.27	38.8	8.1
	554	0.93	500	24.4	13	-	1.52	37.0	3.4
19B	651	0.88	318	11.9	12	-	5.27	33.7	5.3
	672	1.2	306	12.7	11	-	9.65	35.1	10.9
14B	845	1.0	254	16.7	28	40.8	1.58	0.6	14.1
	976	0.96	411	19.4	64	69.3	2.13	72.6	12.4
Average									
Percent deviation	5	5	24	6	14	-	37	8	27

All concentrations in ppm except Fe which is in percent

were: copper, 6 percent; lead, 8 percent; nickel, 14 percent; zinc, 24 percent; and vanadium, 27 percent. The percent average deviations reflect the precision of the analytical procedure. The high average deviation for cadmium reflects the exceedingly small nanogram to subnanogram amounts of total cadmium in the sample. Cadmium has the lowest concentration of all metals determined. Over the three years of study, zinc has presented more problems and yielded more variability in results than any of the other metals. Robertson (1968) has shown multiple contamination sources for zinc in marine analytical procedures, such as reagents, vessels, filters, other apparatus, and even airborne particulate material in the laboratory. Vanadium requires higher atomization temperatures and will show more instrument variability than the other metals. These problems, coupled with the very small amounts of total vanadium in each sample (5 to 20 nanograms), indicate that 27 percent is a reasonable value for relative deviation for vanadium. The relatively low deviations for iron, manganese, copper, and nickel are indicative of the precision of the analysis.

The results of the analyses for the three seasonal suites of samples collected in 1977 are recorded in appendix 2. Average values are shown by table 2. The amounts of zinc for the March and May cruises were too high to be recorded by the atomic absorption spectrophotometer without greatly diluting the samples. Since the samples were obviously contaminated, no analyses were made. Nickel values in March are highly suspect and may be tied to the zinc contamination problem. The March values were plotted, however, on figure 43B. The May nickel samples were obviously contaminated and were not graphed. The nickel blank was an order of magnitude higher for the March and May samples than for the November 1976 samples. Many of

Table 2. Averages of the amounts of trace metals
in suspended sediments

Season	Sample	Mass mg/l	Cd ppm	Cr ppm	Cu ppm	Ni ppm	Pb ppm	Zn ppm	V ppm	Mn ppm	Fe %	C %
Nov. 1976	Top	2.10	19.0 (5.7)*	570 (126)*	59	21	259	1609 (627)*	18	501	1.0	5.1
	Bottom	2.73	3.5	27	29	16	99	420	9	709	1.0	3.4
March 1977	Top	0.70	3.3	341	187	3800	1020	--	71	562	2.3	16.3
	Bottom	2.95 (1.64)*	3.5	349 (73)*	104	129	49	--	99	2240	2.0	5.3
May 1977	Top	1.05	12.1	81	93	938	181	--	112	241	1.0	11.4
	Bottom	3.14	15.2	110	129	1091	341	--	109	908	2.5	15.4

*Values in parentheses are figured when one atypical result is disregarded

the March 1977 samples were inadvertently destroyed when the tray bearing the filtrate samples was dropped in the laboratory, so that the averages for the "top" samples are generally based on three values.

The ranking of elements according to top versus bottom samples indicated in the two previous years was confirmed by the 1977 analyses. Amounts of manganese and iron continued to be larger in the bottom water samples; vanadium was increased in the bottom water in two out of three seasons, and the remaining elements were higher in surface samples except for May. In May all stations showed larger amounts in bottom water samples for all metals, including not only the trace metals themselves but the total particulates in the samples and the percentage of carbon as well. Those metals that previously had larger amounts in the surface samples appear to be tied to carbon concentration. The percent carbon on the average is larger in bottom samples for May 1977 than for any other set of samples in the study. The carbon enrichment is the apparent explanation for the larger amounts of such elements as lead, nickel, cadmium, and copper in the bottom water.

Variations from season to season were not as marked in the third-year's study as was reported for the second year. Amounts of cadmium and lead were larger in May than in November; the results for March were similar to those for November. Total carbon followed a similar pattern, except for a notably higher average for the surface waters in March. Iron, manganese, and chromium remained about the same, showing little seasonal variability. The other metals appeared to be more concentrated in spring and summer. Comparison of the mass values with the values for the previous year showed a similar pattern. The mass values are lower in the spring and summer.

Examination of the areal distribution of the elements (figs. 37-46) shows an apparent seaward increase in amounts of cadmium, lead, nickel, copper, and zinc in surface waters. This pattern is similar to that for total carbon and the inverse of that for total particulates.

The conclusion reached following the second year of study that the distribution pattern for the amounts of trace metals in suspended sediments over the south Texas continental shelf is greatly influenced by planktonic activity seems confirmed by the results for this year. In fact, the data strongly reinforce that conclusion. The other general conclusion that can be made from the third-year's results is that analytical procedures, no matter how carefully planned, proven, and followed, are still subject to contamination at the very low levels of concentration dealt with in this study.

A review of the complete three-year's study reveals the following:

- (1) manganese, iron, and to some extent vanadium, are always more concentrated in bottom-water samples than in near-surface water. This is generally true also of the total particulates. The other elements do not show a clear pattern but do indicate an association with carbon. Bostrom and others (1974) have shown that plankton contains higher concentrations of lead, cadmium, zinc, and copper than were found in shale, but this does not appear to be borne out by the studies for the South Texas Outer Continental Shelf. Lal (1977) suggested that adsorption onto particle surfaces may be an active mechanism for the concentration of trace elements on suspended sediments. If this is true on the south Texas continental shelf, there is sufficient difference between adsorptive properties of organic and inorganic particles to differentiate the trace metals determined in this study.

Seasonal variability does exist but appears to be associated with biological activity as indicated by percent carbon. Areal distribution again shows strong ties to percent carbon with moderate increases in concentration of cadmium, lead, nickel, copper, and zinc seaward and northward. Generally, the pattern reflects an increase in percent carbon or a decrease in total suspended sediment.

The precision of analytical work has been shown to be sufficient to establish a baseline for the trace metals analyzed. Extreme caution should be exercised in using a single analysis or a small group of analyses at a single station, however, as random contamination is a major problem.

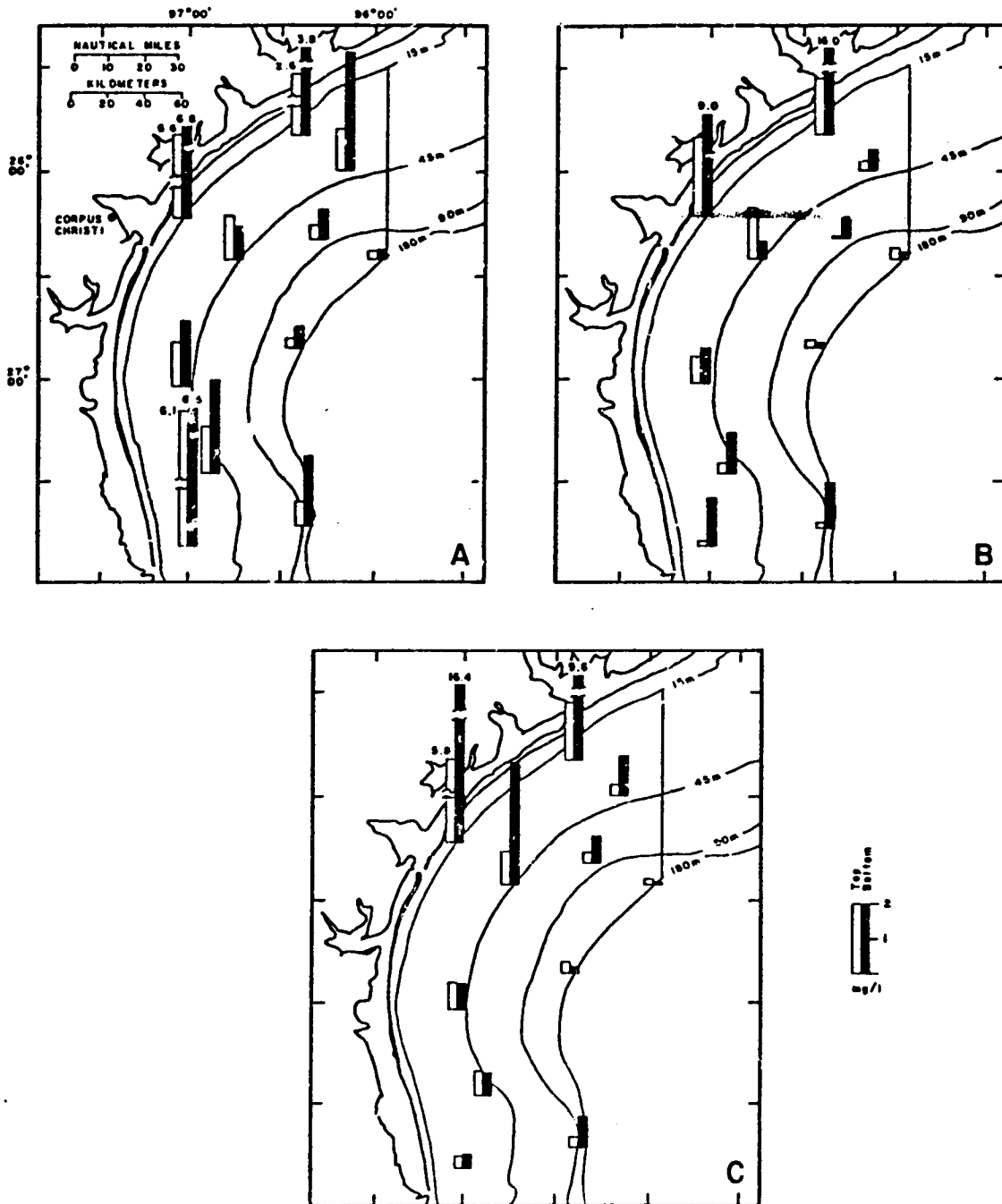


Figure 37. Amounts of suspended sediment: A. November 1976; B. March 1977; and C. May 1977.

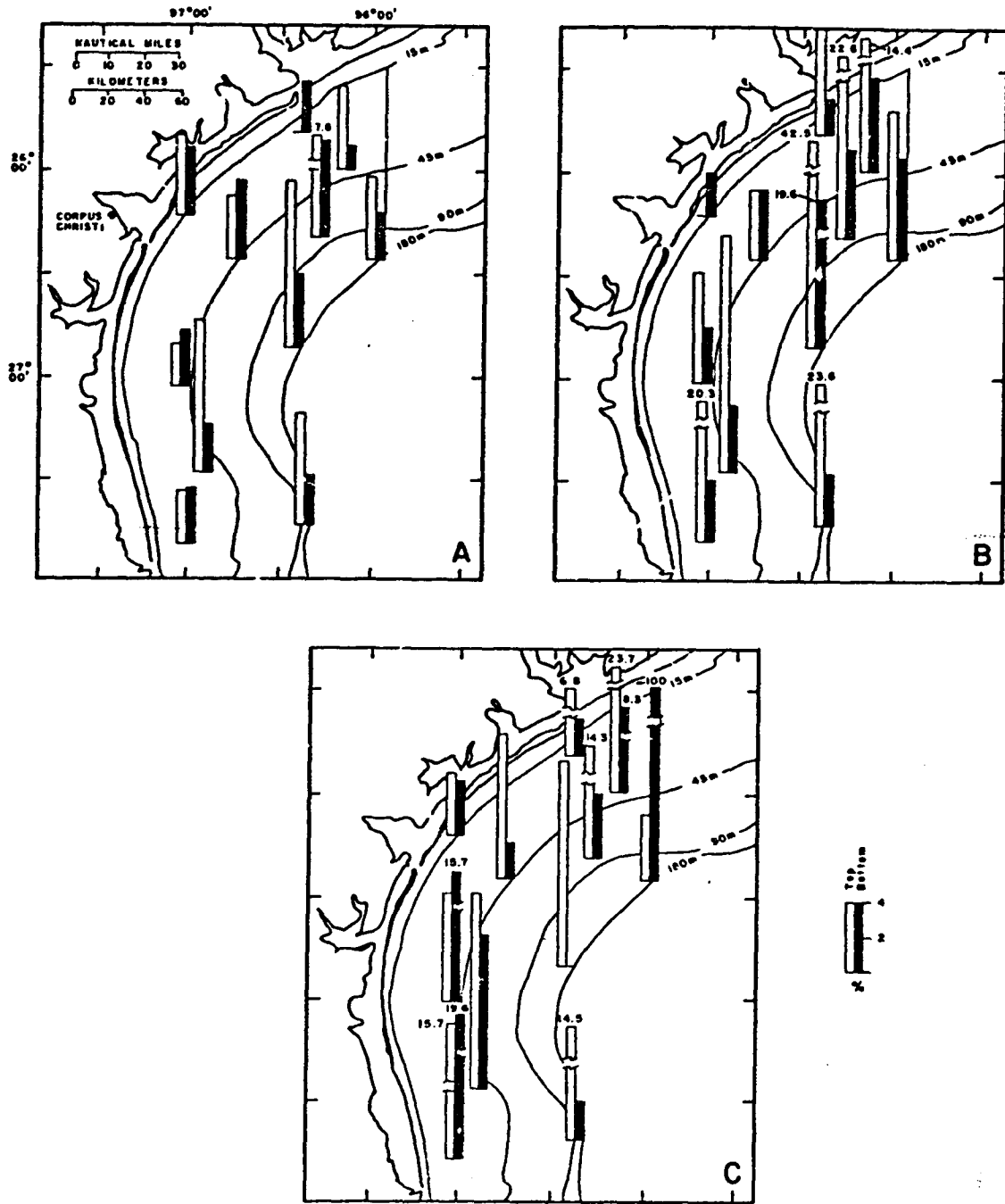


Figure 38. Total particulate carbon in suspended sediments: A. November 1976; B. March 1977; C. May 1977.

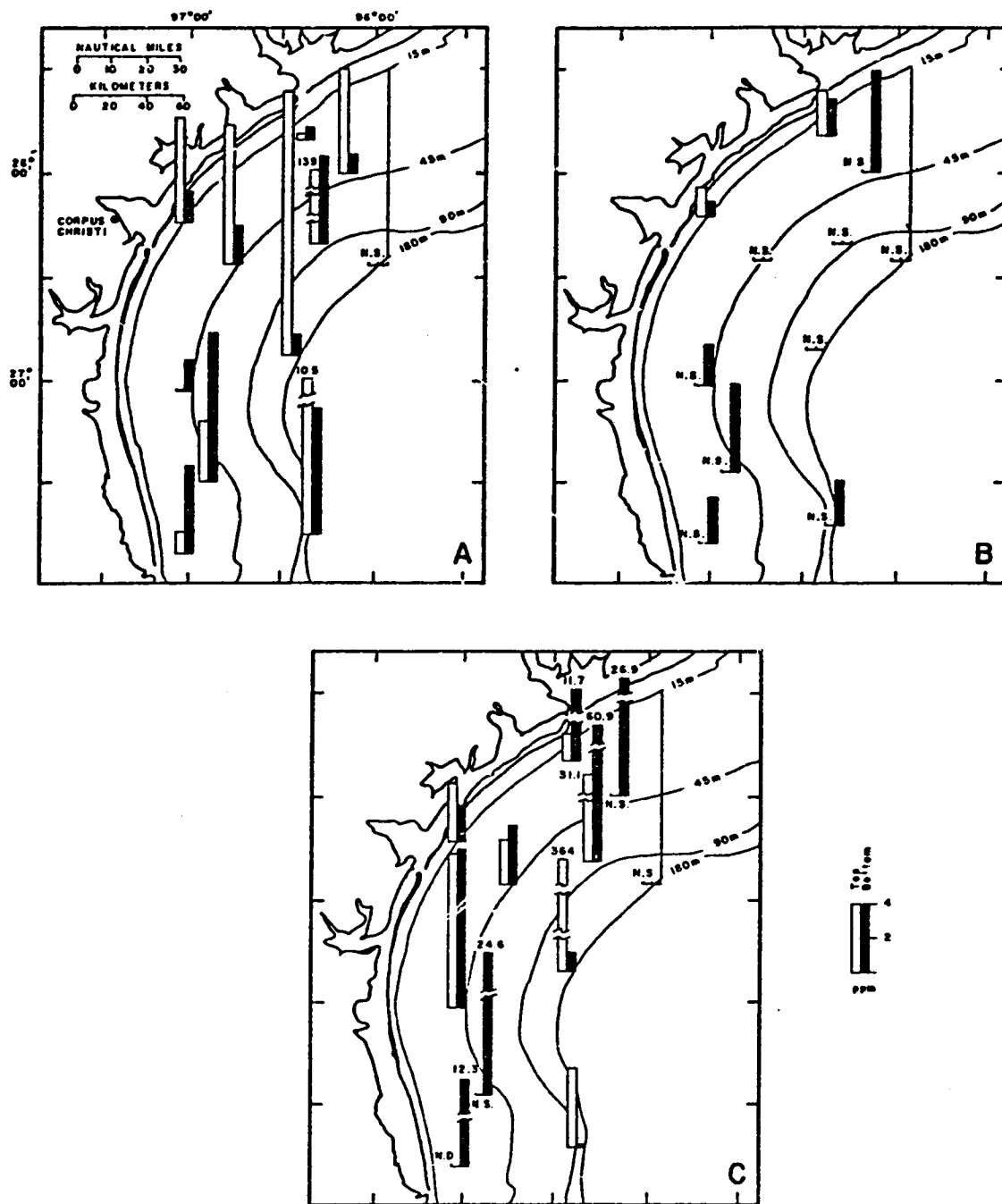


Figure 39. Amounts of cadmium in suspended sediments: A .November 1976; B. March 1977; C. May 1977.

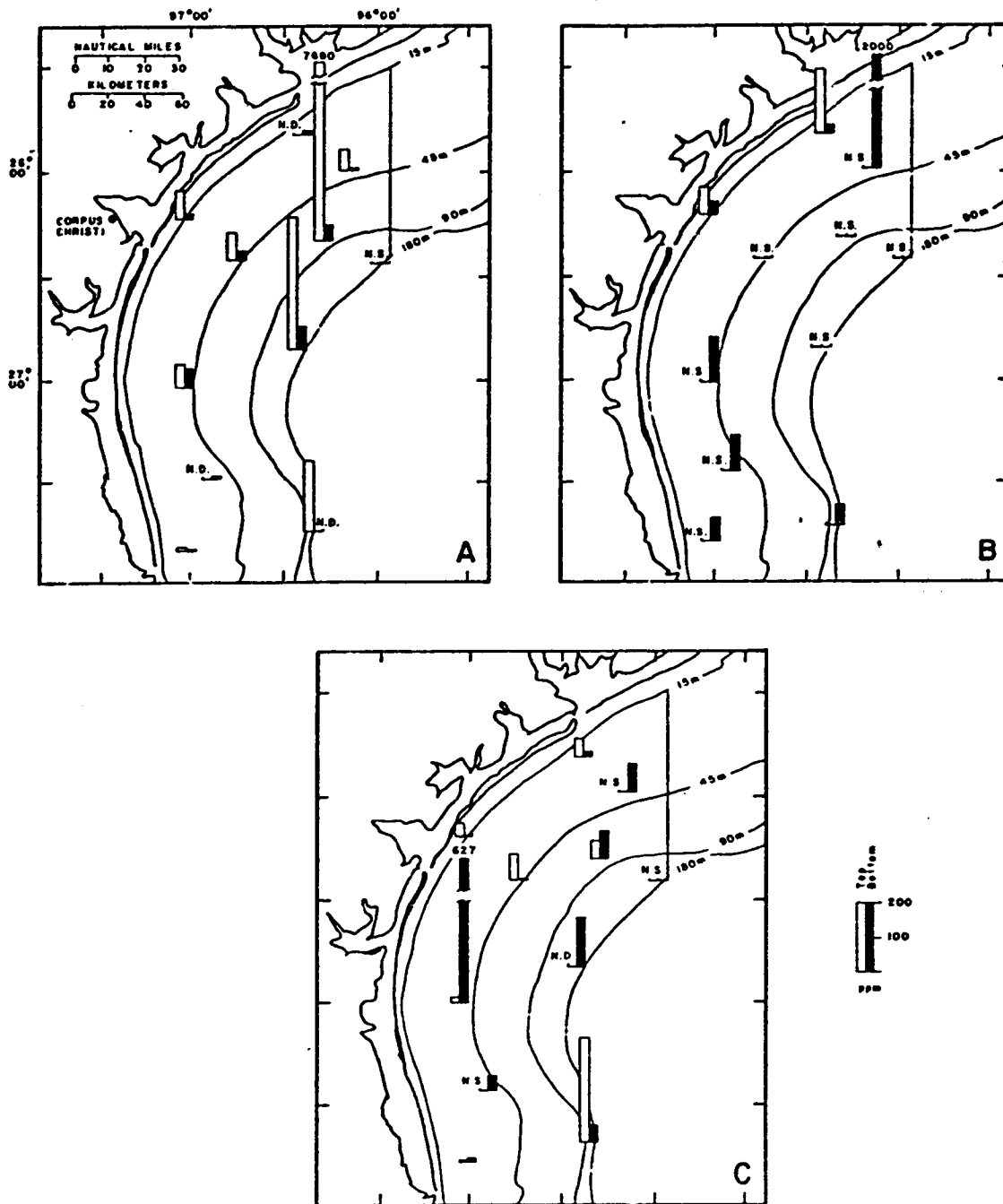


Figure 40. Amounts of chromium in suspended sediments: A. November 1976; B. March 1977; C. May 1977.

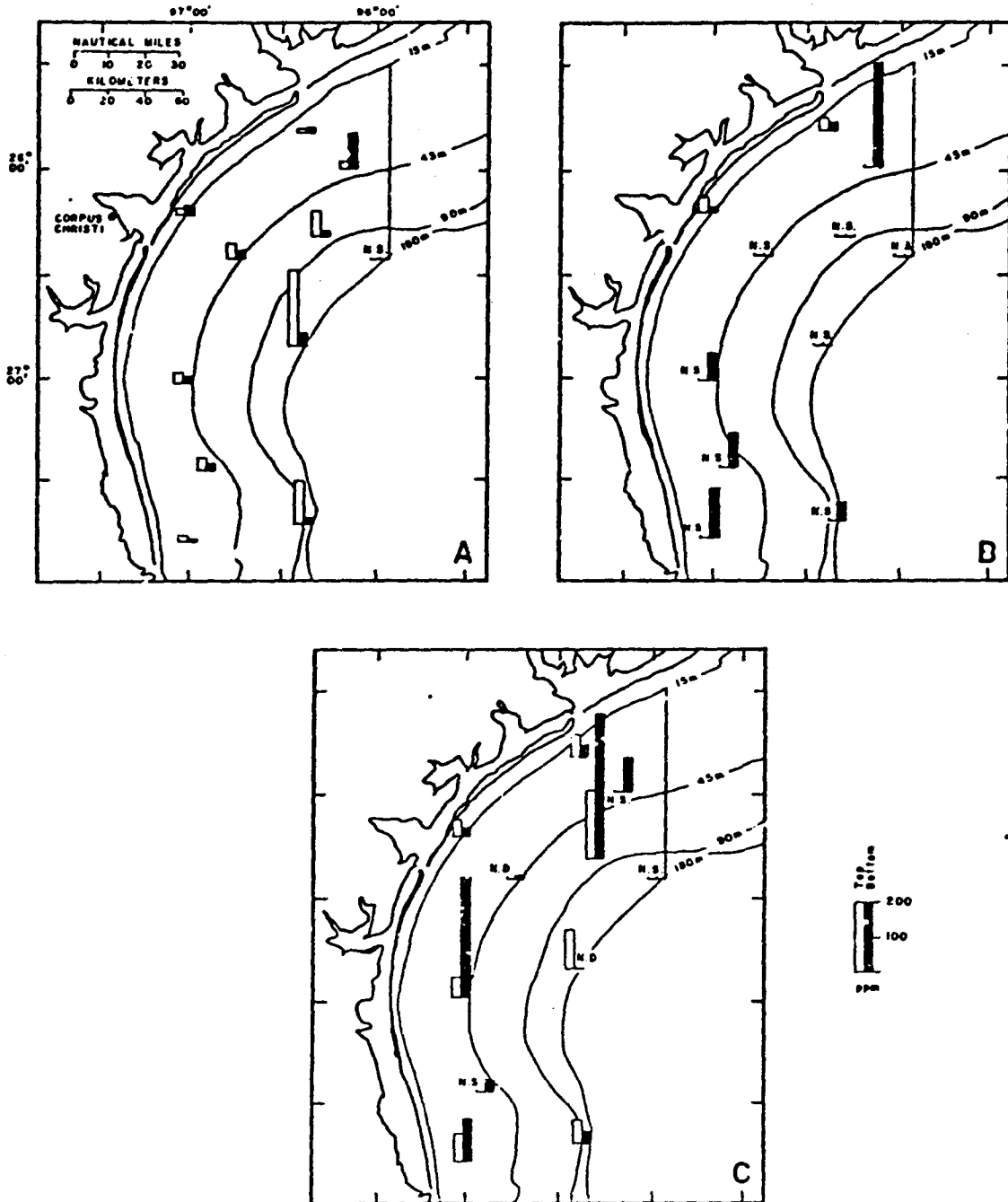


Figure 41. Amounts of copper in suspended sediments: A. November 1976; B. March 1977; C. May 1977.

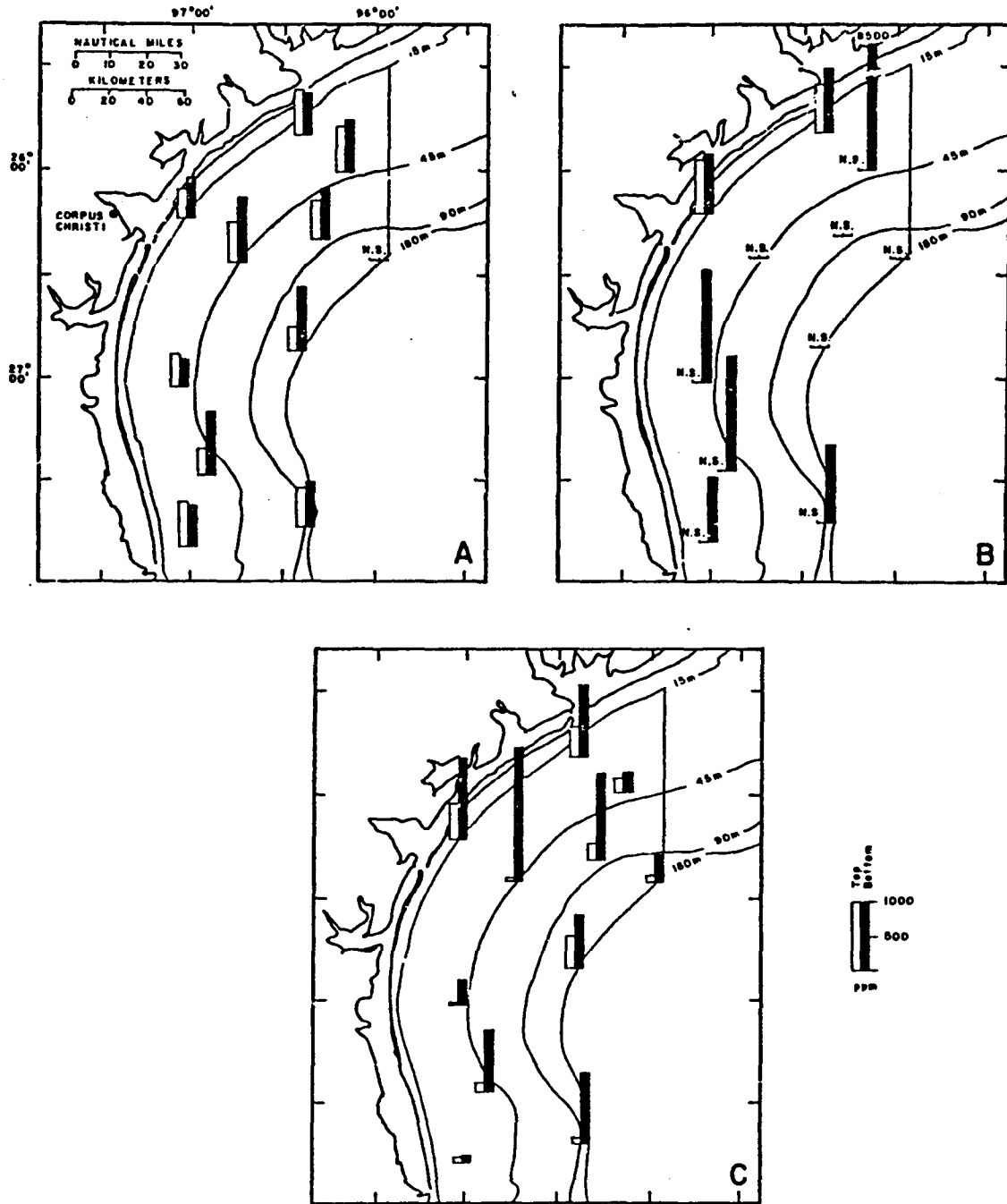


Figure 42. Amounts of manganese in suspended sediments: A. November 1976; B. March 1977; C. May 1977.

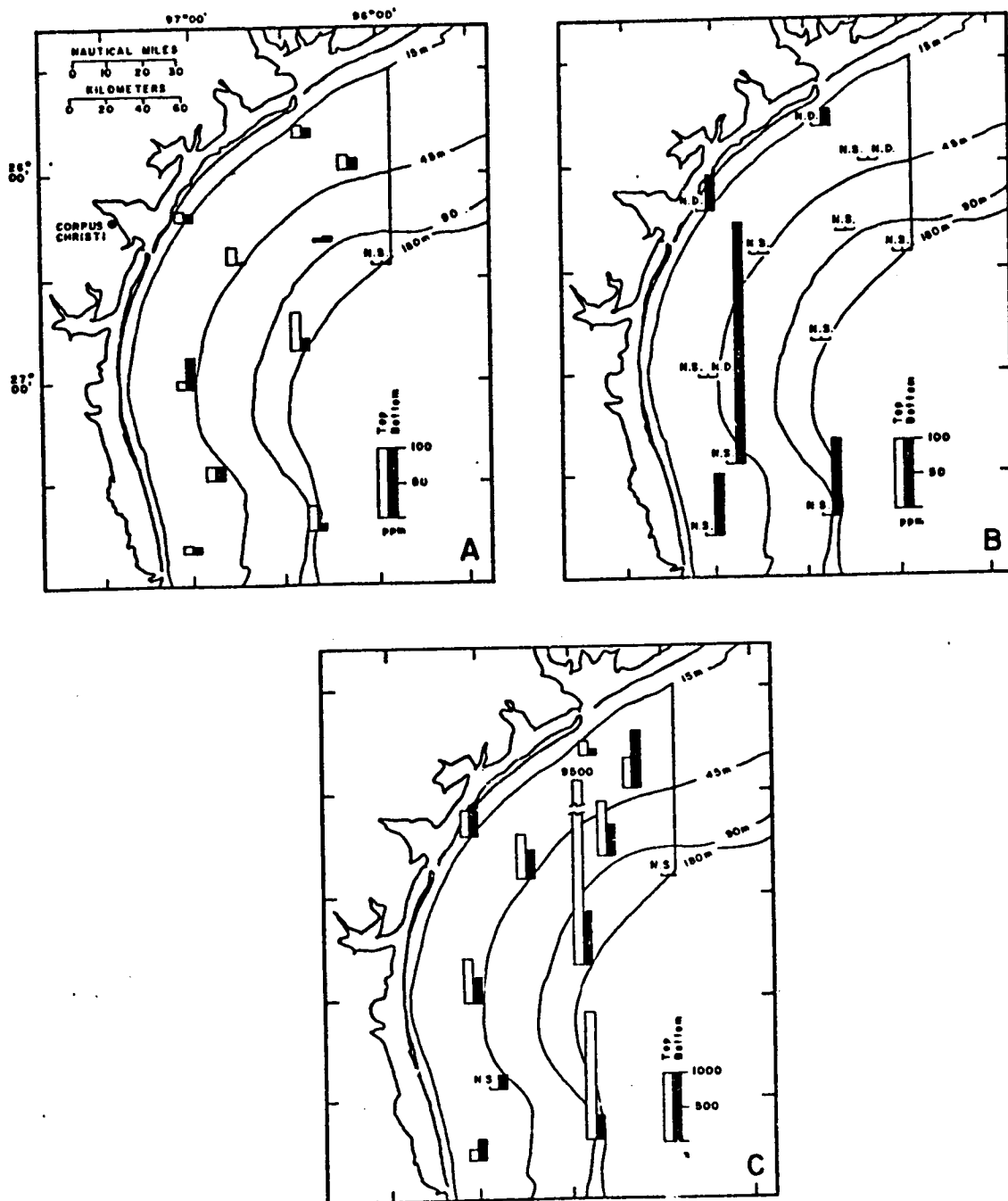


Figure 43. Amounts of nickel in suspended sediments: A. November 1976; B. March 1977. Amounts of zinc in suspended sediments: C. November 1976.

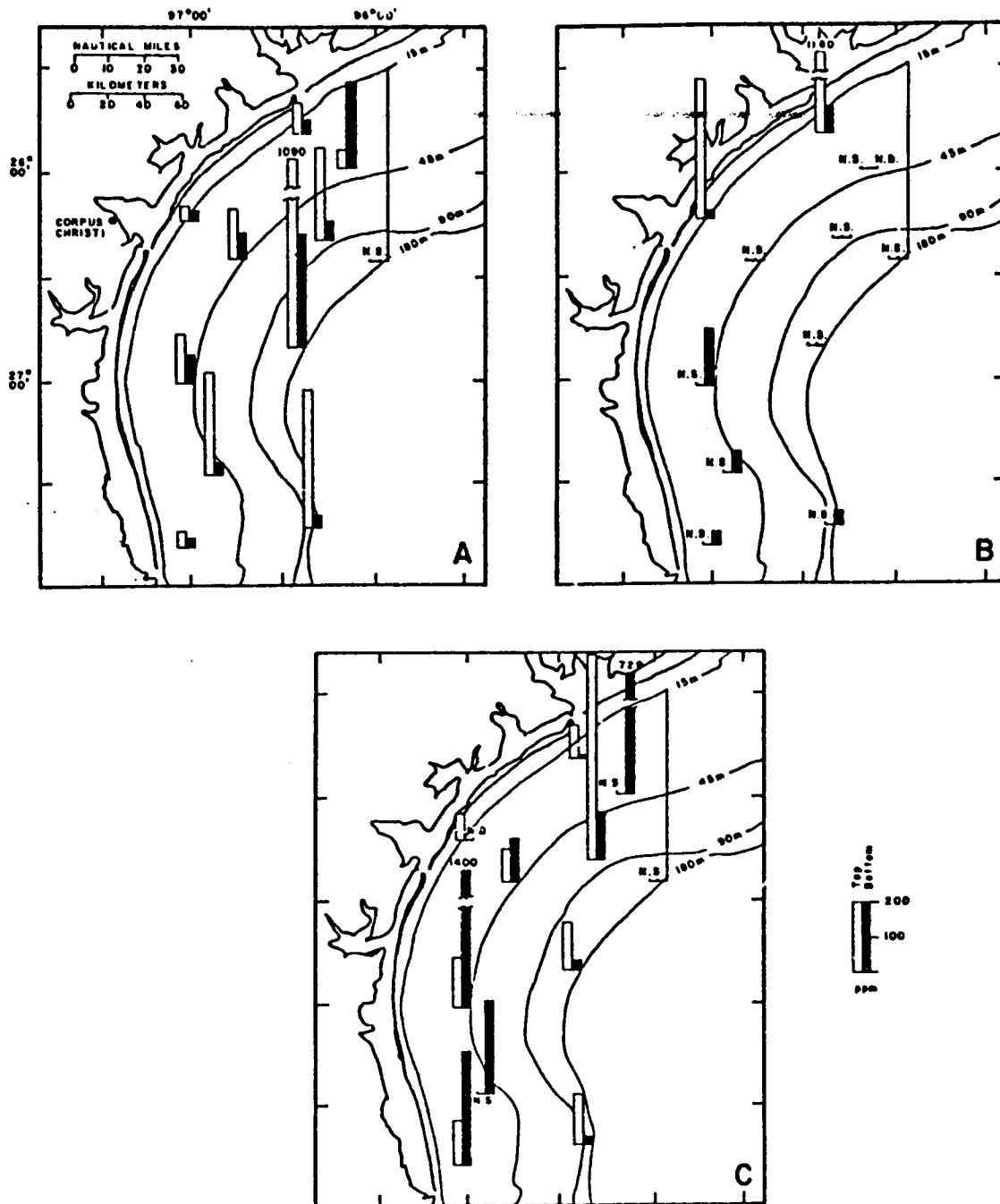


Figure 44. Amounts of lead in suspended sediments: A. November 1976; B. March 1977; C. May 1977.

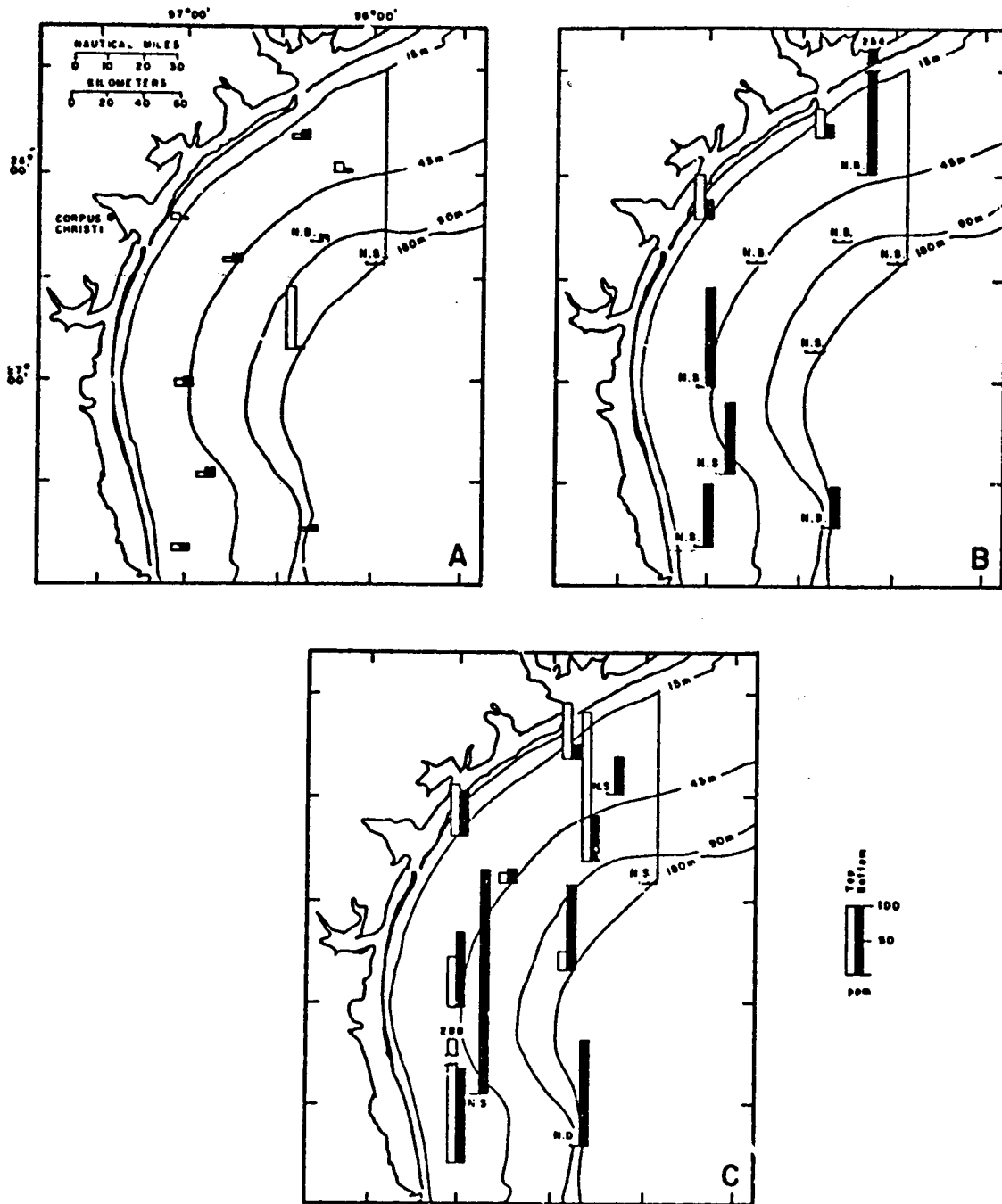


Figure 45. Amounts of vanadium in suspended sediments:
 A. November 1976; B. March 1977; C. May 1977.

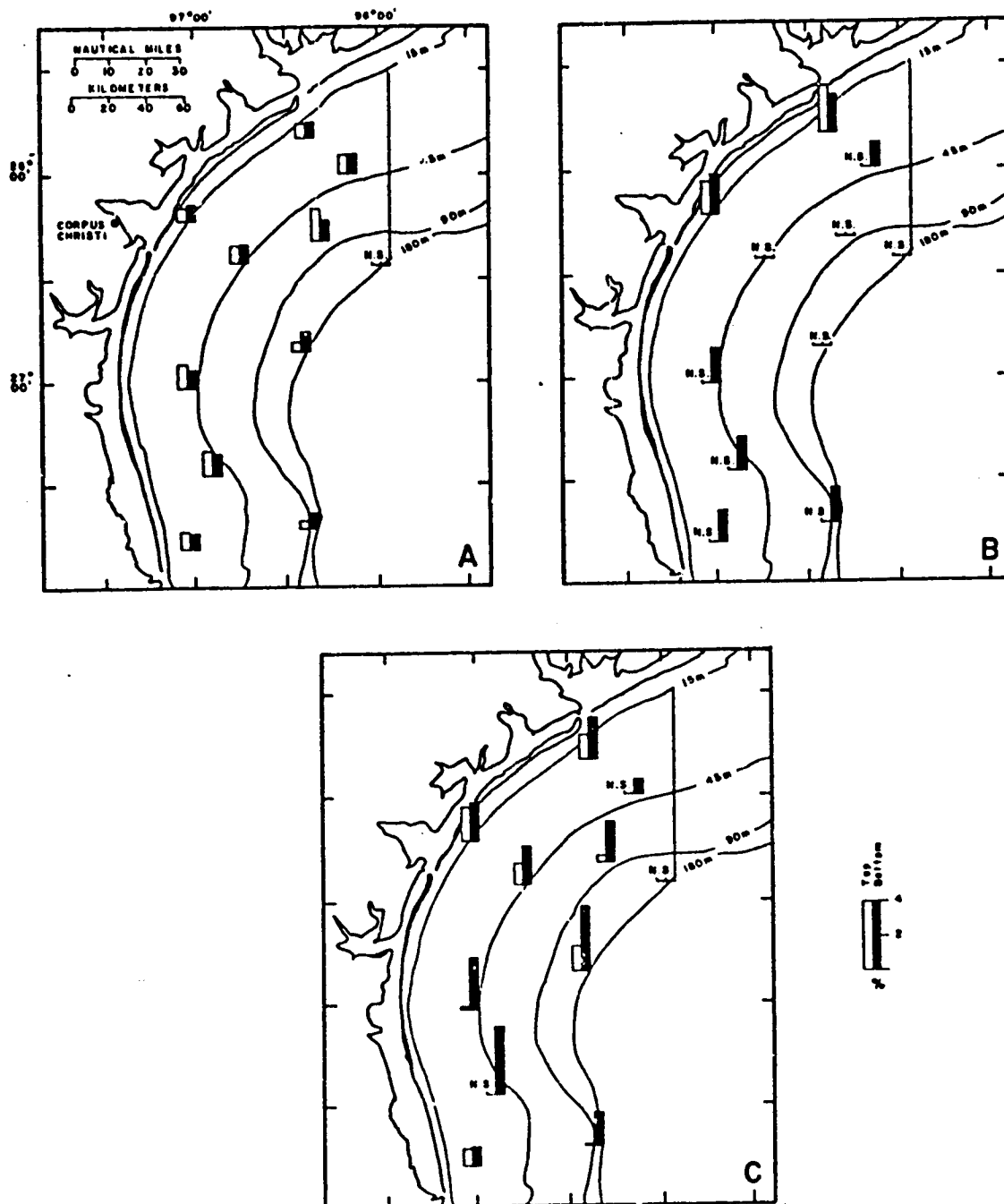


Figure 46. Amounts of iron in suspended sediments:
 A. November 1976; B. March 1977; C. May 1977.

CLAY MINERALOGY, SUSPENDED AND SEA-FLOOR SEDIMENTS

by

Charles W. Holmes

The most chemically active marine inorganic sediment is that fraction classified as clay minerals. The clay minerals of the montmorillonite group possess a large, highly negative surface area (Goldberg, 1965; Neihof and Loeb, 1972) which readily permits the adsorption of positively charged metals and polar organic materials. These clay minerals act both as a substrate and as a carrier of trace substances. Therefore, to determine the means by which the trace substances migrate through and within an environment, some knowledge of the quantity and type of clay minerals present is essential.

In addition to the role of clay minerals as trace substance carriers, the relative proportion of clay minerals within the sea-water column and within the bottom sediment also may indicate the source from which the material is derived. Furthermore, mapping of the clay mineral distribution may identify sedimentary processes at work within a study area, such as directions of dispersal and patterns of deposition; this information is important in constructing predictive models for trace substance migration and/or deposition.

This report is based upon data obtained over the past four years in a baseline environmental investigation of the South Texas Outer Continental Shelf. Suspended and benthic sediments are included together rather than in separate sections so that comparisons can be made and discussed more readily.

METHOD OF STUDY

Suspended Sediment

Samples for suspended sediment extraction were obtained during six cruises spanning the period from fall 1974 until June 1977 (October-November 1974; November 1975; May 1976; November 1976; March 1977 and May 1977). During the fall 1974 cruise, samples were taken at 24 stations (fig. 47A). For the November 1975 and May 1976 cruises, samples were taken at only 11 stations (fig. 47B). Suspended sediment mass determinations for November 1976 and both 1977 cruises were based on these same 11 sampling stations. During November 1976 and March 1977, the sampling density was increased to 23 sites (fig. 47C includes these 23 sites plus stations 1A, 9A, and 23A). Results for stations 1A, 9A, 23A, and 24 were not plotted because of close proximity to other stations. In May 1977, samples were taken at 26 stations (fig. 47C). At each station, the samples were taken with a 30 liter top-drop bottle one meter beneath the surface and one meter from the bottom. In November 1976, March 1977, and May 1977, an additional sample at midwater depth was obtained for clay mineralogy studies.

From each sample, aliquots were obtained for mineralogical analysis (≈ 2 liters). In addition, samples were obtained from the surface and bottom waters at eleven sites from all cruises, except the November 1974 cruise, for total organic carbon (≈ 7.5 liters) and mass (≈ 2 liters). During the 1974 cruise, the samples were filtered immediately. On subsequent cruises, all samples except control samples were frozen and returned to the laboratory for processing.

In the laboratory, aliquots assigned for mass determination were thawed, filtered through a preweighed 27 mm diameter NUCLEOPORE filter with a nominal

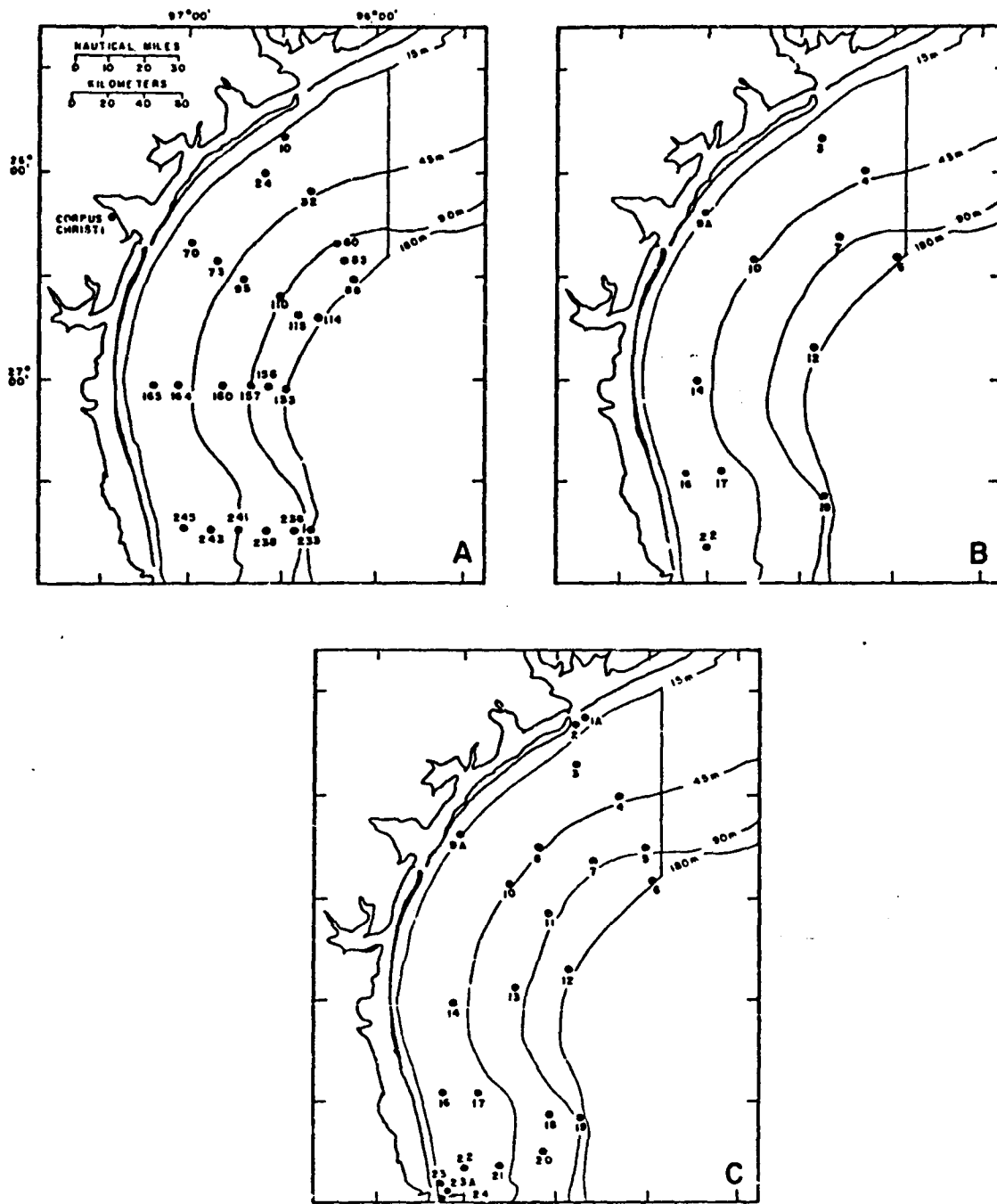


Figure 47. Location of sample stations for suspended sediment studies:
 A. 1974
 B. 1975 and May 1976 for clay mineralogy;
 1975-1977 for total mass and total organic carbon
 C. November 1976-1977 for clay mineralogy

0.45 μ pore diameter, dried, and weighed on a PERKIN ELMER autobalance Model AD-2 in a desiccated environment. Total organic carbon was determined by commercial laboratory after the sample was filtered onto an acid-washed and fired glass filter (47 mm, Type AE, GELMAN).

The mineralogical samples were filtered through a 27 mm SELAS FLOTRONICS silver filter with a nominal pore diameter of 0.4 μ m. The mineralogy was then determined by X-ray diffraction techniques. The samples for the fall cruise of 1974 were analyzed on a PICKER diffractometer, and the analyses were made by subjective measurements of "d" spacings and planimetric areas

Sea-floor Sediment

The clay mineral content of the $<2 \mu$ fraction of the bottom sediment samples was determined on 251 samples. The size fraction was obtained by settling methods after H_2O_2 leaching to destroy the organic matter. The size of the material was checked by COULTER COUNTER analysis, and the concentration of the sample necessary to sediment 5 mg/cm^2 of material consistently on the silver filter was determined. The identification and quantification of the mineral components followed the same procedures used for the suspended sediment samples. All samples were run in duplicate with an additional sample analyzed where the discrepancy was >10 percent between the duplicate analyses. Additional samples were analyzed by increasing the time of the scan in order to define better the clay species present. This procedure increased by one order of magnitude the accuracy of the "d" spacing values.

In addition to the suspended sediment and the $<2 \mu$ fraction of the bottom sediments, selected suspended and bottom sediments in the bordering estuaries also were analyzed, along with some selected silt fraction samples ($>2 \mu$).

RESULTS

In the samples analyzed, three major clay types were recognized: a 17\AA material probably composed of minerals of the montmorillonite group with an expanded lattice after glycolation; 10\AA material interpreted to be illite or some form of hydromica; and a 7.1\AA material that is kaolinite and/or chlorite. The identification of the 7.1\AA substance is extremely difficult and thus far has not been resolved satisfactorily. The lack of any 14\AA clays and the persistence of the 7\AA peak after heating to 400°C . seem to indicate that the substance is kaolinite (Carroll, 1970).

The data for suspended sediments are listed in appendixes 2 and 3, and are summarized graphically in figures 48 to 64. The data for the clay-sized fraction of the bottom sediment ($<2 \mu$) are presented in appendix 4 and in figure 66. Summaries of total suspended sediment and of total particulate carbon are given in table 3.

DISCUSSION

Suspended Sediment

The source, distribution, and composition of suspended sediment in the water column on the continental shelf cannot be proven positively on the basis of nonsynoptic data with samples taken many kilometers apart. Figure 65, an interpretative map based on Landsat imagery that showed the distribution of suspended material on the Texas continental shelf for the period November 21 to November 23, 1973, exhibits many areas of high sediment concentration that are abruptly discordant to adjacent regions (Hunter, 1976). The figure demonstrates that mineralogical analyses of discrete samples alone are of little value in determining sediment sources and processes; identification of the water masses present over the shelf at a given time is necessary to the understanding of dispersal and deposition.

Another problem in determining the true mineral composition of suspended samples is the sample size. In many cases, the amount of filtrate is so small and contains so little inorganic material that the diffraction peaks are diffuse, and the instrument will not record good peaks. This problem may account for the unusual mineral composition at some sites where only one peak was recorded.

Table 3. Summary of total suspended sediment and of total particulate carbon in suspended sediments

<u>Cruise period</u>	<u>Total suspended sediment</u> (mean) (range, percent)		<u>Total particulate carbon</u> (mean) (range, percent)	
November 1974	10.47	140-0.5	N.D.	
November 1975	4.47	21-0.2	2.81	8-0.3
May 1976	1.69	5-0.2	7.0	23-1.5
November 1976	2.39	6.8-0.3	10.8	23-2.9
March 1977	1.47	9-0.13	18.31	50-3.8
May 1977	2.69	16-0.16	23.4	100-1.7

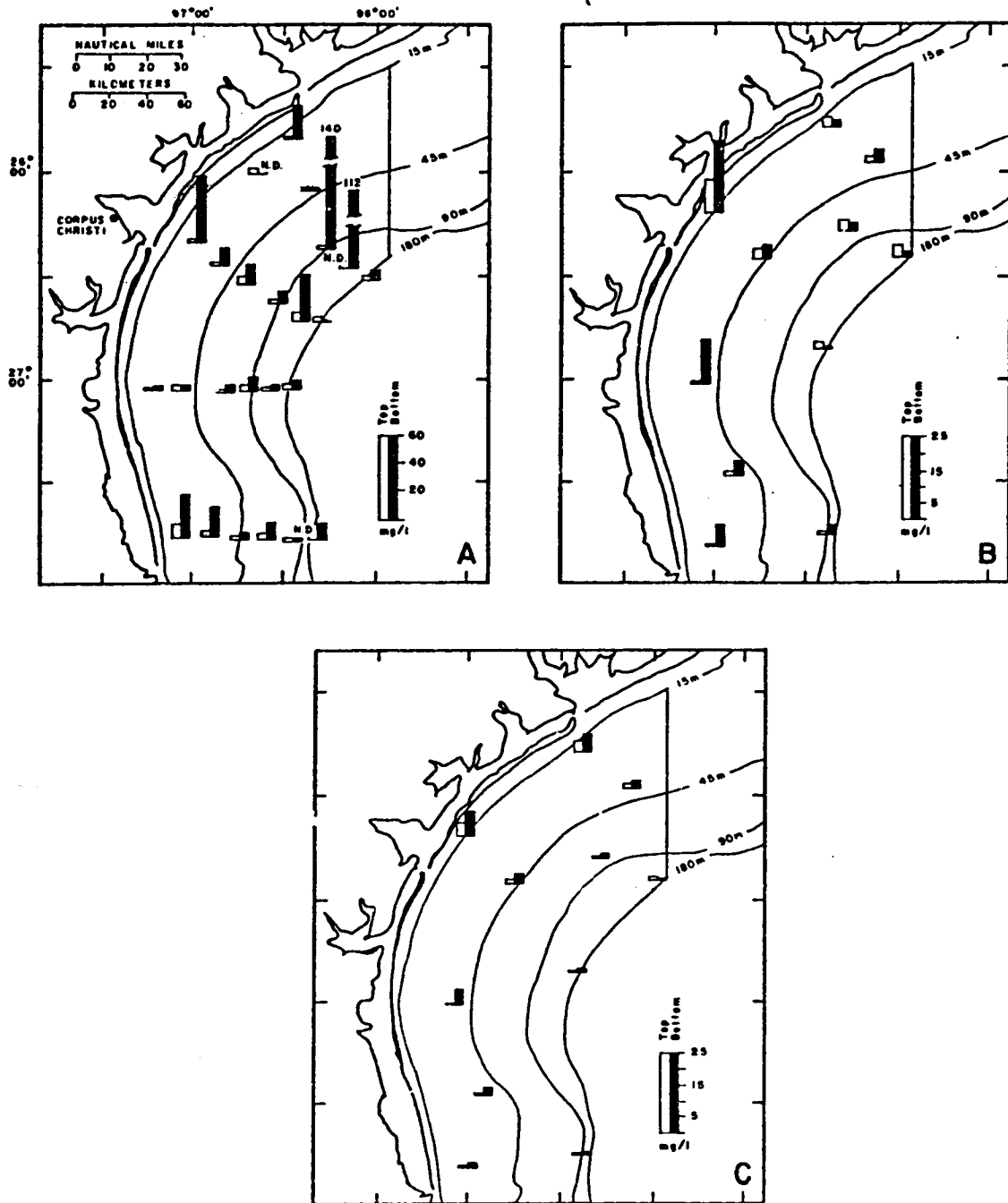


Figure 48. Amounts of suspended sediment; A. November 1974; B. November 1975; C. May 1976.

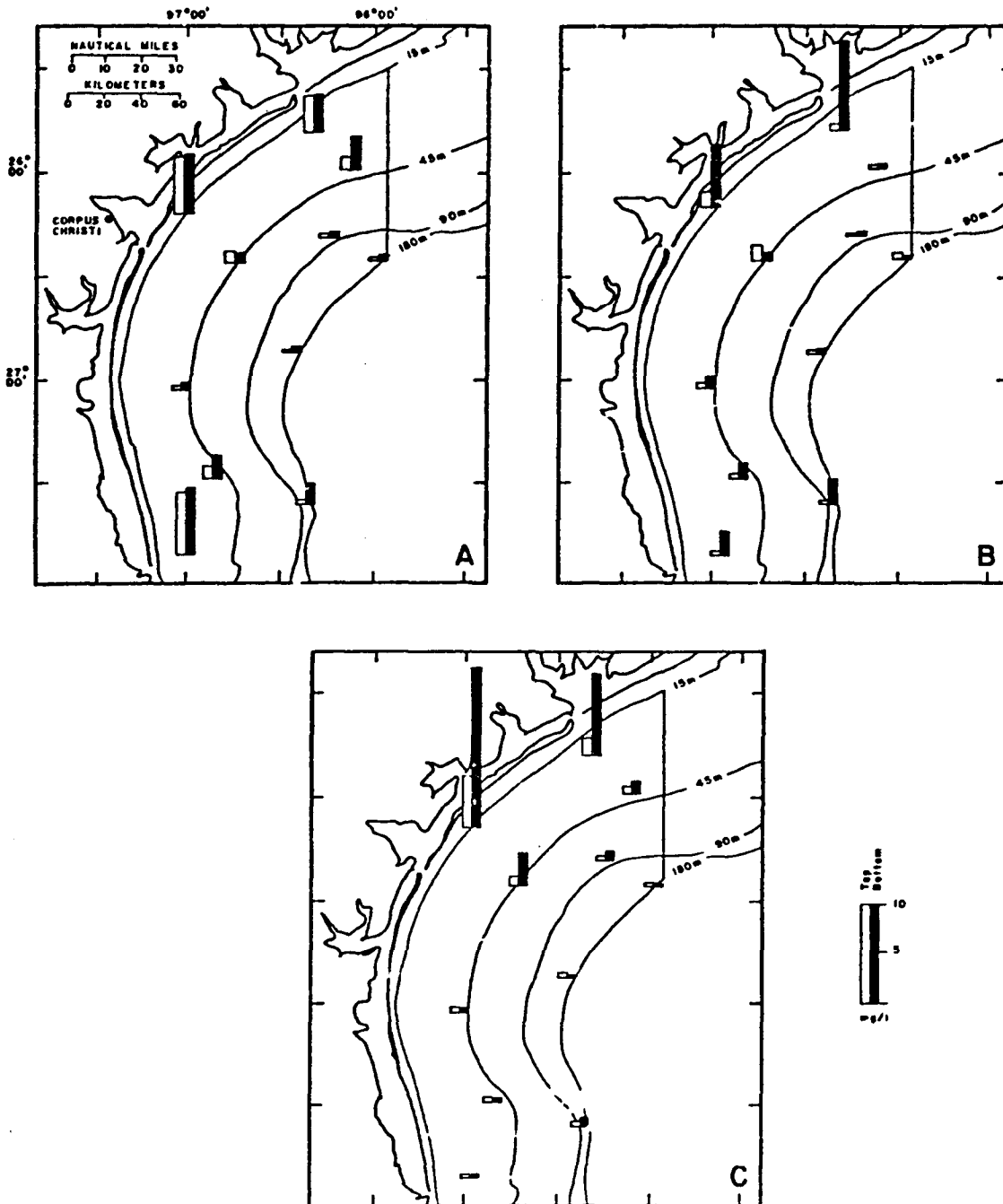


Figure 49. Amounts of suspended sediment:
 A. November 1976; B. March 1977;
 C. May 1977.

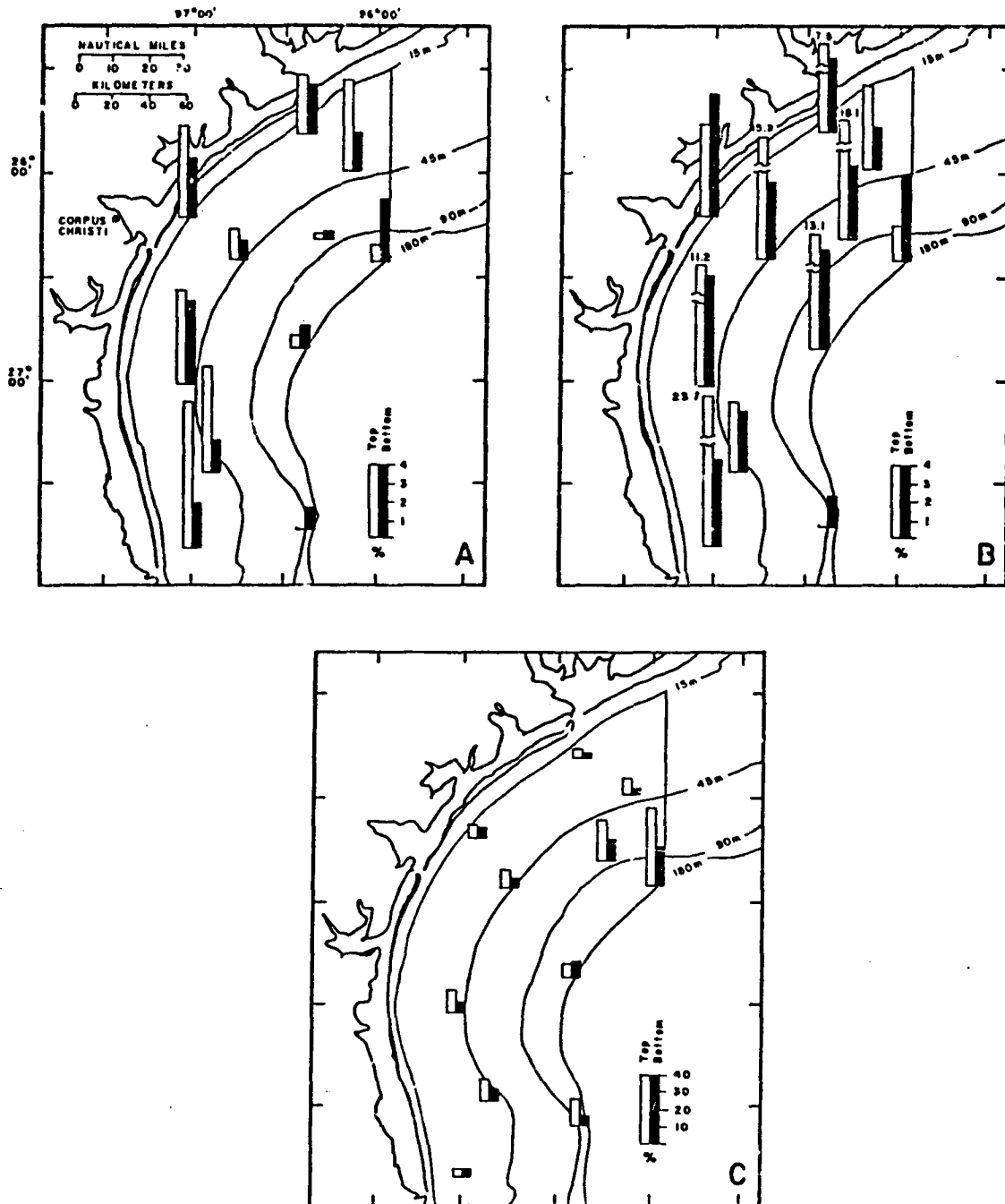


Figure 50. Percentage total particulate carbon in suspended sediments: A, November 1975; B, May 1976; C, November 1976.

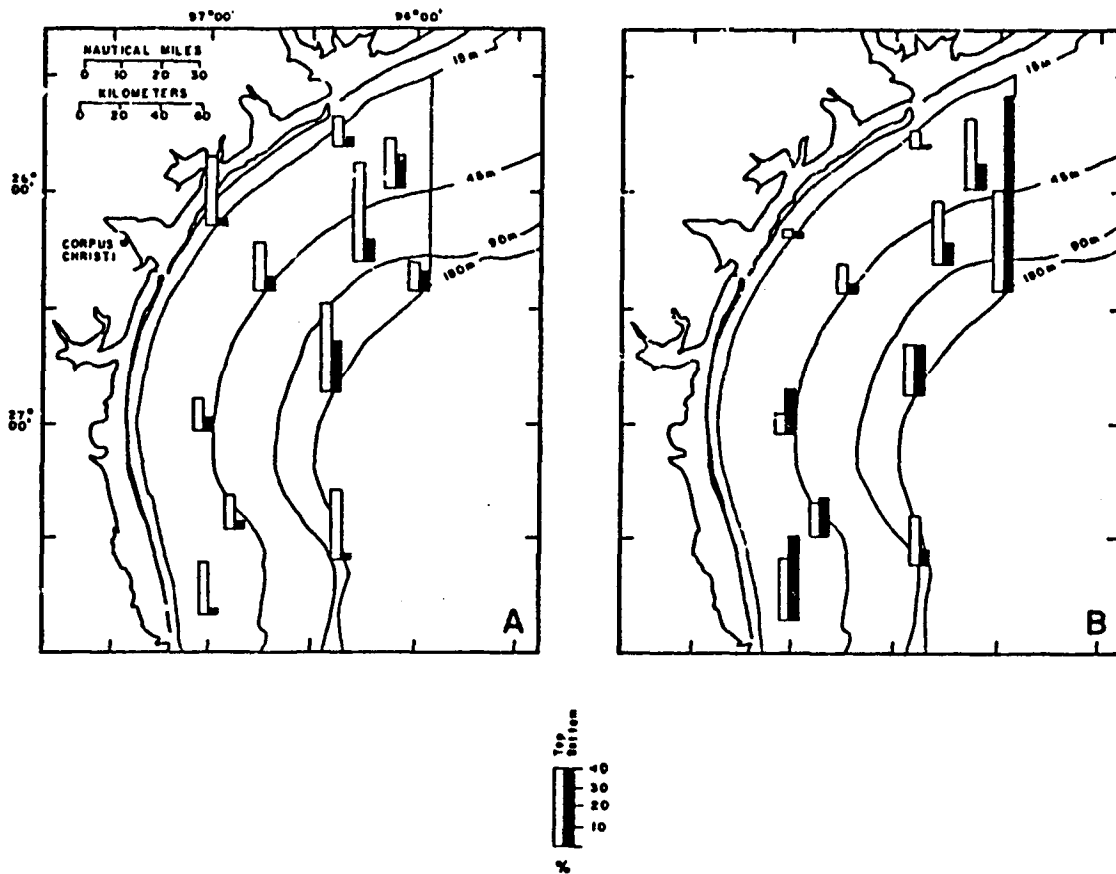


Figure 51. Percentage total particulate carbon in suspended sediments: A. March 1977; B. May 1977.

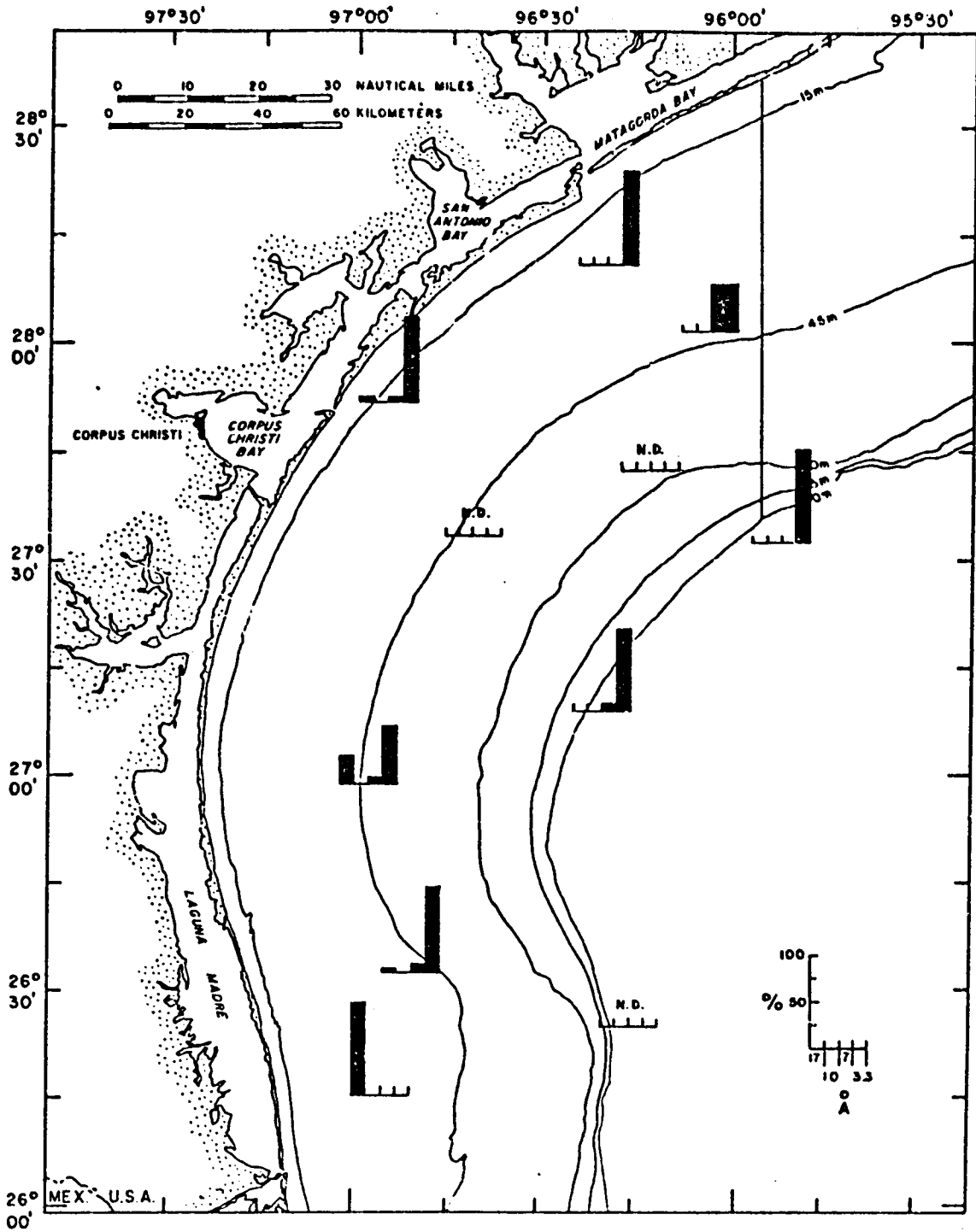
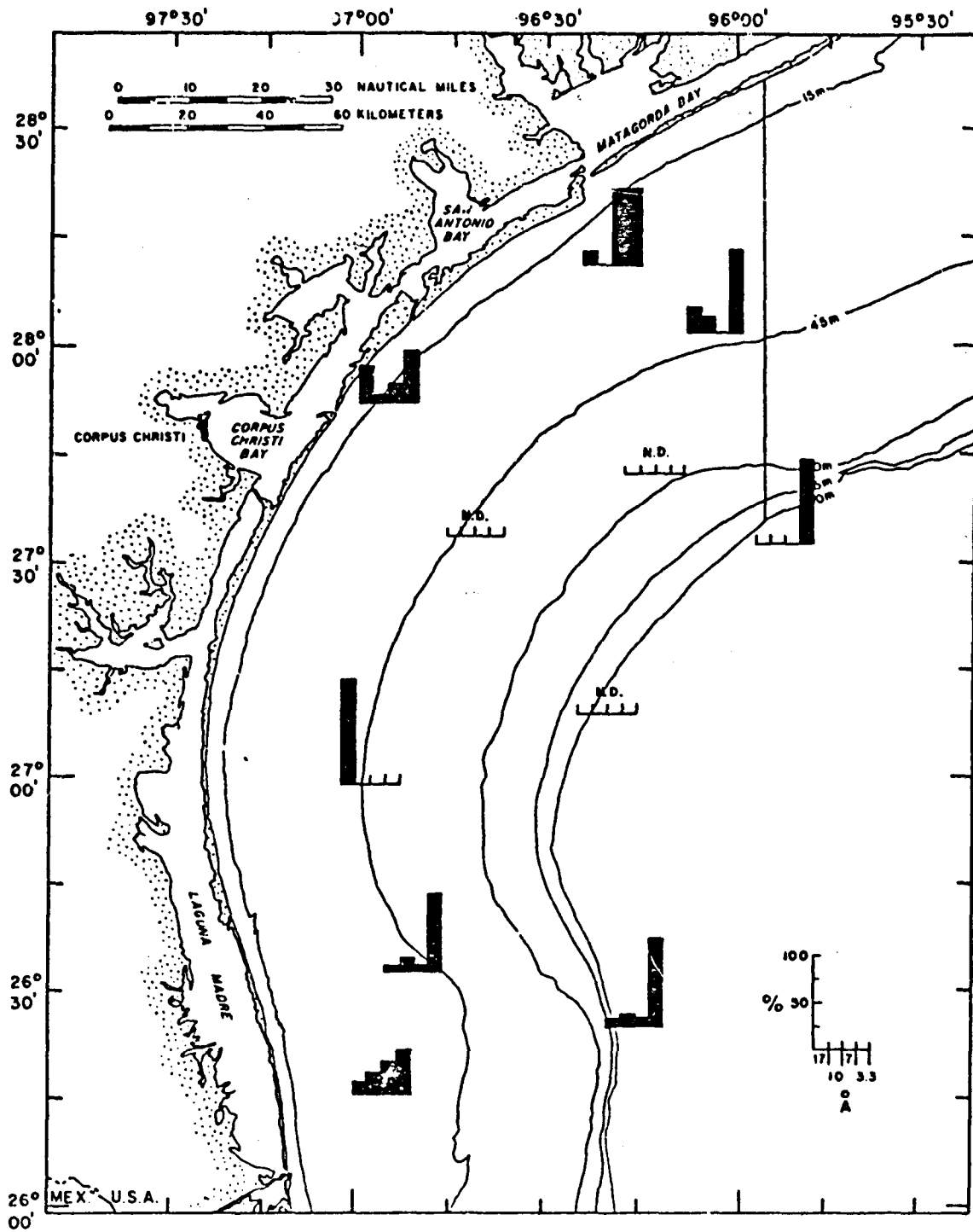


Figure 52. Percentage of clay minerals in suspended sediments, November 1975, one m below the air-water interface.



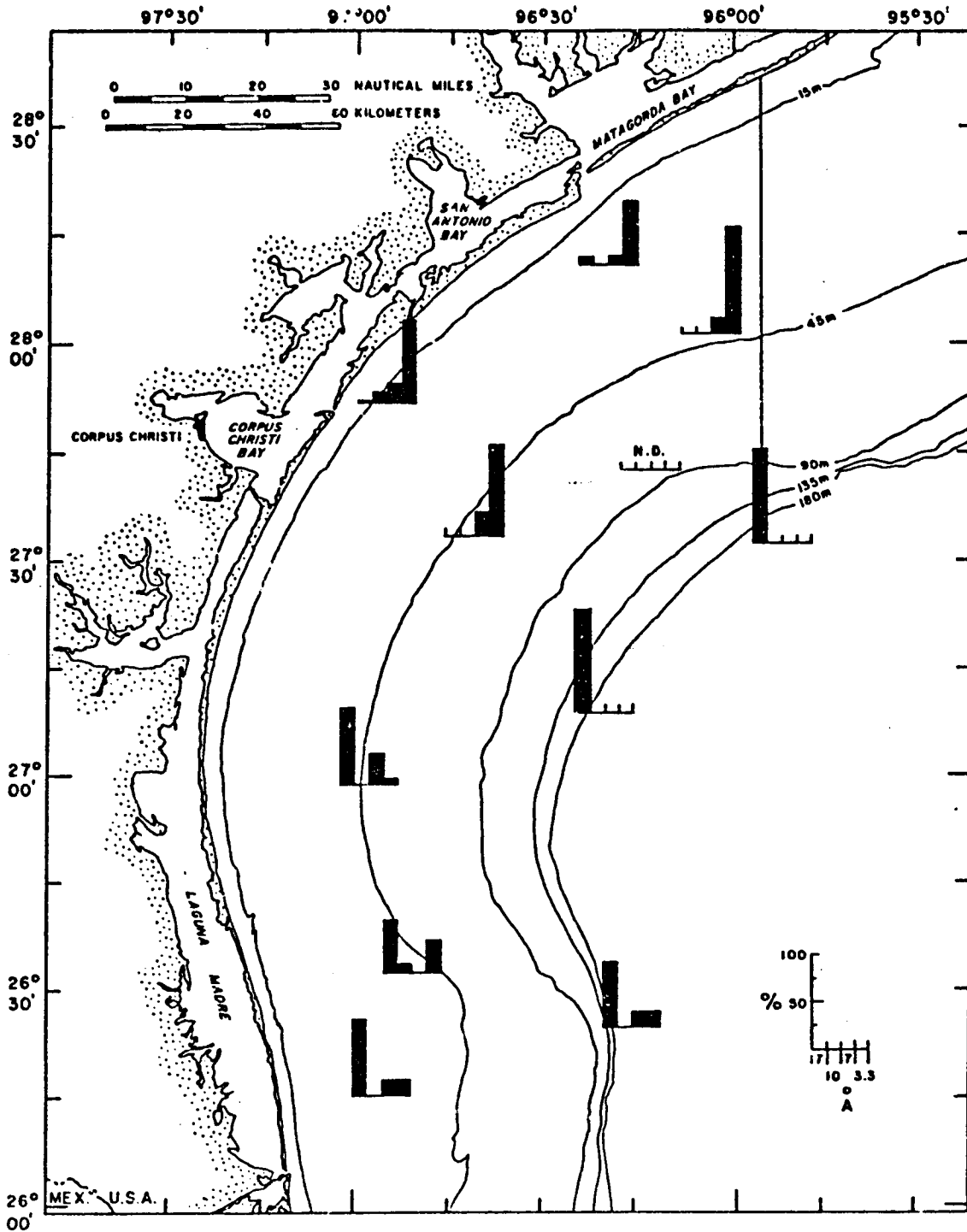


Figure 54. Percentage of clay minerals in suspended sediments, May 1976, one m below the air-water interface.

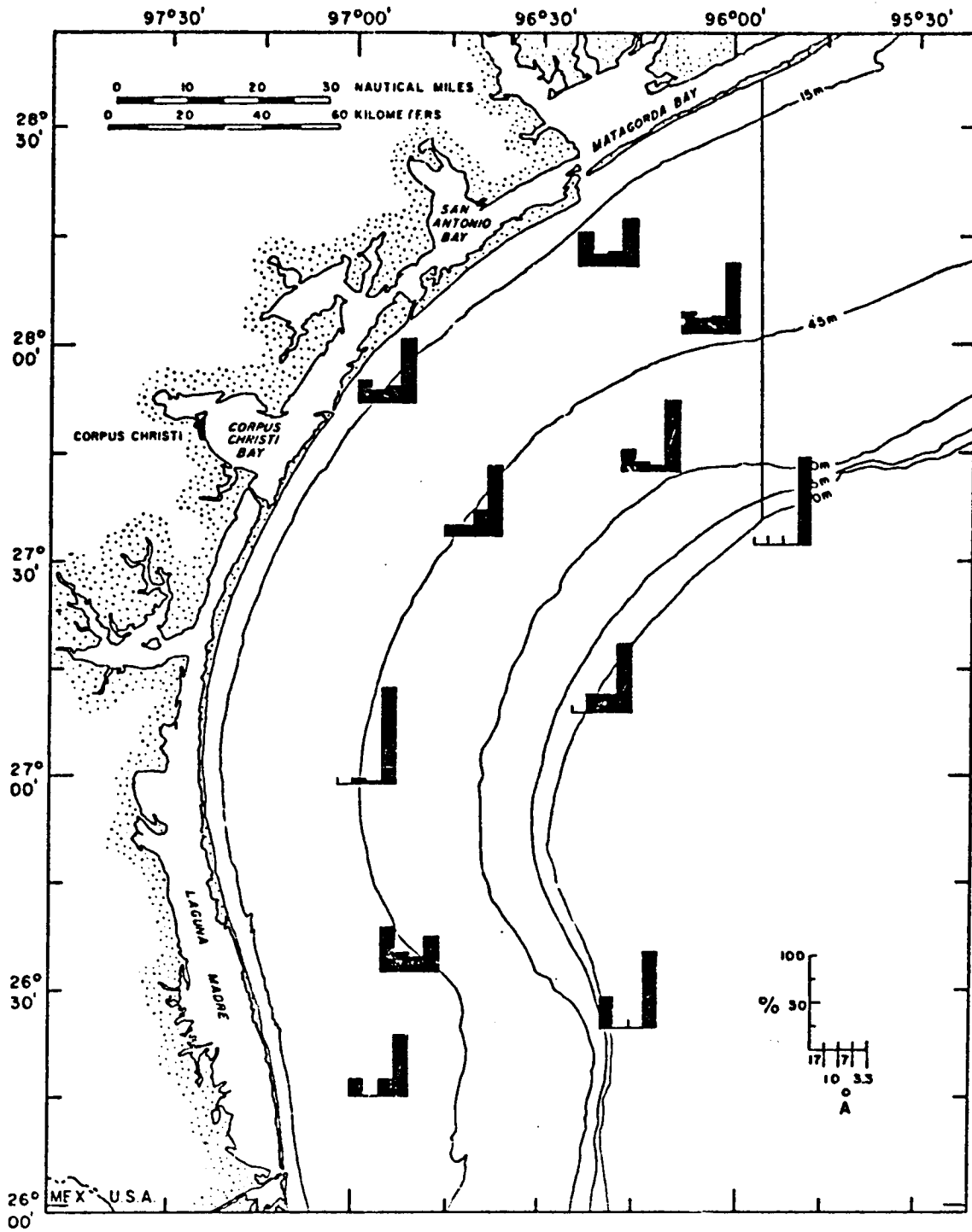


Figure 55. Percentage of clay minerals in suspended sediments, May 1976, one m above the sea-floor surface.

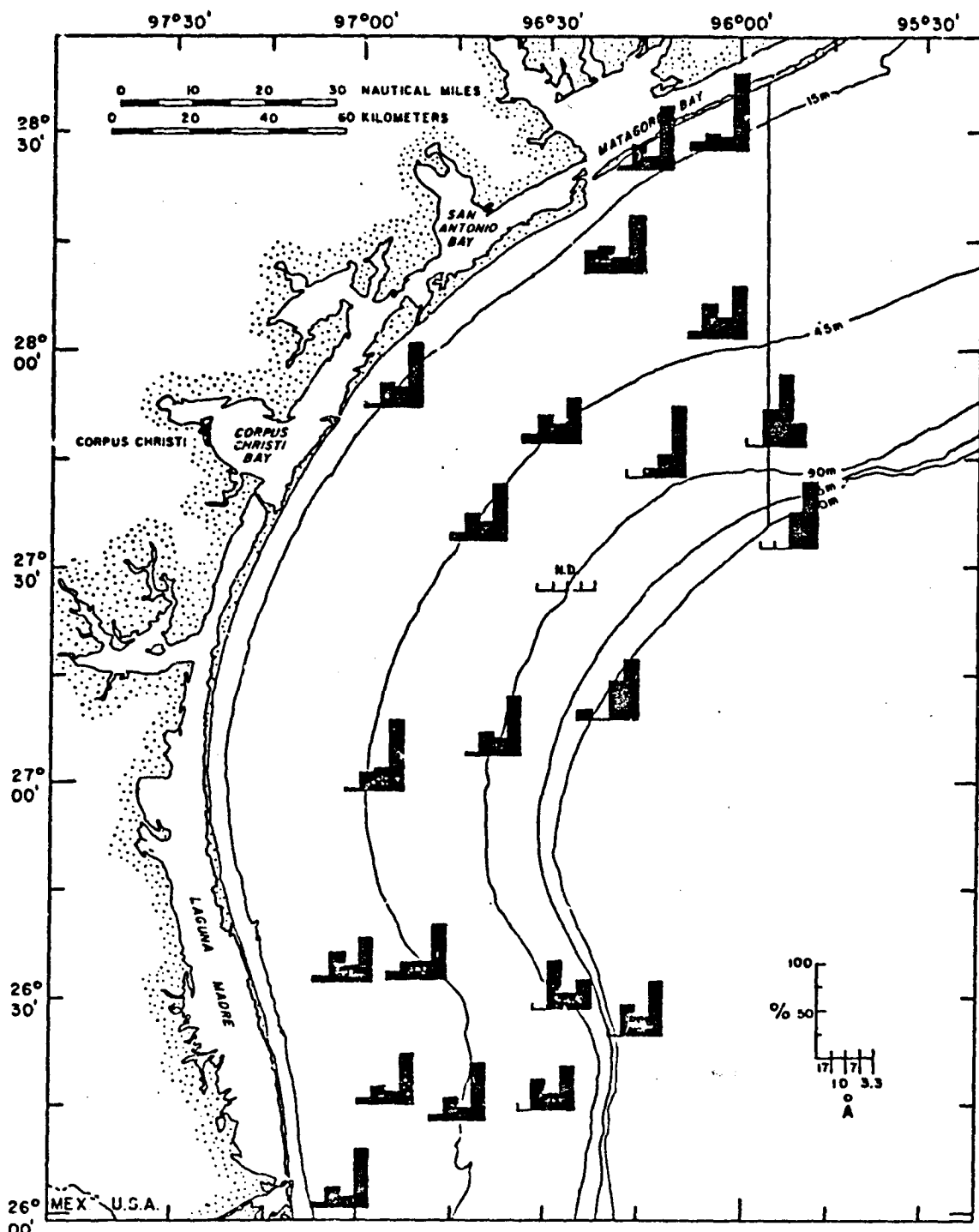


Figure 56. Percentage of clay minerals in suspended sediments, November 1976, one m below the air-water interface.

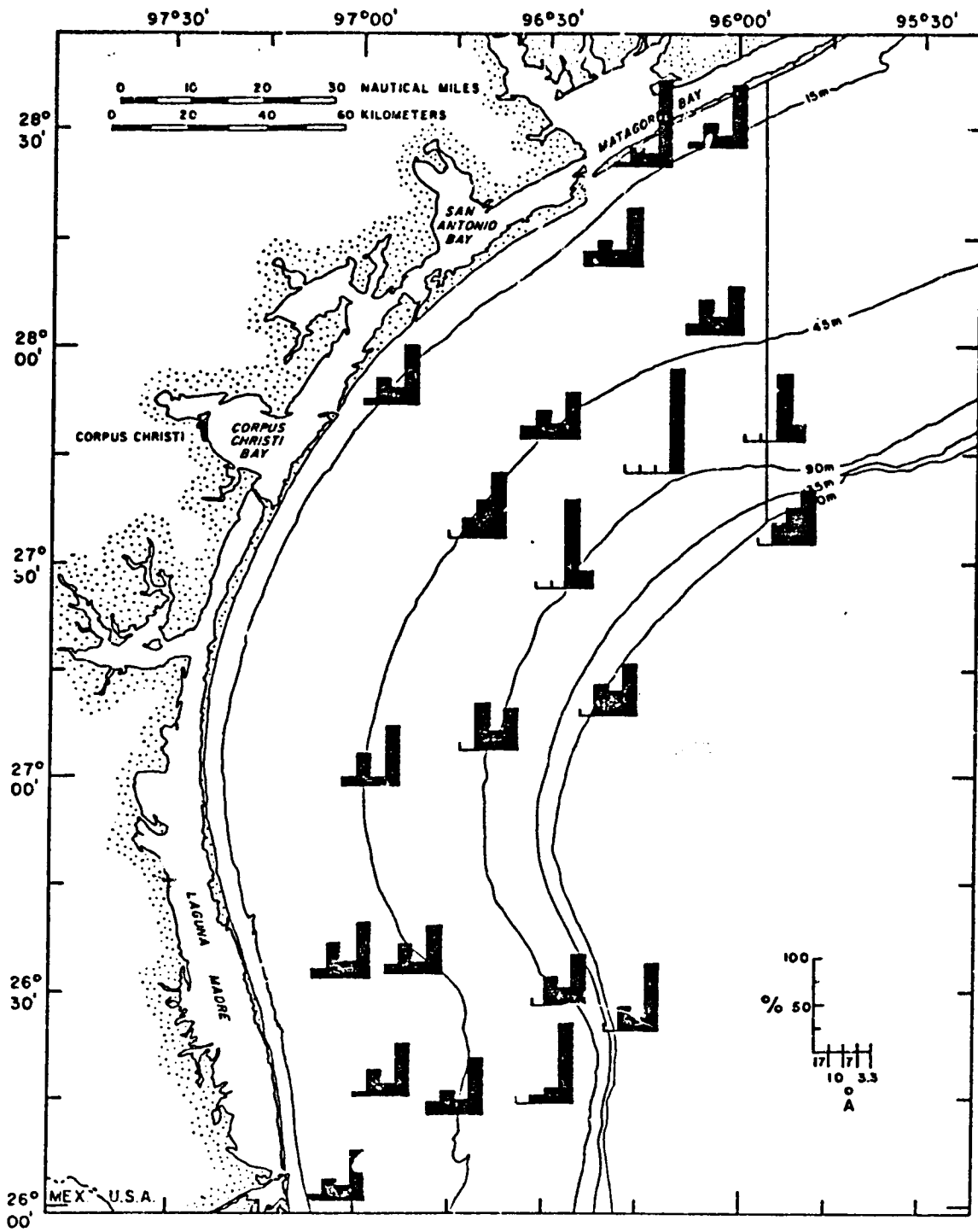


Figure 57. Percentage of clay minerals in suspended sediments, November 1976, mid depth.

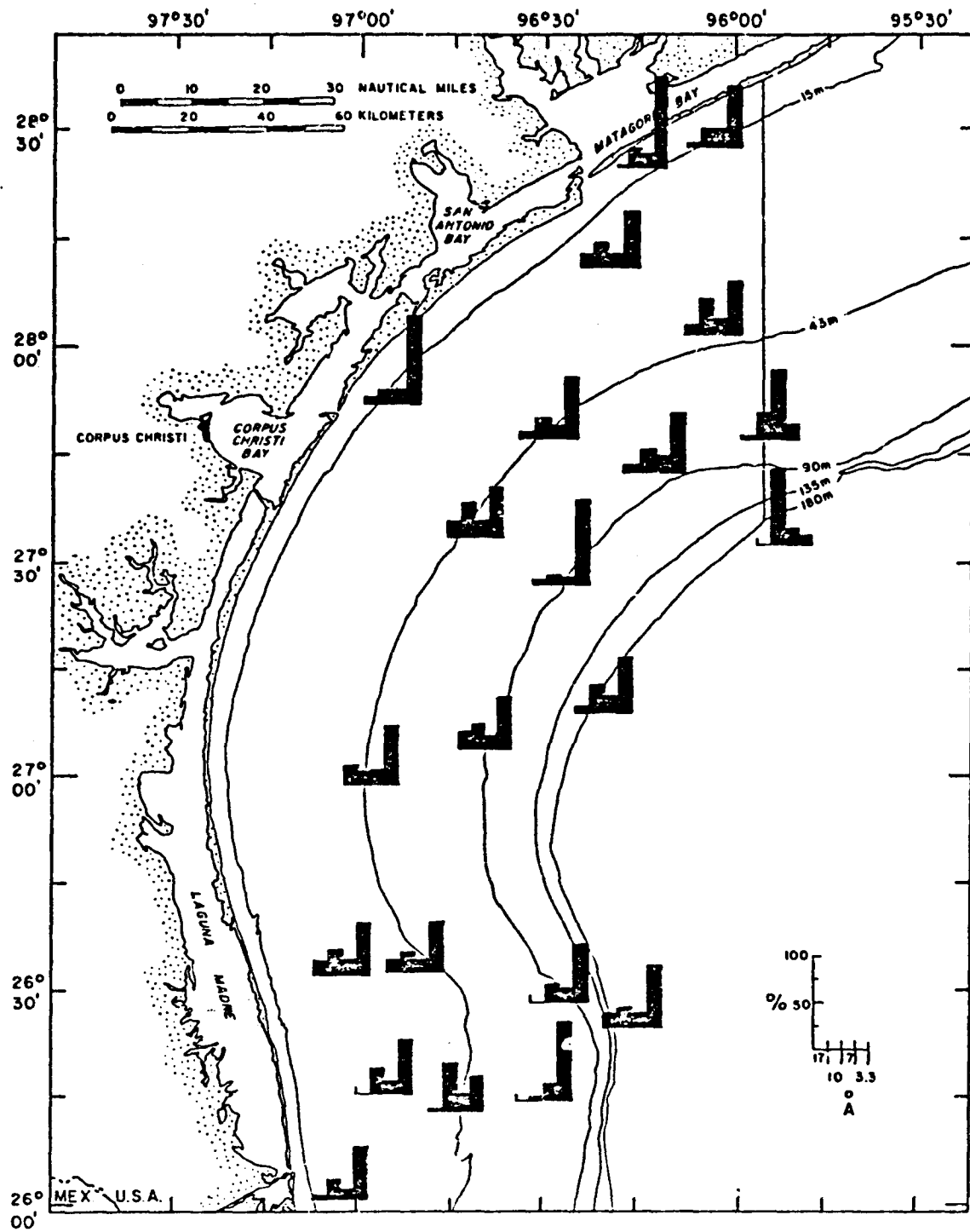


Figure 53. Percentage of clay minerals in suspended sediments, November 1976, one m above the sea-floor surface.

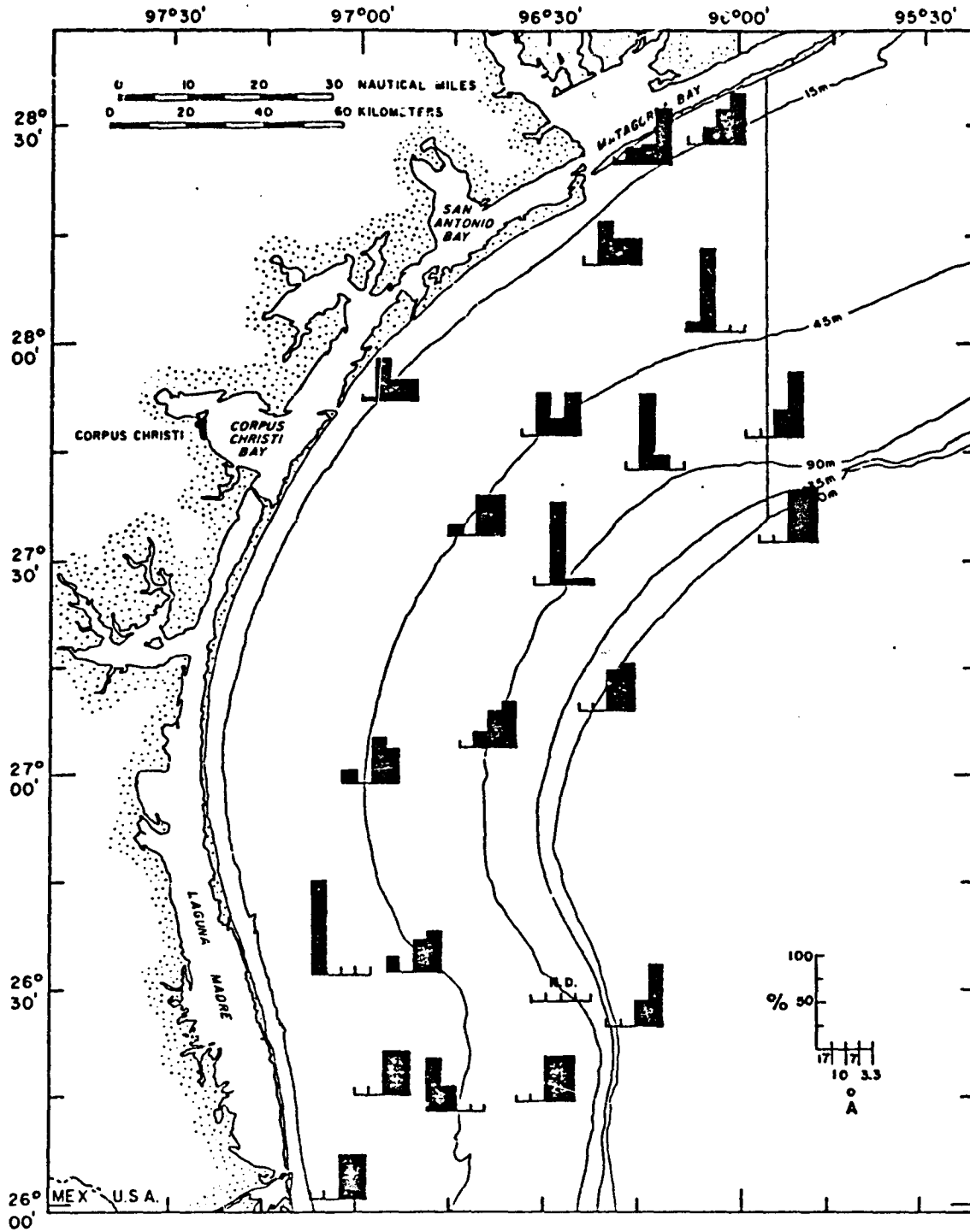


Figure 59. Percentage of clay minerals in suspended sediments, March 1977, one m below the air-water interface.

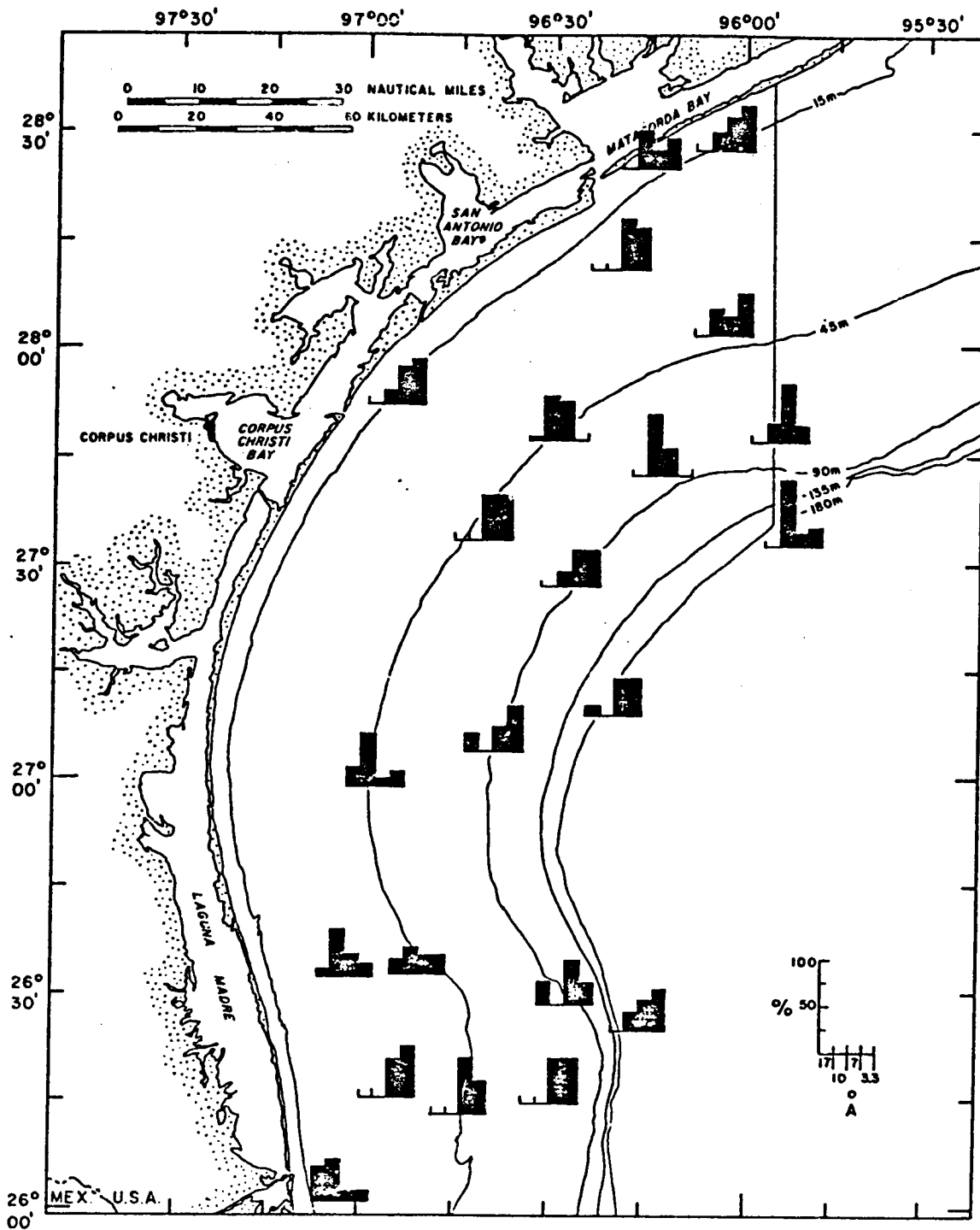


Figure 60. Percentage of clay minerals in suspended sediments, March 1977, mid depth.

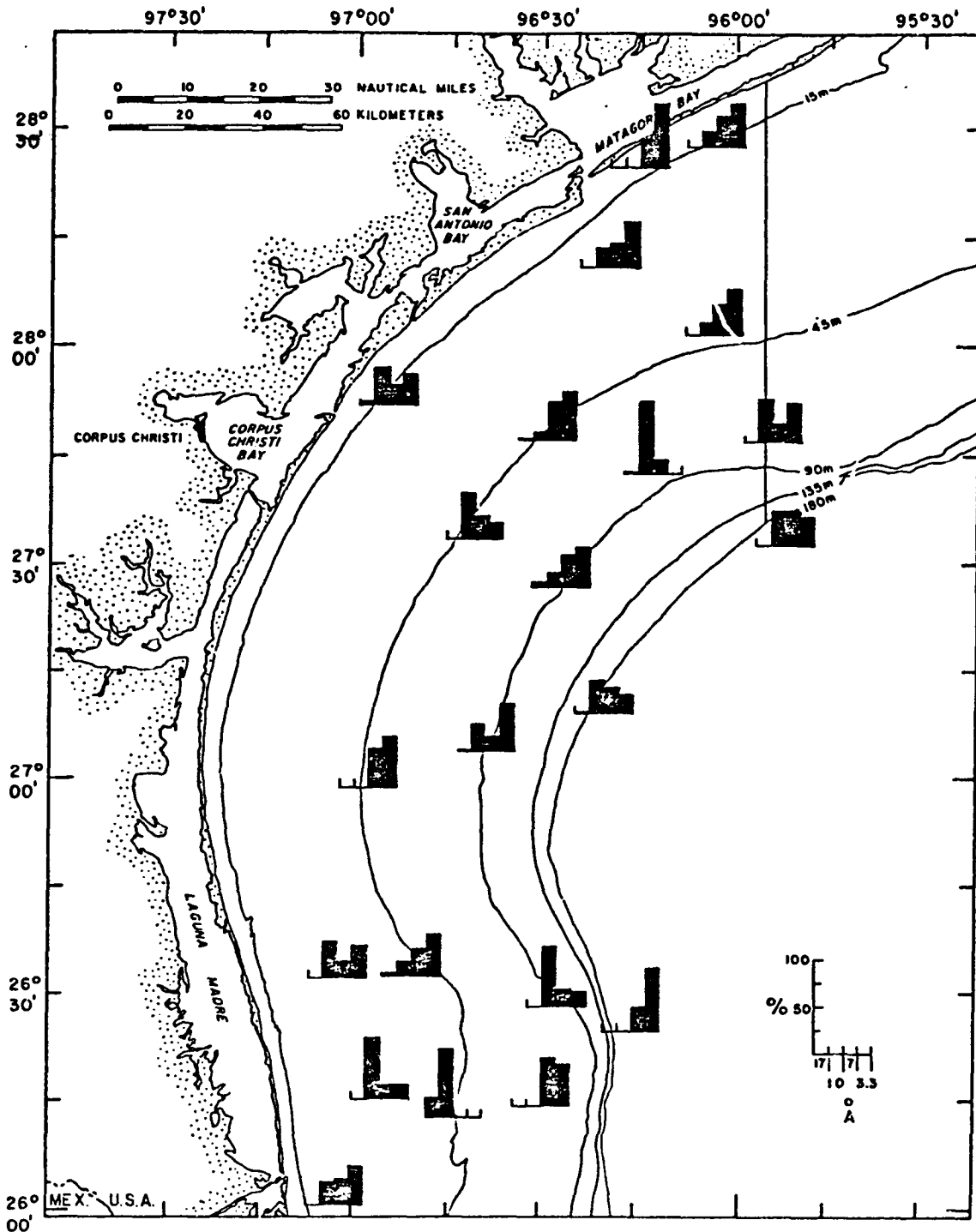


Figure 61. Percentage of clay minerals in suspended sediments, March 1977, one m above the sea-floor surface.

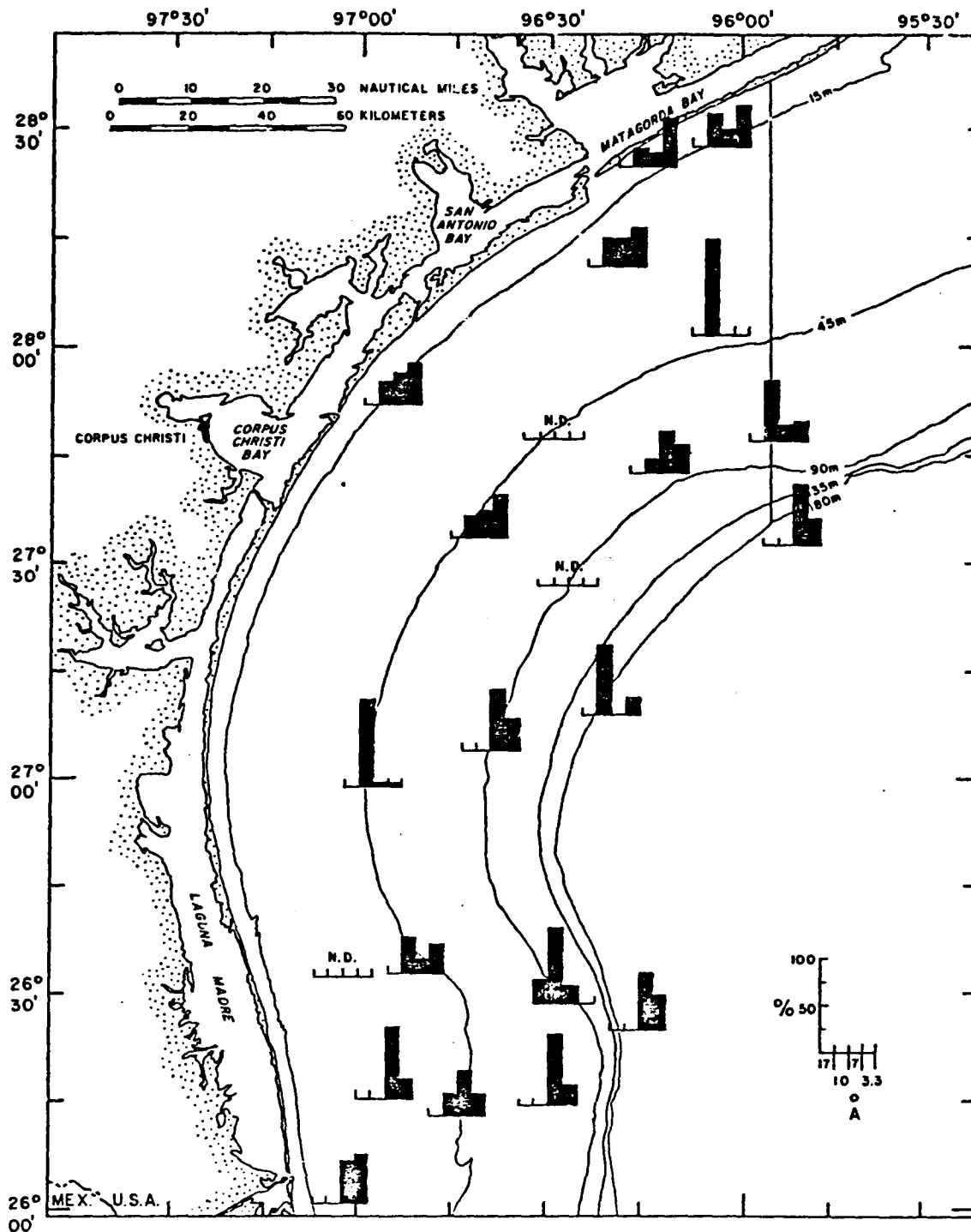


Figure 62. Percentage of clay minerals in suspended sediments, May 1977, one m below the air-water interface.

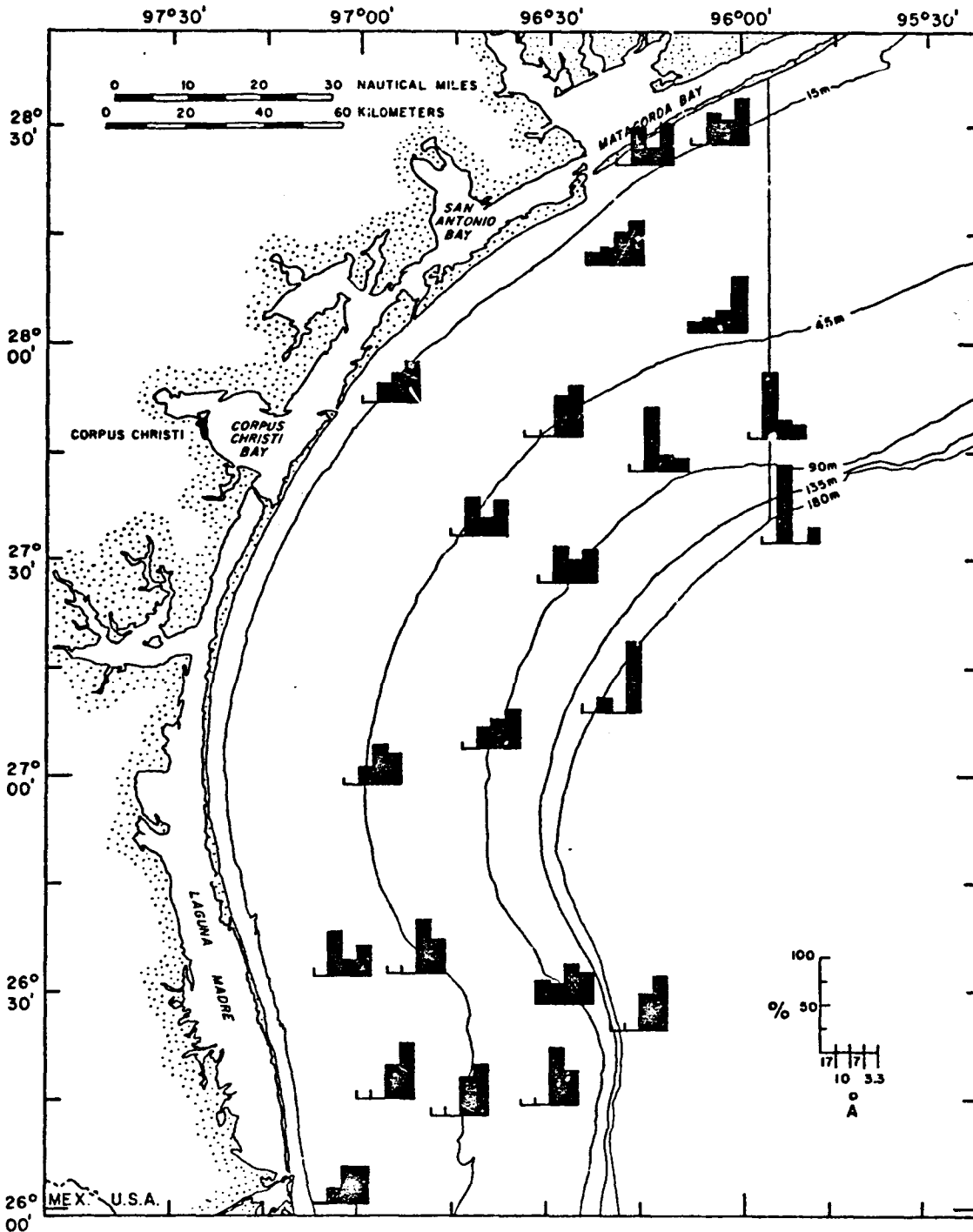


Figure 63. Percentage of clay minerals in suspended sediments, May 1977, mid depth.

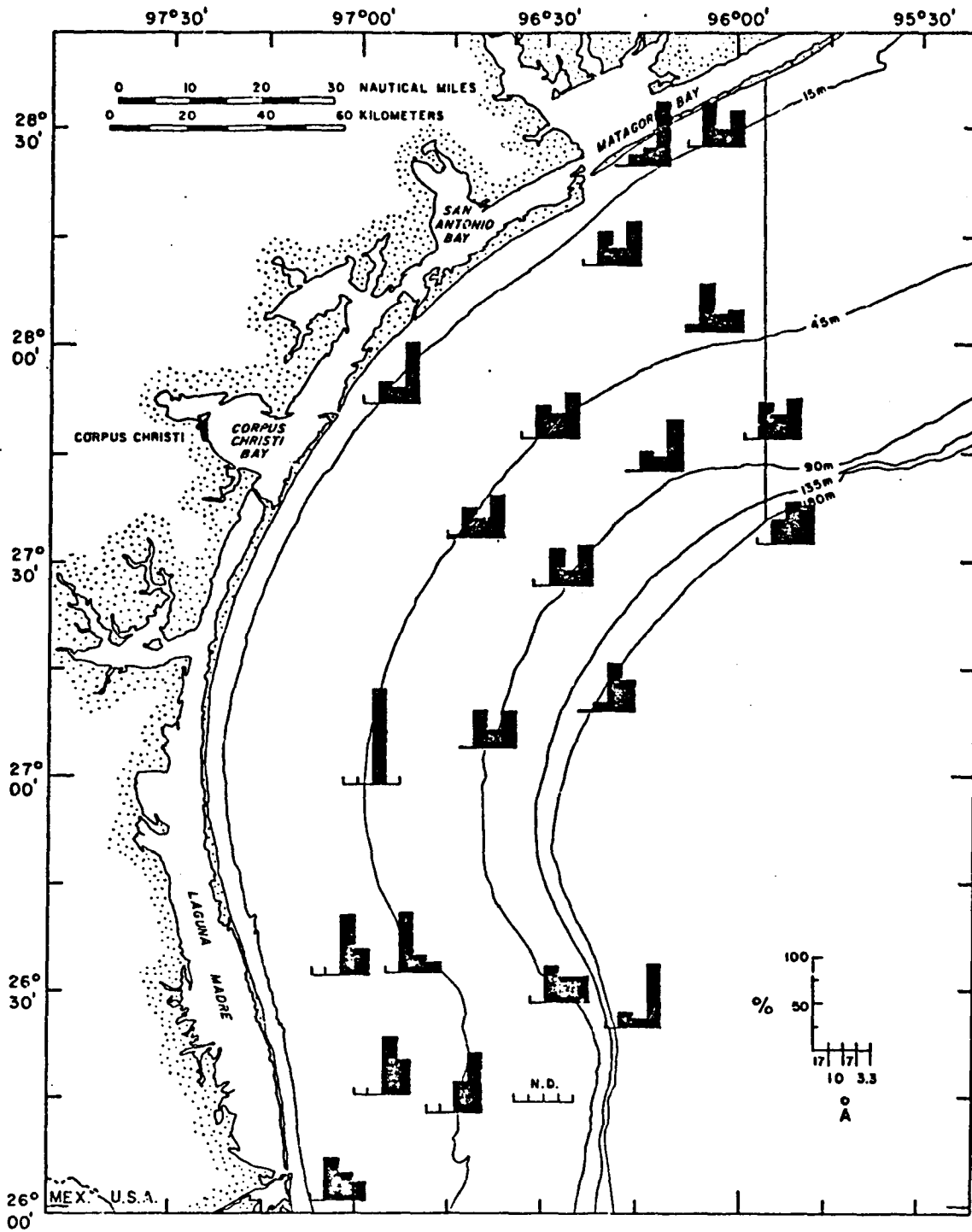


Figure 64. Percentage of clay minerals in suspended sediments, May 1977, one m above the sea-floor surface.

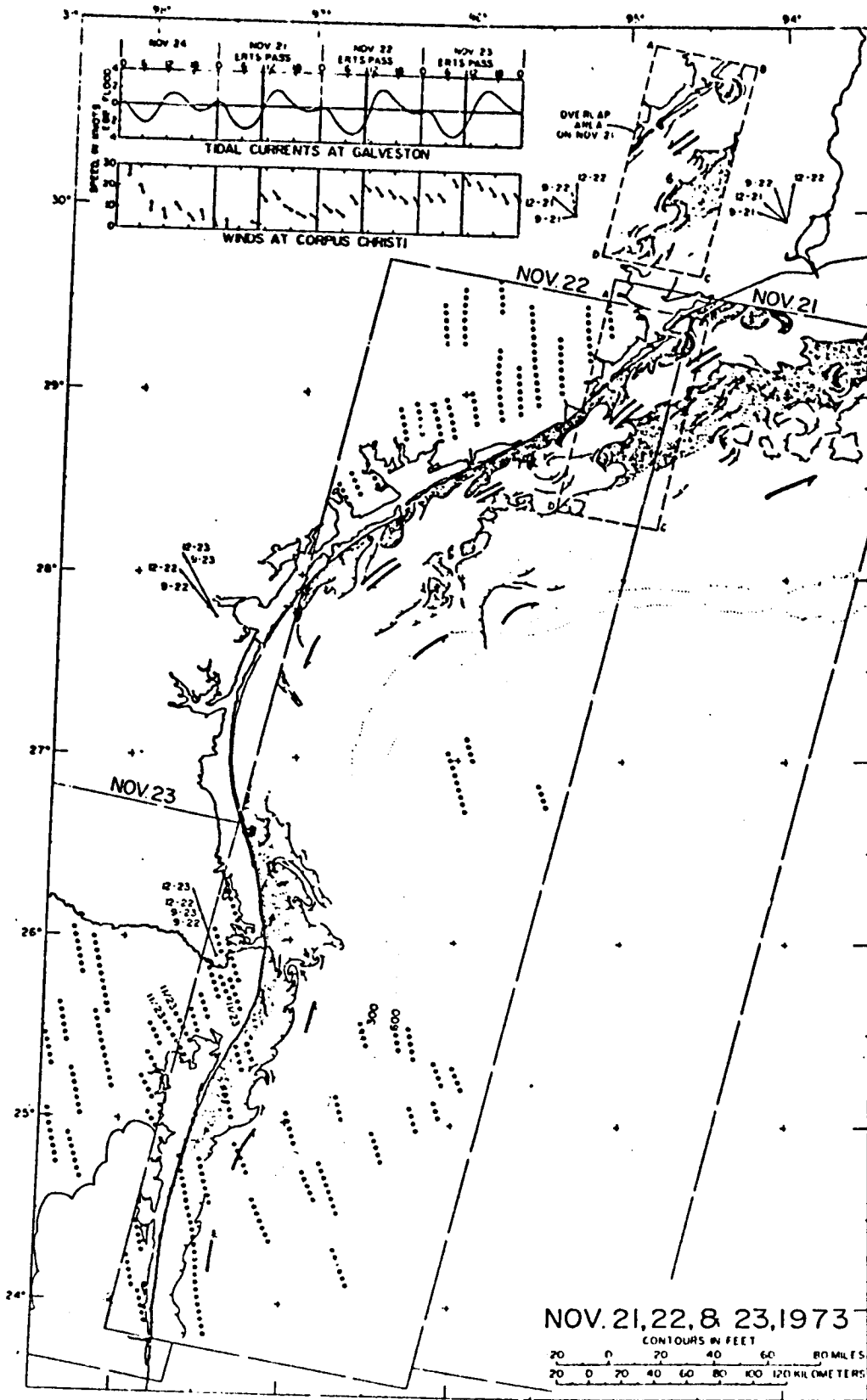


Figure 65. Distribution of suspended material on the Texas continental shelf based on Landsat imagery.

Sediment Concentration

With the exception of the sampling done near Pass Cavallo in November 1975, the highest concentrations of suspended sediment for all sampling periods lie on the inner shelf near the mouths of estuarine systems, a fact supported by the Landsat I data (Hunter, 1976). Moderate sediment concentrations are indicated in the waters over the ancestral Rio Grande delta with a slight decrease in concentration toward the shelf edge. A significant increase in sediment concentration is strongly suggested in the bottom waters along the shelf edge in the fall and early spring, a condition which may be attributed to higher energy during this period coupled with internal waves and tidal forces.

Samples obtained in the fall of 1974 had significantly more sediment within the water column than those of subsequent years. A shift in the national weather pattern during 1975 and 1976 apparently caused climatic moderation along the Texas coast after 1974.

Organic Carbon

The relative amounts of organic and inorganic carbon in the percent total particulate carbon were determined at each station. Regionally, the organic carbon content is higher and the stratification of organic content is more apparent during the late spring when energy conditions needed to transport inorganic constituents and contributions from land sources are at a minimum. Organic content is generally greater in surface water because bottom water is diluted by inorganic material.

Mineralogy

Three major clay types and "quartz" have been identified by X-ray analyses. In some inner shelf samples, feldspar and calcite were also recognized. During the 1974 sample period, the expandable clay mineral identified by its 17Å "d" spacing upon glycolation was present only in the northern portion of the study area. The predominant clay mineral over the rest of the shelf was a 10Å mineral interpreted to be illite. In the subsequent fall samples and in May 1976 and March 1977, 17Å material was detected over the entire shelf. The May 1976 samples along the shelf edge contain 17Å material associated with high organic carbon content, suggesting material of biologic origin. This substance may be attributed to expandable material associated with diatoms (van Bennekom and van der Gaast, 1976). In November 1976, 17Å material was detected at most stations but the largest concentrations were in the northern part of the OCS.

The other clay minerals were measured in varying amounts throughout the region during every sampling period. In the fall of 1974, however, the 10Å clay mineral dominated. Subsequent samples taken during 1975-1977 showed the 3.34Å mineral (quartz) to be the dominant mineral. This discrepancy probably is attributable to the source material. During the fall of 1974, the water column contained a large amount of terrigenous sediment that was diminished in subsequent years. Thus the mineralogy reflected the high concentration of land-derived material. In the 1975 to 1977 period, when land-derived material was less concentrated in the water column, the mineralogy was dominated by water-derived sediment. Diatoms can produce a diffuse X-ray pattern similar to that determined for the suspended sediment in the south Texas region (Gregg and others, 1977). Thus it appears likely that the dominance of the

3.34Å peak is caused by a quartz-like material produced by diatoms in the water column. The 10Å and 7.1Å materials in the 1975, 1976, and 1977 samples follow no discernible pattern except that the 10Å material is usually predominant. Occasionally only 7.1Å material was detected because the filtrate samples were so small that the 10Å or 17Å material, even if present, were below detection limits.

Sea-floor Sediment

Like the suspended sediment, all three clay mineral groups were present in the fine clay fraction (<2 μ). The dominant clay material was the expandable minerals of the montmorillonite group (fig. 66). These minerals made up from 34 to 70 percent of the clay substances present. The distribution over the entire study area is typically around 60 percent ±5 percent. The range of variability indicated is within the analytical error, indicating a rather homogeneous clay mineral suite for the entire shelf. The composition is in agreement with previously published studies in the Gulf of Mexico (Pinsak and Murray, 1960).

MINERALOGY OF SUSPENDED SEDIMENT VERSUS SEA-FLOOR SEDIMENT

Examination and comparison of the data for the three years suggests a significant difference between the mineralogical composition of the clay suspended material and of that in the sea-floor sediment. The difference suggests that illite dominates the suspended sediment whereas montmorillonite dominates the bottom sediments (Jacobs and Ewing, 1969). Tscholke (1974) suggested that such variances are the result of the X-ray preferentially detecting the larger illitic material to the exclusion of the montmorillonitic

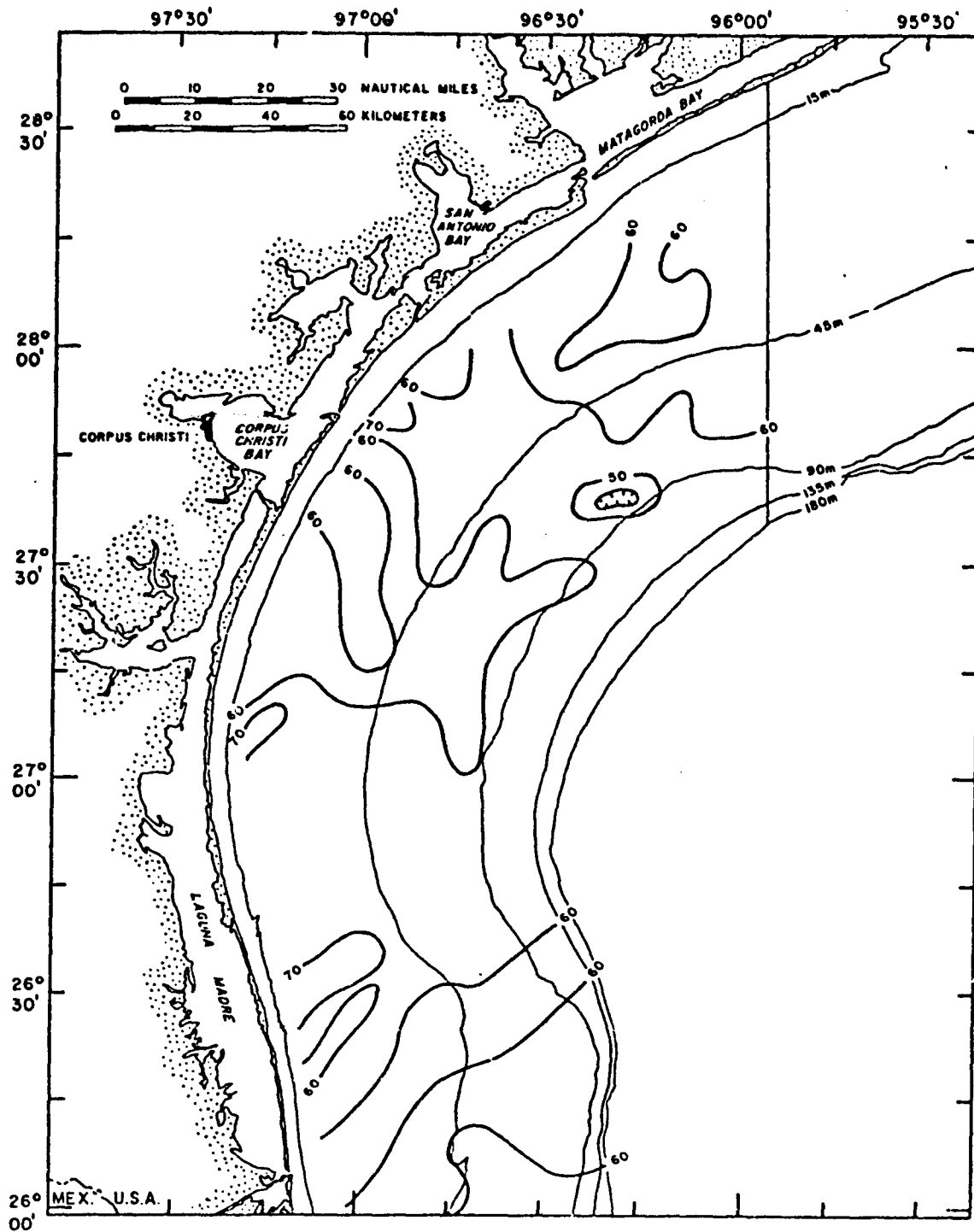


Figure 66. Percent expandable clay in bottom sediments.

substances. Experimentation by Holmes (1977) suggested that such discrimination does not take place on the instrument used in this investigation.

Shideler (1977) has indicated that the dominant size of the suspended material is very fine silt. When this size fraction of the bottom sediment is analyzed, the 10\AA (illite) material dominates as it does in the suspended fraction. The samples that contain significant 17\AA material correspond to samples of the finest suspended sediment. Thus the differences between the reported clay mineral composition and the suspended sediment are an artifact of the analytical procedure, and the material in the water column does mirror that on the sea floor. The composition of the suspended sediment, then, is indicative of the energy conditions on a regional basis and clearly is helpful in the interpretation of the physical processes of sedimentation on the shelf. In the case of the south Texas shelf, significant 17\AA material in the water column indicates a large influx of land-derived detrital material flushed out of the bays. In contrast, dominant 10\AA material in the water column indicates sea-floor derived sediment. Such information can be useful in tagging sediment plumes to their source if two adjacent water masses have different types of clay minerals.

SEA-FLOOR SEDIMENTS

PHYSICAL CHARACTERISTICS

Seasonal Variability of Texture

by

Gerald L. Shideler

Surficial benthic sediment samples were taken during 1977 to determine seasonal variations in sea floor texture in support of other ongoing chemical and/or biological phases of the STOCS program.

Methods

Three seasonal sample suites (winter, spring, summer/fall) were collected along four monitored transects (fig. 67) by the University of Texas Marine Science Institute at Port Aransas. The U.S. Geological Survey did not participate in either the site selection or field work phases of this effort. The three seasonal suites, each containing approximately 50 samples, were analyzed for grain size by the USGS Corpus Christi office.

Laboratory procedures

Laboratory procedures used for determining grain size were as follows:

1. Initial Drying - The original sample was air-dried, and the entire sample was used for analysis.
2. Oxidation of Organic Matter - Carbonaceous organic matter was removed from the sample by oxidation with a 30 percent hydrogen peroxide solution, a step necessary to eliminate potential errors in the COULTER COUNTER analysis of the mud fraction.

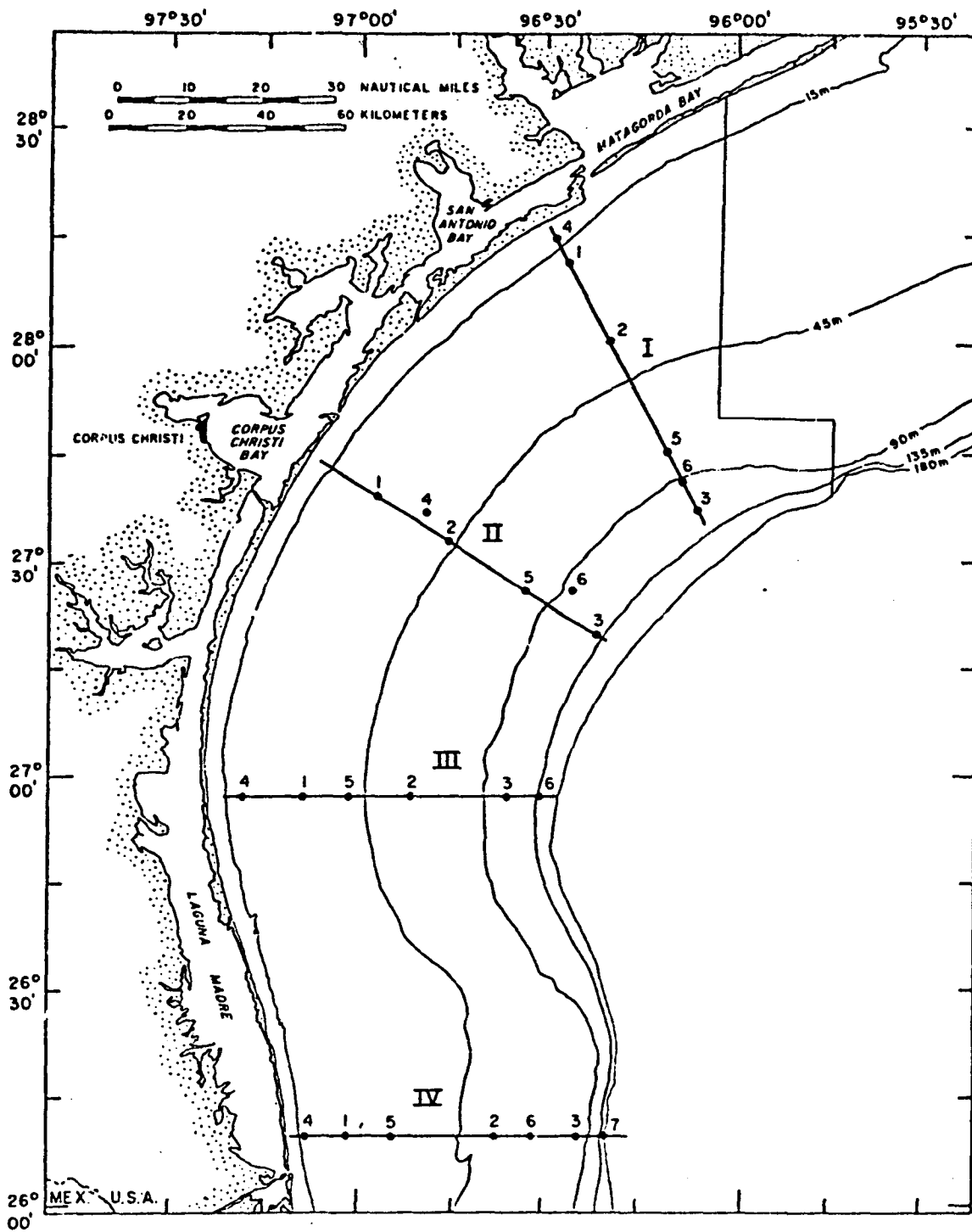


Figure 67. Location of bottom stations for seasonal sampling.

3. Desalinization - Soluble salts were removed from the oxidized sample by washing in 800 ml of distilled water. The sample was agitated, then allowed to settle undisturbed for a minimum of 60 hours. The supernatant wash water was then siphoned off without disturbing the sediment. This step eliminated the weight of salt crystals and allowed sediment dispersion.
4. Final Drying and Weighing - After removal of organic matter and soluble salts, the clean sample was oven-dried at less than 40°C to avoid baking the clay fractions. A final work sample weight was then obtained to within 0.01 g, under the normal ambient temperature and humidity conditions within the USGS Corpus Christi laboratory.
5. Disaggregation and Dispersion - The final work sample was physically disaggregated, then dispersed by soaking in 500 ml of a standard CALGON solution (5 g/liter). The suspension was thoroughly mixed and allowed to settle for 24 hours, then checked for flocculation. If dispersion was complete, the sample was then wet-sieved.
6. Wet Sieving - The dispersed sample was washed through a set of 2 mm (#10) and 63 µm (#230) U.S. standard sieves. The sample was fractionated into gravel (>2 mm), sand (2mm - 63 µm), and mud (<63 µm) fractions; the mud fraction was brought to a standard 800 ml volume.
7. Percentage Determinations - The sand and gravel fractions were washed, oven-dried, and weighed; the percentages of sand, gravel, and mud comprising the total sample were then determined.
8. Settling Tube Analysis (Sand) - The grain-size distributions of sand fractions were determined with a rapid sediment analyzer (RSA) at a half-phi interval. The instrument employs a settling tube 1 m in length, with an 8 cm internal diameter. The settling tube assembly is a modified version of the basic model described by Schlee (1966).

Modifications include incorporation of a different model transducer and the use of a manual sediment introduction device, rather than a motor-driven device. Accessory equipment include a HEWLETT-PACKARD amplifier (Model 321), and a HEATH-SCHLUMBERGER strip-chart recorder (Model EU-205-11). Sediment fall times were converted to phi-size cumulative percentages at a 0.5 ϕ interval by employing the fall time-size overlay technique described by Schlee (1966).

In conducting an analysis, a representative sample of the sand fraction was obtained with a microsplitter. Efforts were made to use 3 gm samples; however, if the total sediment had an insufficient sand content, smaller RSA samples were utilized. Sediments with sand fractions comprising less than 0.4 percent of the total sample weight were considered as "pure mud" texturally; the bulk weight of sand in such samples was so minute (<0.5 g) that it was beyond the capability of the RSA instrument to provide reliable size analyses of the sand fractions. All techniques of sediment introduction, recording, and analog curve interpretation were standardized to minimize operation bias. The recorder sweep speeds employed were 2.5 sec/cm for the first 35 seconds, 5 sec/cm from 35 to 100 seconds, and 10 sec/cm after 100 seconds. All analyses were conducted within a 21-24°C temperature range. On the basis of replicate analyses, the RSA exhibited a precision of ± 2.3 percent in determining Folk's (1965) graphic mean diameters.

9. COULTER COUNTER Analysis (Mud) - The grain-size distributions of the silt and clay fractions (<63 μm) were collectively determined at a half-phi interval electronically, employing a 16-channel model TA COULTER COUNTER. By conducting duplicate analyses with 200 μm and

30 μm tube apertures, the instrument effectively analyzed the 0.63-63 μm size range. The electrolyte consisted of a 4 percent CALGON solution, pre-filtered through a 0.2 μm filter.

For each sample, a 200 μm tube analysis was conducted first to determine the coarser half of the size frequency distribution. The dispersed mud suspension was homogenized in a 1000 ml beaker by agitation on a FLEXA-MIX vibrator equipped with a baffle. A representative sample of the suspension was obtained by sampling with an automatic micro-pipette from the top, middle, and bottom of the beaker. This sampling procedure was repeated until a standard sediment dilution level was achieved which resulted in less than 5 percent coincidence error. The sample was then electronically counted, and the relative percentages of particles in each size class within the operating range of the 200 μm tube (2-40 percent aperture diameter) were determined. During analysis, the sample was agitated and dispersed by a stirring motor operating at a standard speed. Since the state-of-the-art stirring apparatus could not be maintained at a constant number of revolutions per minute, the selected standard speed was just below the level that produced observable turbulence at the surface of the sample beaker.

After the 200 μm tube analysis, the analyzed suspension was then sieved through a 20 μm micro-mesh sieve, and re-analyzed with the 30 μm tube to obtain the finer half of the size distribution. The 30 μm tube analyses were conducted in an unagitated state and were completed within 2 hours of their respective 200 μm tube analyses. The size frequency distributions determined by the COULTER COUNTER are truncated at the lower analytical limit of the 30 μm tube (0.63 μm or 10.62 ϕ), which was weighted as 11.0 ϕ for the purpose of statistical analysis. The size

percentage data from both tubes were arithmetically combined and normalized to provide the full distribution of the mud fraction within the two-tube analytical range. All operational techniques were standardized to minimize operator bias and to eliminate inconsistent analytical artifacts. The precision of the COULTER analyses is equivalent to that of the pipette technique (Shideler, 1976). On the basis of triplicate analyses performed on each of three different samples, the minimal precision in determining Folk's (1965) graphic mean diameters is ± 6.4 percent.

10. Gravel Analysis - A visual inspection of the gravel fractions within the sea-floor sediments revealed that the gravel consisted almost entirely of biogenic shell materials; no significant quantity of non-organic gravel detritus was observed. As the South Texas OCS is essentially a sand-mud province, the inclusion of the gravel-size shell materials within the composite size analyses was not considered to be of any particular sedimentological benefit. In addition, the shells could produce misleading results by distorting the statistical size parameters derived from the sand and mud fractions. For these reasons, the gravel fractions were not included within the size analyses, and all size-frequency distributions are truncated at the 2 mm (-1.0 ϕ) sand/gravel boundary.
11. Interfacing Analytical Results - The individual size frequency distributions determined by RSA (sand) and COULTER COUNTER (silt and clay) were mathematically combined into a composite size frequency distribution characterizing the entire sample. Cumulative weight percentages of size classes were determined at a 0.5 ϕ interval, encompassing a

size range from -1.0 ϕ (2 mm) to 11.0 ϕ (0.49 μ m). These data were then utilized in deriving the statistical size parameters.

12. Textural Parameter Derivation - In deriving textural parameters, data processing was performed by a computer program, employing the computer facilities of the USGS, Reston. The derived parameters consist of the following: sand percentage, silt percentage, clay percentage, sand/mud ratio, silt/clay ratio, and the four moment measures (mean diameter, standard deviation, skewness, kurtosis).

Data presentation

All textural parameters derived are tabulated in appendix 5. In addition, variability graphs were constructed for each of the four transects to illustrate seasonal variations in sand/mud ratios, silt/clay ratios, mean diameters, and standard deviations (figs. 68-71). These specific parameters were considered to be the most appropriate for characterizing the textural variability. The graphs are based on the average values of textural parameters obtained from the analysis of duplicate samples taken at each station. The variability graphs were prepared only for the spring and summer/fall sample suites. Unfortunately, the sampling format used for the winter suite provided neither complete station coverage nor replicate subsampling at individual stations; consequently, the winter suite is not directly comparable with the other two suites. In the winter suite, the following samples were supplied to the USGS for analyses: five or six replicate samples from each of the stations on transect IV, five replicate samples each from stations 1 and 2 of transect III, and one sample each from stations 1, 2, and 3 of transect I. No samples were supplied from any of the remaining stations.

In addition to variability graphs, the statistical significance of differences between mean values of textural parameters from the spring and summer/fall suites was determined by means of t-statistic tests at the 95 percent confidence level, using a computer program (Barr and others, 1976). These results are presented in table 4.

Sand/Mud Ratio Variability

The sand/mud ratios provide a general overview of textural variability (fig. 68) that is most applicable to the inner shelf where sand-size detritus is most abundant. Along transect I, the variation of sand/mud ratios was greatest at station 4 (1.12-2.06 range) located in the shallowest inner-shelf sector. Variability decreased toward the outer shelf. No systematic seasonal trend was apparent. The variations along transect II were greatest at inner-shelf station 4 (0.04-0.29 range) and were minimal throughout the remainder of the transect. The spring sediments were consistently coarser (higher sand/mud ratios) than summer/fall sediments along the entire transect. Variations along transect III were greatest at the shallowest station (station 4; 3.03-5.05 range) and decreased seaward; the spring sediments were consistently coarser than the summer/fall sediments. Seaward of station 5, the sand/mud ratios were essentially zero. Along transect IV, variations were greatest at mid-shelf station 5 (0.80-3.10 range); no systematic seasonal trend was apparent.

In general, the seasonal variability of sand/mud ratios tended to be largest along the inner shelf where sand is most abundantly distributed. In addition, the greater inner-shelf variations may partially reflect a relatively high degree of hydraulic variability. Among the four transects, the southernmost (IV) was most variable because the sea floor is most texturally

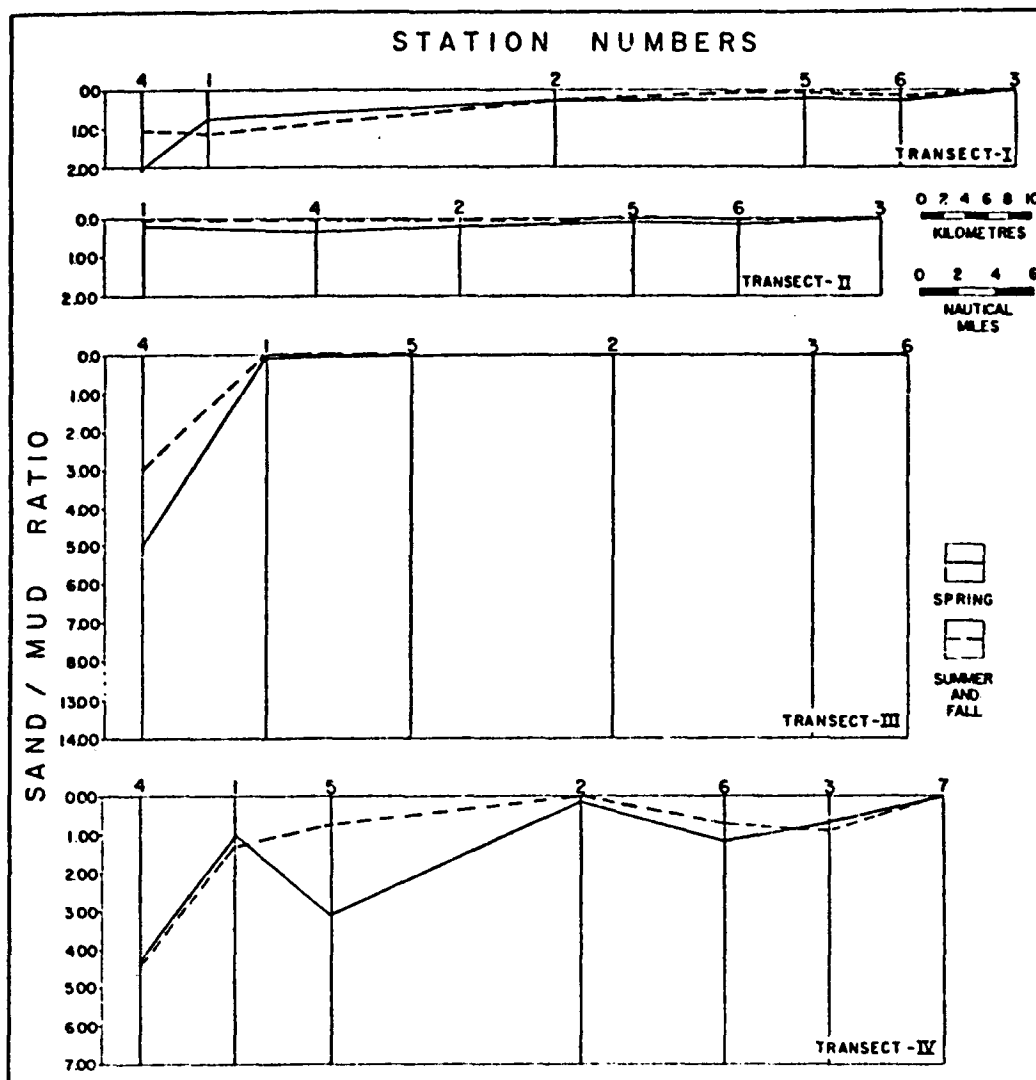


Figure 68. Sand/mud ratios for benthic sediments, biological stations.

heterogeneous along this transect, which crosses the ancestral Rio Grande delta. Systematic seasonal trends were noted only along the two central transects (II and III), where the spring sediments were coarser than the summer/fall sediments. Although no shelfwide seasonal trend was apparent, all four transects showed a general trend of decreasing ratios seaward for both the spring and summer/fall suites. No statistically significant difference occurs between sand/mud ratios of the spring and summer/fall suites (table 4).

Silt/Clay Ratio Variability

The silt/clay ratios provide a somewhat more sensitive general overview of textural variability than do sand/mud ratios. In addition, silt/clay ratios are more widely applicable to the South Texas OCS, where silt and clay are relatively abundant. The silt/clay ratio variability is shown by figure 69. Along transect I, maximum variation occurred at mid-shelf station 2 (1.43-2.18 range); no systematic seasonal trend was apparent. The variations along transect II were greatest at mid-shelf station 2 (1.58-2.59 range), with no apparent seasonal trend. Spring sediments were finer (lower silt/clay ratios) than summer/fall sediments along most of the transect, except along the outer shelf (stations 6;3) where the opposite was true. Along transect III, maximum variation was at mid-shelf station 2 (1.02-1.89 range). The samples of sediment collected during the spring generally were finer than those collected during the summer/fall except at the shallowest station (4). The variations along transect IV were greatest at inner-shelf station 1 (0.66-1.21). No seasonal trend was apparent, and variations appeared to be essentially random.

In general, seasonal variability of silt/clay ratios was substantial along the entire shelf but tended to be greatest toward the mid shelf. No shelfwide seasonal trend was apparent, but sediments in the spring tended to

Table 4. Results of t-statistic tests for seasonal comparison of textural parameters.

Parameter	Spring mean (\bar{x})	Summer/fall mean (\bar{x})	t-value
Sand/mud ratio	0.73	0.58	0.65
Silt/clay ratio	1.24	1.45	1.87
Mean diameter	6.60	6.47	0.48
Standard deviation	2.16	2.17	0.22

d.f. = 99; $t_{0.05} = 1.99$

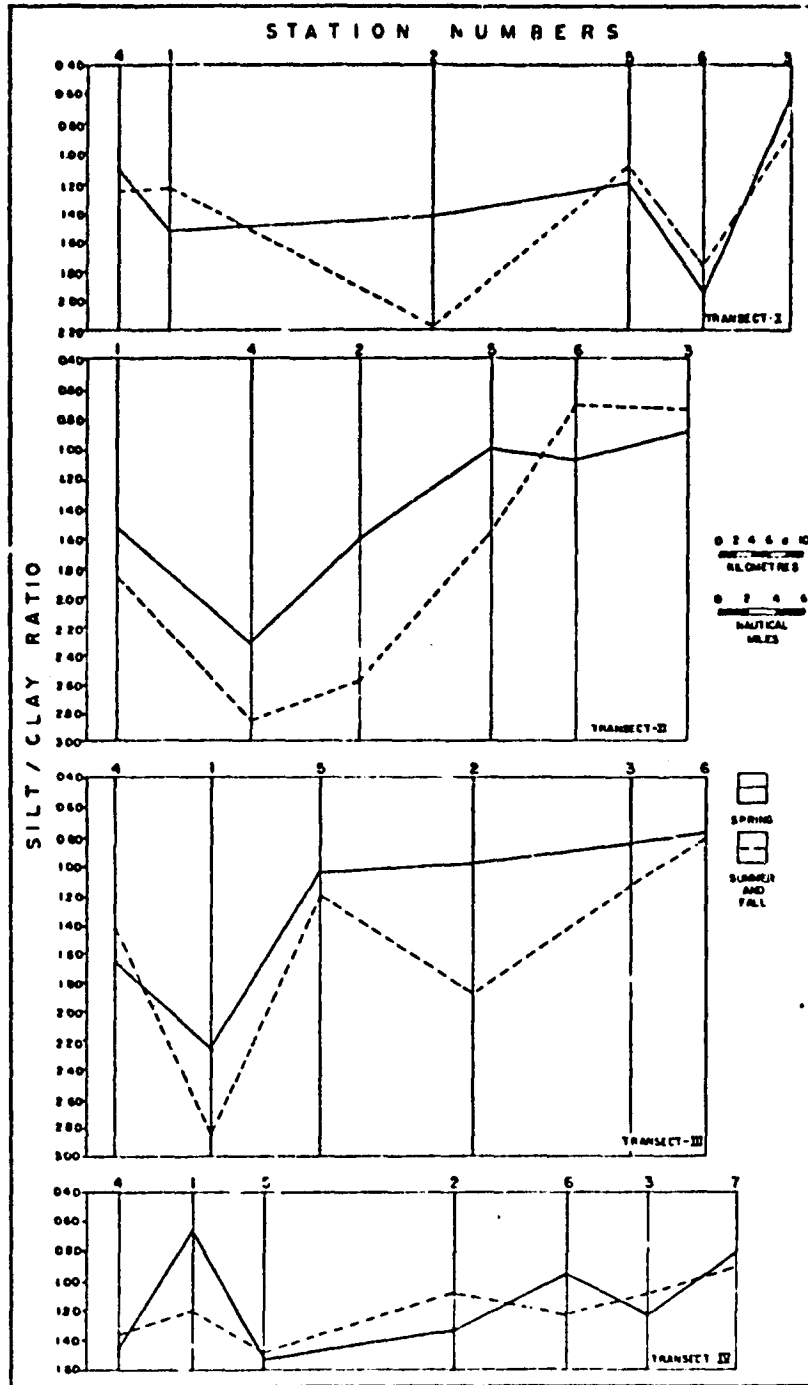


Figure 69. Silt/clay ratios for benthic sediments, biological stations.

be finer grained than during summer/fall along the two central transects. All four transects showed a general seaward trend of decreasing grain size (decreasing ratios) for both the spring and summer/fall suites. No significant statistical difference was evident between silt/clay ratios for the two seasonal suites (table 4).

Mean Diameter Variability

The mean diameter (first moment) provides a sensitive measure of the average grain size of the sediment and indicates the general levels of energy affecting the environment. The mean diameter variability is shown by figure 70. Along transect I, the variation was largest at mid-shelf station 2 (6.17 ϕ -6.93 ϕ range), but no systematic seasonal trend was apparent. The maximum variation along transect II also was at mid-shelf station 2 (6.35 ϕ -6.75 ϕ range), and no seasonal trend was apparent. The variations along transect III were maximum at mid-shelf station 2 (6.93 ϕ -7.85 ϕ range). Except for the shallowest station (4), the spring sediments were finer grained (higher ϕ value) than the summer/fall suite. Along transect IV, variations were maximum at mid-shelf station 5 (3.64 ϕ -5.18 ϕ range), and no seasonal trend was apparent.

In general, seasonal variability was greatest toward the mid-shelf sector and along the southernmost transect (IV). No shelfwide seasonal trend was indicated, but the spring sediments did tend to be finer grained than summer/fall sediments along most of transect III. Along all four transects grain size decreased seaward in both sample suites, thus substantiating the silt/clay variability profiles. No statistically significant difference in mean diameters was noted between the two seasonal suites (table 4).

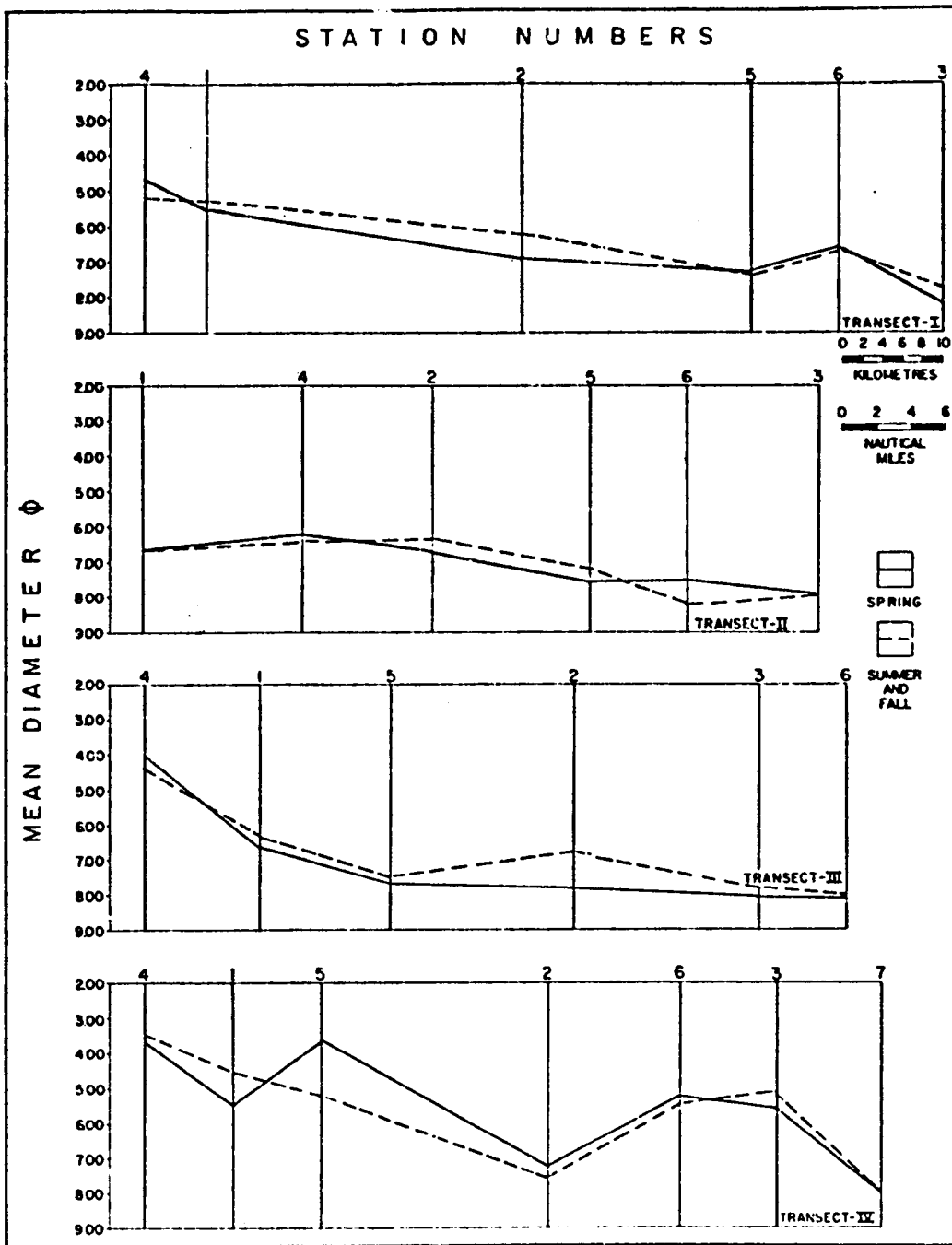


Figure 70. Mean diameters for benthic sediments, biological stations.

Standard Deviation Variability

The standard deviation (second moment) is a measure of sediment sorting characteristics or homogeneity, an aspect that may provide indications of the extent of sediment mixing or of environmental energy consistency. The standard deviation variability is illustrated by figure 71. Along transect I, variation was largest at the shallowest inner-shelf station (station 4; 2.51 ϕ -2.68 ϕ range). Except for station 6, the spring sediments were somewhat better sorted (lower standard deviation values) than the summer/fall sediments. In both seasonal suites, sorting improved seaward. The maximum variation along transect II was at mid-shelf station 6 (1.61 ϕ -2.07 ϕ). This transect showed a systematic seasonal trend: the spring sediments were more poorly sorted than the summer/fall sediments, a relationship opposite to that exhibited by transect I. Along transect II sorting also improved seaward during both seasons. The variations along transect III were maximum at the shallowest inner-shelf station (station 4; 1.62 ϕ -2.01 ϕ range), but no systematic seasonal trend was apparent. Along transect IV, maximum variation was at mid-shelf station 5 (2.36 ϕ -2.83 ϕ range). The variability appeared to be random, exhibiting no seasonal trend.

In general, shelfwide variability tended to be greatest along the southernmost transect (IV) over the ancestral Rio Grande delta. No consistent shelfwide seasonal trend was apparent, although spring sediments were systematically more poorly sorted than summer/fall sediments along central transect II. A general seaward improvement in sorting was indicated along transects I and II. No statistically significant difference in standard deviation values for the two seasonal suites was indicated (table 4).

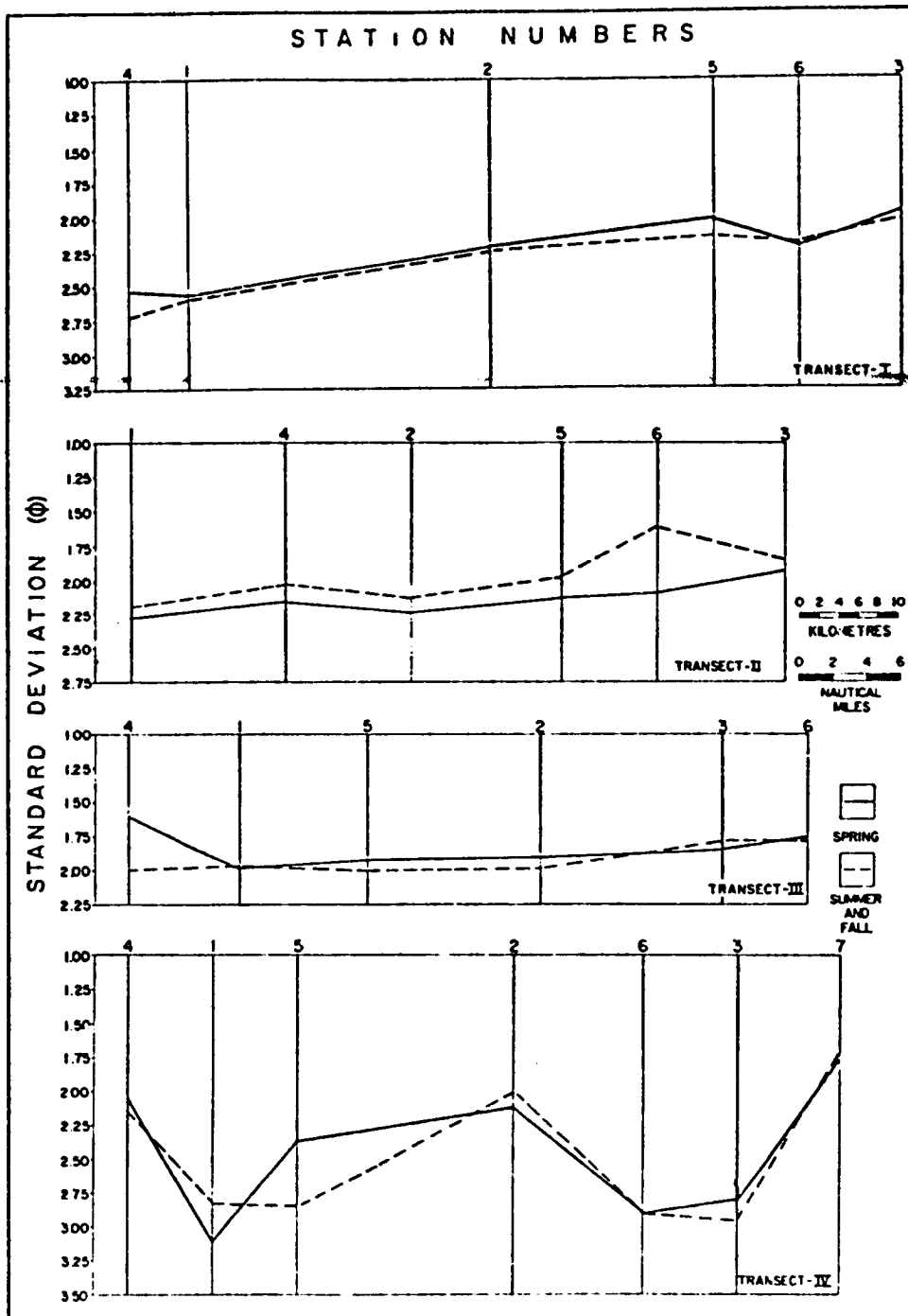


Figure 71. Standard deviations for benthic sediments, biological stations.

Summary .

Sea-floor sediment texture, in terms of both grain size and sorting, showed substantial variability within the spring and summer/fall seasonal suites. The variability appeared to be of a random nature with no consistent seasonal trend on a shelfwide basis. Generally, grain size decreased and sorting improved seaward as a regional trend for both suites of samples. No statistically significant textural differences were noted between the two suites.

ORIGIN OF DISCRETE SAND LAYERS AND MOBILITY OF SEA-FLOOR SEDIMENTS

by

Henry L. Berryhill, Jr.

Introduction

Sediment mobility on the sea floor is a significant aspect of the marine environment and a factor that must be considered in assessing or predicting the impact of any type of offshore activity that will involve the sea floor, either as the foundation for a structure or as a possible repository, inadvertently or otherwise, for anthropogenic substances.

Because the shallow subsurface sediments to depths of about a meter record the depositional history of the shelf during approximately the past thousand years, they have been included in the environmental study plan for the South Texas OCS since inception of the project in the late fall of 1974.

During the first year, emphasis was on description of the textural stratigraphy, or vertical variability in grain size, the extent of sand over the shelf, and the general effect of bioturbation or infaunal burrowing on the sediments (Berryhill and others, 1976). The results for the first year were based on 74 pipe cores ranging in length up to 1.5 m.

The study of shallow subsurface sediments in the second year examined in greater detail the arrangement of sand in the sediments (Berryhill, 1977). The South Texas OCS is characteristically a silt province. Consequently, the distribution of the somewhat coarser sand is a clue to the transporting capacity of bottom currents moving over the sea floor. The number and distribution of the discrete sands is an indication of both the frequency and the areal extent of the higher energy conditions. To relate the dispersal of sand to time, the cores were analyzed in depth increments of 30 cm.

The number, depth, and areal extent of the sand layers within each 30 cm segment were plotted in map form. The results for each segment were compared to determine if patterns of transport and deposition have persisted. For the second year's effort, an additional 101 cores were collected to supplement the original 74 and to fill geographic gaps in coverage (see fig. 72).

In the third year, the focus was on the origin of sand layers that are present at least as far out as midshelf and on the transporting mechanisms for the sediments in general as indicated by the depositional structures. Since the discrete sands at midshelf and beyond may have been spread during and in the aftermath of hurricanes, the vertical distribution of grain size in individual layers was determined to see if sorting characteristics might reveal the mode of transport, as suspension or bed load. In addition the X-radiograph for each core was examined for depositional structures, both within the sand layers and in the finer grained sediments between the discrete sands.

Grain Size Distribution in Sand Layers

The textural analyses from the preceding two years have documented a relatively small range in grain size for all parts of the shelf except the southern and extreme northeastern parts where the relict sediments contain large numbers of shells and some coarse sand. As more than 50 percent of the sediments are of silt size, and as the sand fraction is normally fine to very fine, no great range in grain size would be expected. Consequently no systematic textural analysis of numerous sand layers was attempted. Instead, selected beds in a few cores were analyzed to determine sorting characteristics. Each layer was subsampled in two or three vertical

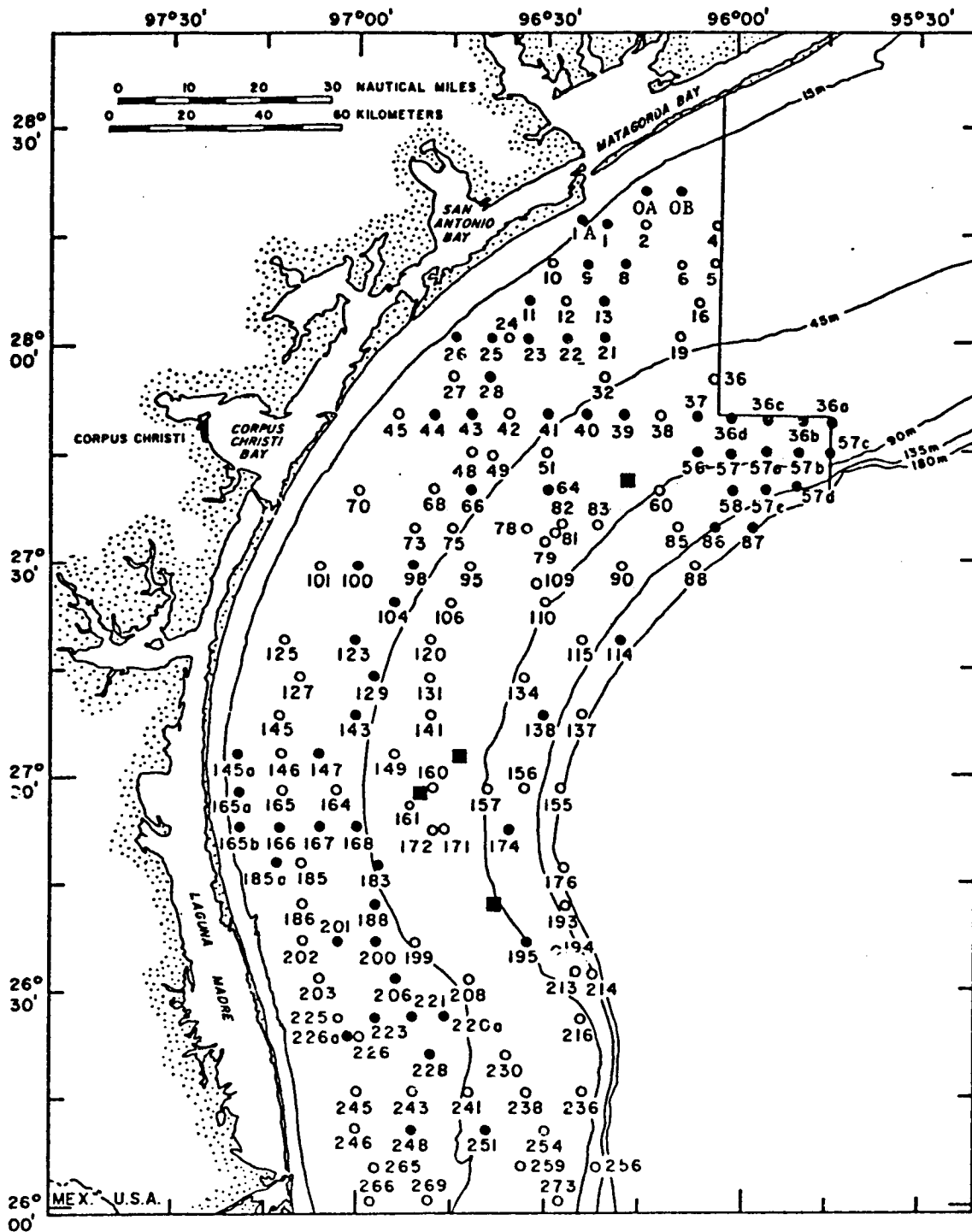


Figure 72. Location of sample stations by number for cores used to study the shallow subsurface sediments. Dots indicate sites cored in 1974. The squares indicate reefs where closely spaced cores were taken in a traverse pattern. Circles indicate sites cored in 1975.

increments and comparative analysis was made at 0.5 phi intervals using the analytical procedures outlined by Shideler elsewhere in this report.

Core OA--The core station is in relatively shallow water at the northwestern corner of the South Texas OCS where sediment moves southward along the inner shelf. The sand layer analyzed is 9 cm thick, and its base is at a core depth of 90 cm. Based on modal diameter, the layer is classified as a very fine grained sand that contains a moderate amount of heavy minerals; comparison of the textural analyses for the three subsamples indicates a relatively narrow range in grain size (fig. 73). The sand in subsample 2 (the middle part of the layer) is slightly coarser than that above and below, but overall the bed is made up of moderately well-sorted sediments. The samples in core OA, as well as almost all samples analyzed, contain a thin tail of fine to very fine sediments that cause an asymmetrical skewness to the sediments that otherwise consist of grain sizes in the coarse silt to fine sand range. Considering the high degree of bioturbation over the inner half of the shelf, the very fine grains may be reworked and mixed into the sand by burrowing. The origin of the fines relative to sorting mechanics is uncertain; some may be transported with the sand/coarse silt, but some may be picked up during transport across the inner shelf.

Core 1A--The core station is in relatively shallow water seaward of the outlet for Matagorda Bay. It lies in an area of considerable sediment movement. The sand layer analyzed texturally is 7 cm thick and its base is at a depth of 32 cm in the core. The modal diameters of the 2 subsamples indicate that the sediment making up the layer is a borderline coarse silt (4.13 ϕ) containing a moderate amount of heavy minerals. Comparison of the

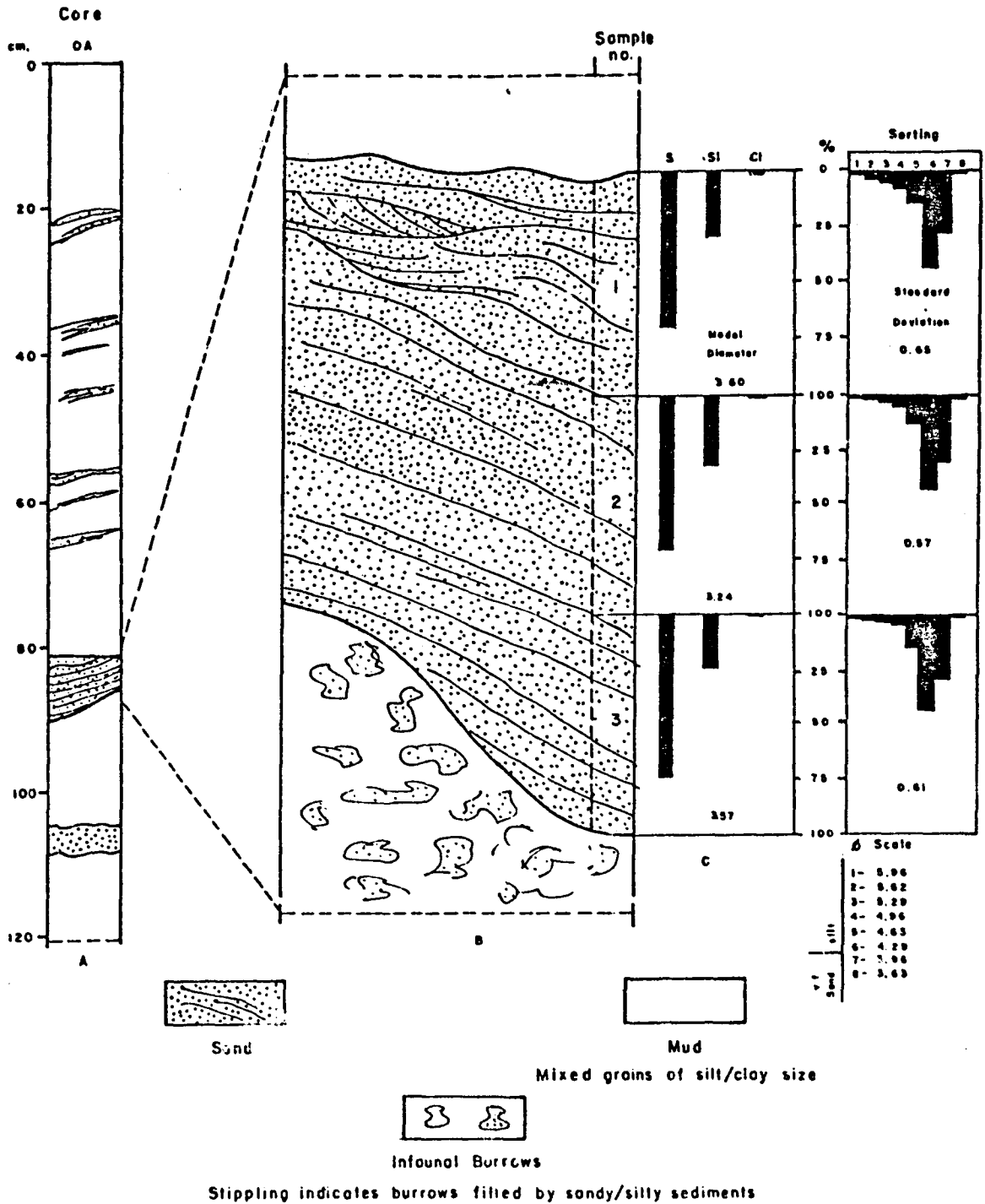


Figure 73. Diagrams for core OA showing the textural stratigraphy of shallow sediments, the sedimentary structures in the specified discrete sand layer, and the textural composition and sorting characteristics of the sand.

analyses for the 2 subsamples indicates moderately good sorting and no textural grading (fig. 74).

Core 23--The core station is midway between the outlets to Matagorda and Corpus Christi Bays at a water depth of about 23.5 m. Analysis of a thin sand layer at a depth of 66 cm in the core indicates that the sediment ranges from fine sand (2.74 ϕ) at the top to very fine (3.14 ϕ) at the base; heavy minerals content is substantial. The results of textural analysis for the two subsamples show that the upper part of the bed is coarser than the lower part, indicating a slight tendency toward reversed grading of grain size. Overall, the sediments are moderately to poorly sorted; the lower subsample is less well sorted than the upper (fig. 75).

Core 28 (A)--The core station lies about 5 miles southwest of core station 23 along the shelf at nearly the same water depth (25 m). The near-surface sand layer analyzed is at a depth in the core of only 8 cm. The modal diameters for both subsamples indicate the sediment is fine-grained sand containing substantial amounts of heavy minerals. Comparison of the analytical results for the subsamples reveal poorly sorted sediments. The skewness pattern has a thin but long tail of very fine particles (fig. 76).

Core 28 (B)--The second layer analyzed from core 28 is at a depth of 67 cm in the core, the same depth as the layer analyzed from core 23. It seems reasonable to assume that both represent the same sand deposit. The analyses indicate that overall the sediment is fine-grained sand (fig. 77). When compared, the results for the 2 sand layers in core 28 show that the lower is less well sorted than the upper and that the upper part of the deeper layer is less well sorted than the lower part. Both layers are near the upper limit

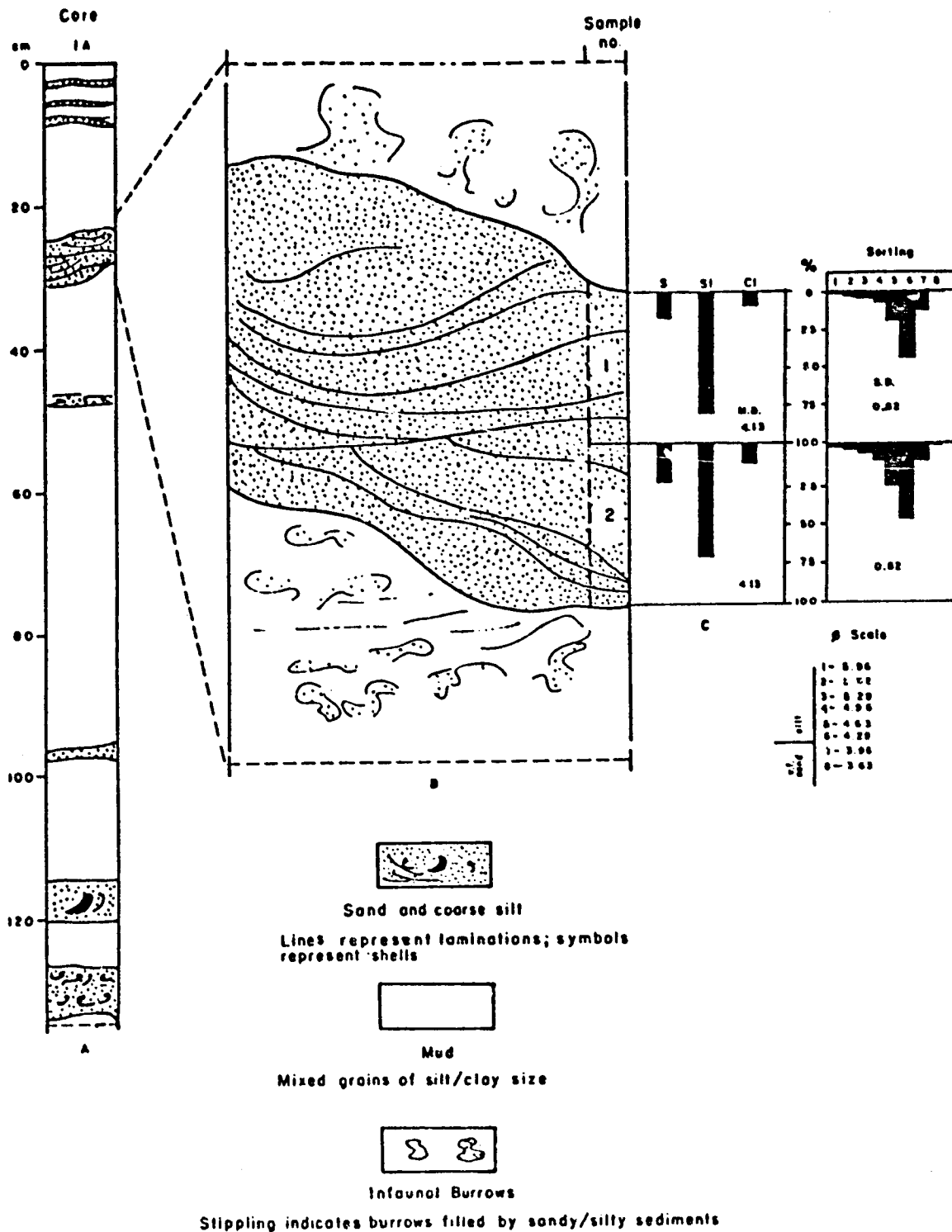


Figure 74. Diagrams for core 1A showing the textural stratigraphy of the shallow sediments, the sedimentary structures in the specified sand layer, and the textural composition and sorting characteristics of the sand.

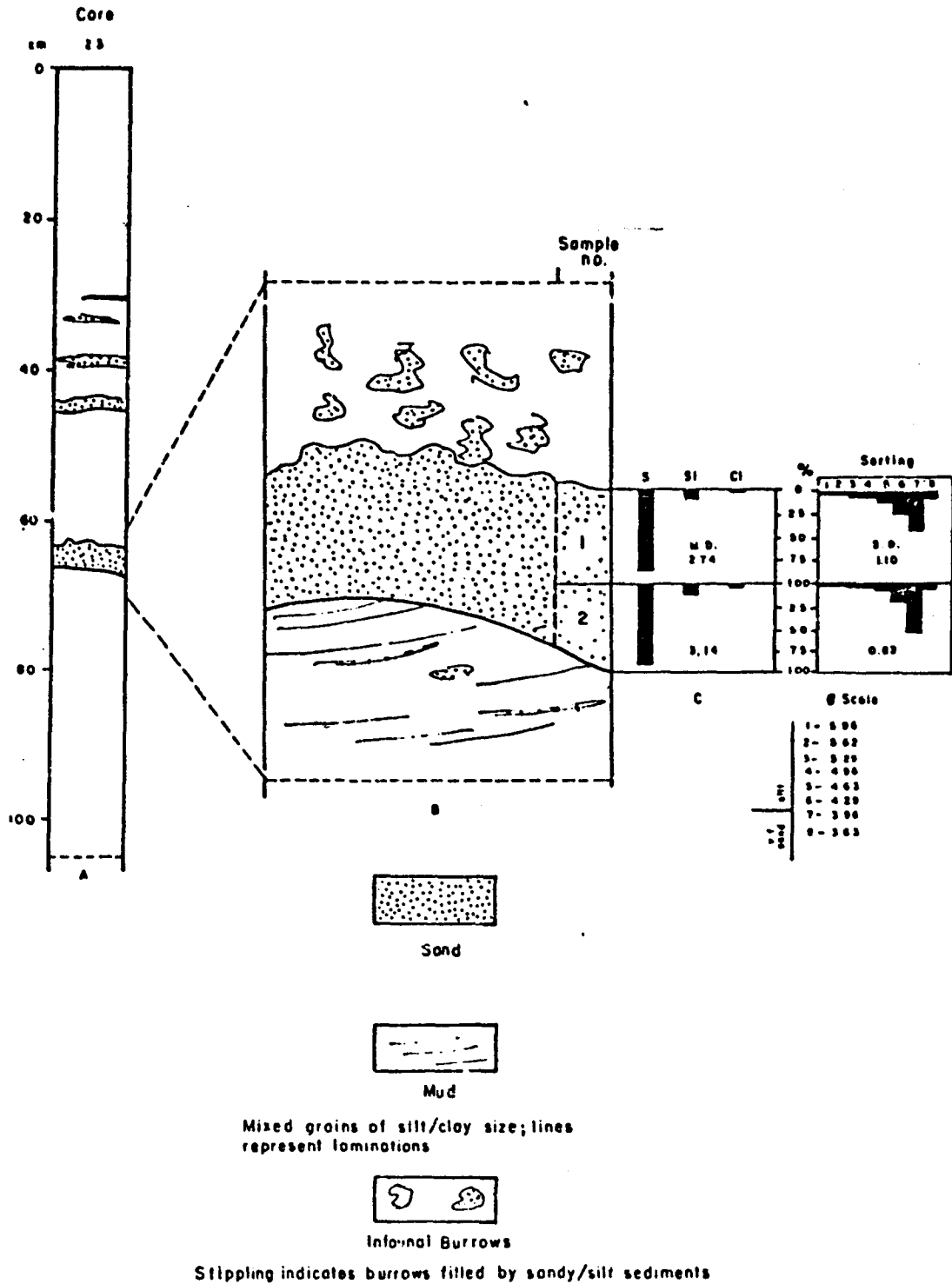


Figure 75. Diagrams for core 23 showing the textural stratigraphy of the shallow subsurface sediments, the sedimentary structures in the specified sand layer, and the textural composition and sorting characteristics of the sand.

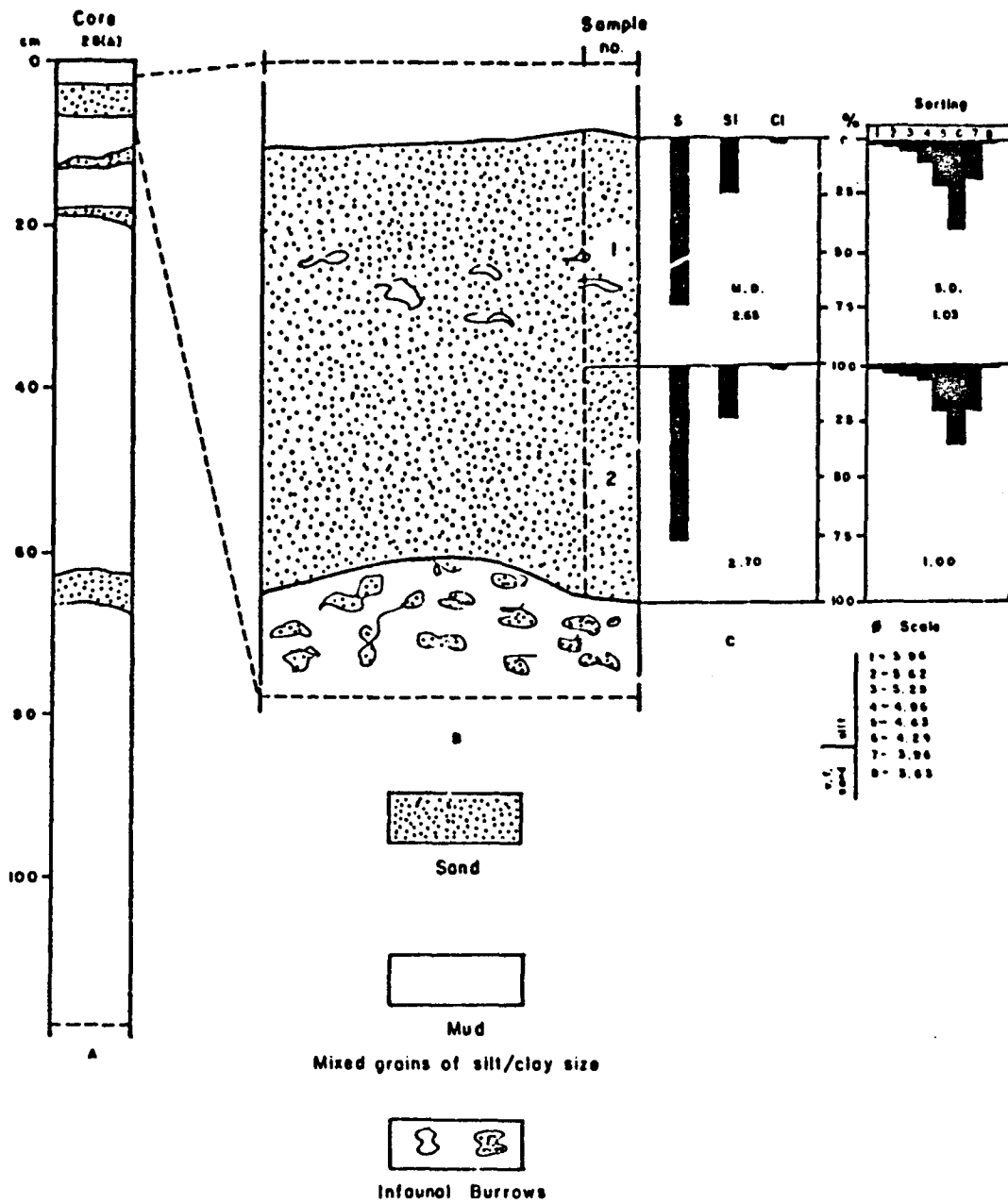


Figure 76. Diagrams for core 28A showing the textural stratigraphy of the shallow subsurface sediments, the sedimentary structures in the specified sand layer, and the textural composition and sorting characteristics of the sand.

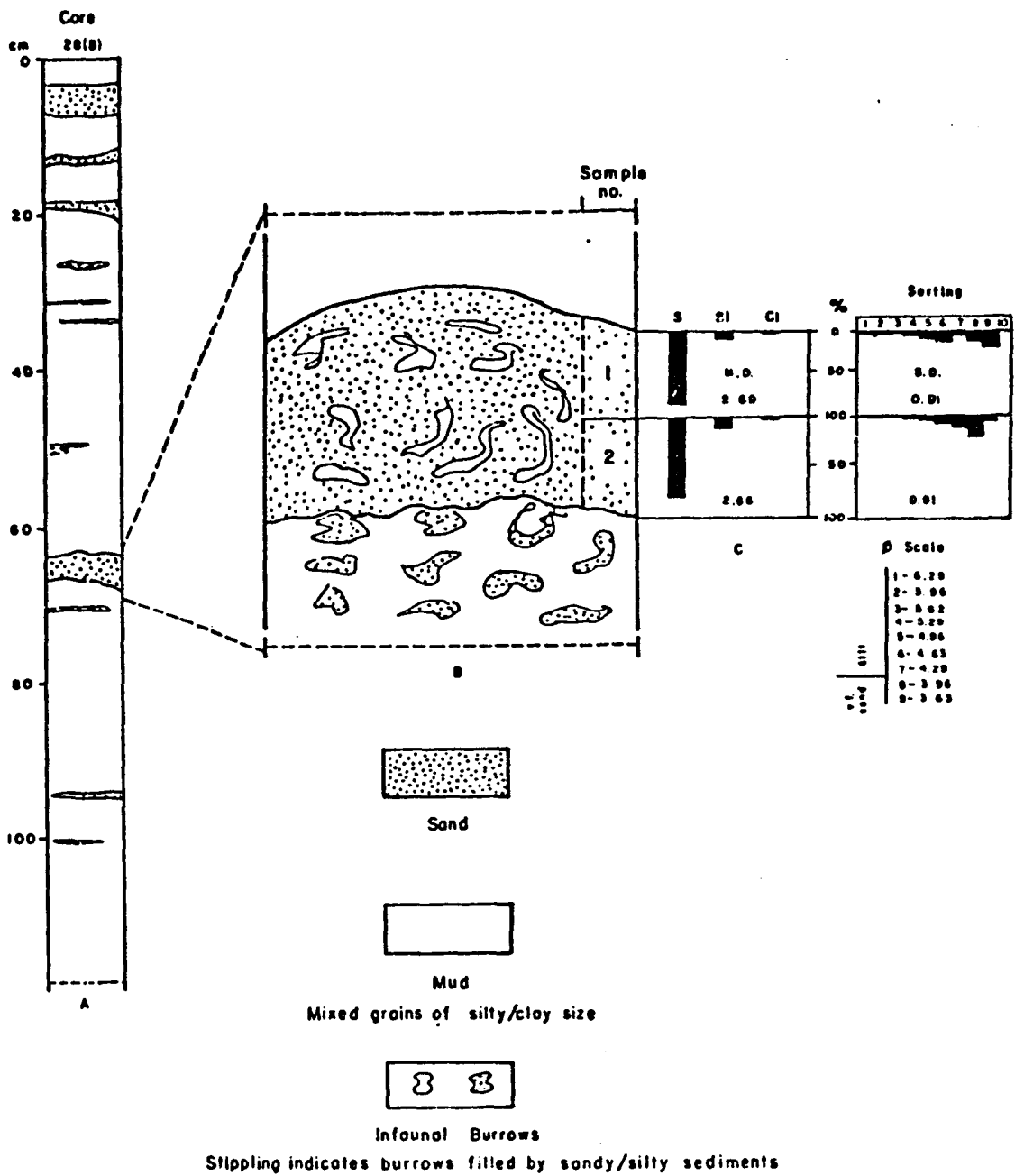


Figure 77. Diagrams for core 28B showing the textural stratigraphy of the shallow subsurface sediments, the sedimentary structures in the specified sand layer and the textural composition and sorting characteristics of the sand.

of a moderately well-sorted sediment. Nevertheless the modal diameters in both are virtually identical.

Core 45--The core was taken at a water depth of 19 m and the layer analyzed is at a core depth of 54 cm. The modal diameters indicate that the sediment is coarse silt (fig. 78). The analytical results for the three subsamples document a slight progressive decrease in grain size and a decrease of very fine sand from the base of the layer to the top, indicating a normally graded bedding profile of decreasing grain size upward. Considering the very small range in grain size involved, the grading is not considered significant relative to the mode of transport.

Core 68--The core station is some 24 km from shoreline in a water depth of 32 m; the layer analyzed is at a depth of 37 cm in the core. The modal diameter in each of the 3 subsamples is that of a borderline coarse silt and very little range is indicated (4.11-4.15 ϕ). When compared, the textural analyses for individual subsamples show a progressive upward reduction in both the median (4.29-4.59 ϕ) and mean diameter (4.56-5.14 ϕ) measures and normal grading is indicated (fig. 79). The reduction in grain size is associated with a progressive upward reduction in sorting (standard deviation range = 1.25-1.59 ϕ). Again, considering the small range in grain sizes involved, the significance of the grading relative to the transporting mechanism is questionable although transport by suspension is suggested. Overall, the sediment is poorly sorted.

Depositional Structures

In conjunction with the textural analyses, the cored sediments were examined in detail for structures formed during deposition, as the types

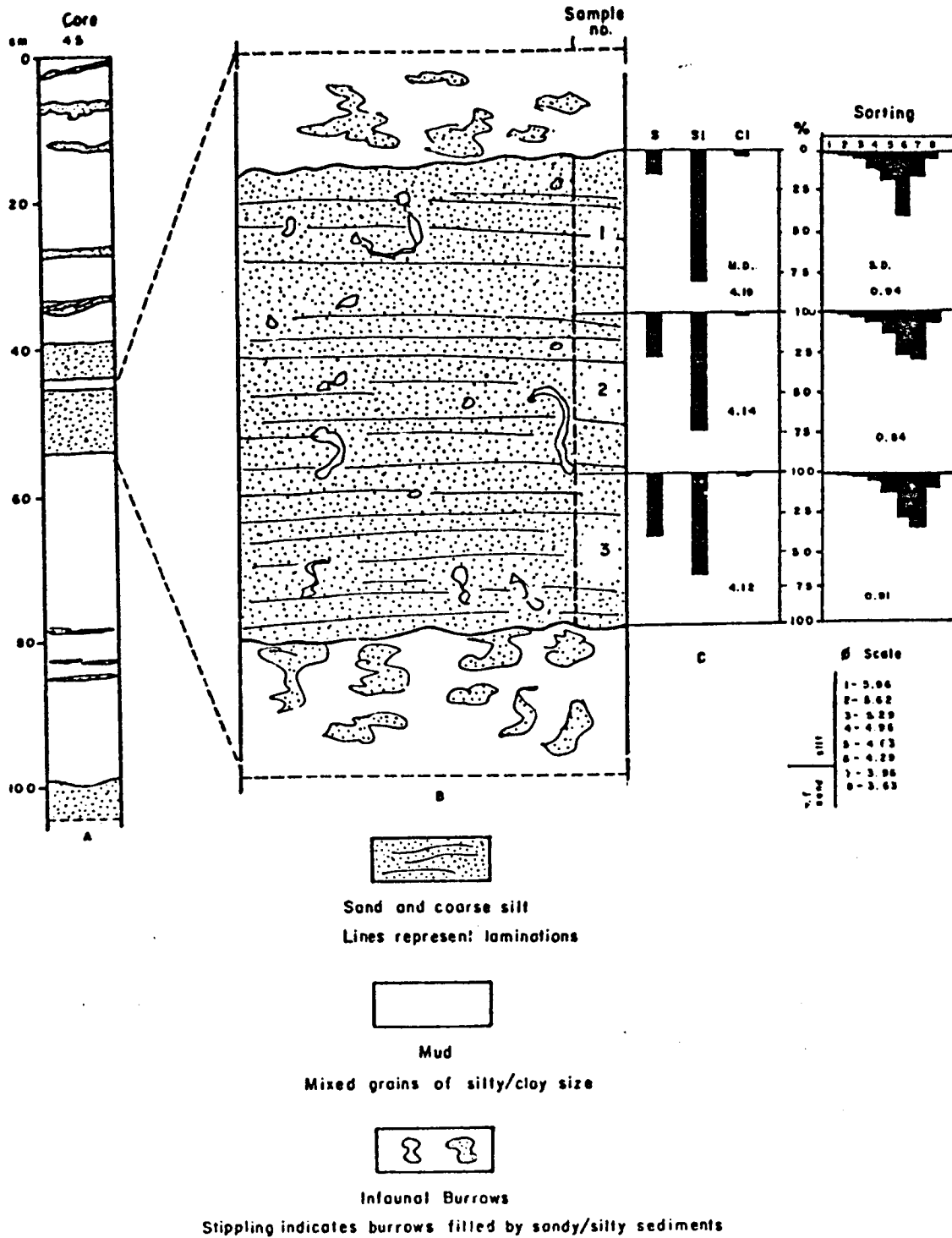


Figure 78. Diagrams for core 45 showing the textural stratigraphy of the shallow subsurface sediments, the sedimentary structures in the specified sand layer, and the textural composition and sorting characteristics of the sand.

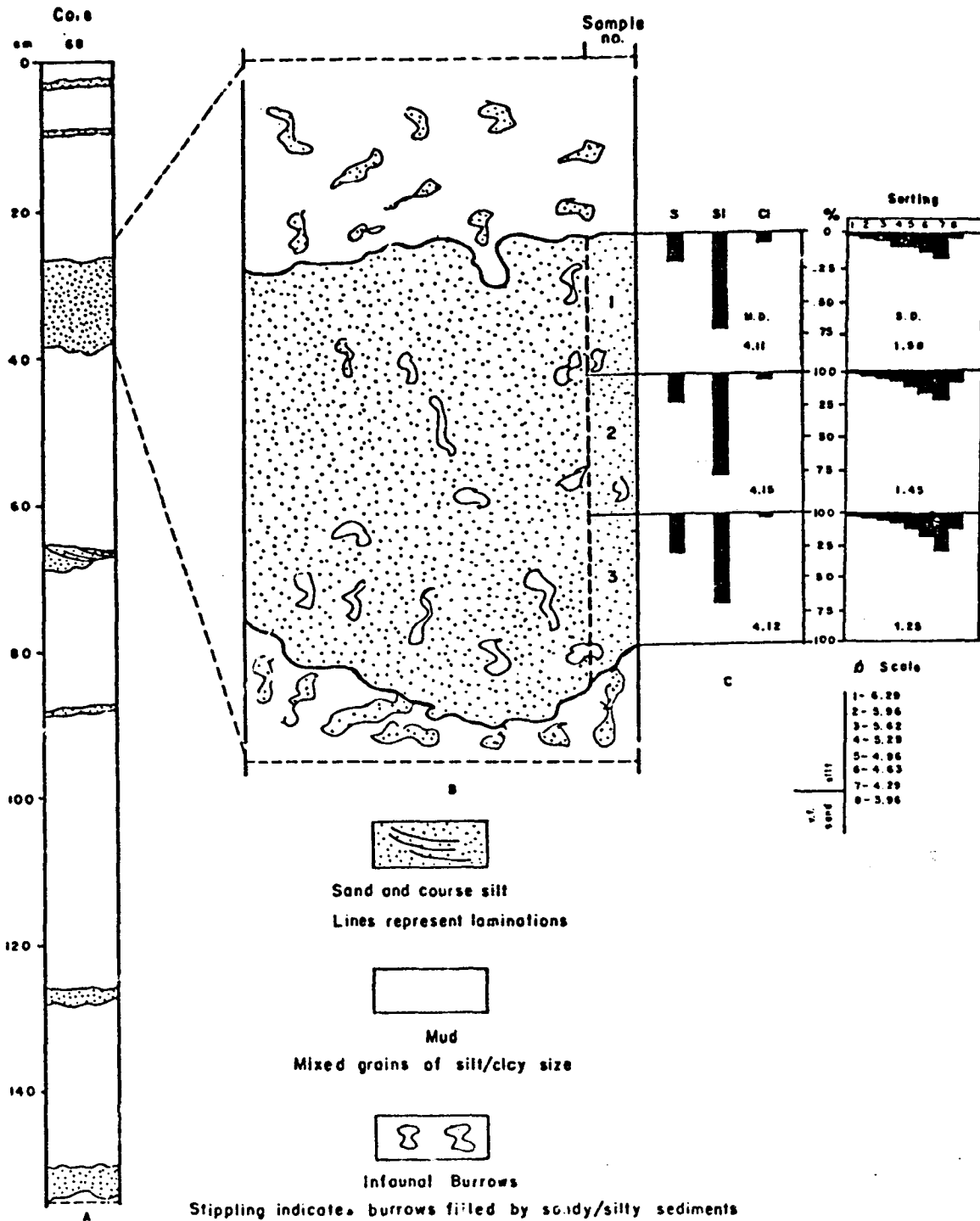


Figure 79. Diagrams for core 68 showing the textural stratigraphy of shallow subsurface sediments, the sedimentary structures in the specified sand layer and the textural composition and sorting characteristics of the sand.

of structures plus their extent and abundance reveal something of the nature and dynamics of the transporting system. The grain size and sedimentary structures are indicators of the carrying power of the water, and the variations of these components, both vertically and geographically in the sediments, indicate variations of energy levels in the water in both time and space. Determination of the carrying capacity of flowing bottom water is a most important environmental concern in any OCS area and recognition of the highest energy level attainable in a specific region is vital to understanding hazard potentials, including the potential for the spread of anthropogenic materials and for damage to structures placed on the sea floor.

Relative to highest potential energy levels, hurricanes cross some part of the Gulf of Mexico almost every year and have affected the continental shelf off Texas on the average of once every two years during the last century according to historical records (Carr, 1967). Water flow over the shelf can reasonably be assumed to reach maximum strength during and immediately following passage of a major hurricane. The return flow of storm surge tides that have reached heights of 4 to 5 m along the south Texas shoreline provides an ample means of redistributing large amounts of sediment from the bays, lagoons, and barrier islands onto the continental shelf. The pertinent questions are: how much of the shelf is affected and how effective is the return flow in moving sediments? The pattern of distribution of sand over the shelf and the flow structures recorded in the sediments during deposition should provide clues to the strength and extent of storm-induced currents.

The radiographs for all 175 cores collected during the previous years of study were examined in detail for evidence of sedimentary structures that document bottom water movement during deposition. The term "sedimentary structure" covers all types of irregular laminations and discontinuities

within a layer as well as very sharp contacts between layers of markedly different grain size such as that at the base of a number of discrete sand layers. Excellent examples of the most common types of sedimentary structures recognized are shown by the 1:1 tracings of the cored sand layers in figures 73 and 74. Both show a range in types of structures, but figure 73 is perhaps the most inclusive. The base of the sand layer shown by figure 73 is very sharp and is discordant to the underlying mud. At intervals upward through the sand are distinct laminae, or aggregates of grains, that also are inclined to the planar orientation of the layer. Near the top of the sand layer are laminae of more irregular and discordant arrangement plus a good example of small-scale cross-lamination and crude ripple-type laminae. The top of the sand is likewise in sharp contact with the overlying mud but is parallel to the sea floor rather than inclined as is the base. The sedimentary structures in the sand document very well its deposition by moving water. The accumulation of the sand was a single event caused by increased strength or carrying power of the bottom current. The sharp base indicates the abrupt onset of sand deposition in this particular situation and the shell fragments in the base of the sands having sharp bases demonstrate both the increased strength of bottom currents that transport the sand as well as the ability of the current to move particles larger than the very fine sand that typifies most of the sand layers on the shelf. Further evidence that the sand in figure 73 represents a single depositional event is the termination of bioturbation at the end of the sand. The mud below the sand is intensely burrowed, yet neither the sand layer itself nor the mud immediately above the sand layer have any indication of burrowing. The deposition of some 10 cm of sand in what must have been a relatively short period of time apparently buried and temporarily killed off the infaunal community at the locality.

The extent of depositional structures in the sediments over the shelf, as represented in the 175 cores, has been plotted on maps. The cores that contain sedimentary structures are shown by figure 80; those in which some bottom scour is indicated as well as small-scale slumping of sediments are shown by figure 81. In the identification and plotting of depositional structures, all sediments in the cores were examined and the structures were coded regardless of the grain size involved. At midshelf and beyond, irregular laminae most commonly involve silts; near the outer edge of the shelf, the flow structures involve foraminiferal tests. Irregular laminae are not common beyond the 90 m isobath. Some of the most intensive and recurrent irregular and inclined laminae in the outer half of the shelf are in cores taken around the dead carbonate reefs (topographic highs).

In using core OA (fig. 73) as the example for giving a text description of typical depositional structures represented on the South Texas OCS, note was taken of its geographic position on the inner shelf where the events involved in the processes of sediment transport are more frequent and more vigorous than farther out on the shelf. Nevertheless, all types of depositional structures in figure 73 are represented in one place or another at least to the approximate position of the 90 m isobath, though not all occurrences involve sand. Furthermore, a sand layer lies within 2 or 3 cm of the 90 cm depth interval in a sizeable number of the 175 cores, the same depth as that in core OA. The geographic areas of occurrence of the sand at 90 cm below the sea floor were shown by Berryhill (1977). The map is included in this report because it bears on the determination of the energy levels generated by hurricane-induced currents and their areal extent over the shelf (fig. 82). No proof exists that the layer is correlative from core to core, considering

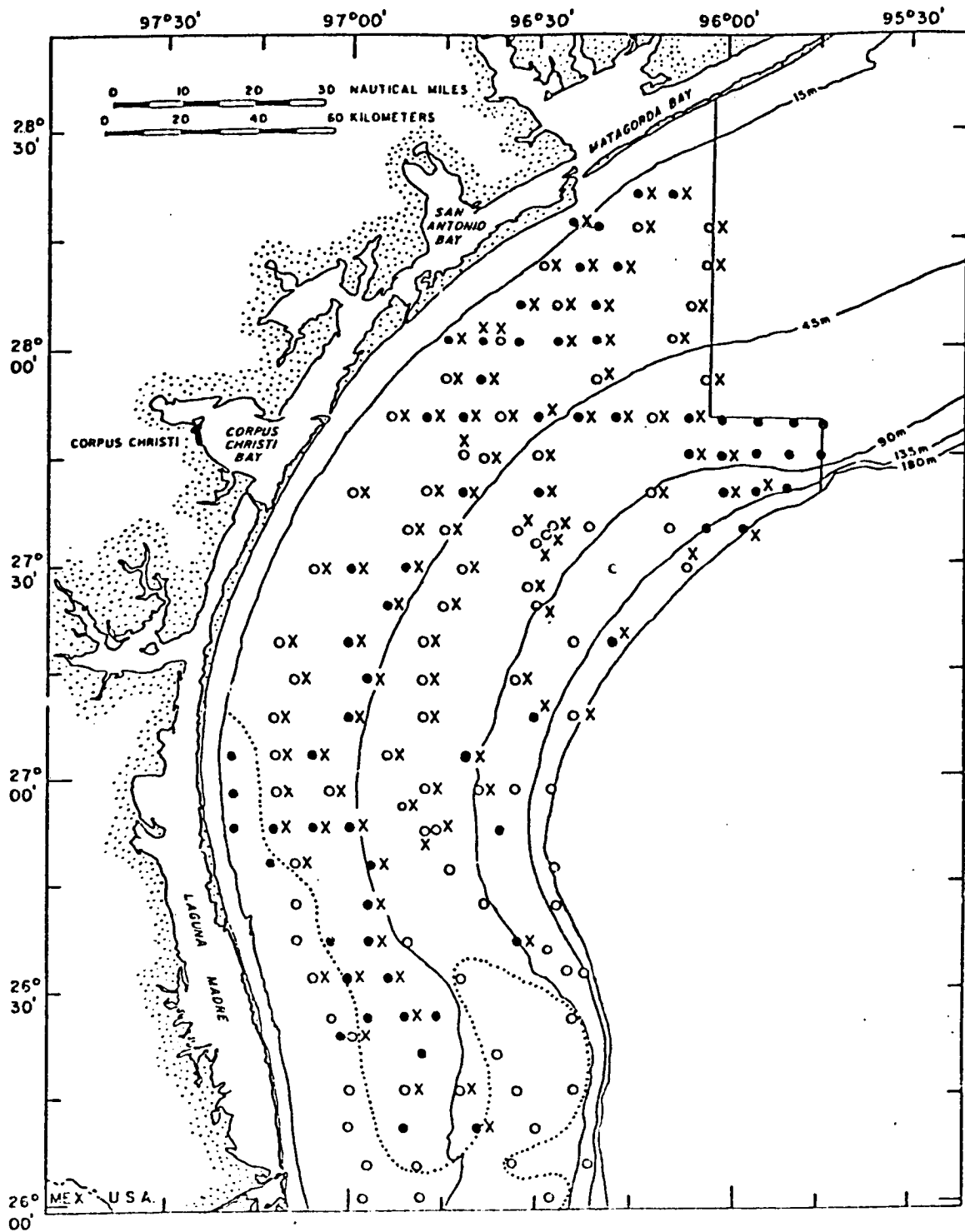


Figure 80. Location of cores (x) that contain sedimentary structures indicating transport and deposition of sediments by flowing bottom water (currents). Dotted line outlines reworked deltaic sediments.

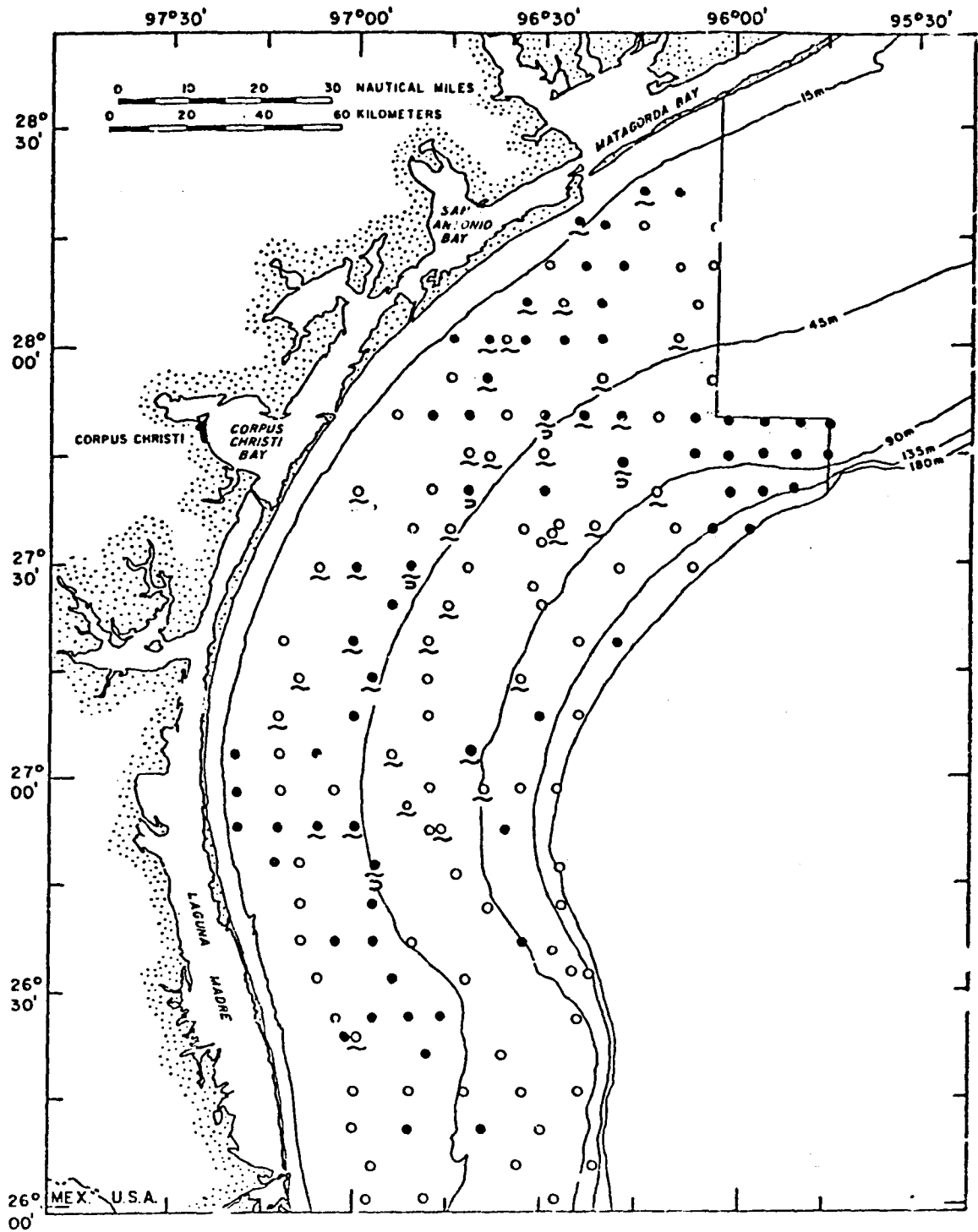


Figure 81. Location of cores in which bottom scour and small-scale slumping of sediments is indicated. ● indicates scour; ○ indicates small-scale slumping.

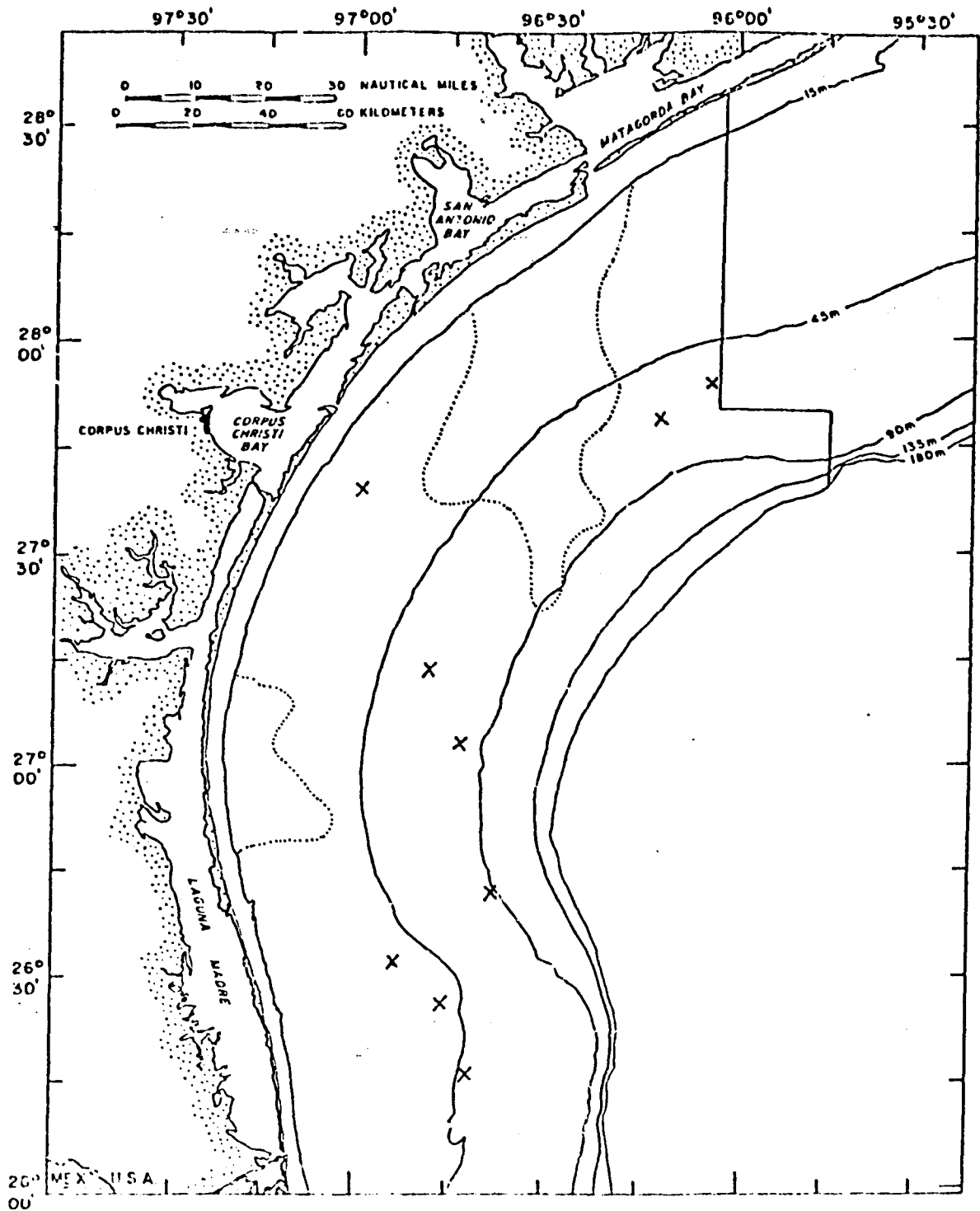


Figure 82. Distribution of the discrete sand layer that is at a subsurface depth of 90 cm in most of the cores in the areas outlined on the map. X's indicate isolated stations where the sand layer is at 90 cm.

the relative distance between cores. However, from a strictly empirical standpoint, the sand layer might be interpreted as the deposit of a single major storm, perhaps of the once-in-a-hundred-years magnitude that is spoken of by meteorologists.

Conclusions

Very few data are available on the three dimensional nature of the current regime that attends a hurricane; available information almost exclusively describes conditions at the sea surface. Consequently, it is difficult to relate the data on grain size and depositional structures quantitatively to the strength of currents involved in eroding and moving sediments on the sea floor. Considering that the depth effect of surface waves is assumed to be one half their length, the strong influence of hurricane-generated waves on the bottom can be readily visualized for the inner shelf in water depths of 30 m or less, though the degree of unidirectional flow and strength of flow along the bottom is not known. Beyond 30 m the movement of the water along the bottom is even more conjectural. A hindcast of hurricane-generated waves from Carla in 1961 was given by Patterson (1971). From the eye of the storm outward to a distance of 180 nautical miles, his calculations were as follows: wave height, 31 to 41 feet; wave periods, 14.7 to 15.1 secs.; wave speed, 46 to 49 knots; and wave length, 1105 to 1160 feet. If the depth effect of a wave is one half the wave length, Patterson's calculations would indicate wave pressure on the bottom virtually all the way across the shelf. Such pressure could possibly lift into suspension incoherent sediments, but the result of flow along the bottom as a function or response to the total hydraulic effect of the storm

over the region is still uncertain. Obviously, if bottom-water flow is independent of wave-induced motion laterally, the process of transport would be enhanced by the increased buoyancy added by the lifting effect of the wave on the sediments. This relationship would be expected to become progressively enforced or strengthened as water depth decreased.

The erodability of bottom sediments for a spectrum of assumed hydraulic conditions has been calculated by Logan (1969). According to his chart, a wave having a periodicity of 12 sec. can move carbonate particles of the following diameters under the conditions stated:

2.5 mm-wave current velocity of 50 cm/sec at a water depth of 260 ft

6 mm-wave current velocity of 100 cm/sec at a depth of 175 ft

10 mm-wave current velocity of 150 cm/sec at a depth of 120 ft

20 mm-wave current velocity of 200 cm/sec at a depth of 90 ft

Logan's calculations modified after Hjustrom (1939) were applied to the morphological subdivisions of reef fronts around the Yucatan carbonate platform and to the types of biotic communities involved. The only possible corollaries on the shelf off south Texas are the Pleistocene reefs whose summits now are in water depths of about 80 m (264 ft); however, these features lie on the flat, open sea floor and perhaps are not directly analogous. Two cores were taken west of the edge of Hospital Reef: one at a distance of 305 m; and the second at 732 m. Core 1 penetrated to 1.2 m and was made up of numerous beds of well-stratified shell and carbonate reef particles up to about 3.5 mm diameter, but averaging about 1.5 mm, interlayered with mud. The number of debris layers decreases upward in the core and mud predominates in the upper 30 cm; however, the uppermost 3 cm of the core is a layer of carbonate particles of various shapes averaging slightly less than 2 mm in diameter. Core 2, which lies 427 m further west, has no reef debris.

Assuming that Logan's calculations are reasonably applicable, the two cores west of Hospital Reef reveal two things about the transporting capacity of bottom currents on the outer South Texas OCS: (1) the currents reach sufficient strength at times to transport particles as large as coarse sand to granule size; (2) the current is able to carry particles of that size upslope across a mud bottom somewhere between 305 and 732 m from the source. The minimum current velocity necessary to move the carbonate particles in core 1 would be 1.8 km/hr by Logan's calculations. Considering the well-sorted nature of the material, its distance from the reef, and the soft mud bottom in the area, a speed of considerably greater than 1.8 km/hr can be reasonably assumed.

The sedimentary structures in the cored sediments amply document that bedload transport of fine sand and coarse silt by moving bottom water has taken place over much of the South Texas OCS, but the amount attributable to bedload transport relative to the amount carried in suspension must remain conjectural in view of the narrow range in grain size involved. Considering that the sand along the shoreline, from which most of the sand on the shelf came originally, is also fine grained, the grain size cannot be used in this case to estimate the velocity of the bottom currents because fine sand virtually is the largest particle size available for transport. The shell fragments along the base of the sand layers in places indicate that the currents do attain velocities in excess of that necessary to move fine sand.

Hurricane-generated currents seem the most likely mechanism for moving the sand over the shelf as well as the granules from the reefs, but aspects of the sediments cored around some of the reefs indicate transport of sediment by currents other than those generated by hurricanes. The sediments around

Baker and South Baker Reefs contain numerous laminae and thin beds of coarse silt to very fine sand whose recurrence in the cores is far in excess of hurricane frequency. Many of the very thin beds and laminae are inclined and some have crude asymmetry that suggests ripples. An example is shown by the copy made from the print of an X-radiograph (fig. 83). Another form of bottom current movement seems obvious for this part of the shelf. Experiments on bottom sediment motion in a laboratory wave tank by Southard and Cacchione (1972) using a two-layered medium of fresh and salt water suggest that breaking internal waves can move particles in the size range of 0.1 to 0.5 mm (fine to medium sand). Their experiment was confined to a two-layered rather than a continuously stratified medium and used acrylic particles, which are less dense than quartz. Nevertheless, their results seem pertinent considering that the layers in the cores contain significant amounts of mica and foraminiferal tests, which also are less dense and more buoyant than quartz. The nature of the laminae and their frequency in cores around the reefs strongly suggest that currents capable of suspending and carrying bottom particles is a normal feature of the outer shelf off south Texas. Only two possible sources of these currents seem likely: either internal waves from the deeper Gulf that regularly feel bottom at about the 90 m isobath or a loop current that swings rather frequently onto the outer shelf.

Finally, moving bottom water capable of transporting sediments for considerable distances is a characteristic of the South Texas OCS. Over the inner half of the shelf the susceptibility of bottom sediments to resuspension and further transport is believed to be considerably enhanced by the intense bioturbation in many areas. The highly burrowed sediments would no doubt be more easily redistributed than those not disturbed by infaunal activity. The

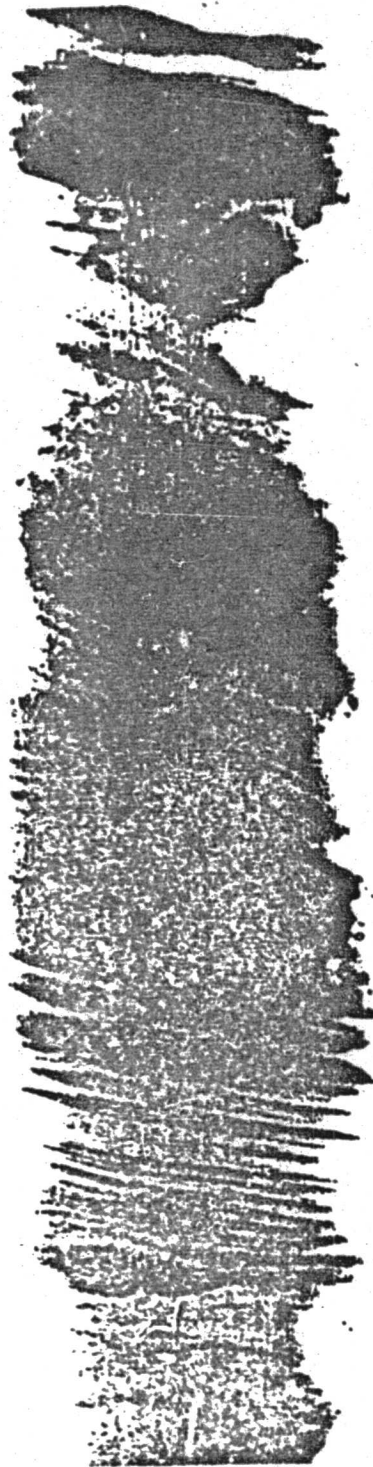


Figure 83. Laminae and thin beds of silt, very fine sand, mica and foraminiferal tests in core from near edge of South Baker Reef, northern part of the South Texas OCS. Note inclined bedding. Scale is 1:1; core diameter is 6 cm.

sand layers are believed to be deposited principally during and immediately after hurricane passage from sources along the shoreline. Currents generated during hurricane passage are believed to be able to transport for long distances over the shelf.

CHEMICAL CHARACTERISTICS

Surface Sediments - Seasonal Variability

in Trace Metals Content

by

E. Ann Martin

and

Charles W. Holmes

Introduction

Seasonal monitoring of the trace metals in the benthic sediments in 1976 indicated that seasonal variations in trace metal content are greater than areal variations within a season. The reasons for this variability are not completely understood, but biologic activity both along the sea floor and/or within the benthic sediments may be a factor. To provide additional data concerning observed seasonal variability of trace metals and to provide additional supportive trace metal data for ongoing biologic and hydrocarbon studies, the 1977 study was undertaken.

Samples were analyzed from the same 25 stations that were occupied in 1976 (fig. 84). (See table 5 for the station locations.) Subsamples representing the upper 5 cm of sediment were taken from "undisturbed" samples retrieved by a SMITH-MACINTYRE grab sampler. The original sampling scheme for the 1977 study was that samples were to be collected in quadruplicate at each station only once during the year. However, completed analyses of the 1975-1976 samples indicated that trace metals variations within an area of a single station are not as great as seasonal variations. The sampling scheme was changed after the winter cruise in order to obtain

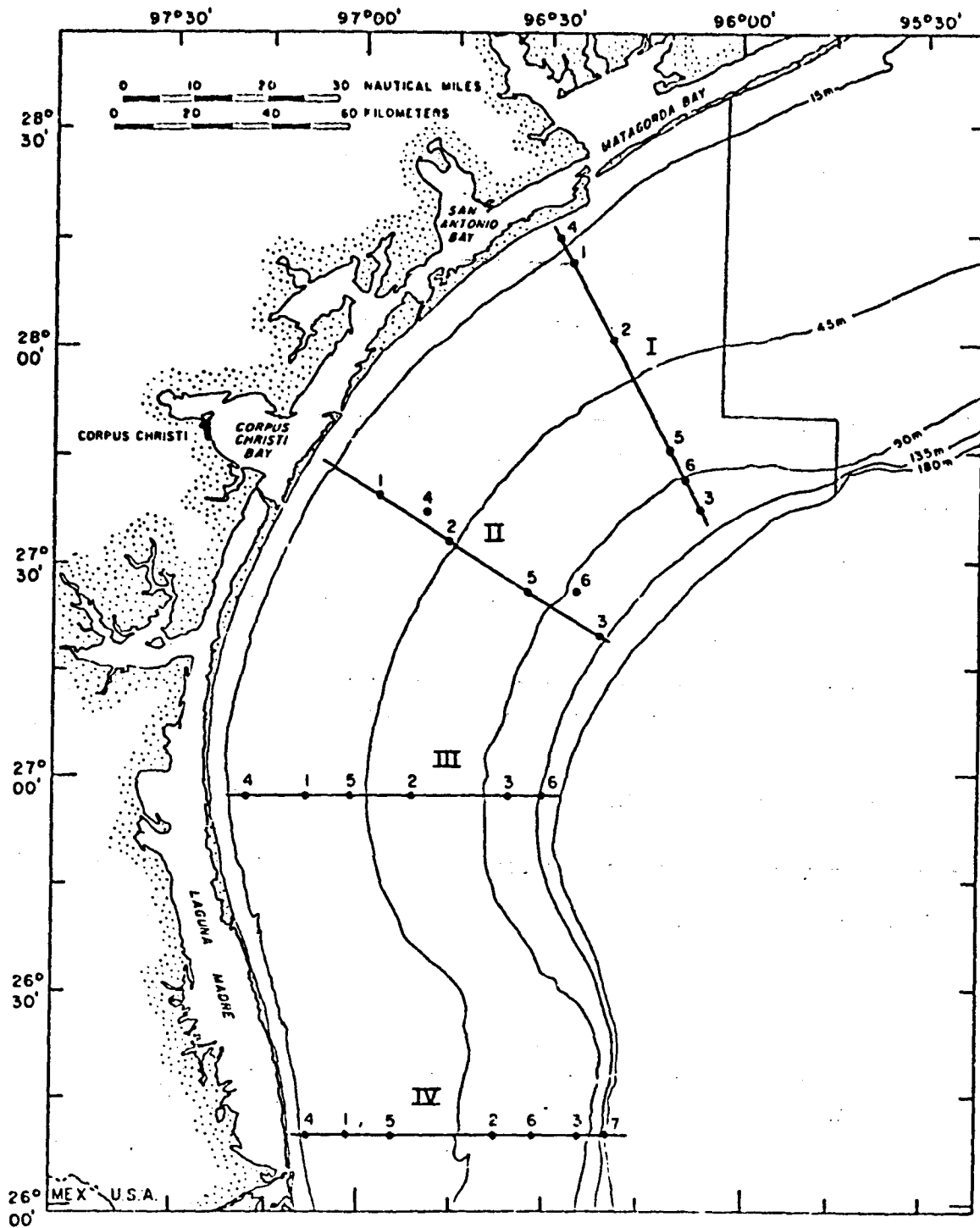


Figure 84. Biologic infaunal stations from which subsamples were taken for trace metal analyses.

Table 5. Location of stations used for studying the seasonal variability of trace metals in benthic sediments

Transect	Station	Latitude	Longitude	Depth (m)
I	1	28°12'N	96°27'W	18
	2	27°55'N	96°20'W	42
	3	27°34'N	96°07'W	134
	4	28°14'N	96°29'W	10
	5	27°44'N	96°14'W	82
	6	27°39'N	96°12'W	100
II	1	27°40'N	96°59'W	22
	2	27°30'N	96°45'W	49
	3	27°18'N	96°23'W	131
	4	27°34'N	96°50'W	34
	5	27°24'N	96°36'W	78
	6	27°24'N	96°29'W	98
III	1	26°58'N	97°11'W	25
	2	26°58'N	96°48'W	65
	3	26°58'N	96°33'W	106
	4	26°58'N	97°20'W	15
	5	26°58'N	97°02'W	40
	6	26°58'N	96°30'W	125
IV	1	26°10'N	97°01'W	27
	2	26°10'N	96°39'W	47
	3	26°10'N	96°24'W	91
	4	26°10'N	97°08'W	15
	5	26°10'N	96°54'W	37
	6	26°10'N	96°31'W	65
	7	26°10'N	96°20'W	130
Winter Stations:				
III	1	26°58'N	97°11'W	25
	2	26°58'N	96°48'W	65
IV	1	26°10'N	97°01'W	27
	2	26°10'N	96°39'W	47
	3	26°10'N	96°24'W	91
	4	26°10'N	97°08'W	15
	5	26°10'N	96°54'W	37
	6	26°10'N	96°31'W	65
	7	26°10'N	96°20'W	130

seasonal samples. As a result, at least two seasonal samplings were taken over the entire area, with three seasonal samplings taken at the nine stations on the southernmost transect (see table 5). During the winter sampling season, 4 grab samples were taken at each of the 9 stations. In the summer and fall seasons, duplicate samples were taken at each of the 25 stations. During each of the three seasons, a composite sample was made in the laboratory of equal amounts of sediment from individual grabs at each station. Individual and composite samples were analyzed by identical procedures. This sampling format permitted both areal and seasonal comparisons and provided for assessment of variability.

In-laboratory calibration and reference samples were also analyzed by atomic absorption methods. The standards included Orchard Leaves and Bovine Liver obtained from the National Bureau of Standards; the marine reference sediment material, USGS MAG 1; the USGS standard rock material, G-2; and a composite sediment sample from the study area, which was exchanged with Texas A&M for an additional analysis. The results of these analyses (table 6) show that both the precision and accuracy of the analytical techniques of the laboratories compare favorably.

Methods

Partial leach (sediment)

For cadmium, chromium, copper, iron, lead, nickel, vanadium, and zinc determinations, the entire sample was dried at 90°C and ground in a ceramic grinder to pass through a 200 µm mesh nylon screen. From this

Table 6. Inter-calibration samples (ppm)

Lab	Ba	Cd	Cr	Cu	Fe	Mn	Ni	Pb	V	Zn
<u>MAG I</u>										
USGS, Corpus Christi Texas A&M	540±1	0.27±.07	108±3	29.0±5	51200±300	666±20	64.5±10	19.7±2	128±8	139±8
	-	-	120±5	30.3±0.6	49300±200	762±24	61.5±3	28.8±2.2	-	140±3
Prof. Paper 841	493	-	121±20	48.8	52400	-	50.7	20.4	132	102
<u>G-2</u>										
USGS, Corpus Christi Prof. Paper 841	1434	0.11	10.3	7.5	-	-	4.3	25.8	-	87.1
	1532	-	8.0	9.7	24400	410	2.4	31.3	44.6	68.2
<u>STOCS I/III</u>										
USGS, Corpus Christi Texas A&M	528±80	0.24±.04	64±1	16.4±3	32800	404	35.4±6	16.4±8	99±8	92±2
	-	-	71±5	17.5±.2	32100±200	468±1	30.9±1	25±1	-	87±2
<u>ON-HARD LEAVES</u>										
USGS, Corpus Christi NBS	-	0.12±0.04	4.3±0.8	10.2±0.2	29300±300	88±5	-	38.7±2	-	26.8±0.1
		0.11±0.02	2.6±0.2	12±1	30000±2000	91±4	-	45±3	-	25±3
<u>BOVINE LIVER</u>										
USGS, Corpus Christi NBS	-	0.20±0.07	-	176±1.8	26200±900	8.9±1.3	-	0.39±0.05	-	117±20
		0.27±0.04	-	193±10	27000±2000	10.3±1.0	-	0.34±0.08	-	130±10

sample, duplicate 1 g subsamples were weighed into preweighed and pre-fired crucibles, and were heated in a muffle furnace at 450°C for 6 hours. After cooling in a dessicator, the samples were reweighed and transferred to precleaned culture tubes; 10 ml of 16N HNO₃ (reagent grade) were added. After heating for 1 hour at 54°C, the solution was transferred to a teflon beaker and evaporated to dryness. The dried sample was brought into solution by the addition of 10 ml of 16N HNO₃, transferred to a culture tube, and analyzed by atomic absorption methods. For barium, the method was modified by the addition of 10 ml of 30 percent H₂O₂ to the sample prior to the addition of the nitric acid. This solution was then mixed well and analyzed for barium. The instrument settings are given in table 7.

Table 7. Instrument Parameters and Mode of Analysis
 -360 FE with an HG2100 Graphite Furnace = flameless
 -303 = flame

Element	Wave Length	Dilution	Mode	Dry Temp.	Ashing Temp.	Atom. Temp.
Ba	2776	1:40(1:200)	Flameless	100°C	1200°C	2700°C
Cd	2293	1:10	Flameless	100°C	250°C	2100°C
Cu	3262	1:10	Flame	--	--	--
Cr	3589	1:100	Flameless	100°C	1200°C	2700°C
Fe	2483	1:1000	Flame	--	--	--
Mn	2801	1:60	Flame	--	--	--
Ni	2330	1:10	Flame	--	--	--
Pb	2842	1:10	Flameless	100°C	550°C	2000°C
V	3194	1:10	Flameless	100°C	1700°C	2700°C
Zn	2146	1:60	Flame	--	--	--

Totals (sediment)

The sample was ground and homogenized. Duplicate 0.25 g samples were placed in preweighed and pre-fired porcelain crucibles and were

fired in a muffle furnace at 450°C for 6 hours. The sample was then cooled in a dessicator, reweighed, carefully transferred into a 50 ml teflon beaker, and wetted with 12N HCL. Four ml of 16N HNO₃ were added. The sample was then stirred and evaporated to dryness. The residue was redissolved in 2 ml of 30 percent H₂O₂, followed by the addition in sequence of 3 ml of 12N HCL, 1 ml of HF, 10 ml of 8N HNO₃ and 1 ml of 12N HCL. One ml of 16N HNO₃ was added to the residue, and it was diluted to a total volume of 10 ml. This solution was analyzed by atomic absorption. The instrument settings are given in table 7.

Total biological material (Bovine Liver and Orchard Leaves)

Duplicate 0.5 g, freeze-dried, homogenized samples were placed into 50 ml teflon beakers, and 6 ml of 3 to 1 concentrated HCL: HNO₃ mixture were added. The sample was covered with a watch glass and allowed to digest at room temperature overnight or until the sample ceased to foam or bubble. It was then slowly heated for 1-1/2 hours and evaporated to near dryness. To this solution, 30 percent H₂O₂ was added until the resulting solution was clear to yellow in color. Again, the sample was taken to near dryness by repeating the last process. To the residue, 5 ml of 16N HNO₃ were added, and the solution was transferred to a 25 ml volumetric flask, brought to volume with 1 to 1 HCL and filtered through a 0.4 µm NUCLEOPORE filter. The solution was analyzed using atomic absorption methods. The instrument settings are given in table 7.

Results

Intercalibration

The results of the intercalibration and standardization with Texas A&M University and the National Bureau of Standards are presented in table 6. For all elements agreement between laboratories is very close. The samples were analyzed by a direct method and in some cases by the method of additions, with consistent results in all instances. To insure quality control, commercially prepared standards were compared to standards prepared in the laboratory by dissolving the appropriate amount of the particular metal or by using a primary standard when available. No significant variation was determined and values were within limits imposed by experimental error.

Seasonal sediment samples

The results of the analyses from the three seasonal samplings are listed in appendix 6. All samples were analyzed in duplicate.

Average Percent Deviation of Duplicate Analyses

Ba	9.0	Mn	2.6
Cd	8.3	Ni	5.9
Cr	7.4	Pb	7.4
Cu	4.4	V	6.9
Fe	3.0	Zn	4.2

Average percent deviations indicate that the reproducibility of duplicate analyses is considerably better for those elements analyzed by flame methods than for those analyzed by flameless methods. This result is due to the increased sensitivity obtained by using the flameless atomic absorption instrument.

Discussion

Areal variation

During the winter cruise, subsamples were taken in quadruplicate at each station and analyzed individually. A composite of the four samples was also analyzed, providing an opportunity to investigate site variability. Figures 85 to 94 show graphically the variability at each site for each element analyzed. The average of the four individual samples was plotted along the abscissa against the value for each individual sample and the composite along the ordinate. The graphs show the variability for each element as well as the concentration range for the winter sampling period. On such a diagram, if no significant variability exists, all values would fall along or close to a 1 to 1 line. Most of the values fall within a 10 percent error envelope indicating very little site variability. Although manganese varied more at individual sites than the other elements, the results for composite samples consistently fall along the 1 to 1 line, suggesting that site variability is overcome by analyzing a composite sample. Generally, site variability is greater at nearshore stations where the sediment texture is highly variable. Composite samples or average values from several grab samples should be used to obtain a representative value rather than relying on the value of any one individual sample for these sites.

Seasonal variability

All of the data from the three years of sampling was used to compare seasonal and areal variability. Some stations from the first year's study did not correspond to the stations occupied during the past two year's studies, and only nine sites were sampled during the winter:

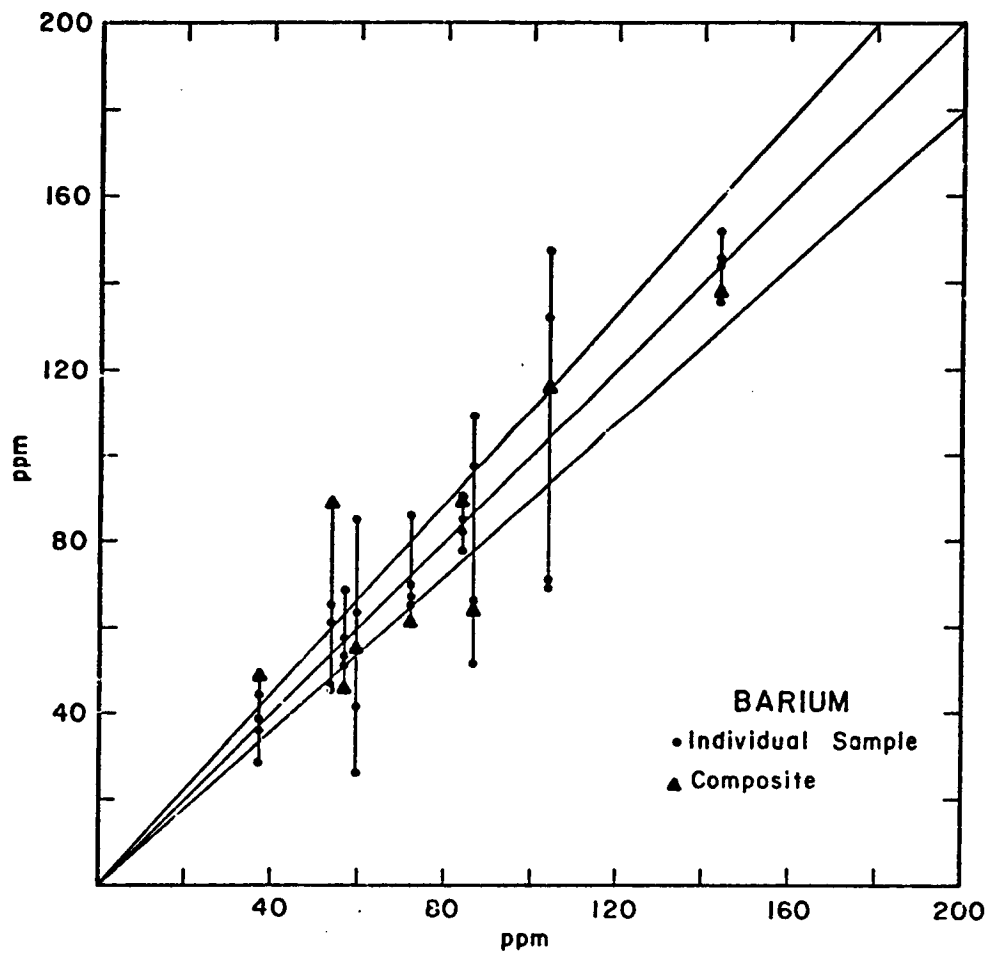


Figure 85. Variations in the concentrations of barium in benthic sediments at individual stations, winter sampling. The divergent lines define an envelope of 10 percent deviation.

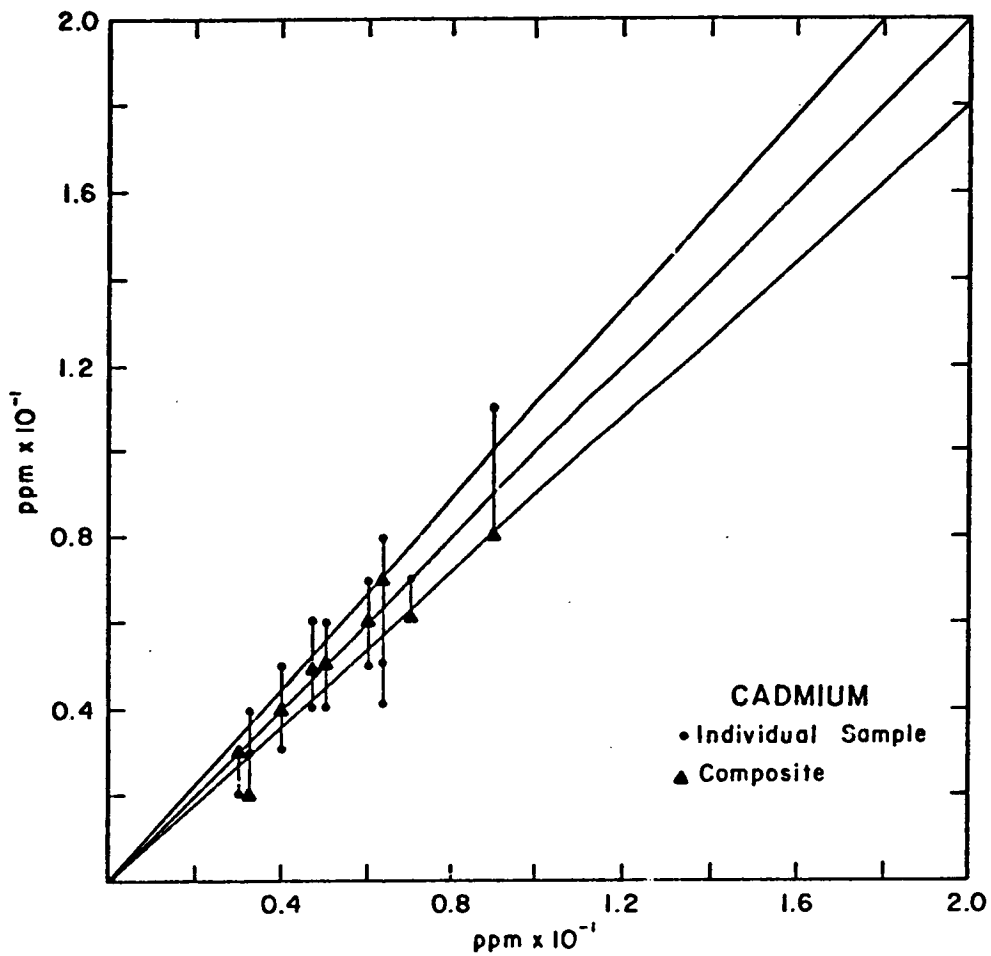


Figure 86. Variations in the concentrations of cadmium in benthic sediments at individual stations, winter sampling. The divergent lines define an envelope of 10 percent deviation.

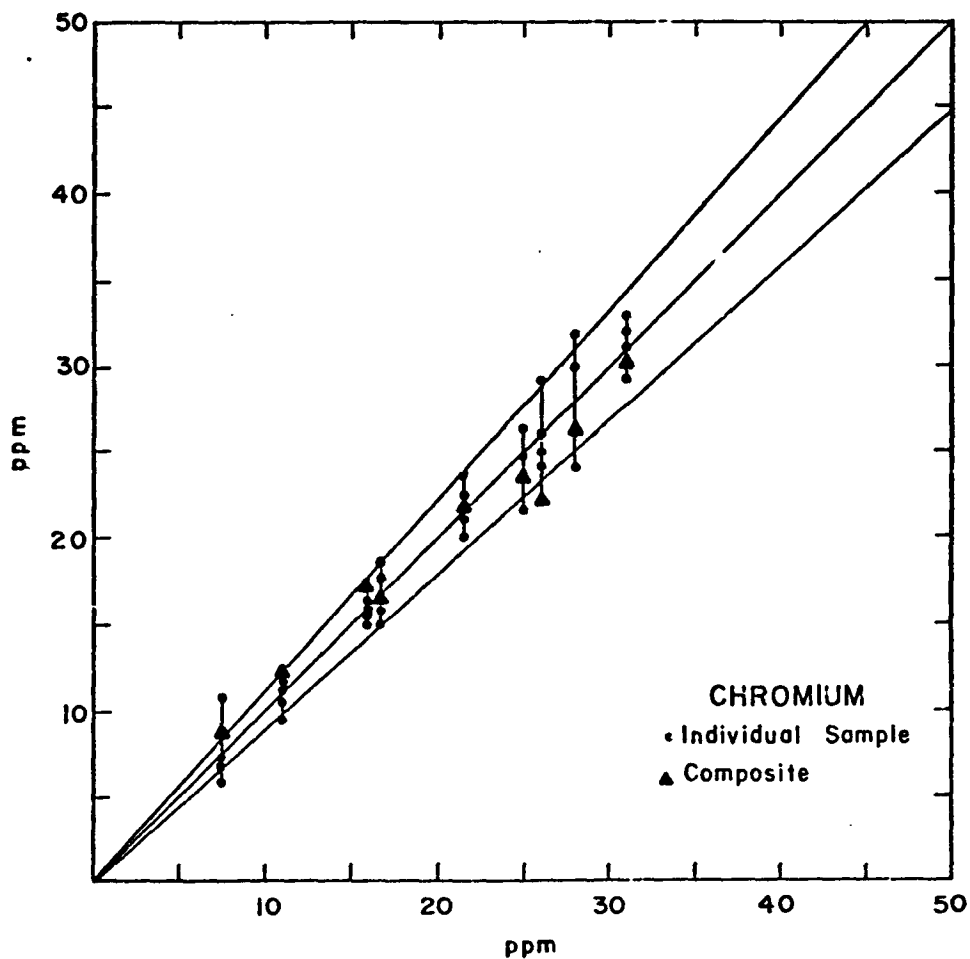


Figure 87. Variations in the concentrations of chromium in benthic sediments at individual stations, winter sampling. The divergent lines define an envelope of 10 percent deviation.

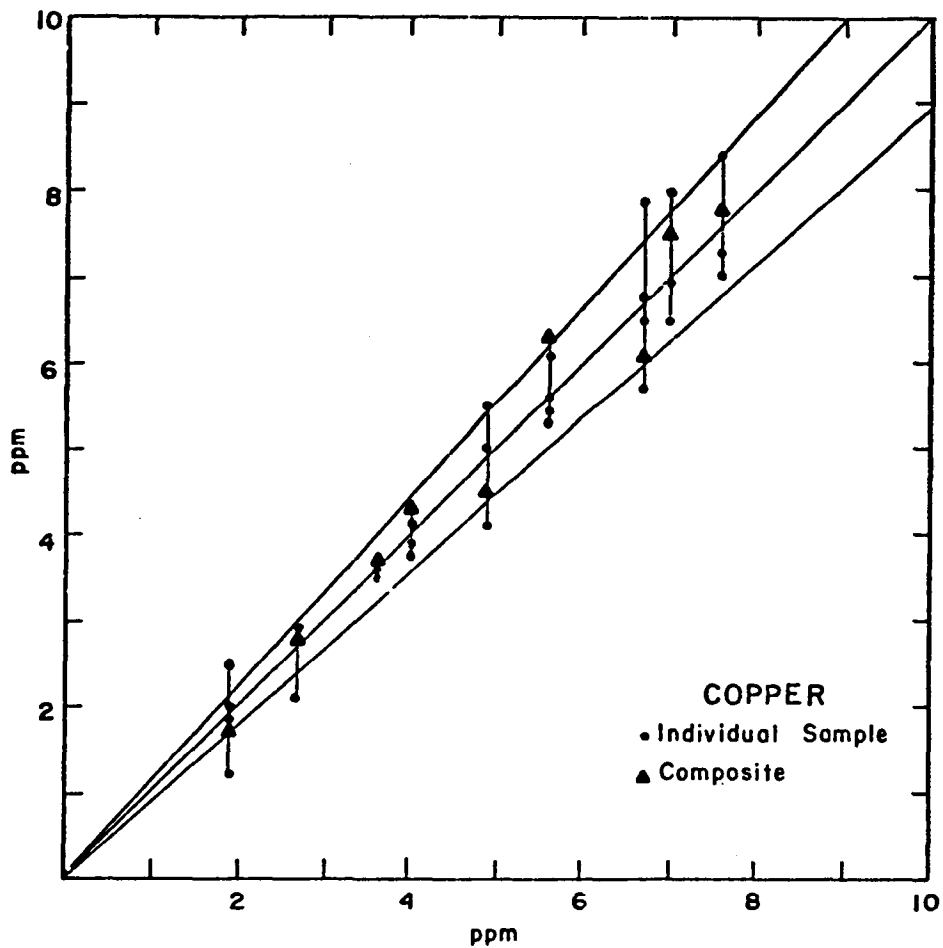


Figure 88. Variations in the concentrations of copper in benthic sediments at individual stations, winter sampling. The divergent lines define an envelope of 10 percent deviation.

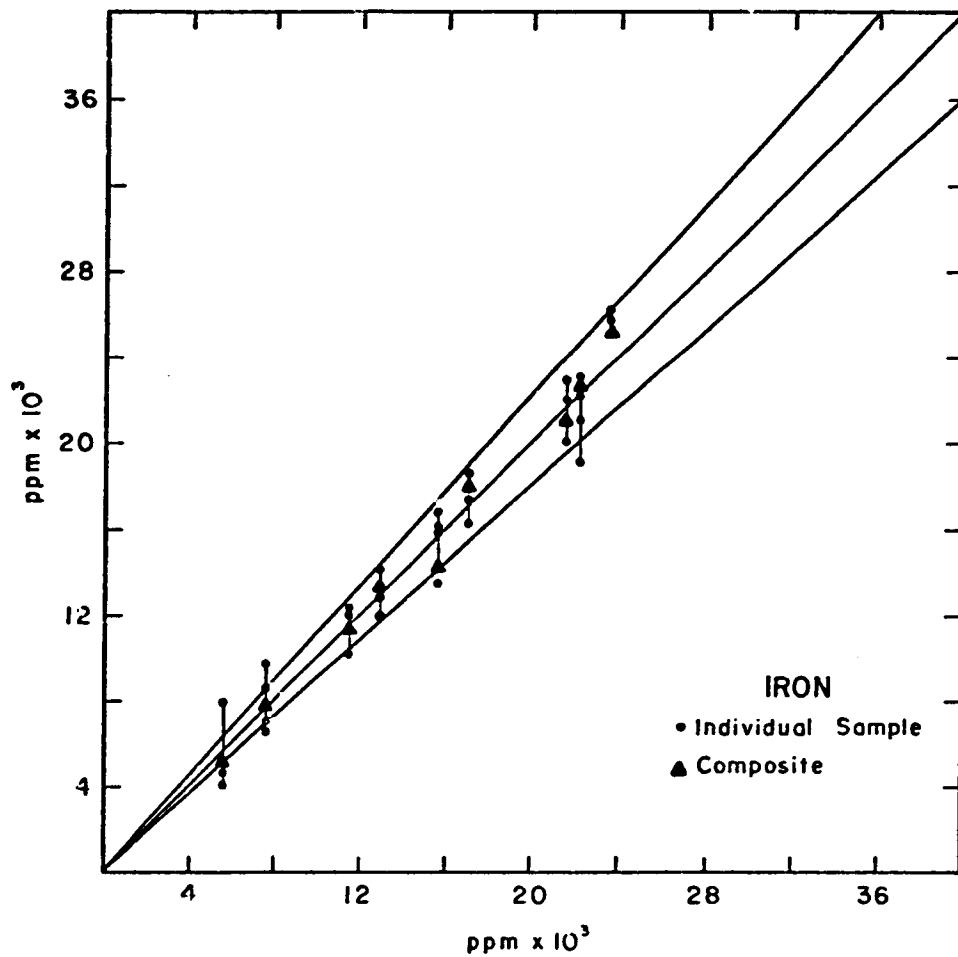


Figure 89. Variations in the concentrations of iron in benthic sediments at individual stations, winter sampling. The divergent lines define an envelope of 10 percent deviation.

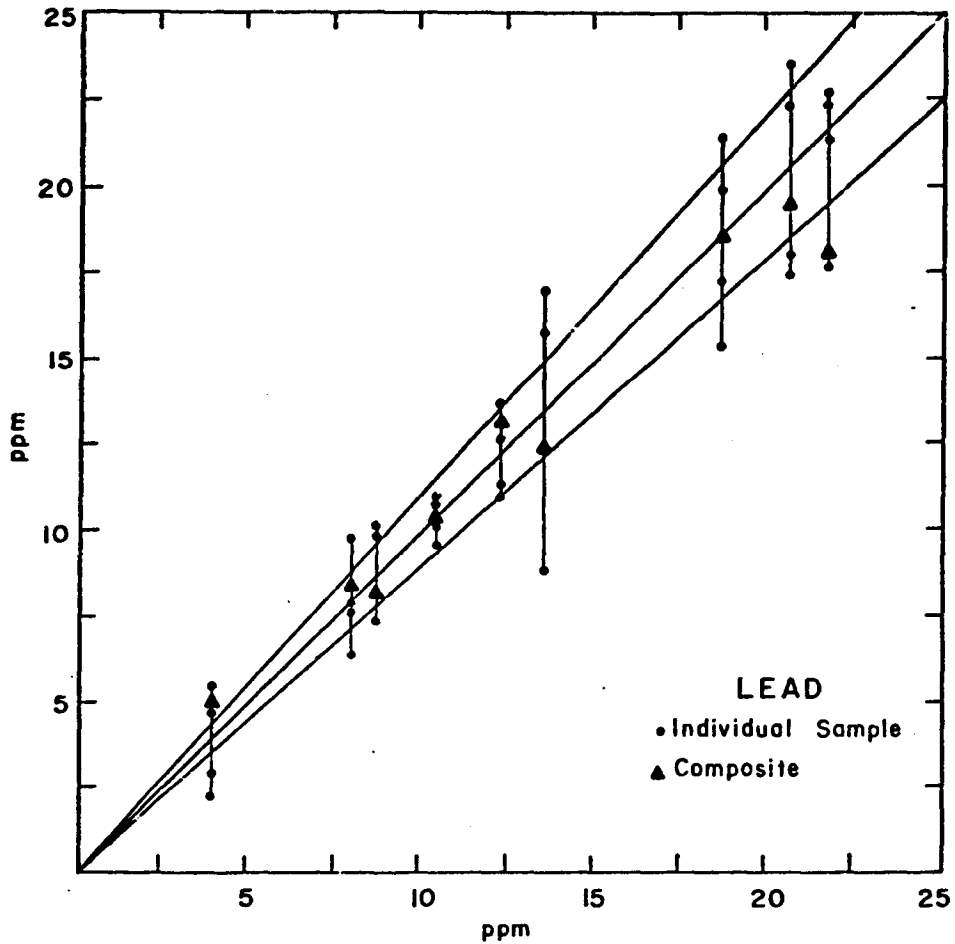


Figure 90. Variations in the concentrations of lead in benthic sediments at individual stations, winter sampling. The divergent lines define an envelope of 10 percent deviation.

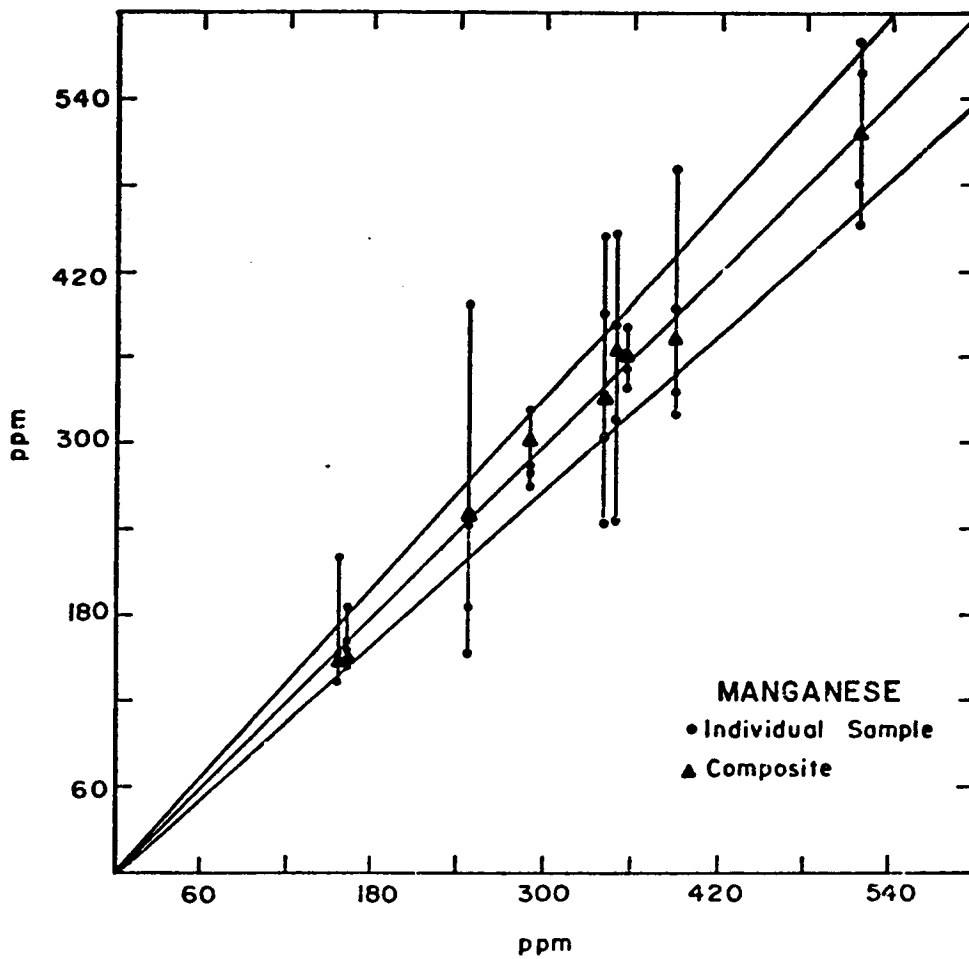


Figure 91. Variations in the concentrations of manganese in benthic sediments at individual stations, winter sampling. The divergent lines define an envelope of 10 percent deviation.

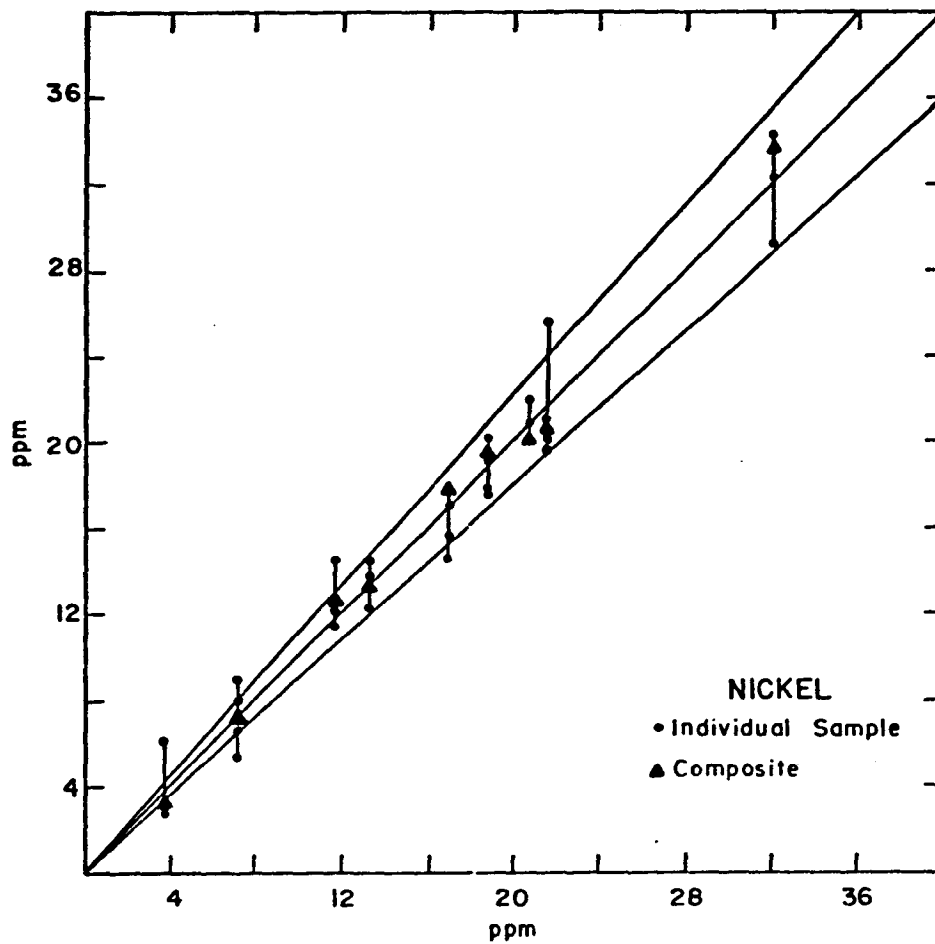


Figure 92. Variations in the concentrations of nickel in benthic sediments at individual stations, winter sampling. The divergent lines define an envelope of 10 percent deviation.

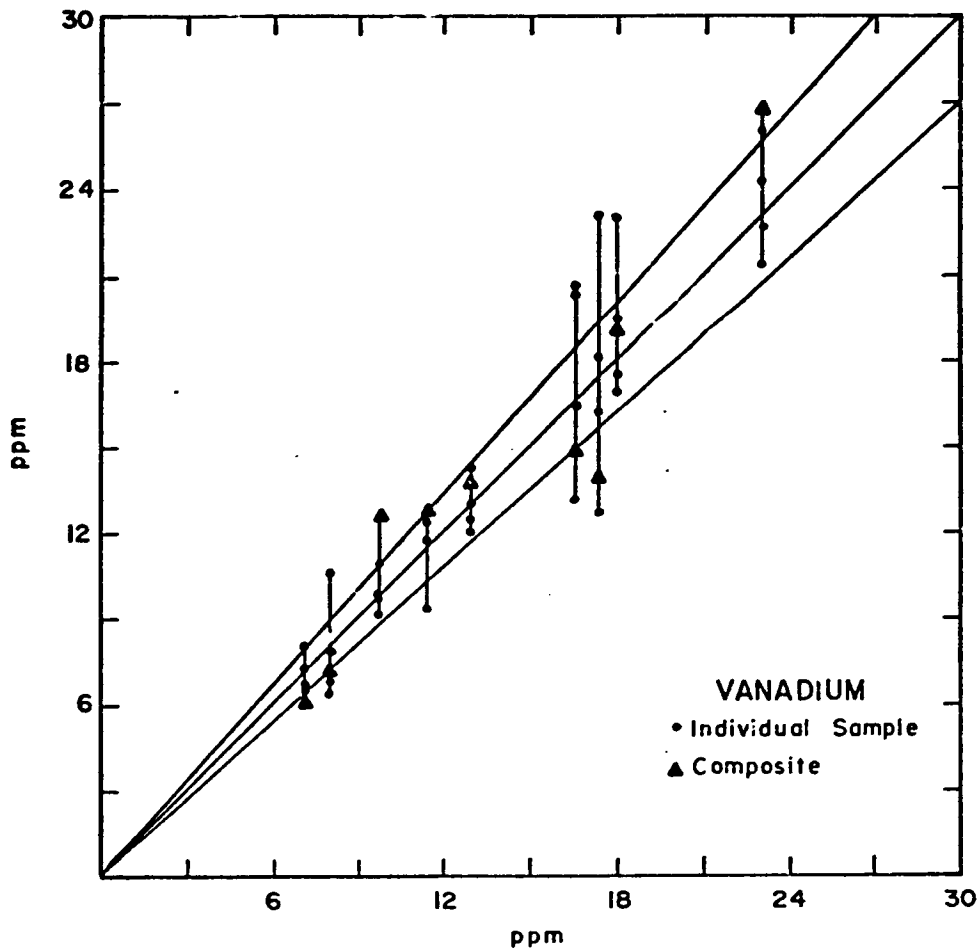


Figure 93. Variations in the concentrations of vanadium in benthic sediments at individual stations, winter sampling. The divergent lines define an envelope of 10 percent deviation.

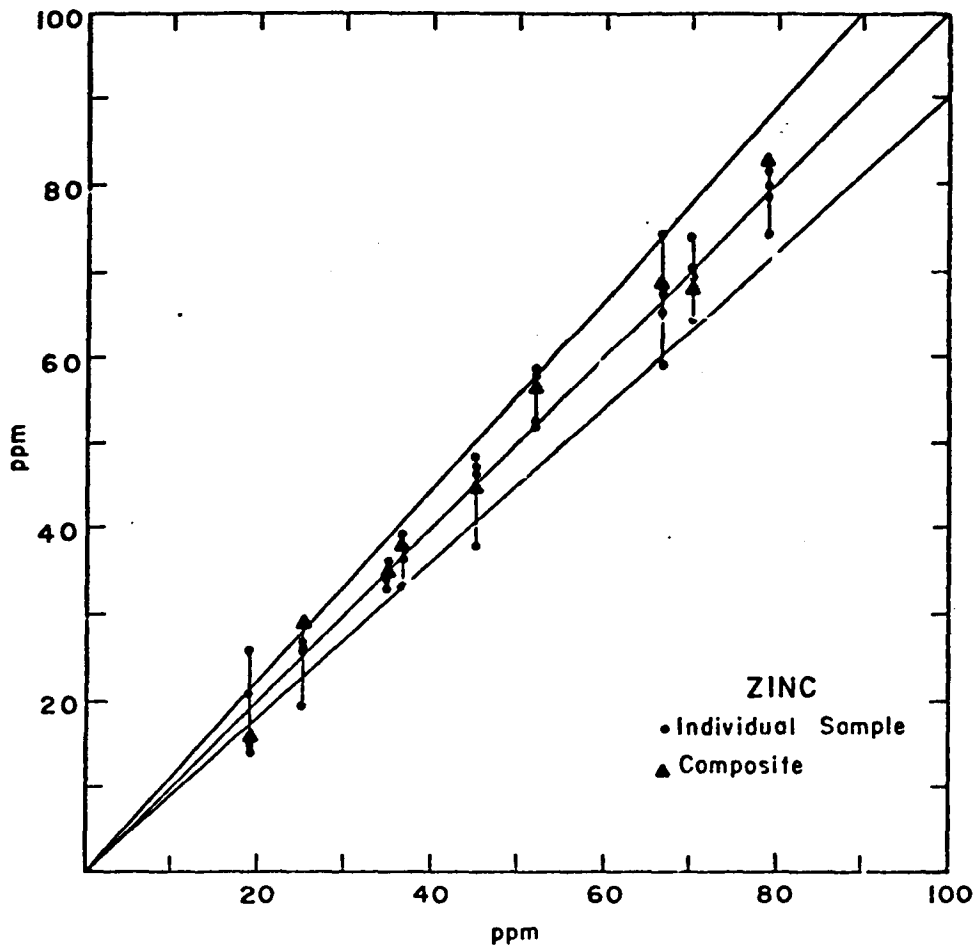


Figure 94. Variations in the concentrations of zinc in benthic sediments at individual stations, winter sampling. The divergent lines define an envelope of 10 percent deviation.

season of 1977. In all instances, however, at least 5 and as many as 7 values were available for each element at each site over the 3-year study.

The plots of the dispersion indices (the standard deviation divided by the mean) for seasonal samples against those from a single station (summer cruise, 1976) are shown by figures 95 to 97. If no significant difference between the seasonal and areal sampling existed, the graphical values should fall along or near the 1 to 1 line. All elements for the sites on transect IV indicated a significant departure from the patterns of variability common to the sites of transects I, II, and III, particularly the nearshore sites IV/1 and IV/4. Values from transect IV, which are indicated by X's on the graphs, vary seasonably more than the values from other transects. Excluding the transect IV values, the zinc, cadmium, iron, and copper values fall very close to the 1 to 1 line, indicating there is no apparent difference between the seasonal and areal values. The remaining element indices fall above and close to the seasonal axis, demonstrating that seasonal variability is probably greater than areal variability. In general, greater variability occurs at the innermost stations and seasonal variations seem to affect some elements more than others.

As each season's samples were analyzed when they were submitted to the laboratory, there was a possibility that some of the variations indicated were caused by inadvertent variations in laboratory processing and procedures. To examine this possibility nine samples from last year's seasonal monitorings were reanalyzed with this year's samples. The results presented in table 8 document very close agreement between the amounts measured last year and those measured during reanalysis.

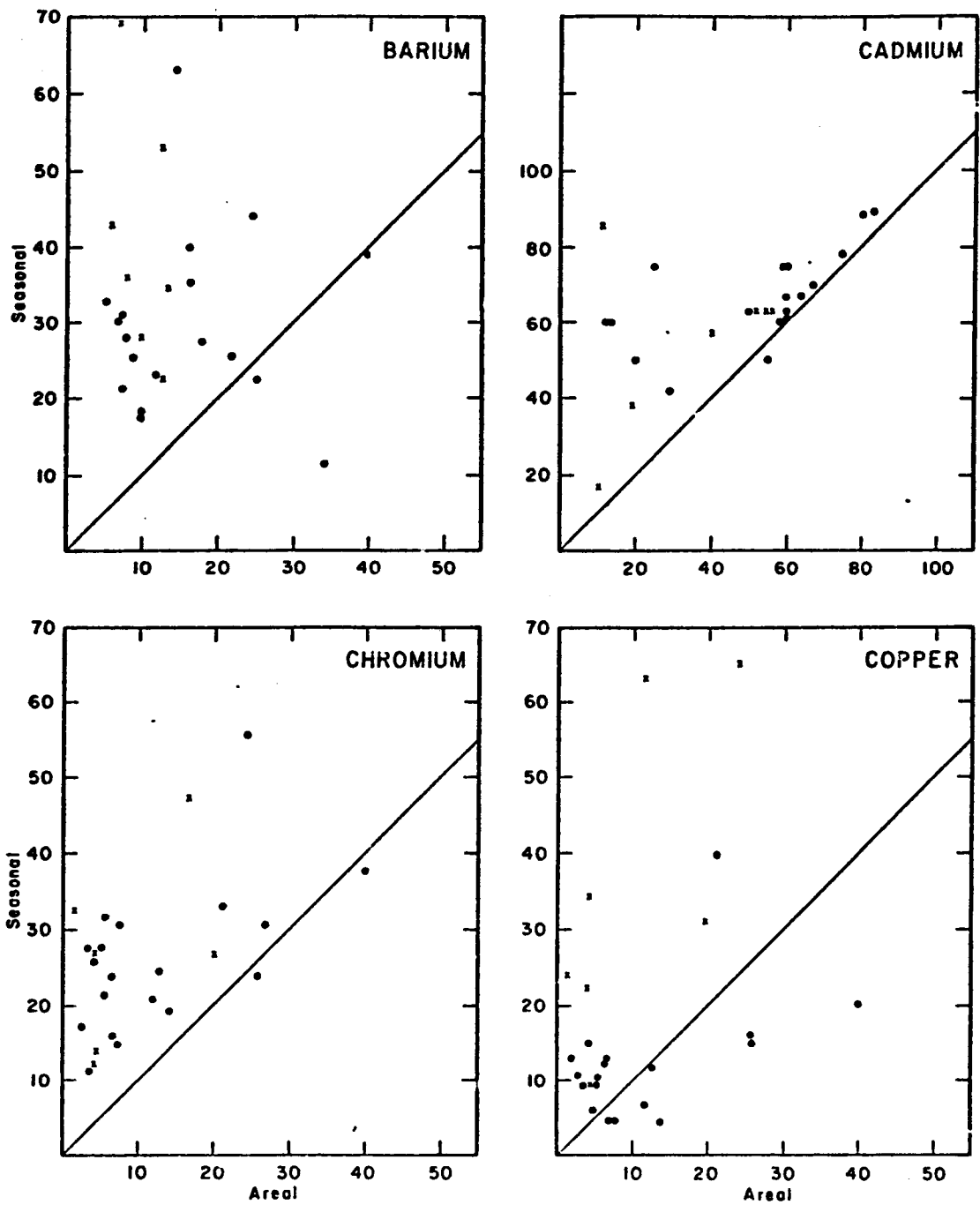


Figure 95. Plot of dispersion indices, seasonal versus areal distribution in benthic sediments.
 . indicates an individual sample
 x indicates an individual sample from transect IV.

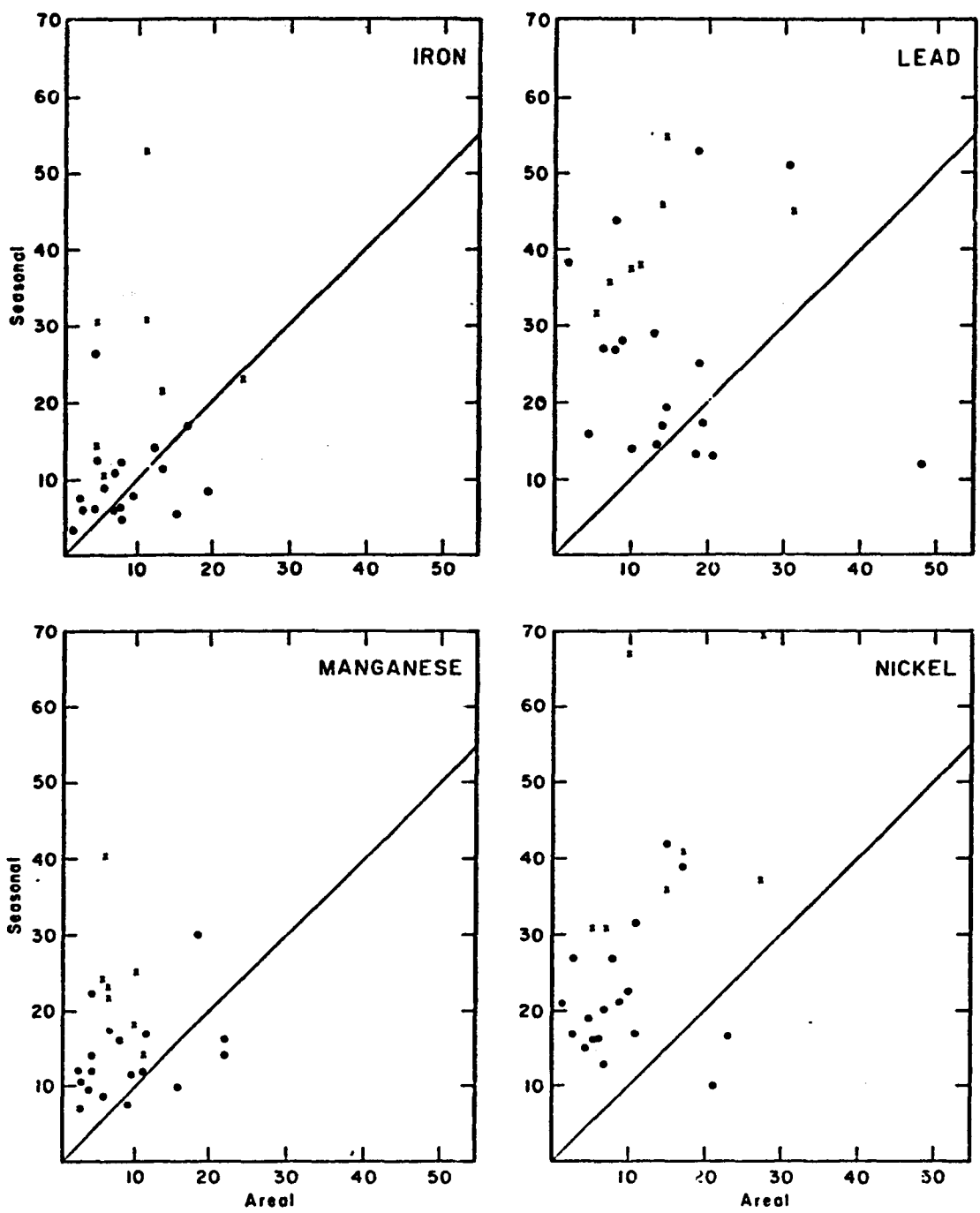


Figure 96. Plot of dispersion indices, seasonal versus areal distribution in benthic sediments.
 . indicates an individual sample
 x indicates an individual sample from transect IV.

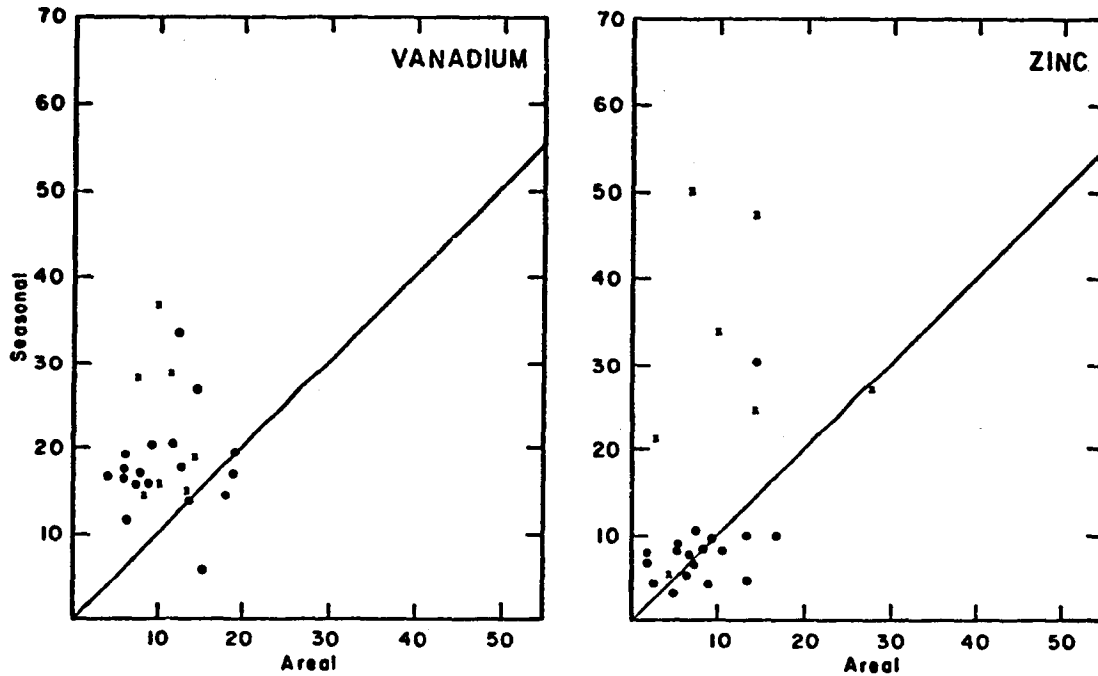


Figure 97. Plot of dispersion indices, seasonal versus areal distribution in benthic sediments.
 . indicates an individual sample
 x indicates an individual sample from transect IV.

Trace metal content

Comparison of the trace metal content of benthic sediments from one year to the next is very difficult because of the sampling patterns. The 1974 sites are not the sites occupied in the 1975-1976 and 1976-1977 programs. Also, the winter data collections of 1974 and 1976 were not repeated at all of the 1977 sites, and no summer or spring data were collected in 1974. If the averages from each year are compared, although the values at a site may vary from season to season, the yearly averages do not change significantly. Since the amounts and general patterns from any year are consistent, when taken together, the averages from these past three years may be considered characteristic of each particular site.

Table 8 . Results of reanalysis of 1976 seasonal samples. Reruns were in duplicate. Concentrations in parts per million.

Sample	Cu	Cu*	Fe	Fe*	Mn	Mn*	Ni	Ni*	Pb	Pb*	Zn	Zn*
Season I												
II/1	6.4	6.0	19,000	16,000	291	268	12.6	12.2	5.5	5.5	59.8	53.8
III/4	1.4	1.7	6,300	6,500	222	195	5.5	5.5	2.4	1.6	30.2	24.8
I/5	6.3	6.9	20,000	23,400	285	256	17.4	17.7	10.0	ND	81.9	75.5
Season II												
I/4	2.9	2.9	9,500	9,000	191	172	6.1	6.6	3.1	3.0	30.1	29.6
III/5	5.9	6.8	19,500	20,200	350	320	15.1	14.2	6.0	6.1	72.7	50.0
IV/6	4.9	5.5	17,300	17,200	252	220	13.9	9.5	3.9	4.3	57.8	47.3
Season III												
I/2	4.7	4.9	18,900	16,000	239	242	14.8	14.2	6.9	6.0	58.8	53.7
II/4	5.3	6.2	19,600	20,100	299	296	14.8	14.7	7.0	7.2	66.1	61.9
IV/2	5.8	6.1	21,700	20,400	298	304	14.3	13.1	7.7	7.9	65.0	62.2

*Reanalysis

N.D. - not determined

Geochemical Anomaly Along the 27° Parallel

by

Charles W. Holmes and E. Ann Martin

Trace metal content distribution of the upper 10 cm of the sediment column mapped in 1974/75 revealed an apparent geochemical discontinuity, roughly along the 27° N. latitude. In the past, many investigators studying the physics, chemistry, biology, and geology of the Texas shelf have recognized similar significant north-south variations; therefore, "27° anomaly" is a term in common usage. In the 1974 sample analyses, the sediments in the north contained less manganese (fig. 98), nickel (fig. 99), and copper (fig. 100) than those south of the 27° parallel. To understand the trace element chemistry of the shelf, the processes causing such discontinuity must be understood.

Methods

In addition to the 273 grab samples analyzed during the first year study and the 44 cores dated by ^{210}Pb in 1976 (see appendix 7 for station locations), 22 cores were taken across the geochemical discontinuity (see table 9 for station locations). Only 60 locations are plotted on figure 101 because 5 cores were either lost or disturbed. These cores were obtained in such a manner that the sediment-water interface was preserved with minimum disturbance; the cores were maintained in the vertical position, frozen, and returned to the laboratory. In the laboratory, the cores were sampled at 1 cm intervals below the surface 2 cm. The samples were analyzed for manganese, nickel, and copper by the atomic absorption methods used throughout the baseline studies on the south Texas shelf (Martin and Holmes, this report).

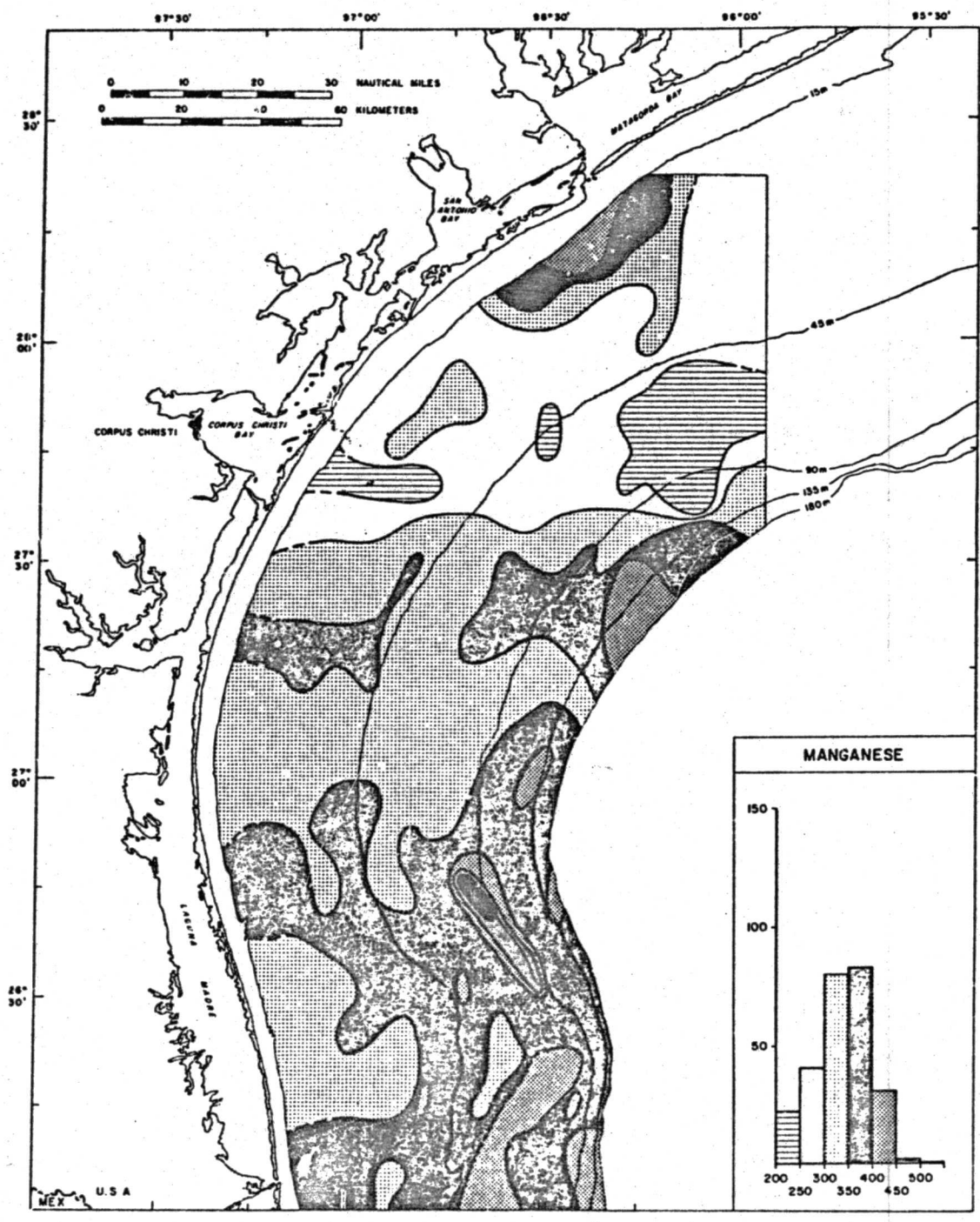


Figure 98. Values for manganese determined from 1974 grab samples.



Figure 99. Values for nickel determined from 1974 grab samples.

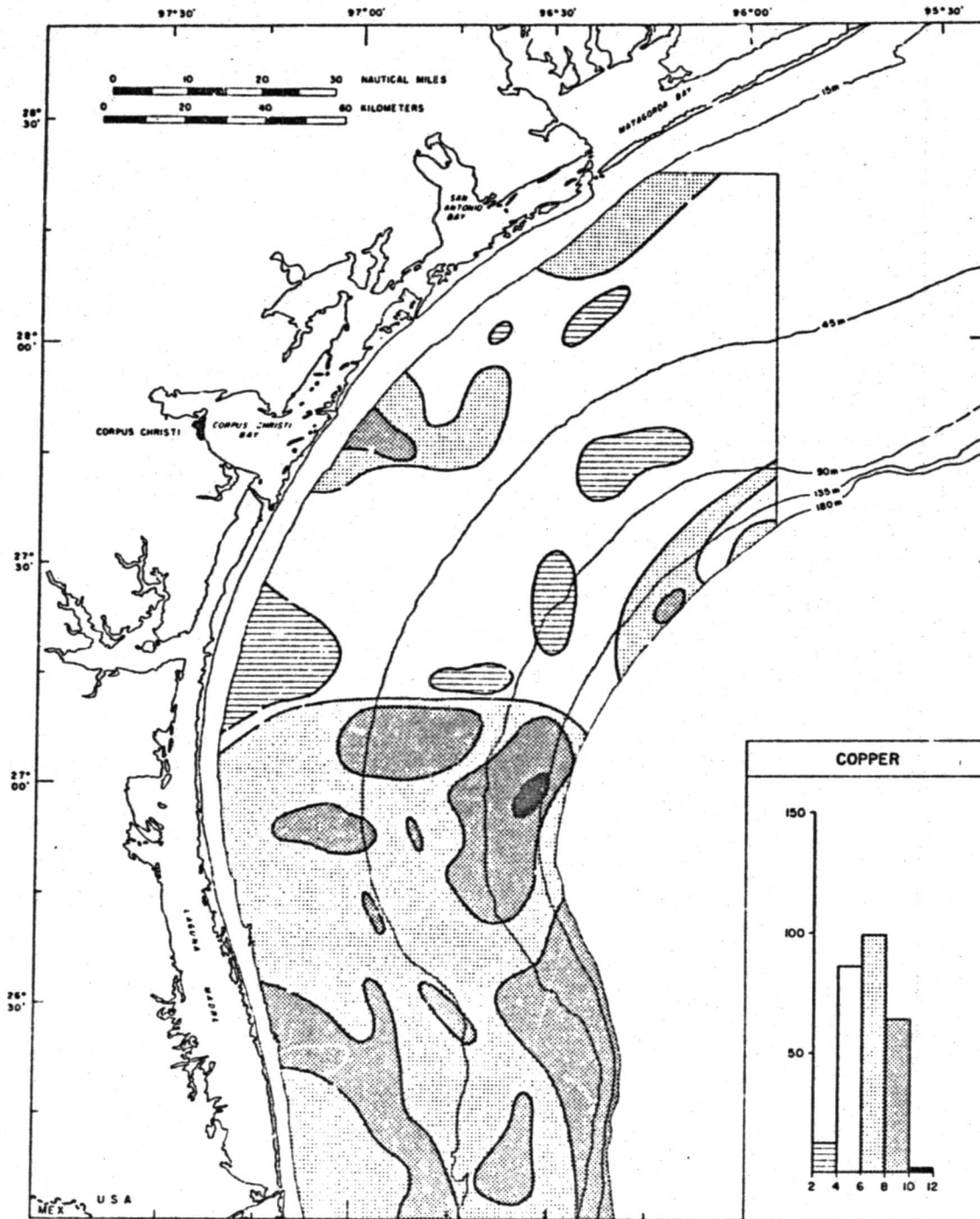


Figure 100. Values for copper determined from 1974 grab samples.

Table 9.

Rates of Sedimentation - 1977 Study

Core number	Latitude	Longitude	Mn ₁₀	Rate (mm/yr)	Remarks
1	27°27'	96°50'	278	7.32	
2	27°19'	96°36'	376	1.91	13 cm surface mixed zone
4	27°05'	96°30'	334	Core disturbed	
5	27°00'	96°30'	344	1.02	
6	26°59'	96°30'	397	Core disturbed	
7	26°55'	96°31'	454	0.66	
8	26°52'	96°30'	379	0.55	9 cm surface mixed zone
9	26°53'	96°34'	404	1.35	8 cm surface mixed zone
10	26°53'	96°36'	431	0.65	
11	26°53'	96°39'	368	1.22	
12	26°53'	97°11'	317	0.645	5 cm sand zone at surface
13	26°57'	97°12'	339	1.12	14 cm surface mixed zone
14	26°58'	97°10'	207	1.06	6 cm sandy zone at surface
15	27°01'	97°10'	348	2.14	sand zone at 9-16 cm
16	27°03'	97°11'	311	0.95	6 cm surface mixed zone
17	27°07'	97°14'	344	3.63	sand zone 5-10 cm
27	27°06'	96°51'	281	1.96	
28	27°04'	96°52'	331	Core disturbed	
29	27°01'	96°51'	355	Core disturbed	
30	26°59'	96°51'	-	Core lost	
31	26°56'	96°51'	343	1.24	
32	26°53'	96°50'	376	Core disturbed	

The ^{210}Pb dating procedures were the same as those used in the second year studies (Holmes and Martin, 1977). The entire sample was dried and ground to a fine powder. A 5 g representative subsample was weighed into a precleaned porcelain crucible and placed in a muffle furnace at 450°C for 6 hours. The sample was allowed to cool in a dessicator and was reweighed in order to obtain a dry sample weight.

The dry sample was transferred to a 100 ml teflon beaker with 5 ml of concentrated reagent grade nitric acid. The appropriate amount of ^{208}Po spike was added, and the sample was evaporated to dryness under heat lamps. Five ml of 30 percent hydrogen peroxide was added and allowed to react with the sample. The solution was again evaporated to dryness. Hydrochloric acid addition was repeated until all traces of the nitric acid were removed.

The sample was redissolved in 5 ml of concentrated hydrochloric acid and transferred to a 100 ml glass beaker. After the addition of 2 ml of 25 percent sodium citrate, 5 ml of hydroxylamine hydrochloride, and 10 mg of bismuth carrier, the pH of the resulting solution was adjusted to 2.0 with ammonium hydroxide. The beaker was placed on a stirring hot plate and heated to $85^{\circ}\text{--}90^{\circ}\text{C}$. Stirring and heating continued for 5 minutes. A silver disc was secured in the teflon plating device and lowered into the solution taking care not to trap air pockets beneath the disc. Heating and stirring continued for a minimum of 90 minutes. The silver disc was removed from the plating apparatus, rinsed with deionized water and allowed to dry. The disc was counted on an alpha spectrometer.

Results

The manganese distribution mirrors that of the grab sample results obtained in 1974 (fig. 98). Amounts of nickel and copper also are similar

to those values determined in 1974, falling within the analytical error of the methods used (Holmes and Martin, 1977; Martin and Holmes, this report) (figs. 99 and 100). In addition to the trace metal data, values for excess ^{210}Po also are listed in appendix 8. Of the 22 cores, 5 were found to be disturbed when opened in the laboratory and were not analyzed. One core was lost during shipping. The estimated rates of sedimentation are listed in table 9. The analytical data are presented in appendix 8.

Discussion

The marine chemistry of manganese has been the subject of many reports (Krauskopf, 1956; Lynn and Bonatti, 1965; Bischoff and Sayles, 1972) which provide a basic understanding of the general mode of the marine chemistry of manganese. The element, either in the ionic form or as a hydroxide film adhering to detrital material, enters the sea via rivers. Manganese hydroxide scavenges many trace metals, in particular copper and nickel. Once in the marine environment the manganese, which enters in the ionic state, also hydrolyzes and precipitates to the sea floor, carrying nickel, copper, cobalt, thorium, and other elements. Thus, distribution of the adsorbed form of manganese will be influenced both by the source and by the sedimentologic environment; regions with the highest clay material will in general have the highest manganese content. The high manganese content of the sediment south of Matagorda Bay and at the shelf edge east of Corpus Christi correlates with the predominantly clay-size sediment in those regions.

Significant manganese concentrations, however, may also be a product of another process. The decay of organic detritus in the deposited sediments produces a reducing chemical environment. Under such conditions, manganese

is reduced to the soluble Mn^{+2} species and migrates by ionic diffusion toward the surface, tending to concentrate in the surface layers of the sediment column. The lower boundary of such an enriched layer is marked by a decrease in the oxidation potential. The rate at which such a migration can occur is dependent upon the amount of organic material, the rate of decay, and the rate of sedimentation.

On the south Texas continental shelf, the organic content is fairly homogeneous (Patrick Parker, pers. commun., 1977) and as there is no severe climatic change throughout the year on the shelf, the decay of the organic material may also be fairly constant. The rate of sedimentation must account for the uneven distribution of manganese. The measured rates of sedimentation on the shelf generally vary from less than 0.5 mm/yr to 7.4 mm/yr, except for a local area near the mouth of the Rio Grande where rates exceed 9 mm/yr (fig. 101). The areas of slow sedimentation rates correlate well with those of high manganese concentrations in the southern part of the study area, thus indicating that manganese, copper, and nickel concentrations are the result of migration within the sediment column and are not diluted by a high rate of sedimentation. Further substantiation for the process is provided by the vertical distribution of manganese in the sediments, which is distinctly higher in the upper 10 cm.

In summary, manganese and associated nickel and copper distributions on the continental shelf are the result of two distinct but not mutually exclusive processes. The region south of Matagorda Bay is a site both of fine sediment deposition and of increased manganese content. There the increased manganese content is caused by rapid deposition of detrital substances coated by a manganese film. Further south the increased manganese content is caused by the migration of manganese upward through the sediment

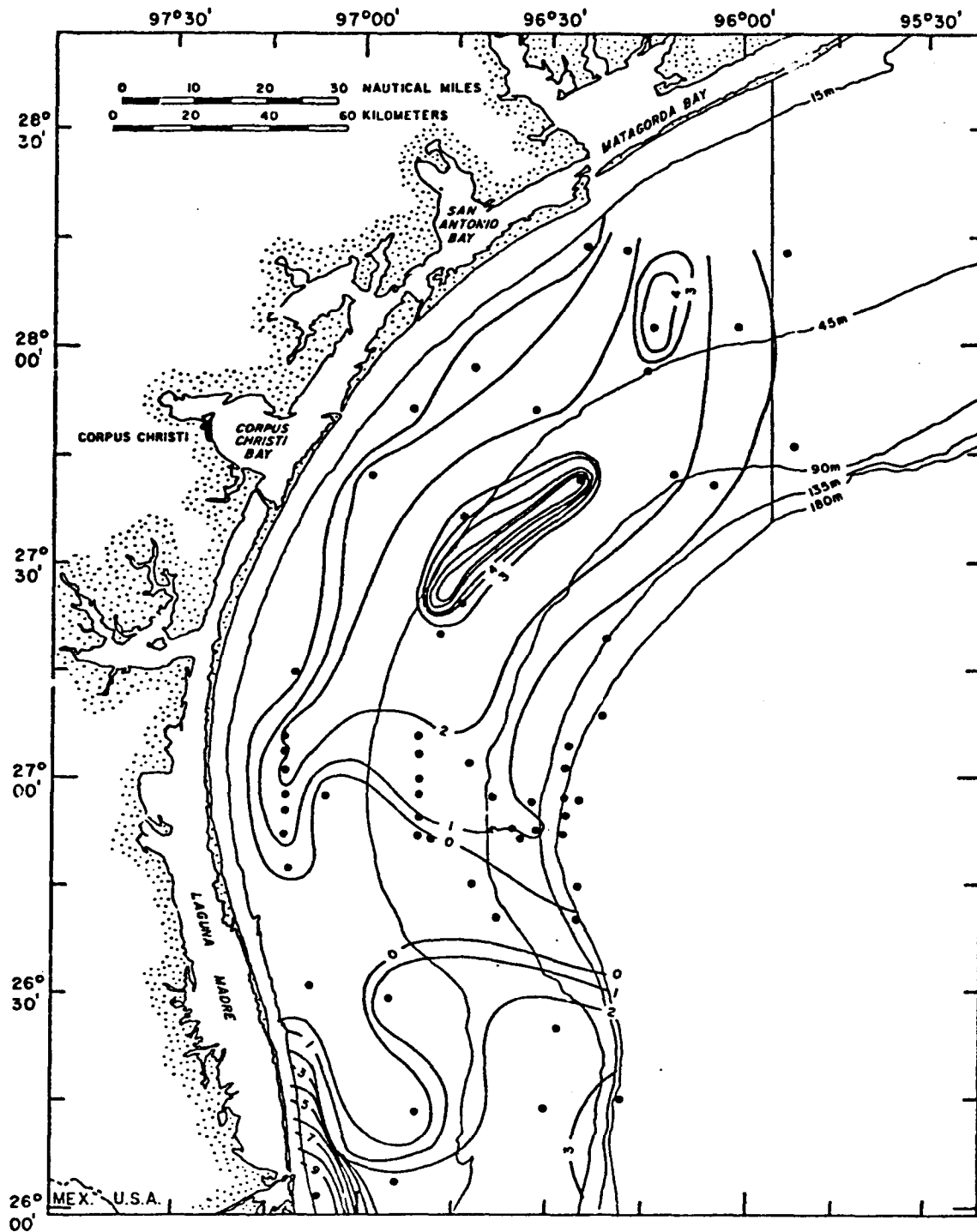


Figure 101. Rates of sedimentation estimated from ^{210}Pb content, in mm/yr.

coupled with slow sedimentation. The manganese concentration at the edge of the shelf, east of Corpus Christi, is caused by both the deposition of clay-sized sediments plus upward migration.

CONCLUSIONS AND INTERRELATIONSHIPS

by

Henry L. Berryhill, Jr.

The more significant results of the studies that involved seasonal sampling during 1977 are summarized in the series of illustrations, figures 102 through 107. The series of small maps showing the results of the suspended sediment studies grouped by season provide for quick visual comparison of regional patterns of distribution and thus help to emphasize both the relation of one aspect to another and the broader trends that reveal regional characteristics.

For comparing summary results for 1977 to those of 1976, the similar maps for 1976 (Berryhill, 1977, p. 433-436) are repeated, following the summary maps for 1977 (figs. 108-112).

The results for 1977 showed a consistent distribution by season for most of the trace metals in the suspended sediments, and an overall inter-relationship of total particulates, total carbon, and clay minerals that strongly confirms the theory that two general masses of water interact over the South Texas OCS: an inner shelf water mass and an outer shelf water mass.

The total particulates, total carbon, and clay minerals analyses for the fall of 1976 indentify in striking, and indeed classic fashion, the nature of the hydrographic regime (figs, 102 and 103). The patterns for both the total particulates and the montmorillonitic clay, signify the inner shelf terrigenous component, which includes the inflowing waters and the higher energy conditions that normally prevail on the inner

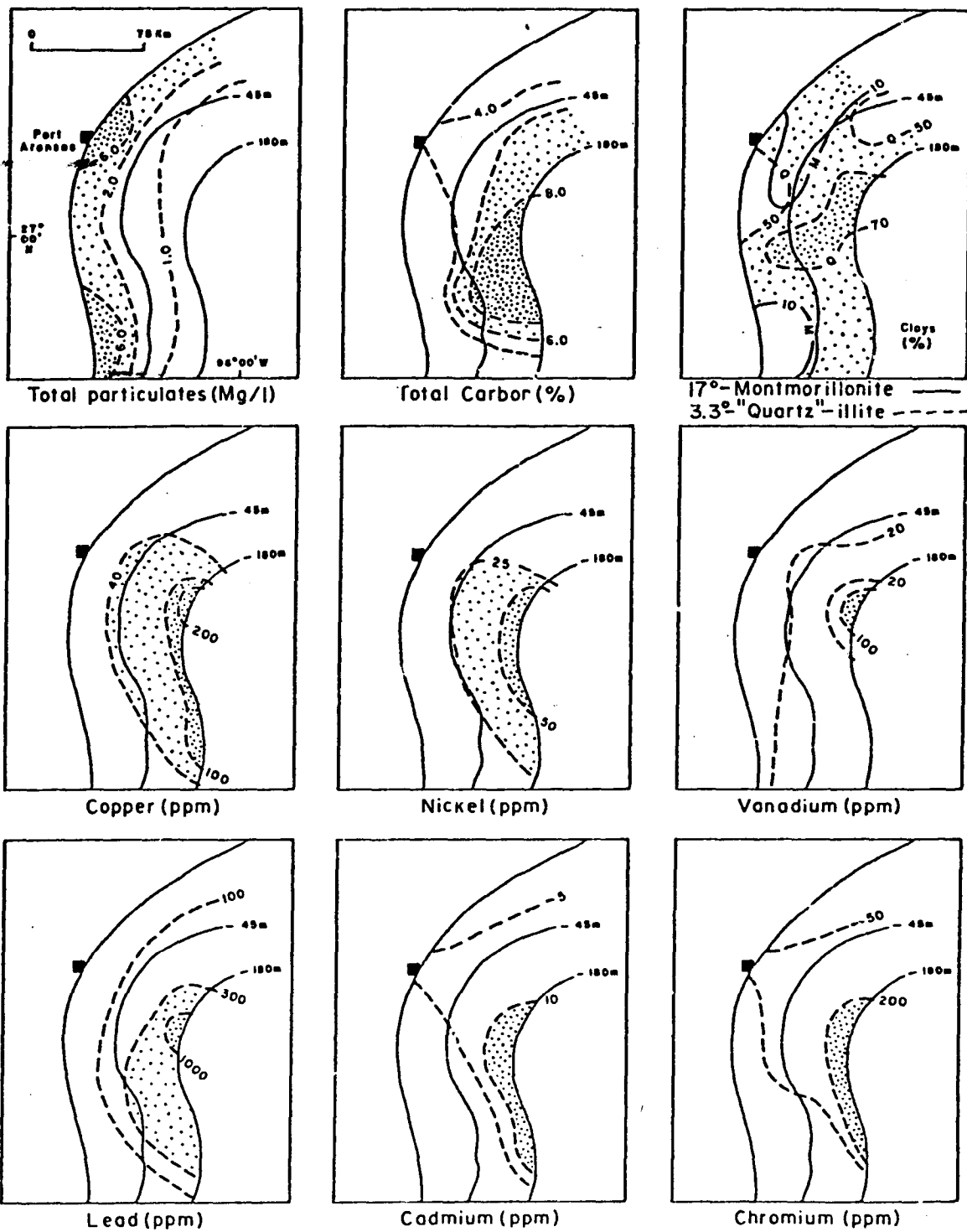


Figure 102. Patterns of distribution for various aspects of the suspended sediments, surface water, October 29 to November 3, 1976.

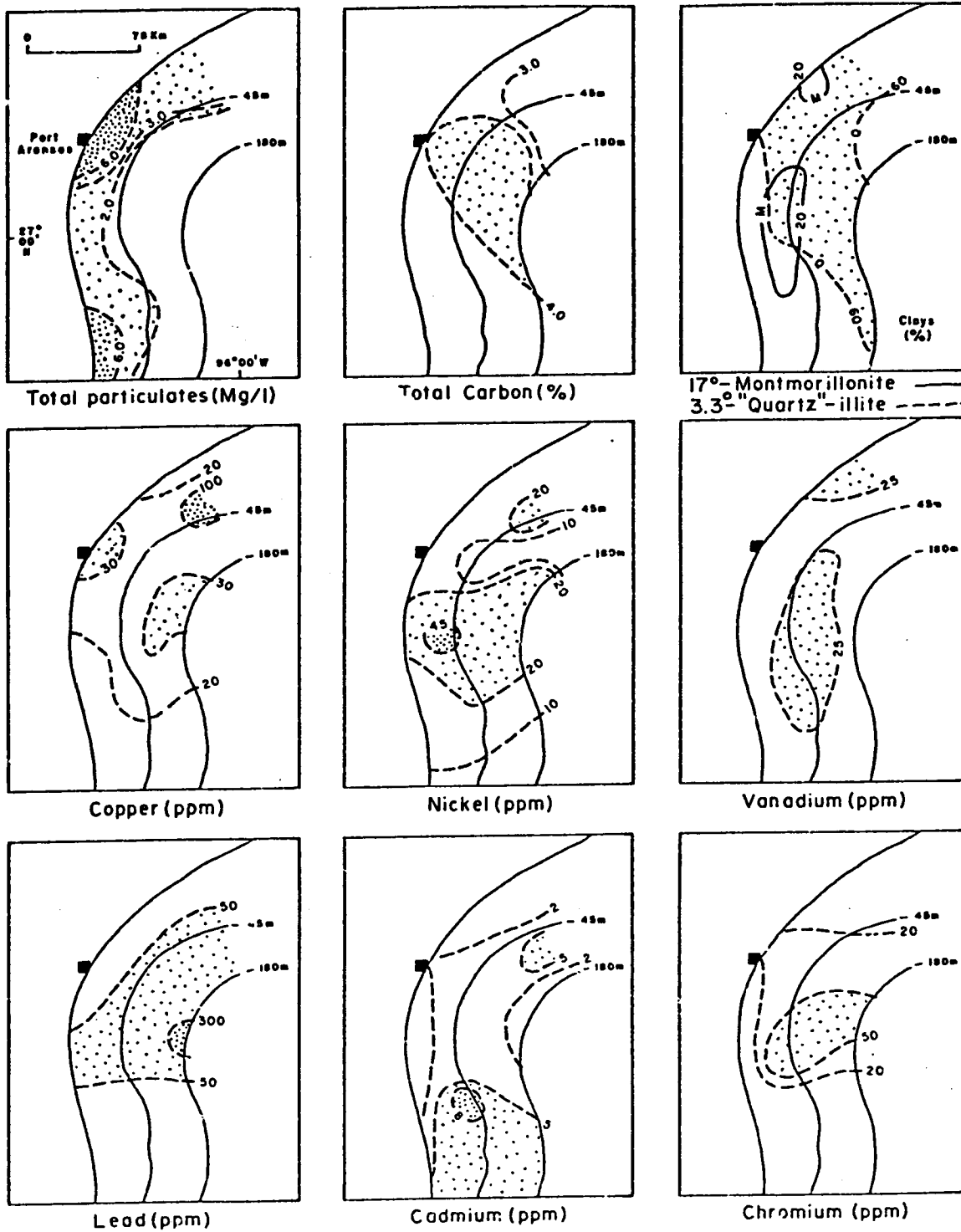


Figure 103. Patterns of distribution for various aspects of the suspended sediments, bottom water, October 29 through November 3, 1976.

shelf. The distributions of total carbon and the "quartz"/illite clays, on the other hand, indicate the strongly organic nature of the particulates in surface waters of the outer shelf. The 3.3° clays over the outer shelf have been tentatively interpreted by Holmes (this report) as siliceous skeletal material from diatoms; on the inner shelf, this material probably is very fine terrigenous quartz. The nature of the interaction of the two masses of water at the surface is revealed when the three maps at the top of figure 102 are compared. The patterns for the period of sampling define a long lobe of water that was moving along the inner shelf; the forward edge of the lobe that forms a southeastward salient across the southern part of the shelf is outlined by the contours showing amounts of montmorillonite. The pattern is further confirmed by the transmissivity pattern for March (see fig. 8, this report).

A more intricate merger of the two waters along the bottom is shown by the patterns of distribution for the particulates (fig. 103). Again, using the patterns for the fall of 1976 as the example (fig. 103), bottom water flow from the outer to the inner shelf is suggested both by the distribution of total carbon and the "quartz"/illite clays pattern. The distribution of some of the trace metals in the bottom water also suggests shoreward movement of water along the bottom.

The most remarkable consistency in the distribution for the trace metals is shown by the analytical results for the fall of 1976 (figs. 102 and 103). The patterns strongly suggest that the trace metals are associated with the microorganisms of the outer shelf, although seeping natural gas possibly may be making some contribution. Petrogenic gas recently has been identified along the outer shelf by Brooks and others

(in press). Areas of seeping gas were outlined earlier by Berryhill, 1977.

When compared with the results for 1976, the distributions for 1977 show expected differences: the amounts differ, but when the contaminated analyses are discounted, the differences are not unusually large; geographic loci for largest amounts are somewhat different in some cases. Nevertheless the patterns taken overall for the two years compare well: the trace metals are most abundant over the outer shelf and particulates, not surprisingly, are most abundant on the inner shelf. The most striking difference between the two years is the concentration of total carbon on the inner shelf in 1976 rather than on the outer shelf as in 1977. Two possibilities may explain the difference in distribution of total carbon. Plankton and organic particulates simply may have been more numerous on the inner shelf in 1976 as a function of nutrient levels. Also, levels of plankton in general may have been lower in 1976/77 and water from the deeper Gulf bearing an abundance of microplankton may have moved onto the shelf. In that vein, a combination of the distribution patterns for the two years is suggested by the results for May 1977 (fig. 107).

For comparison of the components of the suspended sediments with the characteristics of the benthic sediments, the summary maps from the 1976 report are repeated (fig. 112). The correlativity of the patterns is obvious; the finer grained, more organic sediments over the outer shelf have the larger amounts of trace metals.

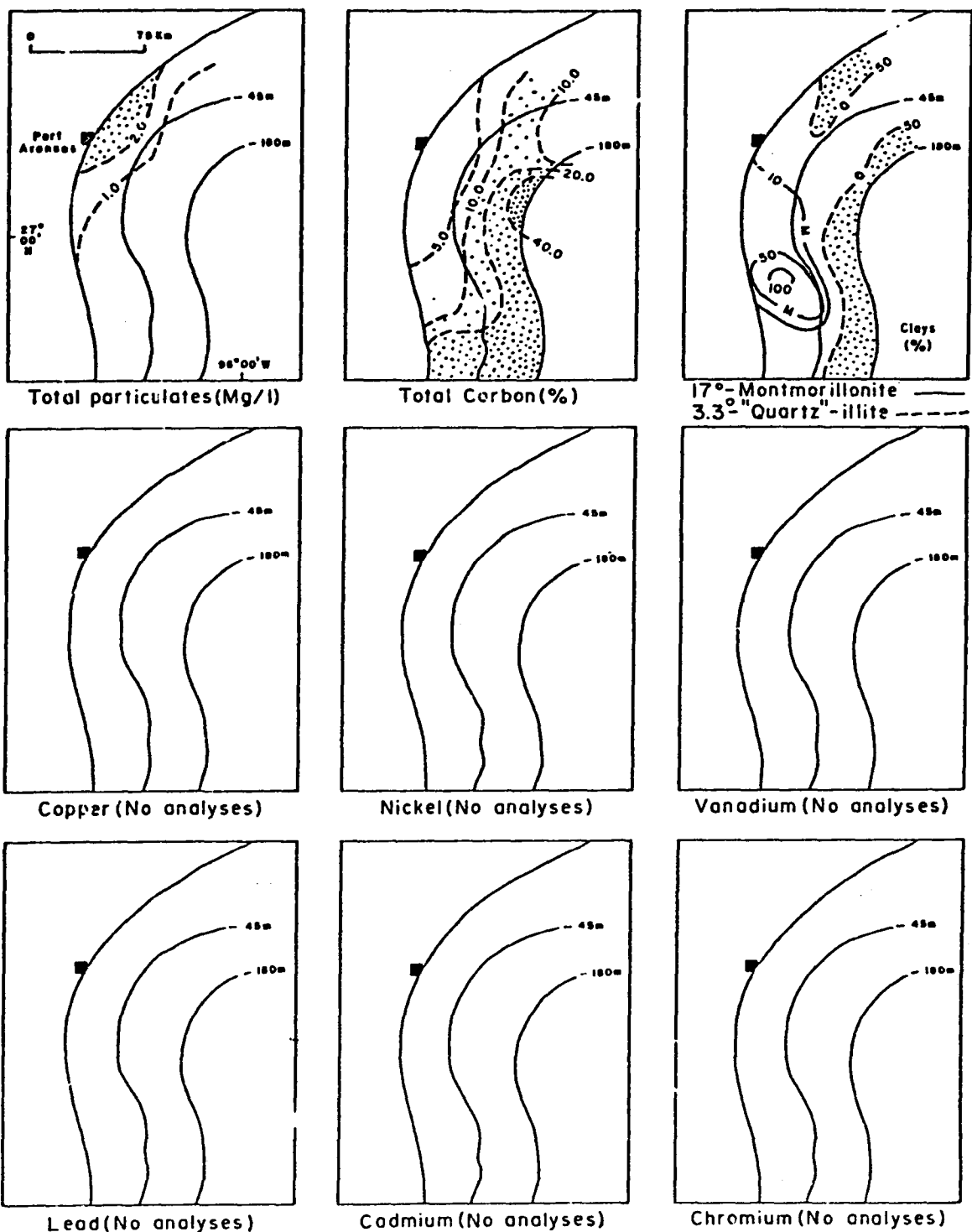


Figure 104. Patterns of distribution for various aspects of the suspended sediments, surface water, March 17 through 21, 1977. No trace metals analyses are available for March because the tray bearing the prepared filtrates was dropped in the laboratory.

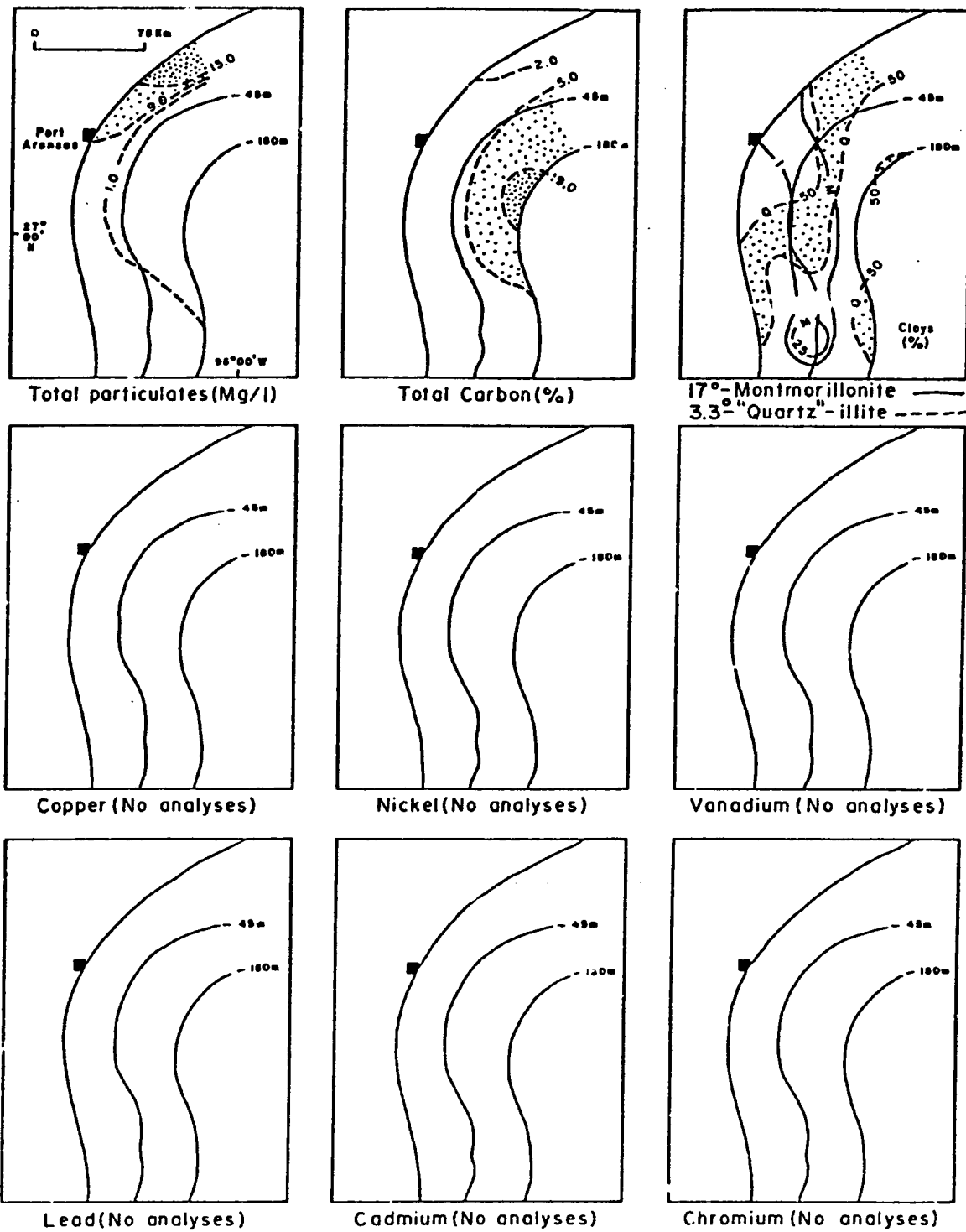


Figure 105. Patterns of distribution for various aspects of the suspended sediments, bottom water, March 17 through 21, 1977.

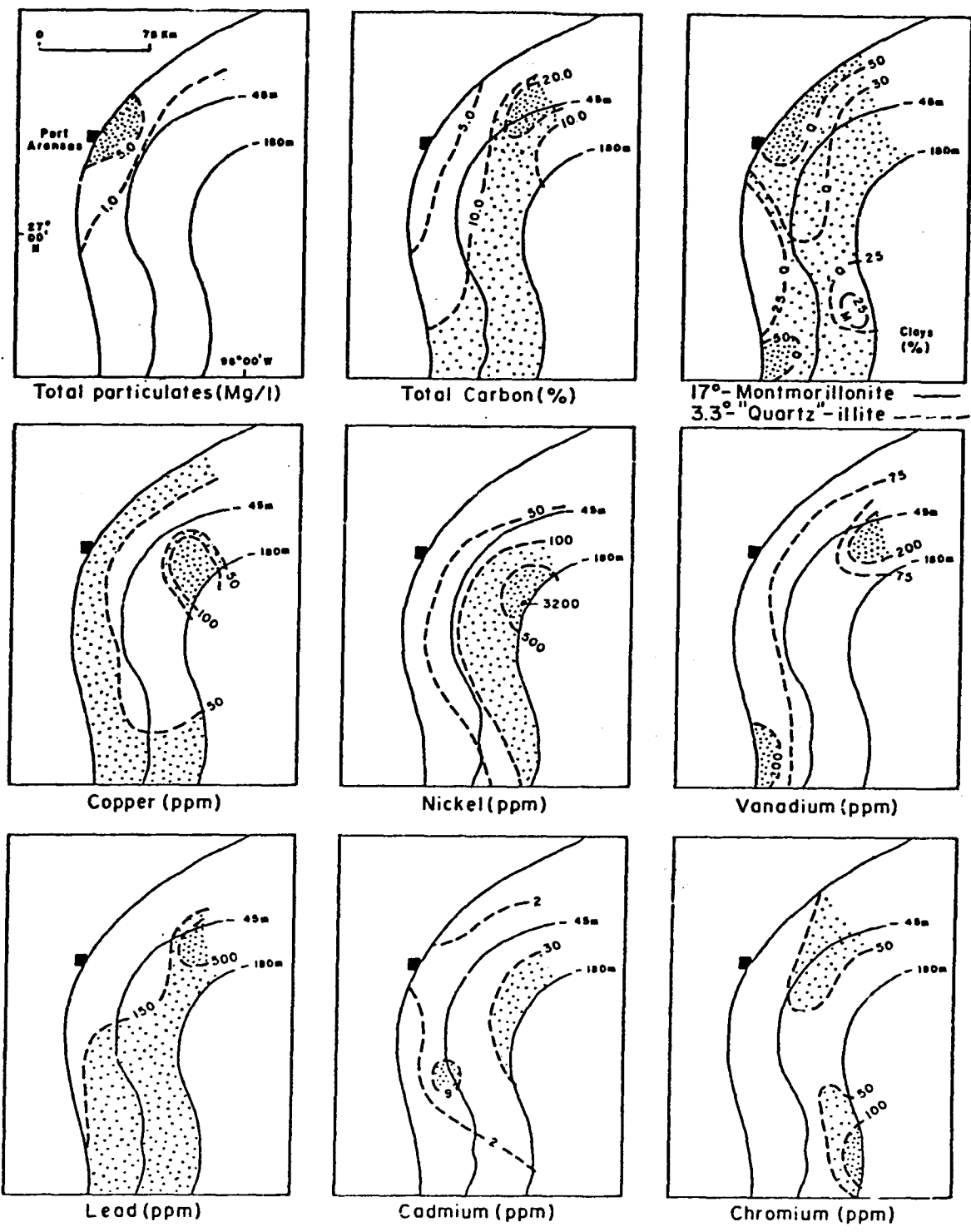


Figure 106. Patterns of distribution for various aspects of the suspended sediments, surface water, May 19 through 23, 1977.

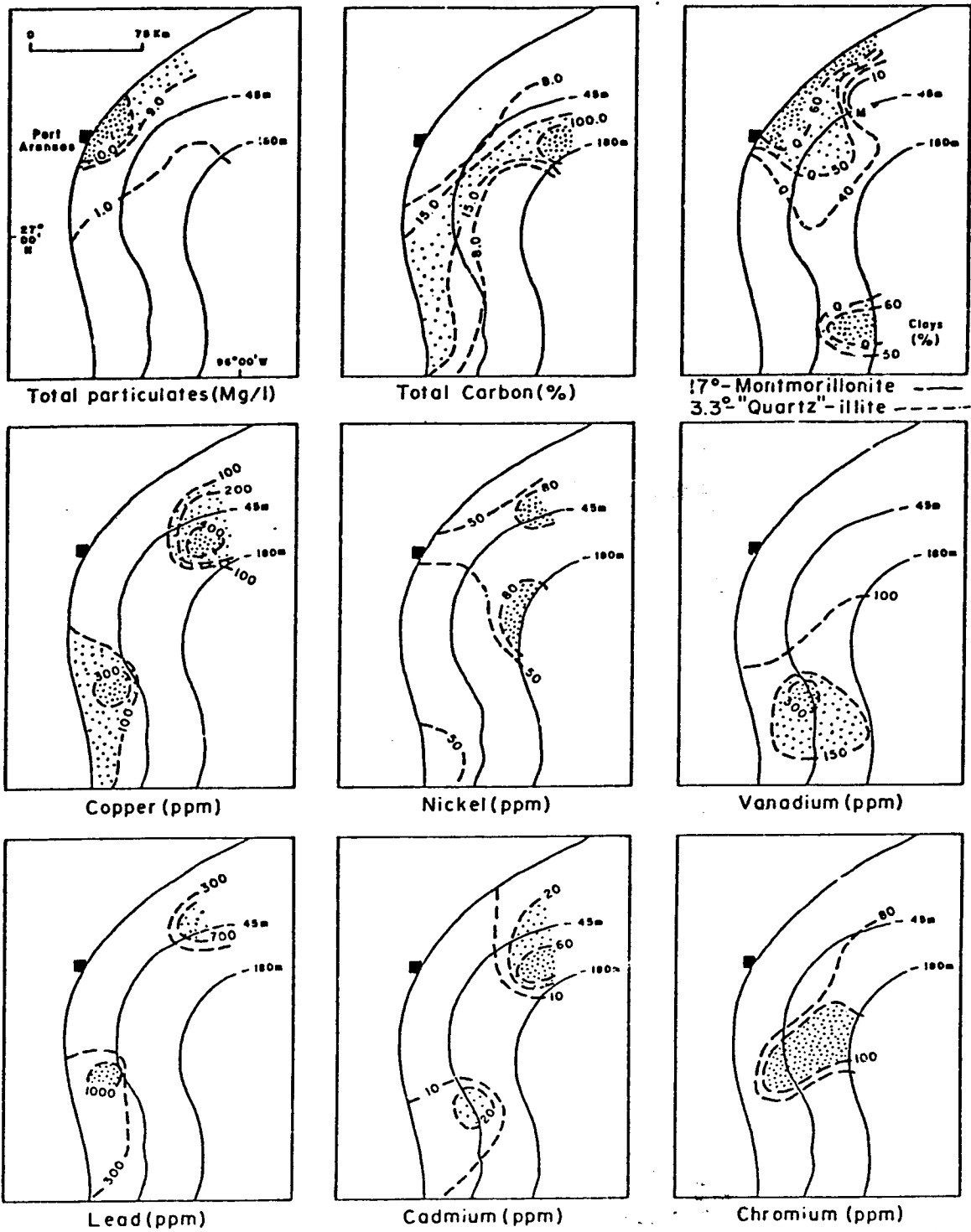


Figure 107. Patterns of distribution for various aspects of the suspended sediments, bottom water, May 19 through 23, 1977.

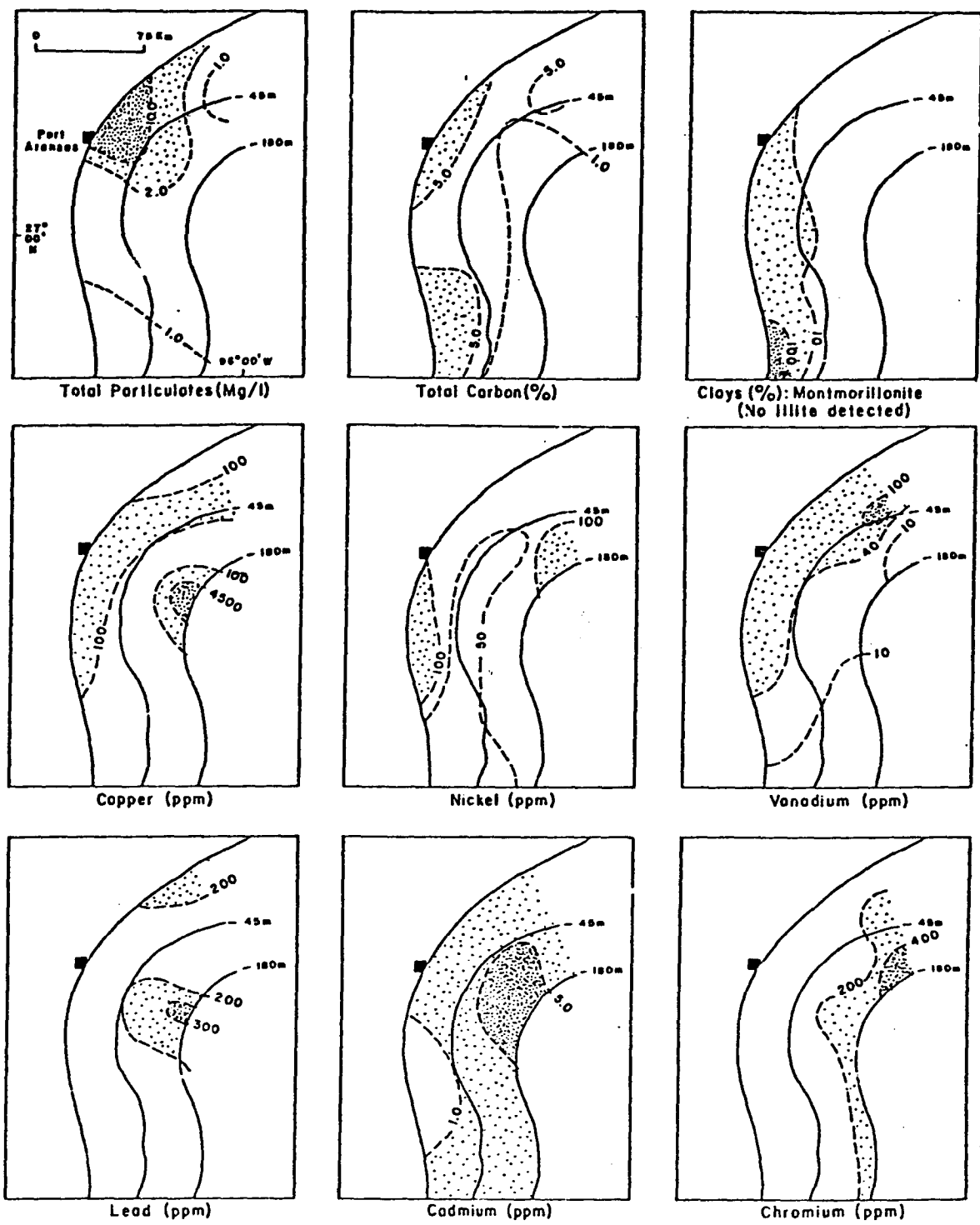


Figure 108. Patterns of distribution for various aspects of the suspended sediments, surface water, November 21 to 26, 1975 (from Berryhill, 1977).

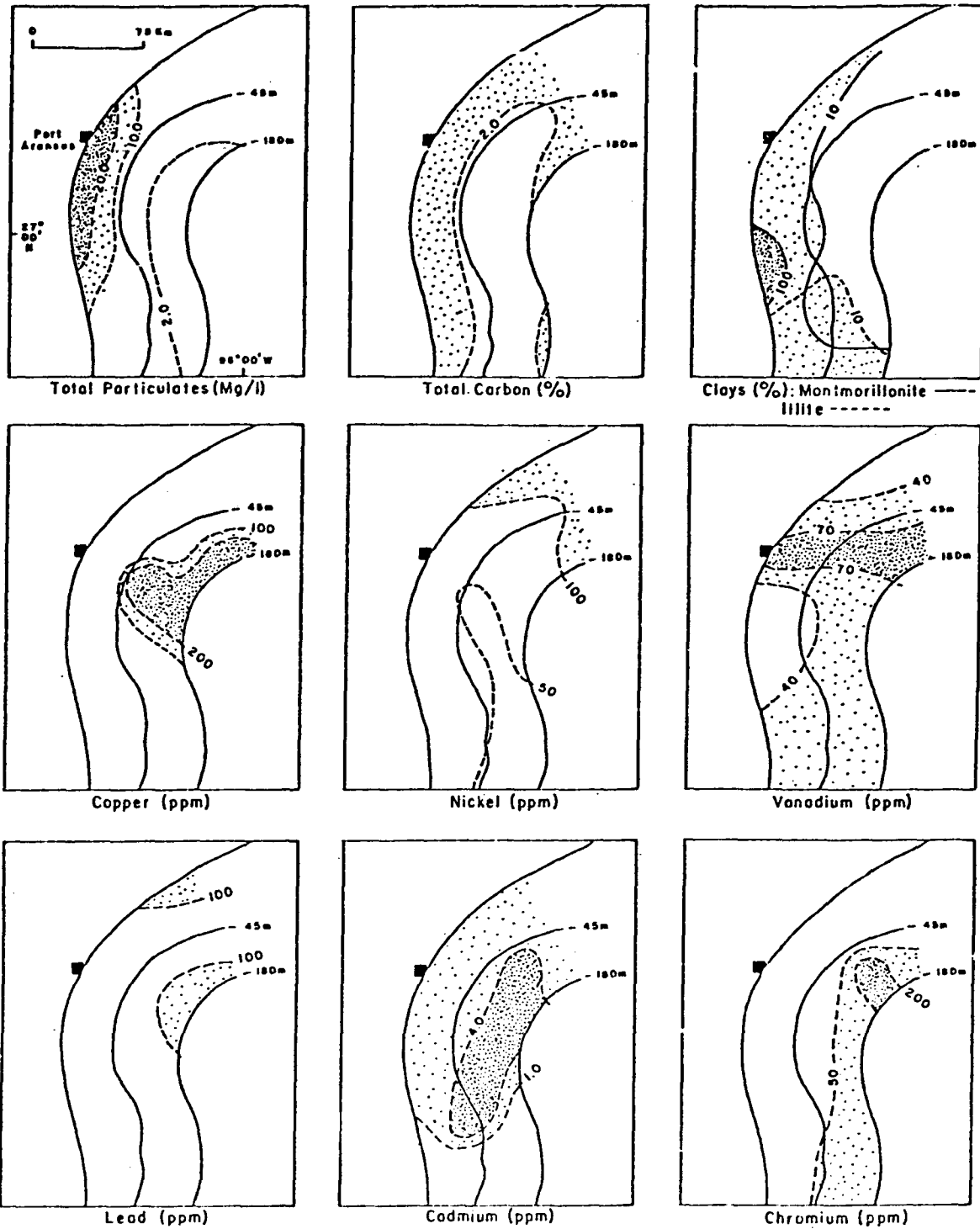


Figure 109. Patterns of distribution for various aspects of the suspended sediments, bottom water, November 21 to 26, 1975 (from Berryhill, 1977).

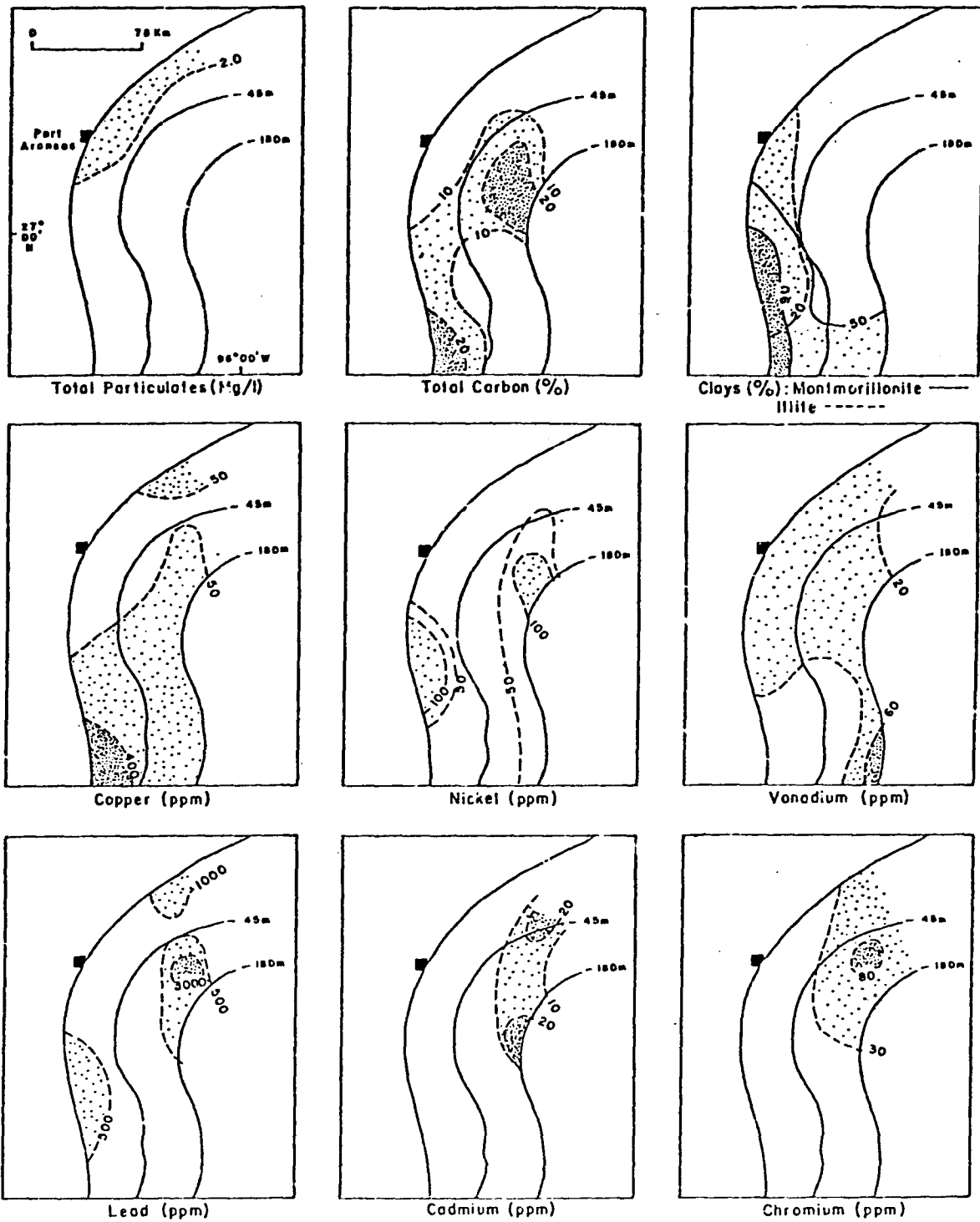


Figure 110. Patterns of distribution for various aspects of the suspended sediments, surface water, May 21 to 26, 1976 (from Ferryhill, 1977).

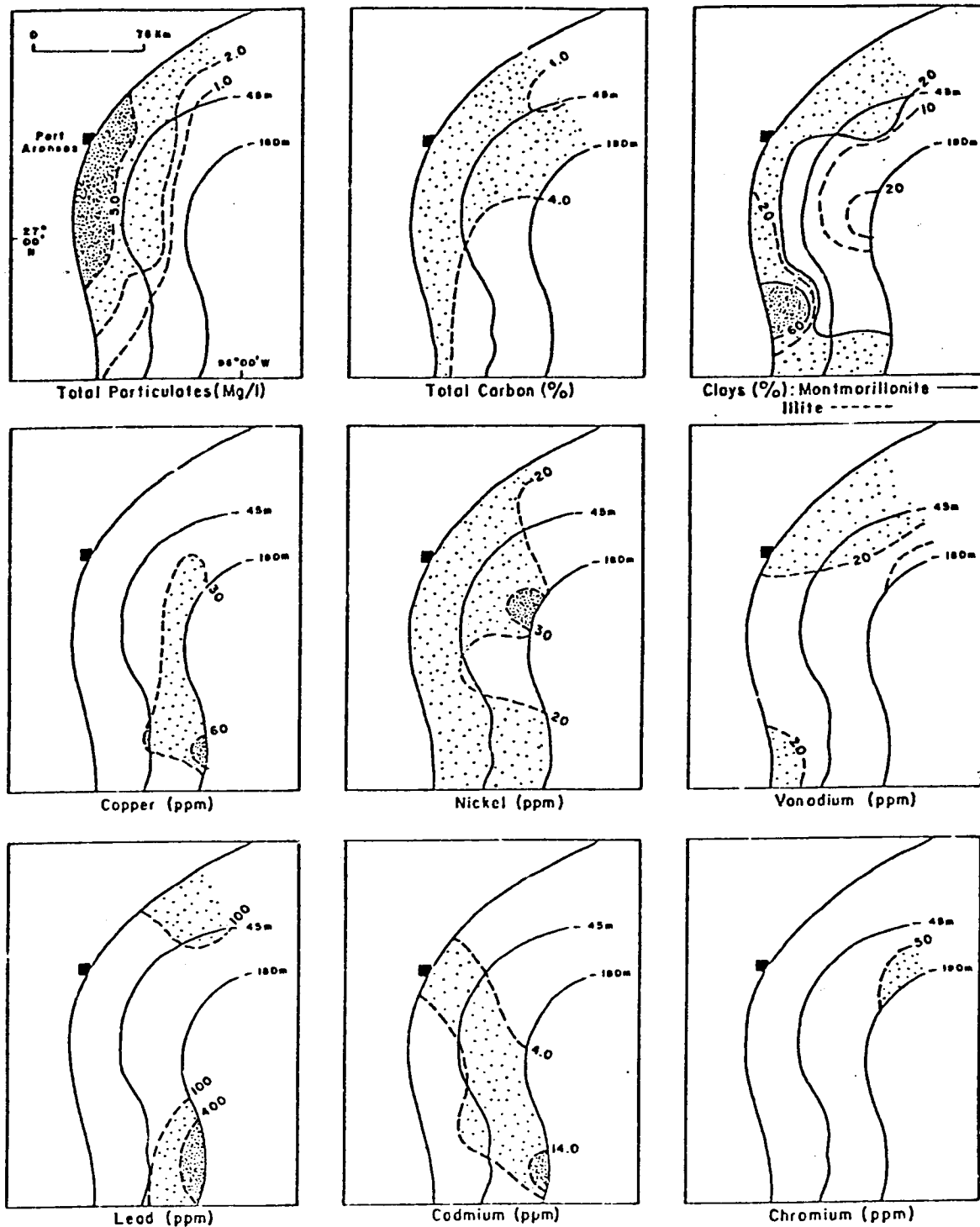


Figure 111. Patterns of distribution for various aspects of the suspended sediments, bottom water, May 21 to 26, 1976 (from Berryhill, 1977).

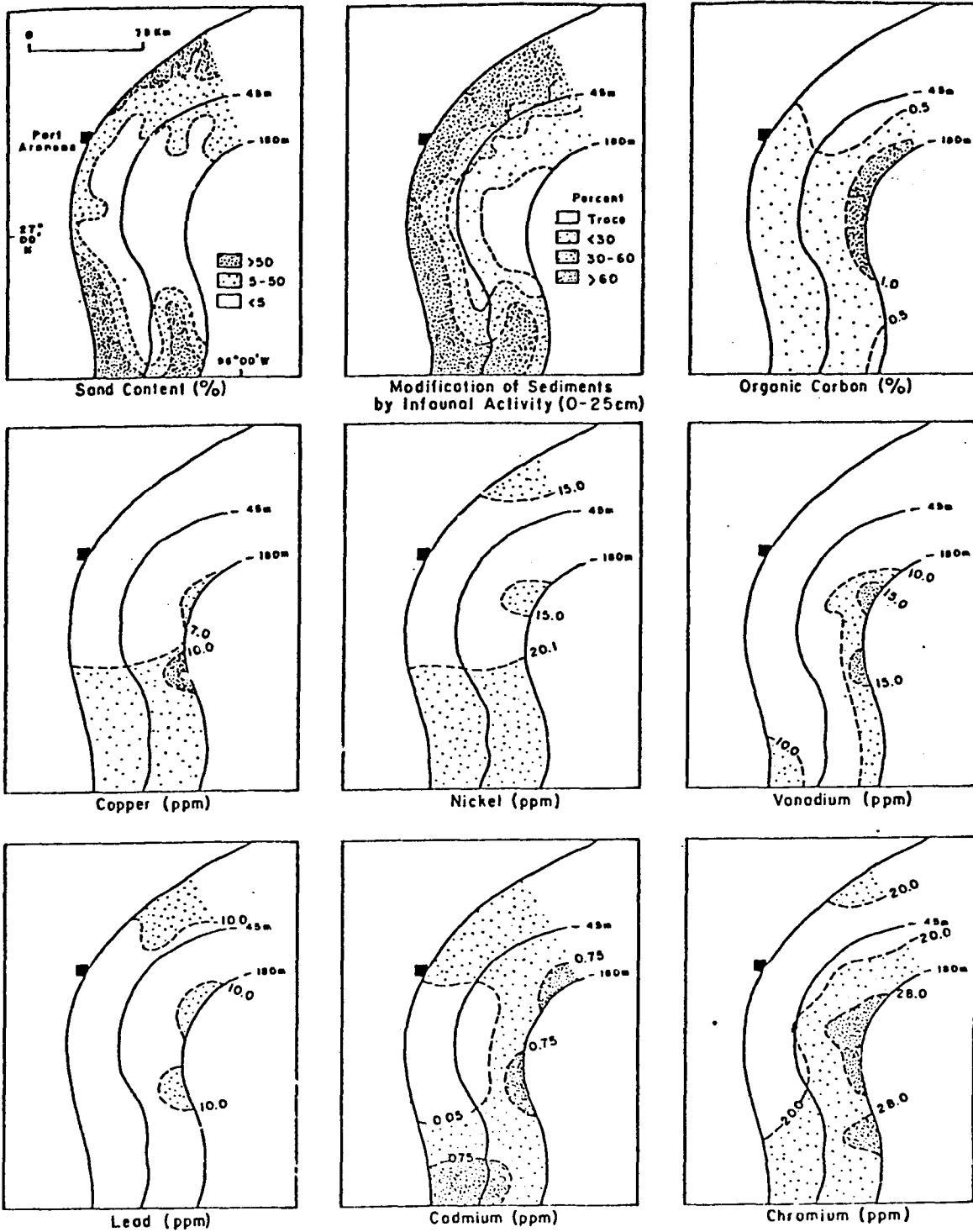


Figure 112. Patterns of distribution for various aspects of the benthic sediments as determined during the first year of study in 1975 (from Berryhill, 1977).

REFERENCES CITED

- Barr, A. J., Goodnight, J. H., Sall, J. P., and Helwig, J. T., 1976, A user's guide to SAS-76: SAS Institute, Inc., Raleigh, N. C., 329 p.
- Berryhill, H. L., Jr., (ed.), 1977, Environmental studies, south Texas outer continental shelf, 1976: Geology: National Technical Information Service, Springfield, Virginia, Pub. accession no. PB277-337/AS, 626 p.
- Berryhill, H. L., Jr., Shideler, G. L., Holmes, C. W., Hill, G. W., Barnes, S. S., and Martin, R. G., Jr., 1976, Environmental studies of the south Texas outer continental shelf, 1975: Geology: Part I, Geologic description and interpretation: National Technical Information Service, Springfield, Virginia, Pub. accession no. PB 251341, 273 p.
- Biscaye, P. E., 1965 Mineralogy and sedimentation of Recent deep-sea clay in the Atlantic Ocean and adjacent seas and oceans: Geological Society of America Bulletin, v. 76, p. 803-832.
- Bischoff, J. L., and Sayles, F. L., 1972, Pore fluid and mineralogical studies of recent marine sediments: Bauer Depression region of East Pacific Rise: Journal of Sedimentary Petrology, v. 42, no. 3, p. 711-724.
- Bostrom, K., Joensuu, O., and Brohm, Irene, 1974, Plankton: its chemical composition and its significance as a source of pelagic sediments: Chemical Geology, v. 14, no. 4, p. 255-271.
- Brooks, J. M., Bernard, B. B., and Sackett, W. M., 1978, Characterization of gases in marine waters and sediments: Preprint, Texas A&M University, College Station, Texas, 16 p., 9 figs.
- Carr, J. T., Jr., 1967, Hurricanes affecting the Texas Gulf Coast: Texas Water Development Board, Report 49.
- Carroll, D., 1970, Clay minerals: A guide to their X-ray identification: Geological Society of America Special Paper 126, 80 p.
- Casey, R. E., 1976, Microzooplankton and microzoobenthos project in Parker, P. L., (ed.), Environmental assessment of the south Texas outer continental shelf - chemical and biological survey component: Report to Bureau of Land Management (Contract 08550-CT5-17), University of Texas, Texas A&M University, and Rice University, p. 82-153.
- _____, 1977, Shelled microzooplankton, general microbenthos of the south Texas outer continental shelf (1976): Report to the Bureau of Land Management (Contract AA550-CT6-17), Rice University, 146 p.
- Davey, Earl W., and Soper, Albert E., 1975, Apparatus for the in situ concentration of trace metals from seawater: Limnology and Oceanography, v. 20, no. 6, p. 1019-1023.

- Feely, R. A., 1975, Major-element composition of the particulate matter in the near-bottom nepheloid layer of the Gulf of Mexico: *Marine Chemistry*, v. 3, no. 2, p. 121-156.
- Fleischer, P., 1970, Mineralogy of hemipelagic basin sediments, California continental borderland: a technical report for Contract #00014-0269-0009C, Ph.D. Dissertation, University of Southern California, 206 p.
- Folk, R. L., 1965, *Petrology of sedimentary rocks*: Hemphill's, Austin, Texas, 159 p.
- Gibbs, R., (ed), 1974, *Suspended solids in water*: Marine Science Series, v. 4, Plenum Press, New York, 320 p.
- Goldberg, E. D., 1965, Minor elements in sea water in Riley, J. P., and Skirrow, G., (eds), *Chemical oceanography*: Academic Press, New York, p. 163-196.
- Gregg, J. M., Goldstein, S. T., Walters, L. J., Jr., 1977, Occurrence of strained quartz in siliceous frustules of cultured freshwater diatoms: *Journal of Sedimentary Petrology*, v. 47, no. 4, p. 1623-1629.
- Hayes, M. O., 1967, Hurricanes as geologic agents - Case studies of hurricanes Carla, 1961, and Cindy, 1963: Bureau of Economic Geology, the University of Texas at Austin, Report of Investigations no. 61, 56 p.
- Hjulstrom, Filip, 1939, Transportation of detritus by moving water in P. D. Trask, (ed), *Recent marine sediments*: American Association of Petroleum Geologists, Tulsa, Oklahoma, p. 5-51.
- Holmes, C. W., 1977, Clay mineralogy in Berryhill, H. L., Jr. (ed), *Environmental studies: South Texas Outer Continental Shelf, 1976*: Geology: NTIS, Springfield, Va., Pub. accession no. PB277-337/AS, 626 p.
- Holmes, C. W., and Martin, E. A., 1977, Rates of sedimentation in Berryhill, H. L., Jr., (ed), *Environmental studies, South Texas Outer Continental Shelf, 1976*: Geology: National Technical Information Service, Springfield, Virginia, Pub. accession no. PB 277-337/AS, 626 p.
- Hunter, R. E., 1976, Movement of turbid-water masses along the Texas coast in Williams, R. S., Jr., and Carter, W. D., (eds), ERTS-1: A new window on our planet: USGS Professional Paper 929, p. 334-336.
- Jacobs, M. B., and Ewing, M., 1969, Mineral source and transport in waters of the Gulf of Mexico and Caribbean Sea: *Science*, v. 163, no. 3869, p. 805-809.
- Jerlov, N. G., 1968, *Optical oceanography*: Elsevier Co., New York, 194 p.
- Krauskopf, K. B., 1956, Factors controlling the concentrations of thirteen rare metals in sea-water: *Geochimica et Cosmochimica Acta*, v. 9, no. 1-2, p. 1-32B.
- Krumbein, W. C., 1934, Size frequency distributions of sediments: *Journal of Sedimentary Petrology*, v. 4, no. 2, p. 65-77.

- Lal, D., 1977, The oceanic microcosm of particles: *Science*, v. 198, no. 4321, p. 997-1009.
- Logan, Brian W., 1969, Part 2: Coral reefs and banks, Yucatan shelf, Mexico (Yucatan Reef unit) in B. W. Logan and others, Carbonate sediments and reefs, Yucatan shelf, Mexico: American Association of Petroleum Geologists, Memoir 11, p. 131-194.
- Lynn, D. C., and Bonatti, E., 1965, Mobility of manganese in diagenesis of deep-sea sediments: *Marine Geology*, v. 3, no. 6, p. 457-474.
- Manheim, F. T., (ed), 1975, Baseline environmental survey of the Mississippi Alabama, Florida, (MAFLA) lease areas: State University System of Florida Institute of Oceanography, St. Petersburg, Florida, 114 p. (unpublished).
- Neihof, R. A., and Loeb, G. I., 1972, The surface charge of particulate matter in seawater: *Limnology and Oceanography*, v. 17, no. 1, p. 7-16.
- Patterson, M. M., 1971, Hindcasting hurricane waves in the Gulf of Mexico: Preprints, 1971 Offshore Technology Conference, v. 11, p. 191-206.
- Pinsak, A. P., and Murray, H. H., 1960, Regional clay mineral patterns in the Gulf of Mexico in Swineford, A., (ed), Clays and clay minerals: National Conference Clays and Clay Minerals, 7th, Washington, D.C., Oct. 1958, Proc., p. 162-177.
- Robertson, D. E., 1968, Role of contamination in trace element analysis of sea water: *Analytical Chemistry*, v. 40, no. 7, p. 1067-1072.
- Schlee, J., 1966, A modified Woods Hole rapid sediment analyzer: *Journal of Sedimentary Petrology*, v. 36, p. 403-413.
- Shideler, G. L., 1976, A comparison of electronic particle counting and pipette techniques in routine mud analysis: *Journal of Sedimentary Petrology*, v. 46, no. 4, p. 1017-1025.
- Shideler, G. L., 1977, Suspended sediments-physical characteristics in Berryhill, H. L., Jr., (ed), Environmental studies, South Texas Outer Continental Shelf, 1976: *Geology: National Technical Information Service*, Springfield, VA, Pub. accession no. PB 277-337/AS, 626 p.
- Scuthard, J. B., and Cacchione, D. A., 1972, Experiments on bottom sediment movement by breaking internal waves in D. J. P. Swift, D. B. Duane, and O. H. Pilkey, (eds), Shelf sediment transport: Process and pattern: Dowden, Hutchinson & Ross, Inc., Stroudsburg, Pennsylvania, P. 83-97.
- Tuohetke, B. E., 1974, Determination of montmorillonite in small samples and implications for suspended-matter studies: *Journal of Sedimentary Petrology*, v. 44, no. 1, p. 254-258.
- van Bennekom, A. J., and van der Gaast, Sjierk J., 1976, Possible clay structures in frustules of living diatoms: *Geochimica et Cosmochimica Acta*, v. 40, p. 1149-1152.

APPENDIXES

	<u>Page</u>
1. Properties of suspended sediments in water-column samples -----	223
2. Trace metals content of suspended sediments, seasonal sampling -----	242
3. Clay mineralogy, seasonal suspended sediment samples -----	246
4. Clay mineralogy, bottom sediment samples -----	253
5. Textural properties of seasonal benthic sediment samples -----	258
6. Trace metals content, seasonal benthic sediment samples -----	271
7. Rates of sedimentation (1976 study) -----	282
8. 27° geochemical anomaly -----	285

EXPLANATION FOR APPENDIX 1:

Properties of Suspended Sediments in Water-Column Samples

- Column 1 - Sample station number: OCSS2 = STOCS 1977 program, second character = station locality, third character = water column sampling level (T = Top, M = mid depth, B = Bottom)
- Column 2 - Sampling date
- Column 3 - Station latitude
- Column 4 - Station longitude
- Column 5 - Water sample depth (meters)
- Column 6 - Water sample in situ temperature (C°)
- Column 7 - Water sample light transmissivity (% transmission/meter)
- Column 8 - Data sheet designation number (#1 = first data sheet)
- Column 9 - Sample station number (reiteration)
- Column 10 - Total sediment particle counts (0.63-81 μm size range) $\times 10^4/\text{cc}$ of water sample
- Column 11 - Suspended-sediment silt/clay ratio
- Column 12 - Suspended-sediment mean diameter in phi units (first moment)
- Column 13 - Suspended-sediment standard deviation in phi units (second moment)
- Column 14 - Suspended-sediment skewness (third moment)
- Column 15 - Suspended-sediment kurtosis (fourth moment)
- Column 16 - Data sheet designation number (#2 = second data sheet)
- Note: The designation "ND" indicated no data for that specific item

October-November 1976

1	2	3	4	5	6	7	8
OCSS2-1-T	10-30-76	28.41774	96.27237	0.0	17.25	0.0	1
OCSS2-1-M	10-30-76	28.41774	96.27237	5.5	17.25	0.0	1
OCSS2-1-R	10-30-76	28.41774	96.27237	9.0	17.25	0.0	1
OCSS2-1A-T	10-30-76	28.38739	96.32788	0.0	16.75	0.0	1
OCSS2-1A-M	10-30-76	28.38739	96.32788	5.0	16.75	0.0	1
OCSS2-1A-R	10-30-76	28.38739	96.32788	8.0	16.75	0.0	1
OCSS2-2-T	10-30-76	28.34666	96.37500	0.0	17.00	0.0	1
OCSS2-2-M	10-30-76	28.34666	96.37500	3.0	17.00	0.0	1
OCSS2-2-R	10-30-76	28.34666	96.37500	6.0	17.00	0.0	1
OCSS2-3-T	10-30-76	28.17822	96.38748	0.0	16.75	0.6	1
OCSS2-3-M	10-30-76	28.17822	96.38748	14.0	16.75	0.7	1
OCSS2-3-R	10-30-76	28.17822	96.38748	21.0	17.50	1.4	1
OCSS2-4-T	10-30-76	27.99858	96.14554	0.0	22.75	30.8	1
OCSS2-4-M	10-30-76	27.99858	96.14554	21.0	22.75	26.1	1
OCSS2-4-R	10-30-76	27.99858	96.14554	39.0	22.75	26.1	1
OCSS2-5-T	10-30-76	27.73987	96.00642	0.0	24.50	70.1	1
OCSS2-5-M	10-30-76	27.73987	96.00642	26.0	24.50	78.1	1
OCSS2-5-R	10-30-76	27.73987	96.00642	80.0	17.50	48.6	1
OCSS2-6-T	10-30-76	27.56316	95.95906	0.0	24.50	96.1	1
OCSS2-6-M	10-30-76	27.56316	95.95906	52.0	23.00	96.1	1
OCSS2-6-R	10-30-76	27.56316	95.95906	178.0	13.25	96.1	1
OCSS2-7-T	10-31-76	27.68718	96.29082	0.0	24.25	74.8	1
OCSS2-7-M	10-31-76	27.68718	96.29082	40.0	24.25	81.5	1
OCSS2-7-R	10-31-76	27.68718	96.29082	79.0	24.25	83.2	1
OCSS2-8-T	10-31-76	27.78411	96.50290	0.0	22.75	21.4	1
OCSS2-8-M	10-31-76	27.78411	96.50290	20.5	22.75	22.0	1
OCSS2-8-R	10-31-76	27.78411	96.50290	39.0	22.75	22.7	1
OCSS2-9-T	10-31-76	27.84696	96.98851	0.0	18.50	0.2	1
OCSS2-9-M	10-31-76	27.84696	96.98851	6.0	18.50	0.3	1
OCSS2-9-R	10-31-76	27.84696	96.98851	10.0	18.50	0.3	1

	9	10	11	12	13	14	15	16
OCSS2-1-T	247.4	0.63	8.22	1.20	-0.33	1.10		2
OCSS2-1-M	248.3	0.70	8.14	1.09	-0.30	2.00		2
OCSS2-1-R	229.9	0.79	8.04	1.15	-0.35	1.02		2
OCSS2-1A-T	432.8	1.63	7.61	1.18	-0.10	0.01		2
OCSS2-1A-M	463.8	1.99	7.33	1.69	0.21	-1.14		2
OCSS2-1A-H	620.6	0.95	7.95	1.23	-0.24	0.60		2
OCSS2-2-T	166.0	0.63	8.19	1.24	-0.37	1.25		2
OCSS2-2-M	219.3	0.71	8.14	1.20	-0.29	1.04		2
OCSS2-2-H	315.7	0.71	8.20	1.17	-0.19	0.72		2
OCSS2-3-T	56.3	0.76	8.05	1.32	-0.41	1.48		2
OCSS2-3-M	58.6	0.80	8.00	1.33	-0.41	1.26		2
OCSS2-3-H	85.8	0.87	8.07	1.14	-0.18	1.24		2
OCSS2-4-T	35.3	1.02	7.94	1.39	-0.19	0.20		2
OCSS2-4-M	27.0	1.27	7.87	1.28	-0.01	-0.08		2
OCSS2-4-H	31.3	1.35	7.80	1.29	-0.01	-0.15		2
OCSS2-5-T	17.0	1.66	7.20	1.99	0.08	-1.13		2
OCSS2-5-M	14.8	2.14	7.02	1.85	0.05	-0.87		2
OCSS2-5-R	13.3	2.01	7.41	1.50	0.02	-0.30		2
OCSS2-6-T	14.5	0.97	7.55	2.20	-0.11	-1.31		2
OCSS2-6-M	5.2	1.22	7.26	2.20	-0.03	-1.34		2
OCSS2-6-R	9.3	1.56	7.53	1.75	-0.00	-0.89		2
OCSS2-7-T	11.9	0.79	8.06	1.58	-0.19	-0.74		2
OCSS2-7-M	13.3	0.87	7.87	1.84	-0.19	-0.93		2
OCSS2-7-R	18.5	1.23	7.85	1.31	-0.04	-0.23		2
OCSS2-8-T	31.1	0.96	8.01	1.29	-0.15	0.32		2
OCSS2-8-M	27.9	0.88	8.11	1.21	-0.08	0.10		2
OCSS2-8-H	24.8	1.15	7.95	1.21	0.02	-0.15		2
OCSS2-9-T	93.3	0.57	8.26	1.26	-0.33	0.74		2
OCSS2-9-M	98.1	0.63	8.18	1.25	-0.33	0.66		2
OCSS2-9-R	338.5	1.22	7.84	1.10	-0.05	0.02		2

1	2	3	4	5	6	7	8
OCSS2-9A-T	10-31-76	27.79668	97.02267	0.0	17.50	0.0	1
OCSS2-9A-M	10-31-76	27.79668	97.02267	6.0	18.25	0.1	1
OCSS2-9A-R	10-31-76	27.79668	97.02267	10.0	19.00	0.0	1
OCSS2-10-T	10-31-76	27.57692	96.74031	0.0	22.50	45.2	1
OCSS2-10-M	10-31-76	27.57692	96.74031	20.5	22.50	48.6	1
OCSS2-10-R	10-31-76	27.57692	96.74031	39.0	22.50	49.8	1
OCSS2-11-T	10-31-76	27.43317	96.53265	0.0	24.00	21.4	1
OCSS2-11-M	10-31-76	27.43317	96.53265	56.0	23.00	24.7	1
OCSS2-11-R	10-31-76	27.43317	96.53265	70.0	20.00	7.3	1
OCSS2-12-T	11-01-76	27.13619	96.40814	0.0	24.50	12.5	1
OCSS2-12-M	11-01-76	27.13619	96.40814	48.0	23.75	13.0	1
OCSS2-12-R	11-01-76	27.13619	96.40814	183.0	ND	ND	1
OCSS2-13-T	11-01-76	27.05201	96.71562	0.0	24.00	44.1	1
OCSS2-13-M	11-01-76	27.05201	96.71562	62.5	22.25	35.1	1
OCSS2-13-R	11-01-76	27.05201	96.71562	75.0		13.8	1
OCSS2-14-T	11-01-76	26.96700	97.04292	0.0	22.00	19.0	1
OCSS2-14-M	11-01-76	26.96700	97.04292	18.0	22.00	16.0	1
OCSS2-14-R	11-01-76	26.96700	97.04292	36.0	22.25	13.0	1
OCSS2-16-T	11-01-76	26.53405	97.09422	0.0	19.75	7.0	1
OCSS2-16-M	11-01-76	26.53405	97.09422	12.0	19.75	4.0	1
OCSS2-16-R	11-01-76	26.53405	97.09422	21.0	21.00	0.0	1
OCSS2-17-T	11-01-76	26.53075	96.90106	0.0	21.50	10.0	1
OCSS2-17-M	11-01-76	26.53075	96.90106	11.0	22.25	12.0	1
OCSS2-17-R	11-01-76	26.53075	96.90106	34.0	23.50	3.0	1
OCSS2-18-T	11-01-76	26.44037	96.51613	0.0	23.75	63.5	1
OCSS2-18-M	11-01-76	26.44037	96.51613	35.0	23.75	62.0	1
OCSS2-18-R	11-01-76	26.44037	96.51613	69.0	19.25	0.0	1
OCSS2-19-T	11-01-76	26.41209	96.34731	0.0	24.00	60.0	1
OCSS2-19-M	11-01-76	26.41209	96.34731	56.0	24.75	91.5	1
OCSS2-19-R	11-01-76	26.41209	96.34731	108.0	ND	ND	1

	9	10	11	12	13	14	15	16
OCSS2-9A-T	153.6	0.75	8.13	1.29	-0.24	0.27		2
OCSS2-9A-M	131.1	0.54	8.25	1.23	-0.39	1.10		2
OCSS2-9A-R	169.5	0.63	8.17	1.16	-0.31	1.06		2
OCSS2-10-T	30.8	1.38	7.64	1.44	-0.16	-0.06		2
OCSS2-10-M	30.0	1.07	7.88	1.36	-0.22	0.38		2
OCSS2-10-R	32.8	1.10	7.96	1.15	-0.11	0.86		2
OCSS2-11-T	16.9	1.50	7.21	2.06	0.02	-1.17		2
OCSS2-11-M	15.0	1.24	7.56	1.94	-0.06	-1.06		2
OCSS2-11-R	30.9	1.37	7.60	1.50	-0.14	-0.52		2
OCSS2-12-T	23.3	0.54	8.36	1.74	-0.37	-0.55		2
OCSS2-12-M	13.9	0.80	7.87	1.80	-0.23	-0.92		2
OCSS2-12-R	16.4	1.20	7.79	1.51	-0.11	-0.45		2
OCSS2-13-T	23.6	0.87	7.90	1.77	-0.21	-0.64		2
OCSS2-13-M	27.2	0.81	8.09	1.64	-0.24	-0.58		2
OCSS2-13-R	23.5	0.86	8.02	1.30	-0.30	1.40		2
OCSS2-14-T	34.6	1.08	7.92	1.29	-0.12	0.10		2
OCSS2-14-M	34.2	0.96	8.05	1.18	-0.06	0.16		2
OCSS2-14-R	41.4	1.23	7.86	1.18	-0.09	0.41		2
OCSS2-16-T	73.5	0.54	8.36	1.50	-0.43	0.09		2
OCSS2-16-M	63.7	0.32	8.73	1.15	-0.51	1.19		2
OCSS2-16-R	90.6	0.55	8.37	1.14	-0.33	0.91		2
OCSS2-17-T	56.0	0.66	8.26	1.20	-0.28	0.58		2
OCSS2-17-M	51.2	0.50	8.48	1.13	-0.26	0.48		2
OCSS2-17-R	51.4	0.81	8.18	1.21	-0.16	0.03		2
OCSS2-18-T	33.2	0.62	8.27	1.78	-0.33	-0.63		2
OCSS2-18-M	26.7	0.81	8.04	1.87	-0.22	-0.90		2
OCSS2-18-R	19.8	0.86	8.11	1.55	-0.22	-0.47		2
OCSS2-19-T	31.4	0.72	8.21	1.69	-0.24	-0.77		2
OCSS2-19-M	8.9	1.80	7.07	1.91	0.01	-0.96		2
OCSS2-19-R	37.2	1.26	7.81	1.27	-0.08	-0.00		2

1	2	3	4	5	6	7	8
OCSS2-20-T	11-01-76	26.26283	96.56506	0.0	22.75	10.0	1
OCSS2-20-M	11-01-76	26.26283	96.56506	36.5	23.75	42.0	1
OCSS2-20-R	11-01-76	26.26283	96.56506	48.0	24.25	24.0	1
OCSS2-21-T	11-02-76	26.18097	96.81056	0.0	22.00	16.5	1
OCSS2-21-M	11-02-76	26.18097	96.81056	19.0	21.75	17.5	1
OCSS2-21-R	11-02-76	26.18097	96.81056	36.0	22.00	15.0	1
OCSS2-22-T	11-02-76	26.17506	96.99780	0.0	20.75	1.0	1
OCSS2-22-M	11-02-76	26.17506	96.99780	13.0	20.75	1.0	1
OCSS2-22-R	11-02-76	26.17506	96.99780	24.0	20.75	1.5	1
OCSS2-23-T	11-02-76	26.08895	97.11304	0.0	19.50	2.5	1
OCSS2-23-M	11-02-76	26.08895	97.11304	8.0	19.50	0.5	1
OCSS2-23-R	11-02-76	26.08895	97.11304	14.0	19.50	0.5	1
OCSS2-23A-T	11-02-76	26.03070	97.10454	0.0	19.25	4.0	1
OCSS2-23A-M	11-02-76	26.03070	97.10454	8.0	19.50	0.0	1
OCSS2-23A-R	11-02-76	26.03070	97.10454	14.0	19.50	0.0	1
OCSS2-24-T	11-02-76	25.99561	97.10997	0.0	19.25	0.5	1
OCSS2-24-M	11-02-76	25.99561	97.10997	7.0	19.75	0.5	1
OCSS2-24-R	11-02-76	25.99561	97.10997	12.0	19.75	0.0	1

March, 1977

OCSS2-1-T	3-18-77	28.41774	96.27237	0.0	18.00	2.7	1
OCSS2-1-M	3-18-77	28.41774	96.27237	5.5	17.25	7.3	1
OCSS2-1-R	3-18-77	28.41774	96.27237	9.4	15.50	14.8	1
OCSS2-1A-T	3-18-77	28.38739	96.32788	0.0	17.25	0.4	1
OCSS2-1A-M	3-18-77	28.38739	96.32788	5.0	16.50	1.7	1
OCSS2-1A-R	3-18-77	28.38739	96.32788	8.0	15.50	26.1	1

	9	10	11	12	13	14	15	16
OCSS2-20-T	65.7	1.27	7.61	1.54	-0.22	-0.02		2
OCSS2-20-M	27.0	1.34	7.85	1.36	0.01	-0.16		2
OCSS2-20-R	31.5	0.84	8.15	1.15	-0.11	0.76		2
OCSS2-21-T	36.0	0.92	8.08	1.29	-0.16	0.38		2
OCSS2-21-M	24.1	1.63	7.64	1.51	0.62	-0.40		2
OCSS2-21-R	39.8	1.10	7.88	1.33	-0.22	0.62		2
OCSS2-22-T	77.9	1.30	7.78	1.16	-0.18	0.61		2
OCSS2-22-M	85.2	1.04	7.94	1.12	-0.16	0.68		2
OCSS2-22-R	77.7	1.46	7.71	1.16	-0.13	0.58		2
OCSS2-23-T	158.3	0.58	7.97	1.56	-0.57	0.88		2
OCSS2-23-M	130.5	0.51	8.20	1.23	-0.57	2.47		2
OCSS2-23-R	133.5	0.51	8.28	1.06	-0.39	2.11		2
OCSS2-23A-T	167.0	0.49	8.30	1.13	-0.50	2.26		2
OCSS2-23A-M	151.3	0.46	8.34	1.04	-0.39	2.14		2
OCSS2-23A-R	144.9	0.62	8.15	1.12	-0.43	1.89		2
OCSS2-24-T	134.8	0.58	8.21	1.10	-0.42	2.10		2
OCSS2-24-M	135.1	0.86	7.92	1.29	-0.40	1.01		2
OCSS2-24-R	253.9	1.11	7.78	1.21	-0.22	0.14		2

March, 1977

OCSS2-1-T	127.5	0.63	8.12	1.63	-0.34	-0.18		2
OCSS2-1-M	92.5	0.77	8.02	1.62	-0.21	-0.68		2
OCSS2-1-R	87.2	0.93	7.91	1.60	-0.14	-0.75		2
OCSS2-1A-T	128.0	0.79	8.04	1.50	-0.24	-0.32		2
OCSS2-1A-M	151.3	0.83	8.02	1.48	-0.21	-0.37		2
OCSS2-1A-R	71.9	0.80	8.06	1.33	-0.25	0.40		2

1	2	3	4	5	6	7	8
OCSS2-2-T	3-18-77	28.34666	96.37500	0.0	18.50	0.0	1
OCSS2-2-M	3-18-77	28.34666	96.37500	4.5	15.50	1.7	1
OCSS2-2-H	3-18-77	28.34666	96.37500	7.0	15.25	0.9	1
OCSS2-3-T	3-18-77	28.17822	96.38748	0.0	19.00	11.7	1
OCSS2-3-M	3-18-77	28.17822	96.38748	11.5	15.75	45.2	1
OCSS2-3-R	3-18-77	28.17822	96.38748	21.0			1
OCSS2-4-T	3-18-77	27.99858	96.14554	0.0	17.75	73.2	1
OCSS2-4-M	3-18-77	27.99858	96.14554	21.0	15.50	71.6	1
OCSS2-4-R	3-18-77	27.99858	96.14554	40.5	ND	ND	1
OCSS2-5-T	3-18-77	27.73987	96.00642	0.0	19.50	76.4	1
OCSS2-5-M	3-18-77	27.73987	96.00642	42.0	18.00	73.2	1
OCSS2-5-R	3-18-77	27.73987	96.00642	81.0	ND	ND	1
OCSS2-6-T	3-18-77	27.56316	95.95996	0.0	19.50	88.5	1
OCSS2-6-M	3-18-77	27.56316	95.95996	92.0	17.00	94.1	1
OCSS2-6-R	3-18-77	27.56316	95.95996	183.0			1
OCSS2-7-T	3-18-77	27.68718	96.29082	0.0	17.50	73.2	1
OCSS2-7-M	3-18-77	27.68718	96.29082	39.0	16.50	68.6	1
OCSS2-7-R	3-18-77	27.68718	96.29082	76.0	ND	ND	1
OCSS2-8-T	3-19-77	27.78411	96.59290	0.0	18.00	34.2	1
OCSS2-8-M	3-19-77	27.78411	96.59290	20.0	15.50	78.1	1
OCSS2-8-R	3-19-77	27.78411	96.59290	38.0	ND	ND	1
OCSS2-9-T	3-19-77	27.84696	96.98851	0.0	15.75	2.3	1
OCSS2-9-M	3-19-77	27.84696	96.98851	6.0	14.25	0.1	1
OCSS2-9-H	3-14-77	27.84696	96.98851	10.5	13.50	0.0	1
OCSS2-9A-T	3-19-77	27.79668	97.02267	0.0	15.75	4.9	1
OCSS2-9A-M	3-19-77	27.79668	97.02267	7.0	14.00	2.3	1
OCSS2-9A-H	3-19-77	27.79668	97.02267	12.0	13.25	0.0	1
OCSS2-10-T	3-19-77	27.57692	96.74031	0.0	17.75	44.1	1
OCSS2-10-M	3-19-77	27.57692	96.74031	22.0	17.50	74.8	1
OCSS2-10-R	3-19-77	27.57692	96.74031	41.5	ND	ND	1

	9	10	11	12	13	14	15	16
OCSS2-2-T	177.3	1.18	7.70	1.56	-0.13	-0.62		2
OCSS2-2-M	101.4	1.62	7.44	1.56	-0.03	-0.74		2
OCSS2-2-R	130.2	1.01	7.79	1.45	-0.24	-0.15		2
OCSS2-3-T	94.2	0.50	4.36	1.48	-0.41	0.37		2
OCSS2-3-M	37.8	0.70	8.13	1.58	-0.28	-0.31		2
OCSS2-3-R	157.4	0.93	8.00	1.03	-0.23	1.43		2
OCSS2-4-T	14.3	2.14	6.90	1.88	0.13	-0.90		2
OCSS2-4-M	10.3	2.05	6.86	1.94	0.13	-0.09		2
OCSS2-4-R	17.7	1.81	7.27	1.83	0.06	-0.92		2
OCSS2-5-T	14.7	1.28	7.25	2.30	0.03	-1.41		2
OCSS2-5-M	8.1	1.72	6.88	2.00	0.08	-1.21		2
OCSS2-5-R	22.2	3.03	6.98	1.57	0.08	-0.42		2
OCSS2-6-T	14.1	1.60	7.06	2.16	0.12	-1.32		2
OCSS2-6-M	4.8	2.26	6.77	1.89	0.16	-0.97		2
OCSS2-6-R	4.6	3.31	6.29	1.88	0.27	-0.82		2
OCSS2-7-T	16.4	2.39	6.59	2.03	0.28	-0.91		2
OCSS2-7-M	10.5	1.52	7.29	1.93	0.01	-1.06		2
OCSS2-7-R	16.8	1.85	7.62	1.35	0.00	-0.14		2
OCSS2-8-T	36.6	1.00	7.79	1.74	-0.12	-0.81		2
OCSS2-8-M	4.8	1.69	7.08	1.90	0.05	-1.11		2
OCSS2-8-R	26.7	1.68	7.62	1.34	-0.03	0.04		2
OCSS2-9-T	135.3	0.55	8.33	1.34	-0.31	0.24		2
OCSS2-9-M	116.7	0.44	8.44	1.17	-0.31	0.79		2
OCSS2-9-R	115.3	0.50	8.37	1.09	-0.22	0.69		2
OCSS2-9A-T	91.7	0.67	8.16	1.54	-0.26	-0.52		2
OCSS2-9A-M	96.4	0.51	8.36	1.24	-0.34	0.76		2
OCSS2-9A-R	154.9	0.46	8.35	0.99	-0.29	1.72		2
OCSS2-10-T	23.8	1.75	7.22	1.77	0.07	-0.89		2
OCSS2-10-M	8.7	2.12	6.92	1.92	0.13	-1.03		2
OCSS2-10-R	9.9	5.50	6.18	1.67	0.30	-0.15		2

1	2	3	4	5	6	7	8
OCSS2-11-T	3-19-77	27.43317	96.53265	0.0	18.25	65.6	1
OCSS2-11-M	3-19-77	27.43317	96.53265	40.0	16.75	73.2	1
OCSS2-11-R	3-19-77	27.43317	96.53265	78.0	15.50	0.0	1
OCSS2-12-T	3-19-77	27.13619	96.40814	0.0	18.25	65.6	1
OCSS2-12-M	3-19-77	27.13619	96.40814	92.0	16.50	74.8	1
OCSS2-12-R	3-19-77	27.13619	96.40814	183.0	ND	ND	1
OCSS2-13-T	3-19-77	27.05201	96.71562	0.0	18.50	48.6	1
OCSS2-13-M	3-19-77	27.05201	96.71562	40.0	17.00	64.2	1
OCSS2-13-R	3-19-77	27.05201	96.71562	78.0			1
OCSS2-14-T	3-19-77	26.96700	97.04292	0.0	17.50	32.5	1
OCSS2-14-M	3-19-77	26.96700	97.04292	19.0	15.50	37.0	1
OCSS2-14-R	3-19-77	26.96700	97.04292	36.0	ND	ND	1
OCSS2-16-T	3-20-77	26.53405	97.09422	0.0	17.75	62.7	1
OCSS2-16-M	3-20-77	26.53405	97.09422	7.0	17.50	58.6	1
OCSS2-16-R	3-20-77	26.53405	97.09422	23.0	16.25	0.0	1
OCSS2-17-T	3-20-77	26.53075	96.90106	0.0	16.50	60.0	1
OCSS2-17-M	3-20-77	26.53075	96.90106	20.0	15.50	62.7	1
OCSS2-17-R	3-20-77	26.53075	96.90106	38.0	ND	ND	1
OCSS2-18-T	3-20-77	26.44037	96.51613	0.0	17.50	73.2	1
OCSS2-18-M	3-20-77	26.44037	96.51613	35.0	16.75	73.2	1
OCSS2-18-R	3-20-77	26.44037	96.51613	68.0	ND	ND	1
OCSS2-19-T	3-20-77	26.41209	96.34731	0.0	17.50	73.2	1
OCSS2-19-M	3-20-77	26.41209	96.34731	55.0	16.75	81.5	1
OCSS2-19-R	3-20-77	26.41209	96.34731	108.0	ND	ND	1
OCSS2-20-T	3-20-77	26.26283	96.56506	0.0	18.00	83.2	1
OCSS2-20-M	3-20-77	26.26283	96.56506	24.0	15.50	84.9	1
OCSS2-20-R	3-20-77	26.26283	96.56506	47.0	ND	ND	1
OCSS2-21-T	3-20-77	26.18097	96.81056	0.0	16.50	76.4	1
OCSS2-21-M	3-20-77	26.18097	96.81056	20.5	15.25	84.9	1
OCSS2-21-R	3-20-77	26.18097	96.81056	39.0	14.25	0.2	1

	9	10	11	12	13	14	15	16
OCSS2-11-T	17.6	1.27	7.52	1.98	-0.00	-1.24		2
OCSS2-11-M	10.7	1.24	7.38	2.05	-0.31	-1.19		2
OCSS2-11-R	20.6	1.65	7.66	1.31	-0.05	0.23		2
OCSS2-12-T	22.9	2.72	6.68	1.91	0.28	-0.84		2
OCSS2-12-M	8.8	1.49	7.61	1.70	0.01	-0.72		2
OCSS2-12-R	7.9	2.23	7.04	1.75	0.07	-0.75		2
OCSS2-13-T	24.5	1.39	7.50	1.79	0.04	-1.07		2
OCSS2-13-M	14.5	1.61	7.69	1.44	-0.02	-0.15		2
OCSS2-13-R	33.1	1.35	7.86	1.04	-0.09	1.24		2
OCSS2-14-T	28.5	1.41	7.49	1.77	-0.01	-0.97		2
OCSS2-14-M	27.2	1.16	7.51	1.83	-0.15	-0.86		2
OCSS2-14-R	21.2	1.97	7.51	1.42	0.03	-0.19		2
OCSS2-16-T	19.7	0.98	7.74	1.93	-0.12	-1.14		2
OCSS2-16-M	20.6	0.86	7.75	1.99	-0.19	-1.06		2
OCSS2-16-R	40.0	1.59	7.70	1.29	-0.07	0.24		2
OCSS2-17-T	15.2	1.72	7.17	1.95	0.08	-1.01		2
OCSS2-17-M	10.4	1.31	7.27	2.06	-0.03	-1.23		2
OCSS2-17-R	26.4	1.69	7.60	1.43	-0.06	-0.01		2
OCSS2-18-T	15.0	1.37	7.25	2.07	0.01	-1.17		2
OCSS2-18-M	11.9	1.55	7.19	2.04	0.04	-1.22		2
OCSS2-18-R	18.5	1.13	7.89	1.36	-0.17	0.33		2
OCSS2-19-T	13.6	1.21	7.37	2.09	-0.03	-1.31		2
OCSS2-19-M	6.8	2.07	6.80	2.05	0.16	-1.05		2
OCSS2-19-R	16.8	2.25	7.45	1.23	0.05	0.17		2
OCSS2-20-T	19.2	1.14	7.54	2.04	-0.06	-1.25		2
OCSS2-20-M	17.2	1.15	7.63	1.79	-0.19	-0.57		2
OCSS2-20-R	25.6	0.99	7.84	1.61	-0.27	-0.92		2
OCSS2-21-T	13.3	1.53	7.13	2.08	0.03	-1.23		2
OCSS2-21-M	10.6	6.88	6.43	1.44	0.26	0.51		2
OCSS2-21-R	31.4	1.97	7.34	1.56	0.02	-0.49		2

1	2	3	4	5	6	7	8
OCSS2-22-T	3-20-77	26.17506	96.99780	0.0	16.50	81.5	1
OCSS2-22-M	3-20-77	26.17506	96.99780	11.0	16.00	79.7	1
OCSS2-22-R	3-20-77	26.17506	96.99780	21.0	15.50	0.0	1
OCSS2-23-T	3-20-77	26.08895	97.11304	0.0	16.75	35.1	1
OCSS2-23-M	3-20-77	26.08895	97.11304	8.5	16.25	57.3	1
OCSS2-23-H	3-20-77	26.08895	97.11304	15.0	14.25	11.9	1
OCSS2-23A-T	3-20-77	26.03070	97.10454	0.0	16.50	91.5	1
OCSS2-23A-M	3-20-77	26.03070	97.10454	8.0	16.00	30.0	1
OCSS2-23A-R	3-20-77	26.03070	97.10454	14.0	14.50	0.0	1
OCSS2-24-T	3-20-77	25.99561	97.10997	0.0	16.75	22.0	1
OCSS2-24-M	3-20-77	25.99561	97.10997	7.5	16.75	33.4	1
OCSS2-24-H	3-20-77	25.99561	97.10997	15.0	ND	ND	1

May, 1977

OCSS2-1-T	5-24-77	28.41774	96.27237	0.0	26.75	0.2	1
OCSS2-1-M	5-24-77	28.41774	96.27237	5.5	26.75	0.1	1
OCSS2-1-R	5-24-77	28.41774	96.27237	9.0	26.25	0.0	1
OCSS2-1A-T	5-24-77	28.38739	96.32788	0.0	27.00	0.0	1
OCSS2-1A-M	5-24-77	28.38739	96.32788	5.0	26.75	0.0	1
OCSS2-1A-H	5-24-77	28.38739	96.32788	8.0	27.00	0.0	1
OCSS2-2-T	5-24-77	28.34666	96.37500	0.0	25.00	0.0	1
OCSS2-2-M	5-24-77	28.34666	96.37500	3.5	26.75	0.0	1
OCSS2-2-R	5-24-77	28.34666	96.37500	5.0	27.00	0.0	1
OCSS2-3-T	5-24-77	28.17822	96.38748	0.0	26.25	10.2	1
OCSS2-3-M	5-24-77	28.17822	96.38748	10.5	26.00	16.8	1
OCSS2-3-R	5-24-77	28.17822	96.38748	19.0	25.50	0.1	1

	9	10	11	12	13	14	15	16
OCSS2-22-T	13.1	4.74	6.40	1.72	0.35	-0.05		2
OCSS2-22-M	12.4	5.90	6.37	1.55	0.41	0.60		2
OCSS2-22-R	35.7	2.23	7.25	1.55	0.05	-0.49		2
OCSS2-23-T	18.2	0.96	7.83	1.77	-0.19	-0.71		2
OCSS2-23-M	26.3	1.01	7.70	1.88	-0.15	-0.91		2
OCSS2-23-R	40.6	1.29	7.75	1.59	-0.08	-0.42		2
OCSS2-23A-T	44.1	0.66	8.17	1.68	-0.29	-0.43		2
OCSS2-23A-M	43.2	0.63	8.22	1.69	-0.31	-0.38		2
OCSS2-23A-R	60.9	1.18	7.84	1.34	-0.12	0.04		2
OCSS2-24-T	43.0	0.61	8.25	1.70	-0.32	-0.35		2
OCSS2-24-M	47.8	0.63	8.20	1.71	-0.34	-0.25		2
OCSS2-24-R	88.7	1.51	7.73	1.15	-0.05	0.27		2

May, 1977

OCSS2-1-T	256.3	0.46	8.39	1.24	-0.41	1.14		2
OCSS2-1-M	148.4	0.58	8.25	1.31	-0.36	0.63		2
OCSS2-1-R	279.7	0.57	8.25	1.20	-0.35	0.90		2
OCSS2-1A-T	374.1	0.48	8.42	1.01	-0.08	-0.13		2
OCSS2-1A-M	277.2	0.64	8.09	1.37	-0.39	0.45		2
OCSS2-1A-R	308.4	0.76	8.00	1.33	-0.34	0.32		2
OCSS2-2-T	316.9	0.63	8.13	1.37	-0.41	0.74		2
OCSS2-2-M	258.3	0.67	8.12	1.32	-0.34	0.47		2
OCSS2-2-R	308.5	0.76	7.97	1.47	-0.36	0.15		2
OCSS2-3-T	96.4	0.82	7.96	1.77	-0.18	-0.77		2
OCSS2-3-M	77.9	0.80	8.06	1.62	-0.23	-0.33		2
OCSS2-3-R	90.7	1.62	7.68	1.18	-0.01	0.14		2

1	2	3	4	5	6	7	8
OCSS2-4-T	5-25-77	27.99858	96.14554	0.0	25.00	61.4	1
OCSS2-4-M	5-25-77	27.99858	96.14554	19.0	25.00	78.1	1
OCSS2-4-P	5-25-77	27.99858	96.14554	36.0	23.75	26.1	1
OCSS2-5-T	5-25-77	27.73987	96.00642	0.0	25.25	74.8	1
OCSS2-5-M	5-25-77	27.73987	96.00642	42.0	23.75	88.5	1
OCSS2-5-P	5-25-77	27.73987	96.00642	82.0	21.00	60.0	1
OCSS2-6-T	5-25-77	27.56316	95.95996	0.0	25.00	62.7	1
OCSS2-6-M	5-25-77	27.56316	95.95996	98.0	20.50	88.5	1
OCSS2-6-P	5-25-77	27.56316	95.95996	194.0	17.25	96.1	1
OCSS2-7-T	5-25-77	27.68718	96.29082	0.0	27.00	62.7	1
OCSS2-7-M	5-25-77	27.68718	96.29082	38.5	23.00	68.6	1
OCSS2-7-P	5-25-77	27.68718	96.29082	75.0	20.75	47.5	1
OCSS2-8-T	5-25-77	27.78411	96.59290	0.0	26.75	57.3	1
OCSS2-8-M	5-25-77	27.78411	96.59290	20.0	24.50	58.6	1
OCSS2-8-P	5-25-77	27.78411	96.59290	38.0	24.25	37.0	1
OCSS2-9-T	5-25-77	27.84696	96.98851	0.0	27.75	4.4	1
OCSS2-9-M	5-25-77	27.84696	96.98851	7.0	26.75	7.3	1
OCSS2-9-P	5-25-77	27.84696	96.98851	10.8	26.75	0.3	1
OCSS2-9A-T	5-25-77	27.79668	97.02267	0.0	28.00	1.3	1
OCSS2-9A-M	5-25-77	27.79668	97.02267	6.0	26.75	2.7	1
OCSS2-9A-P	5-25-77	27.79668	97.02267	10.0	26.50	0.3	1
OCSS2-10-T	5-25-77	27.57692	97.74031	0.0	27.50	34.2	1
OCSS2-10-M	5-25-77	27.57692	97.74031	21.0	24.75	53.4	1
OCSS2-10-P	5-25-77	27.57692	97.74031	39.5	23.75	17.3	1
OCSS2-11-T	5-25-77	27.43317	96.53265	0.0	27.25	74.8	1
OCSS2-11-M	5-25-77	27.43317	96.53265	39.0	22.50	65.6	1
OCSS2-11-P	5-25-77	27.43317	96.53265	75.0	20.75	48.6	1
OCSS2-12-T	5-26-77	27.13619	96.40814	0.0	27.00	67.1	1
OCSS2-12-M	5-26-77	27.13619	96.40814	92.0	19.75	70.1	1
OCSS2-12-P	5-26-77	27.13619	96.40814	183.0			1

	9	10	11	12	13	14	15	16
OCSS2-4-T	37.9	1.41	7.24	2.20	0.10	-1.36		?
OCSS2-4-V	26.0	1.23	7.39	2.02	-0.01	-1.17		?
OCSS2-4-P	34.3	1.34	7.41	1.99	0.03	-1.27		?
OCSS2-5-T	25.4	1.13	7.63	2.01	-0.03	-1.24		?
OCSS2-5-M	21.8	1.80	7.07	1.99	0.14	-1.08		?
OCSS2-5-P	26.2	1.45	7.71	1.43	-0.04	-0.28		?
OCSS2-6-T	19.4	2.55	6.70	1.91	0.24	-0.81		?
OCSS2-6-M	10.1	2.46	6.91	1.81	0.23	-0.74		?
OCSS2-6-R	9.7	1.48	7.49	1.79	0.00	-0.94		?
OCSS2-7-T	43.6	1.16	7.61	2.09	-0.00	-1.32		?
OCSS2-7-M	17.0	1.61	7.12	2.08	0.09	-1.24		?
OCSS2-7-R	21.4	1.39	7.77	1.35	-0.07	0.04		?
OCSS2-8-T	43.1	1.04	7.56	2.19	-0.01	-1.44		?
OCSS2-8-M	25.0	1.62	7.19	2.02	0.12	-1.21		?
OCSS2-8-R	32.1	1.66	7.39	1.66	-0.05	-0.65		?
OCSS2-9-T	176.9	0.68	7.96	1.84	-0.29	-0.76		?
OCSS2-9-M	121.6	0.06	8.27	1.68	-0.55	0.38		?
OCSS2-9-R	173.4	1.17	7.79	1.44	-0.09	-0.47		?
OCSS2-9A-T	219.9	0.52	8.29	1.60	-0.44	0.38		?
OCSS2-9A-M	179.5	0.60	8.17	1.64	-0.38	0.03		?
OCSS2-9A-R	226.0	0.89	8.01	1.30	-0.26	0.47		?
OCSS2-10-T	43.7	1.05	7.65	2.06	-0.06	-1.29		?
OCSS2-10-M	26.2	2.05	6.89	1.99	0.17	-1.05		?
OCSS2-10-R	38.7	1.55	7.66	1.44	-0.05	-0.18		?
OCSS2-11-T	25.8	1.66	7.11	2.16	0.15	-1.27		?
OCSS2-11-M	21.1	1.07	7.92	1.49	-0.07	-0.56		?
OCSS2-11-P	34.7	1.49	7.75	1.24	-0.04	0.12		?
OCSS2-12-T	27.7	6.51	6.09	1.59	0.50	0.61		?
OCSS2-12-M	7.0	2.90	6.91	1.71	0.29	-0.48		?
OCSS2-12-R	8.1	2.44	7.06	1.59	0.07	-0.40		?

1	2	3	4	5	6	7	8
OCSS2-13-T	5-26-77	27.05201	96.71562	0.0	27.00	73.2	1
OCSS2-13-M	5-26-77	27.05201	96.71562	39.0	22.50	67.1	1
OCSS2-13-R	5-26-77	27.05201	96.71562	75.0	20.50	0.8	1
OCSS2-14-T	5-26-77	26.96700	97.04292	0.0	27.25	43.0	1
OCSS2-14-M	5-26-77	26.96700	97.04292	20.0	25.25	64.2	1
OCSS2-14-R	5-26-77	26.96700	97.04292	37.0	23.00	3.7	1
OCSS2-16-T	5-26-77	26.53405	97.09422	0.0	27.25	48.6	1
OCSS2-16-M	5-26-77	26.53405	97.09422	13.0	25.75	27.6	1
OCSS2-16-R	5-26-77	26.53405	97.09422	24.0	25.25	19.0	1
OCSS2-17-T	5-26-77	26.53075	96.90106	0.0	27.50	56.0	1
OCSS2-17-M	5-26-77	26.53075	96.90106	20.0	24.00	36.1	1
OCSS2-17-R	5-26-77	26.53075	96.90106	38.0	22.75	0.9	1
OCSS2-18-T	5-27-77	26.44037	96.51613	0.0	27.00	67.1	1
OCSS2-18-M	5-27-77	26.44037	96.51613	35.0	22.75	39.4	1
OCSS2-18-R	5-27-77	26.44037	96.51613	69.0	20.00	31.6	1
OCSS2-19-T	5-27-77	26.41209	96.34731	0.0	26.75	68.6	1
OCSS2-19-M	5-27-77	26.41209	96.34731	56.0	21.50	64.2	1
OCSS2-19-R	5-27-77	26.41209	96.34731	110.0	18.50	49.8	1
OCSS2-20-T	5-27-77	26.26283	96.56506	0.0	27.00	70.1	1
OCSS2-20-M	5-27-77	26.26283	96.56506	27.0	23.50	71.6	1
OCSS2-20-R	5-27-77	26.26283	96.56506	52.0	21.75	0.0	1
OCSS2-21-T	5-27-77	26.18077	96.81056	0.0	26.75	73.2	1
OCSS2-21-M	5-27-77	26.18077	96.81056	20.0	23.75	61.3	1
OCSS2-21-R	5-27-77	26.18077	96.81056	38.0			1
OCSS2-22-T	5-26-77	26.17506	96.99780	0.0	26.75	57.3	1
OCSS2-22-M	5-26-77	26.17506	96.99780	14.0	26.50	39.0	1
OCSS2-22-R	5-26-77	26.17506	96.99780	26.0	25.00	32.5	1
OCSS2-23-T	5-27-77	26.08895	97.11304	0.0	27.00	17.9	1
OCSS2-23-M	5-27-77	26.08895	97.11304	8.0	26.50	29.1	1
OCSS2-23-R	5-27-77	26.08895	97.11304	14.0	26.00	10.9	1

	9	10	11	12	13	14	15	16
OCSS2-13-T	27.9	0.83	7.77	2.23	-0.13	-1.33		2
OCSS2-13-M	18.6	2.15	7.04	1.78	0.07	-0.79		2
OCSS2-13-R	31.8	0.91	8.07	1.13	-0.14	0.74		2
OCSS2-14-T	42.7	1.23	7.46	2.09	0.00	-1.29		2
OCSS2-14-M	43.0	1.30	7.41	2.12	0.02	-1.32		2
OCSS2-14-R	46.9	1.23	7.57	2.01	-0.01	-1.22		2
OCSS2-16-T	65.7	1.14	7.57	2.13	-0.02	-1.38		2
OCSS2-16-M	65.9	1.76	7.18	1.90	0.04	-1.00		2
OCSS2-16-R	61.7	0.68	8.16	1.83	-0.25	-0.72		2
OCSS2-17-T	57.2	1.34	7.35	2.23	0.05	-1.44		2
OCSS2-17-M	55.1	0.95	7.66	2.23	-0.10	-1.38		2
OCSS2-17-R	56.1	1.09	7.61	2.11	-0.07	-1.26		2
OCSS2-18-T	34.3	0.92	7.78	2.12	-0.09	-1.31		2
OCSS2-18-M	22.4	1.28	7.76	1.51	-0.07	-0.48		2
OCSS2-18-R	31.9	0.90	8.04	1.22	-0.28	1.12		2
OCSS2-19-T	22.5	1.26	7.33	2.17	0.03	-1.35		2
OCSS2-19-M	16.6	1.48	7.47	1.78	-0.07	-0.70		2
OCSS2-19-R	16.5	1.38	7.72	1.39	-0.11	0.04		2
OCSS2-20-T	28.4	0.96	7.60	2.17	-0.09	-1.33		2
OCSS2-20-M	26.1	1.03	7.58	2.13	-0.07	-1.26		2
OCSS2-20-R	23.4	1.01	7.77	1.95	-0.12	-1.03		2
OCSS2-21-T	36.2	1.07	7.55	2.17	-0.05	-1.34		2
OCSS2-21-M	31.5	1.02	7.58	2.16	-0.08	-1.28		2
OCSS2-21-R	41.3	1.05	7.71	1.79	-0.18	-0.61		2
OCSS2-22-T	34.2	0.83	7.65	2.32	-0.14	-1.35		2
OCSS2-22-M	39.0	0.59	8.30	2.03	-0.28	-0.98		2
OCSS2-22-R	35.8	0.80	7.88	2.12	-0.18	-1.12		2
OCSS2-23-T	81.1	0.94	8.01	1.54	-0.11	-0.41		2
OCSS2-23-M	90.2	0.78	8.18	1.32	-0.14	0.26		2
OCSS2-23-R	80.9	0.93	8.02	1.49	-0.15	-0.09		2

1	2	3	4	5	6	7	8
NCSS2-23A-T	5-27-77	26.03070	97.10454	0.0	26.75	62.7	1
NCSS2-23A-M	5-27-77	26.03070	97.10454	9.0	26.00	52.2	1
NCSS2-23A-H	5-27-77	26.03070	97.10454	15.0	25.75	17.9	1
NCSS2-24-T	5-27-77	25.99561	97.10997	0.0	27.25	67.1	1
NCSS2-24-U	5-27-77	25.99561	97.10997	8.0	26.00	37.0	1
NCSS2-24-H	5-27-77	25.99561	97.10997	13.0	25.75	5.1	1

9	10	11	12	13	14	15	16
OCSS2-23A-T	41.0	0.74	8.03	2.09	-0.20	-1.07	2
OCSS2-23A-M	34.2	1.10	7.59	2.09	-0.03	-1.29	2
OCSS2-23A-R	33.4	1.28	7.15	2.25	0.03	-1.30	2
OCSS2-24-T	46.7	1.08	7.58	2.13	-0.04	-1.26	2
OCSS2-24-V	47.9	1.17	7.49	2.15	-0.02	-1.25	2
OCSS2-24-R	46.9	1.18	7.57	2.02	-0.03	-1.17	2

EXPLANATION FOR APPENDIX 2:

Trace Metals Content of Suspended Sediments, Seasonal Sampling

- Column 1 - Station number (T = top; B = bottom)
- Column 2 - Amounts of suspended sediment in mg/liter
- Column 3 - Cadmium, in ppm
- Column 4 - Chromium, in ppm
- Column 5 - Copper, in ppm
- Column 6 - Manganese, in ppm
- Column 7 - Nickel, in ppm
- Column 8 - Lead, in ppm
- Column 9 - Vanadium, in ppm
- Column 10 - Zinc, in ppm
- Column 11 - Percentage of iron
- Column 12 - Percentage of total particulate carbon

October - November 1976

STA.	MASS	CD.	CD.	CU.	MM.	MT.	DR.	V.	7N.	FF.	C.
1	2	3	4	5	6	7	8	9	10	11	12
2T	3.40	.4	10	13	597	14	92	6	108	.8	0.0
2D	3.00	.5	12	14	551	12	48	10	104	1.0	3.0
4T	1.20	5.0	40	27	635	20	53	15	452	1.0	4.8
4D	3.40	1.0	2	106	751	18	256	6	874	1.1	1.3
6T	.20	MS	MS	MS	MS	MS	MS	MS	MS	MS	4.8
6D	.34	MS	MS	MS	MS	MS	MS	MS	MS	MS	2.4
7T	.34	125.5	3680	76	531	4	266	ND	762	1.0	7.6
7D	.70	5.2	50	10	706	0	55	0	424	1.3	5.5
9AT	6.65	6.0	70	10	301	15	40	10	378	.7	4.7
9AR	6.86	1.0	12	25	560	14	38	6	309	1.0	4.0
10T	1.33	0.2	05	44	541	22	146	6	634	.0	3.8
10D	.00	2.2	26	27	810	2	81	13	426	1.0	4.6
12T	.35	15.3	370	222	303	54	1022	06	0470	.4	0.7
12D	.72	1.1	67	26	971	16	332	3	768	1.1	4.3
14T	1.25	.2	70	56	493	11	145	12	624	1.3	2.4
14D	1.08	1.0	55	19	455	46	77	13	411	1.0	3.2
17T	1.30	3.4	10	34	354	18	297	6	ND	1.3	8.8
17D	2.70	0.6	5	21	047	18	30	10	203	1.1	2.0
10T	.60	10.5	204	122	536	36	308	3	1820	.6	6.5
10D	2.02	7.5	ND	12	662	12	36	8	312	1.0	3.0
22T	6.07	1.3	2	15	621	12	50	12	145	1.0	3.1
22D	6.51	5.2	2	10	567	11	25	11	283	.8	3.2

March 1977

STA.	WASS	CD.	CH.	CH.	UN.	HT.	DR.	V.	7N.	FF.	C.
1	2	3	4	5	6	7	8	9	10	11	12
2T	1.67	2.6	100	30	730	ND	1160	43	ND	2.6	6.6
30	16.00	4.6	25	26	902	27	40	20	ND	2.2	2.2
4T	.26	NS	NS	NS	NS	NS	NS	NS	NS	NS	14.4
40	.66	5.0	2000	207	2400	ND	ND	254	ND	1.3	5.3
6T	.26	NS	NS	NS	NS	NS	NS	NS	NS	NS	9.9
60	.21	NS	NS	NS	NS	NS	NS	NS	NS	NS	6.1
7T	.15	NS	NS	NS	NS	NS	NS	NS	NS	NS	22.6
70	.65	NS	NS	NS	NS	NS	NS	NS	NS	NS	5.1
9AT	2.25	1.0	80	42	771	ND	402	65	ND	2.1	ND
9AD	0.00	.0	21	20	400	54	30	30	ND	2.2	2.7
10T	1.40	NS	NS	NS	NS	NS	NS	NS	NS	NS	4.0
100	.50	NS	NS	NS	NS	NS	NS	NS	NS	NS	4.0
12T	.20	NS	NS	NS	NS	NS	NS	NS	NS	NS	42.5
120	.15	NS	NS	NS	NS	NS	NS	NS	NS	NS	10.6
14T	.70	NS	NS	NS	NS	NS	NS	NS	NS	NS	6.4
140	1.00	2.4	141	77	1660	ND	92	142	ND	2.0	3.2
17T	.21	NS	NS	NS	NS	NS	NS	NS	NS	NS	13.8
170	1.26	5.2	104	100	1650	256	62	103	ND	2.0	4.0
10T	.12	NS	NS	NS	NS	NS	NS	NS	NS	NS	23.6
100	1.30	2.7	65	51	1180	115	50	60	ND	2.2	3.1
22T	.14	5.4	760	401	176	3000	1500	105	ND	ND	20.3
220	1.63	2.0	76	150	010	01	41	00	ND	1.0	3.5

May 1977

STATION	MASS	CD.	CP.	CH.	WH.	NT.	DI.	V.	ZN.	FF.	G.
21	1.70	1.5	62	64	303	527	93	85	1.5	ND	6.8
20	0.58	11.7	18	37	1110	316	4	22	2.4	ND	2.3
6T	.37	NS	NS	NS	NS	NS	NS	NS	NS	NS	23.7
6B	1.16	26.0	05	105	202	1100	720	59	.8	ND	8.2
6T	.19	NS	NS	NS	NS	NS	NS	NS	NS	NS	NS
6B	.04	NS	NS	NS	NS	NS	NS	NS	NS	NS	NS
7T	.27	51.1	58	106	252	65	608	220	.4	ND	14.3
7B	.70	60.0	87	420	1270	177	134	45	2.2	ND	3.8
0AT	5.74	3.5	61	54	594	60	91	75	2.0	ND	3.6
0AB	16.43	2.2	2	30	1220	325	40	69	2.2	ND	3.2
1AT	.07	2.6	04	NS	52	1700	101	13	1.2	ND	8.6
10B	3.66	3.5	7	10	1000	180	130	10	2.5	ND	2.2
12T	.20	366.0	NS	116	483	465	137	26	1.5	ND	12.1
12B	.10	1.1	160	NS	801	NS	28	125	4.0	ND	0.0
14T	.75	0.2	22	66	10	2200	166	77	.2	ND	6.4
14B	.71	0.3	627	360	370	2600	1400	111	3.0	ND	15.7
17T	.62	NS	NS	NS	NS	NS	NS	NS	NS	NS	8.8
17B	.70	26.5	64	36	013	2100	275	326	4.1	ND	11.6
170	.20	6.5	202	71	51	NS	150	NS	.1	ND	14.5
10T	.06	.1	53	35	1030	003	20	156	2.1	ND	2.3
22T	.37	NS	2	05	78	562	120	224	1.1	ND	15.7
22B	.38	12.3	23	120	87	2300	540	140	1.2	ND	19.6

EXPLANATION FOR APPENDIX 3:

Clay Mineralogy, Seasonal Suspended Sediment Samples

Column 1 - Station number (T = top; M = middle; B = bottom)

Column 2 - Amounts of suspended sediment in mg/liter

Column 3 - Percentage of 17Å clay mineral

Column 4 - Percentage of 10Å clay mineral

Column 5 - Percentage of 7.1Å clay mineral

Column 6 - Percentage of 3.3Å clay mineral

November 1976

NO	MASS	17A	10A	7.1A	3.3A
1T	ND	4	10	0	74
1M	ND	6	23	10	50
1P	ND	4	12	12	64
2T	ND	2	23	12	61
2M	ND	3	17	12	74
2P	ND	3	15	14	70
3T	3.50	17	10	10	51
3M	ND	11	23	11	53
3P	3.00	15	16	12	54
4T	1.20	5	30	17	45
4M	ND	4	30	12	47
4P	3.48	19	37	33	9
5T	ND	0	20	50	11
5M	ND	0	0	25	17
5P	ND	2	25	15	55
6T	0.20	0	0	22	66
6M	ND	0	20	21	47
6P	0.33	0	42	12	4
7T	0.34	0	0	20	70
7M	ND	0	0	0	100
7P	0.77	7	21	14	56
8T	ND	0	25	18	45
8M	ND	10	20	14	45
8P	ND	4	16	11	54
9T	6.66	0.1	22	14	62
9M	ND	5	20	14	60
9P	6.03	4	4	4	70
10T	1.33	7	24	14	53
10M	ND	0	12	28	57
10P	0.00	11	21	12	44
11T	ND	0	0	0	0
11M	ND	0	0	01	18
11P	ND	4	0	0	74
12T	0.35	5	0	31	64
12M	ND	0	30	23	44
12P	0.71	3	27	16	52

247

[Faint, illegible handwritten notes or signatures at the bottom of the page.]

November 1976

NO	MASS	17A	10A	7.1A	3.3A
13T	ND	3	23	19	53
13M	ND	0	42	17	39
13R	ND	15	22	12	40
14T	0.86	4	13	16	65
14M	ND	8	27	8	54
14R	1.89	16	12	14	55
16T	ND	7	29	13	40
16M	ND	6	27	14	51
16R	ND	11	25	12	51
17T	1.38	5	16	19	50
17M	ND	8	32	10	48
17R	2.70	10	24	13	52
18T	ND	0	40	16	33
18M	ND	0	26	20	52
19R	ND	0	19	16	64
19T	0.68	0	27	20	51
19M	ND	0	24	10	65
19R	2.01	10	15	12	62
20T	ND	0	39	15	45
20M	ND	0	8	13	78
20R	ND	0	2	18	79
21T	ND	4	24	14	57
21M	ND	8	21	16	53
21R	ND	1	48	11	38
22T	6.06	4	20	14	61
22M	ND	2	26	12	50
22R	6.51	0	27	13	58
23T	ND	7	22	14	55
23M	ND	11	17	13	57
23R	ND	4	17	16	61
24T	ND	4	21	11	62
24M	ND	2	20	12	63
24R	ND	5	17	11	65

March 1977

NO	PASS	17A	10A	7.1A	3.3A
1F	ND	0	14	25	51
1G	ND	0	10	14	47
1H	ND	0	17	25	49
2T	ND	2	16	20	43
2A	ND	0	46	22	34
2B	ND	0	0	32	50
3T	0.84	0	46	20	24
3A	ND	0	0	56	44
3B	0.50	2	21	27	50
4T	0.34	0	22	0	0
4A	ND	0	20	24	47
4B	0.47	0	12	27	50
5T	ND	0	0	20	71
5A	ND	0	21	63	16
5B	ND	0	44	22	36
6T	0.44	0	0	46	54
6A	ND	0	76	10	16
6B	0.25	0	34	35	31
7T	0.14	0	21	10	0
7A	ND	0	67	32	0
7B	0.71	1	80	10	0
8T	ND	0	40	10	42
8A	ND	6	40	45	0
8B	ND	1	7	42	50
9T	1.25	4	47	22	26
9A	ND	1	11	42	40
9B	6.20	4	40	22	23
10T	1.42	0	0	46	45
10A	ND	0	0	50	50
10B	0.75	1	53	24	22
11T	ND	0	88	6	6
11A	ND	0	17	42	41
11B	ND	5	12	36	46
12T	0.24	0	0	46	54
12A	ND	0	0	46	45
12B	0.25	2	40	32	26

March 1977

NO	WASS	17A	10A	7.1A	3.3A
137	MO	0	14	30	40
138	MO	21	0	20	50
139	MO	0.7	32	15	53
141	0.52	13	0	40	30
142	MO	22	57	7	16
143	1.00	0	0	43	57
147	MO	100	0	0	0
148	MO	7	53	27	13
149	MO	0	40	23	37
177	0.50	19	0	36	46
178	MO	20	32	24	24
179	1.77	6	15	31	50
181	MO	0	0	0	0
182	MO	23	0	51	26
183	MO	0	40	17	15
187	0.30	0	0	31	40
188	MO	0	22	33	45
189	2.81	0	0	29	71
201	MO	0	0	50	50
202	MO	0	0	50	50
203	MO	0	0	54	44
217	MO	42	30	6	4
218	MO	0	0	42	34
219	MO	25	75	0	0
221	0.22	0	0	50	50
222	MO	0	0	42	52
223	2.43	0	70	15	15
237	MO	0	0	50	50
238	MO	30	44	8	8
239	MO	0	26	20	45
247	MO	1	23	40	36
248	MO	11	0	30	50
249	MO	2	0	18	71

May 1977

NO	MASS	17A	10A	7.1A	3.3A
1T	ND	0	35	21	44
1M	ND	0	31	24	45
1R	ND	0	45	17	38
1AT	ND	0	21	21	58
1AM	ND	2	22	17	59
1AR	ND	0	15	21	64
2T	ND	1	23	20	56
2M	ND	0.1	38	17	45
2R	ND	0.4	0	21	70
3T	1.70	0	30	20	41
3M	ND	10	15	31	44
3R	0.57	2	35	19	44
4T	0.36	0	100	0	0
4M	ND	0	15	24	61
4R	1.15	6	53	17	24
5T	ND	0	62	17	21
5M	ND	0	60	19	12
5R	ND	0	36	25	39
6T	0.10	0	0	67	33
6M	ND	0	26	0	14
6R	0.08	0	26	30	35
7T	0.27	0	16	49	35
7M	ND	0	70	16	14
7R	0.70	2	25	17	56
8T	ND	0	0	0	0
8M	ND	0	0	44	56
8R	ND	1	34	25	40
9T	ND	0	25	32	43
9M	ND	0	24	32	44
9R	ND	1	20	16	63
9AT	5.76	5	0	48	47
9AM	ND	0	64	15	21
9AR	16.43	0.2	20	25	46
10T	0.06	0	25	30	45
10M	ND	0	42	22	36
10R	3.63	3	30	23	44
11T	ND	0	0	0	0
11M	ND	0.5	40	25	34
11R	ND	0	30	19	42

May 1977

NO	MASS	17A	10A	7.1A	3.3A
12T	0.27	0	78	0	22
12M	ND	0	17	0	83
12R	0.18	1	7	56	36
13T	ND	0	0	67	33
13M	ND	0	25	33	42
13R	ND	1	38	23	38
14T	0.75	0	92	4	4
14M	ND	0	20	45	35
14R	0.70	0	0	100	0
16T	ND	0	0	0	0
16M	ND	0.3	48	20	32
16R	ND	0	0	67	33
17T	0.61	1	41	22	36
17M	ND	0	0	61	39
17R	0.09	0	68	21	11
18T	ND	0	81	17	2
18M	ND	0	22	46	32
18R	ND	1	42	28	29
19T	0.29	0	0	64	36
19M	ND	0	0	39	61
19R	0.93	0	21	8	71
20T	ND	0	0	78	22
20M	ND	0	0	64	36
20R	ND	0	0	0	0
21T	ND	0	26	49	25
21M	ND	0	0	44	56
21R	ND	0	0	34	66
22T	0.36	0	0	77	23
22M	ND	0	0	34	66
22R	0.37	0	0	66	34
23T	ND	0	0	47	53
23M	ND	1	16	41	42
23R	ND	0	47	31	22
23AT	ND	0	0	39	61
23AM	ND	0	160	0	0
23AR	ND	0	0	0	0
24T	ND	0	14	36	50
24M	ND	0	0	44	56
24R	ND	0	0	50	50

EXPLANATION FOR APPENDIX 4:

Clay Mineralogy, Bottom Sediment Samples

Column 1 - Sample number

Column 2 - Percentage 17Å clay mineral

Column 3 - Percentage 10Å clay mineral

Column 4 - Percentage 7Å clay mineral

SAMPLE	*17	*10	*7
1	56	26	10
2	61*	25	15
5	55	27	10
6	57	22	11
7	51	21	12
8	62*	22	15
9	52	20	10
10	55	20	17
11	57	27	17
12	59*	25	17
13	62	10	19
14	62	22	16
15	63	24	14
16	74	17	10
17	60	25	16
18	50	26	17
20	53	22	16
22	62	22	16
23	54	27	10
26	50	26	17
25	61	24	16
27	52	26	16
28	62	22	15
29	60	26	14

SAMPLE	*17	*10	*7
30	60*	26*	15
31	56	28	16
32	55	28	18
33	56	27	17
34	50	24	14
35	60	22	18
37	55	21	15
38	64*	20*	14
39	55	20	17
40	62	24	14
41	62	26	14
42	62	25	14
43	70	20	11
44	60	20	12
45	70	21	10
46	54	25	12
47	60	22	9
48	67	21	12
50	66	22	12
51	62	24	12
52	61	20*	10
54	65	22	14
55	62	24	15
56	64	22	14
57	58	28	14
58	70	10	12
59	62	27	10

SAMPLE	*17	*10	*7
60	65	22	14
61	55	24	11
62	58	25	10
63	67	40	14
64	62	25	14
65	69	21	10
66	62	24	15
67	56	27	18
68	67	22	11
69	50	26	16
71	62	24	14
72	66	22	12
73	59	28	12
74	62	25	14
75	70	20	11
76	61	24	15
77	58	25	17
80	62	24	15
82	67	22	12
84	62	26	12
85	62	24	14
86	61	22	14
87	62	22	16
88	61	24	16

SAMPLE	%17	%10	%7
00	60	25	16
01	62	23	16
02	58	27	16
03	61	25	16
04	63	24	14
05	60	26	15
06	61	24	15
07	62	24	15
08	59	27	16
09	55	20	16
100	60	10	12
101	56	32	12
102	53	31	17
103	63	24	13
104	50	28	14
105	62	23	16
106	63	23	15
107	58	25	17
108	60	26	15
110	62*	24	14
111	63	24	13
112	66	21	13
113	67	20	13
114	59	25	16
115	62	23	16
116	50	27	14
117	61	24	16
118	54	31	15
119	58	27	16

SAMPLE	%17	%10	%7
120	58	28	15
121	50	33	25
122	62	24	14
123	62	24	15
124	50	23	17
125	57	27	17
126	58	27	16
127	62	25	13
128	58	20	14
129	57	26	20
130	50	26	14
131	53	20	21
132	61	25	15
133	67	21	12
134	54	24	22
135	61	26	14
136	71*	10	12
140	54	26	21
141	67	21	13
142	61	25	15
143	63	23	15
144	68	20	13
145	70	18	13
146	68	21	12
147	59	23	13
148	62	21	17
149	64	24	13

SAMPLE	%17	%10	%7
150	65	20	15
151	55	20	17
152	60	26	14
153	68	21	11
154	65	20	15
155	56	26	18
156	67	22	12
157	61	20	11
158	64	21	15
159	67	21	13
160	61	20	12
161	54	30	17
162	68	20	13
163	67	20	14
164	63*	26	12
165	55	35	11
166	60	25	15
167	57	26	14
168	58	20	14

SAMPLE	%17	%10	%7
170	56	20	17
171	50	26	15
172	45	22	7
174	66	23	12
175	60	21	12
176	66	21	14
177	66	22	12
179	68	21	12
170	41	21	24
180	65	25	11
181	62	23	15
182	55*	25*	11
183	62	24	15
184	63	22	15
185	58	26	15
186	68	10	13
187	68	20	12
188	64	23	15
189	60	25	16
190	62	24	15
191	67	10	15
192	66	22	15
193	57	27	17
194	64	21	16
195	58	20	15
196	60	22	17
197	58	24	10
198	54	10	12
199	66*	21*	14

SAMPLE	%17	%10	%7
200	72	14	15
201	72	15	13
202	63	23	15
203	72	17	13
204	53	20	14
205	57	15	0
206	66	20	14
207	67	21	13
208	55	20	17
209	66	22	13
210	57*	28	17
211	64	10	17
212	68	20	13
216	57	26	10
217	60	24	17
218	64	24	22
219	74	42	24
220	60	10	12
221	61	21	10
222	64	21	25
223	65	24	12
224	64	21	15
225	56	28	16
226	66	21	13
227	65	22	13
228	55	23	22
229	51	24	24

SAMPLE	%17	%10	%7
230	64	21	15
231	68	22	10
232	66	20	15
233	61	23	16
234	60*	27*	13
235	63	21	17
236	54	27	20
237	61	25	15
238	60	24	16
239	62	23	15
240	77	14	0
241	67	20	13
242	70	18	13
243	67	20	13
244	57	27	16
245	60	23	18
246	47	35*	15
247	60	25	16
248	59	27	15
249	68	10	14

SAMPLE	217	210	27
250	55	20	16
251	61*	22	17
252	65	10	17
253	64	22	15
254	65	22	13
255	71	10	11
256	64	22	15
257	62	22	15
258	67	22	12
259	56	27	17
260	54	20	13
261	62	22	16
262	58	24	17
263	63	21	17
264	62	22	15
265	52	27	22*
266	62*	25*	13
267	71	17	12
268	61	22	18
269	71	16	12
270	65	10	17
271	55*	20*	10
272	59	25	17
273	57*	24	20
274	59	24	17

EXPLANATION FOR APPENDIX 5:

Textural Properties of Seasonal Benthic Sediment Samples

- Column 1 - Sample station number (Univ. Texas Marine Science Institute designation)
- Column 2 - Sample station number (USGS designation): TS = Texas seasonal samples, second character = station number, third character = transect number, fourth character = subsample designation, fifth character = seasonal suite (1 = winter, 2 = spring, 3 = summer/fall)
- Column 3 - Station latitude: first two digits = degrees, last two digits = minutes
- Column 4 - Station longitude: first two digits = degrees, last two digits = minutes
- Column 5 - Station water depth (meters)
- Column 6 - Sand percentage (%)
- Column 7 - Silt percentage (%)
- Column 8 - Clay percentage (%)
- Column 9 - Sand/Mud ratio
- Column 10 - Data sheet designation numbers (#1 = first data sheet)
- Column 11 - Sample station number reiteration (Univ. Texas Marine Science Institute designation)
- Column 12 - Sample station number reiteration (USGS designation)
- Column 13 - Silt/Clay ratio
- Column 14 - Mean diameter in phi units (first moment)
- Column 15 - Standard deviation in phi units (second moment)
- Column 16 - Skewness (third moment)
- Column 17 - Kurtosis (fourth moment)
- Column 18 - Data sheet designation number (#2 = second data sheet)

1	2	3	4	5	6	7	8	9	10
1-1-RRFF-SFD	TS2-1-1-A-1	28.12	06.27	14	58.76	18.10	23.14	1.43	1
2-1-RRGO-SFD	TS2-2-1-A-1	27.55	06.20	42	26.70	50.07	23.23	0.36	1
3-1-RRTR-SFD	TS2-3-1-A-1	27.24	06.07	134	3.74	51.40	44.77	0.04	1
1-3-RRKA-SFD	TS2-1-3-A-1	26.58	07.11	25	3.12	46.20	50.68	0.03	1
1-3-RRKD-SFD	TS2-1-3-B-1	26.58	07.11	25	3.14	58.14	38.72	0.03	1
1-3-RRKG-SFD	TS2-1-3-C-1	26.58	07.11	25	24.31	52.01	23.58	0.32	1
1-3-RRKJ-SFD	TS2-1-3-D-1	26.58	07.11	25	1.82	47.17	51.01	0.02	1
1-3-RRKY-SFD	TS2-1-3-Y-1	26.58	07.11	25	7.46	55.76	36.70	0.08	1
2-3-RRME-SFD	TS2-2-3-A-1	26.58	06.48	65	0.88	43.81	55.30	0.01	1
2-3-RRMH-SFD	TS2-2-3-B-1	26.58	06.48	65	1.28	50.80	47.92	0.01	1
2-3-RRMK-SFD	TS2-2-3-C-1	26.58	06.48	65	1.32	49.94	48.74	0.01	1
2-3-RRMN-SFD	TS2-2-3-D-1	26.58	06.48	65	2.64	53.75	43.61	0.03	1
2-3-RRMZ-SFD	TS2-2-3-Y-1	26.58	06.48	65	1.61	57.57	40.82	0.02	1
1-4-RRHA-SFD	TS2-1-4-A-1	26.10	07.01	27	48.70	21.63	29.58	0.05	1
1-4-RRHD-SFD	TS2-1-4-B-1	26.10	07.01	27	27.89	36.21	35.01	0.39	1
1-4-RRHC-SFD	TS2-1-4-C-1	26.10	07.01	27	62.24	17.78	19.98	1.65	1
1-4-RRHI-SFD	TS2-1-4-D-1	26.10	07.01	27	61.52	20.34	18.14	1.60	1
1-4-RRHY-SFD	TS2-1-4-E-1	26.10	07.01	27	55.82	26.26	17.01	1.26	1
1-4-RRHZ-SFD	TS2-1-4-Y-1	26.10	07.01	27	52.06	25.34	22.60	1.00	1
2-4-RRWK-SFD	TS2-2-4-A-1	26.10	06.30	47	55.26	20.00	24.65	1.23	1
2-4-RRWL-SFD	TS2-2-4-B-1	26.10	06.30	47	47.61	23.48	28.91	0.01	1
2-4-RRWN-SFD	TS2-2-4-C-1	26.10	06.30	47	52.90	23.40	23.71	1.12	1
2-4-RRWT-SFD	TS2-2-4-D-1	26.10	06.30	47	58.05	10.57	22.48	1.44	1
2-4-RRWY-SFD	TS2-2-4-Y-1	26.10	06.30	47	54.48	20.53	25.00	1.20	1
3-4-RRYU-SFD	TS2-3-4-A-1	26.10	06.24	91	50.38	27.28	22.34	1.02	1
3-4-RRYS-SFD	TS2-3-4-B-1	26.10	06.24	91	39.08	27.68	32.34	0.67	1
3-4-RRYV-SFD	TS2-3-4-C-1	26.10	06.24	91	30.68	29.30	30.93	0.66	1
3-4-RRYX-SFD	TS2-3-4-D-1	26.10	06.24	91	48.67	22.52	28.81	0.95	1
3-4-RRYF-SFD	TS2-3-4-Y-1	26.10	06.24	91	43.91	27.08	29.00	0.78	1
4-4-RRAS-SFD	TS2-4-4-A-1	26.10	07.08	15	73.25	12.87	13.88	2.74	1

	11	12	13	14	15	16	17	18
1-1-BBEE-SFD	TS2-1-1-A-1	0.78	5.23	2.63	0.42	-0.36		2
2-1-BBCH-SFD	TS2-2-1-A-1	2.16	5.98	2.24	-0.29	-0.89		2
2-1-BBTR-SFD	TS2-2-1-A-1	1.15	7.54	1.91	-0.17	-0.50		2
1-2-BBKA-SFD	TS2-1-2-A-1	0.91	7.71	2.12	-0.16	-1.13		2
1-2-BBKN-SFD	TS2-1-2-B-1	1.50	7.16	2.16	0.03	-1.20		2
1-2-BBKC-SFD	TS2-1-2-C-1	2.20	5.88	2.30	0.38	-0.79		2
1-2-BBKJ-SFD	TS2-1-2-D-1	0.93	7.86	1.46	-0.15	-1.01		2
1-2-BBKY-SFD	TS2-1-2-Y-1	1.52	6.00	2.23	0.05	-1.27		2
2-2-BBME-SFD	TS2-2-2-A-1	0.70	8.06	1.97	-0.20	-0.93		2
2-2-BBMH-SFD	TS2-2-2-B-1	1.16	7.52	2.05	-0.07	-1.29		2
2-2-BBHK-SFD	TS2-2-2-C-1	1.02	7.72	2.02	-0.08	-1.23		2
2-2-BBHN-SFD	TS2-2-2-D-1	1.23	7.31	2.22	-0.02	-1.38		2
2-2-BBG7-SFD	TS2-2-2-Y-1	1.41	7.32	2.09	0.01	-1.25		2
1-4-BBHA-SFD	TS2-1-4-A-1	0.73	5.40	3.08	0.16	-1.50		2
1-4-BBHN-SFD	TS2-1-4-B-1	1.01	6.44	2.95	-0.15	-1.16		2
1-4-BBHG-SFD	TS2-1-4-C-1	0.89	4.59	2.94	0.47	-0.60		2
1-4-BBHJ-SFD	TS2-1-4-D-1	1.12	4.47	2.78	0.49	-0.55		2
1-4-BBHM-SFD	TS2-1-4-E-1	1.47	4.66	2.72	0.43	-0.66		2
1-4-BBHQ-SFD	TS2-1-4-Y-1	1.22	5.02	2.87	0.31	-1.13		2
2-4-BBWK-SFD	TS2-2-4-A-1	0.91	4.93	3.11	0.29	-1.25		2
2-4-BBWN-SFD	TS2-2-4-B-1	0.91	5.41	3.10	0.17	-1.48		2
2-4-BBWC-SFD	TS2-2-4-C-1	0.99	4.96	3.06	0.26	-1.24		2
2-4-BBWT-SFD	TS2-2-4-D-1	0.83	4.71	3.03	0.37	-1.08		2
2-4-BBWD-SFD	TS2-2-4-Y-1	0.92	4.95	3.13	0.28	-1.27		2
2-4-BBYD-SFD	TS2-2-4-A-1	1.22	5.14	2.87	0.28	-1.15		2
2-4-BBYS-SFD	TS2-2-4-B-1	0.86	5.90	3.00	0.06	-1.52		2
2-4-BBYV-SFD	TS2-2-4-C-1	0.95	5.91	3.04	0.06	-1.49		2
2-4-BBYY-SFD	TS2-2-4-D-1	0.78	5.45	3.07	0.18	-1.45		2
2-4-BBYE-SFD	TS2-2-4-Y-1	0.93	5.53	3.07	0.13	-1.47		2
4-4-BBGS-SFD	TS2-4-4-A-1	0.93	4.11	2.50	0.70	-0.57		2

1	2	3	4	5	6	7	8	9	10
4-4-RCAM-SED	TS2-4-4-R-1	26.10	97.08	15	84.49	9.21	6.30	5.45	1
4-4-RCAY-SED	TS2-4-4-C-1	26.10	97.09	15	76.46	12.21	11.33	3.25	1
4-4-RCDD-SED	TS2-4-4-D-1	26.10	97.08	15	76.18	12.85	10.97	3.20	1
4-4-RCHH-SED	TS2-4-4-Y-1	26.10	97.08	15	75.04	13.14	11.91	3.01	1
5-4-RCOM-SED	TS2-5-4-A-1	26.10	96.54	37	37.16	45.10	17.74	0.59	1
5-4-ROCD-SED	TS2-5-4-P-1	26.10	96.54	37	53.83	23.59	22.58	1.17	1
5-4-ROCS-SED	TS2-5-4-C-1	26.10	96.54	37	29.61	33.79	45.60	0.26	1
5-4-ROCV-SED	TS2-5-4-D-1	26.10	96.54	37	24.61	31.07	44.31	0.33	1
5-4-RCHJ-SED	TS2-5-4-Y-1	26.10	96.54	37	35.84	35.27	28.89	0.56	1
6-4-RCFI-SED	TS2-6-4-A-1	26.10	96.31	65	59.73	17.76	22.51	1.48	1
6-4-RCFI-SED	TS2-6-4-P-1	26.10	96.31	65	59.74	21.78	18.49	1.48	1
6-4-RCFO-SED	TS2-6-4-C-1	26.10	96.31	65	50.07	21.84	28.08	1.00	1
6-4-RCFD-SED	TS2-6-4-D-1	26.10	96.31	65	48.72	21.69	29.60	0.95	1
6-4-RCHI-SED	TS2-6-4-Y-1	26.10	96.31	65	56.27	19.00	24.72	1.29	1
7-4-RCGF-SED	TS2-7-4-A-1	26.10	96.20	130	0.00	36.61	63.39	0.00	1
7-4-RCGH-SED	TS2-7-4-P-1	26.10	96.20	130	0.94	40.90	54.17	0.01	1
7-4-RCGK-SED	TS2-7-4-C-1	26.10	96.20	130	0.47	39.27	60.26	0.00	1
7-4-RCGN-SED	TS2-7-4-D-1	26.10	96.20	130	0.44	35.04	64.52	0.00	1
7-4-RCHN-SED	TS2-7-4-Y-1	26.10	96.20	130	0.51	40.13	59.35	0.00	1
1-1-RCXF-SED	TS2-1-1-A-2	29.12	96.27	18	44.07	33.91	22.01	0.79	1
1-1-RCMH-SED	TS2-1-1-P-2	29.12	96.27	18	42.83	34.52	22.65	0.75	1
2-1-RCYD-SED	TS2-2-1-A-2	27.55	96.20	42	15.16	49.66	35.17	0.18	1
2-1-RCYG-SED	TS2-2-1-P-2	27.55	96.20	42	15.90	49.80	34.40	0.19	1
3-1-RCAT-SED	TS2-3-1-A-2	27.34	96.07	134	4.48	41.04	54.48	0.05	1
3-1-RCAL-SED	TS2-3-1-P-2	27.34	96.07	134	4.39	30.10	65.51	0.05	1
4-1-RCDF-SED	TS2-4-1-A-2	29.14	96.29	10	60.70	17.23	22.06	1.55	1
4-1-RCDI-SED	TS2-4-1-P-2	29.14	96.29	10	72.01	16.54	11.45	2.57	1
5-1-RCFF-SED	TS2-5-1-A-2	27.44	96.14	82	1.29	47.03	51.68	0.01	1

		11	12	13	14	15	16	17	18
4-4-PCAV-SED	TS2-4-4-P-1	1.46	3.42	1.92	1.11	4.23			?
4-4-PCAY-SED	TS2-4-4-C-1	1.08	3.69	2.49	0.72	1.16			?
4-4-PCBP-SED	TS2-4-4-D-1	1.17	3.04	2.29	0.82	1.48			?
4-4-PCHP-SED	TS2-4-4-Y-1	1.11	3.08	2.36	0.79	1.21			?
5-4-PCCV-SED	TS2-5-4-A-1	2.54	4.07	2.63	0.33	-0.66			?
5-4-PCCP-SED	TS2-5-4-P-1	1.05	4.03	2.93	0.34	-1.10			?
5-4-PCCS-SED	TS2-5-4-C-1	0.74	6.89	2.85	-0.20	-1.20			?
5-4-PCCV-SED	TS2-5-4-D-1	0.70	6.77	2.95	-0.18	-1.30			?
5-4-PCCH-SED	TS2-5-4-Y-1	1.22	5.62	2.96	0.13	-1.36			?
6-4-PCFT-SED	TS2-6-4-A-1	0.70	4.80	3.03	0.35	-1.18			?
6-4-PCFL-SED	TS2-6-4-P-1	1.18	4.61	2.80	0.44	-0.71			?
6-4-PCFD-SED	TS2-6-4-C-1	0.78	5.31	3.14	0.19	-1.47			?
6-4-PCFD-SED	TS2-6-4-D-1	0.73	5.40	3.15	0.17	-1.51			?
6-4-PCHI-SED	TS2-6-4-Y-1	0.77	4.07	3.07	0.29	-1.23			?
7-4-PCGF-SED	TS2-7-4-A-1	0.58	8.47	1.64	-0.22	-0.88			?
7-4-PCGH-SED	TS2-7-4-P-1	0.70	8.26	1.72	-0.19	-0.84			?
7-4-PCGK-SED	TS2-7-4-C-1	0.65	8.30	1.80	-0.23	-0.92			?
7-4-PCGN-SED	TS2-7-4-D-1	0.54	8.49	1.67	-0.28	-0.65			?
7-4-PCHN-SED	TS2-7-4-Y-1	0.68	8.28	1.70	-0.20	-0.87			?
1-1-PCVF-SED	TS2-1-1-A-2	1.54	5.51	2.53	0.31	2.52			?
1-1-PCVU-SED	TS2-1-1-B-2	1.52	5.56	2.54	0.30	-1.02			?
2-1-PCVQ-SED	TS2-2-1-A-2	1.41	6.07	2.21	-0.01	-1.06			?
2-1-PCVQ-SED	TS2-2-1-B-2	1.45	6.89	2.24	0.01	-1.10			?
3-1-PCWJ-SED	TS2-3-1-A-2	0.75	7.08	2.02	-0.30	-0.37			?
3-1-PCWJ-SED	TS2-3-1-B-2	0.46	8.41	1.91	-0.52	0.67			?
4-1-PCWF-SED	TS2-4-1-A-2	0.78	4.08	2.82	0.38	-1.02			?
4-1-PCWJ-SED	TS2-4-1-B-2	1.44	4.42	2.20	0.74	0.96			?
5-1-PCWF-SED	TS2-5-1-A-2	0.01	8.08	1.56	-0.13	-0.34			?

1	2	3	4	5	6	7	8	9	10
5-1-04FH-SFD	TS2-5-1-0-2	27.44	96.14	92	25.68	44.74	20.59	0.35	1
6-1-04GC-SFD	TS2-6-1-A-2	27.39	96.12	100	12.33	56.10	31.57	0.14	1
4-1-04GF-SFD	TS2-6-1-0-2	27.39	96.12	100	10.80	54.49	25.72	0.25	1
1-2-04HY-SFD	TS2-1-2-A-2	27.40	96.59	22	8.29	57.59	34.12	0.09	1
1-2-04YA-SFD	TS2-1-2-0-2	27.40	96.50	22	23.54	44.44	32.02	0.31	1
1-2-04WJ-SFD	TS2-1-2-C-2	27.40	96.59	22	9.67	47.75	42.58	0.11	1
2-2-04KD-SFD	TS2-2-2-A-2	27.30	96.45	49	24.15	50.84	25.01	0.32	1
2-2-04KN-SFD	TS2-2-2-0-2	27.30	96.45	49	6.03	49.63	44.35	0.06	1
2-2-04KI-SFD	TS2-2-2-C-2	27.30	96.45	49	8.06	52.34	39.60	0.04	1
3-2-04ME-SFD	TS2-3-2-A-2	27.18	96.23	131	2.99	44.40	52.11	0.03	1
3-2-04MT-SFD	TS2-3-2-0-2	27.18	96.23	131	1.76	48.10	50.14	0.02	1
3-2-04MC-SFD	TS2-3-2-C-2	27.18	96.23	131	1.84	45.85	52.31	0.02	1
4-2-04DP-SFD	TS2-4-2-A-2	27.34	96.50	34	9.26	61.89	28.85	0.10	1
4-2-04DH-SFD	TS2-4-2-0-2	27.34	96.50	34	31.84	48.84	19.32	0.47	1
5-2-04DV-SFD	TS2-5-2-A-2	27.24	96.36	78	8.82	41.74	49.44	0.10	1
5-2-04DY-SFD	TS2-5-2-0-2	27.24	96.36	78	6.03	50.66	43.32	0.06	1
5-2-04DT-SFD	TS2-6-2-A-2	27.24	96.29	98	5.58	52.07	42.35	0.06	1
6-2-04HC-SFD	TS2-6-2-0-2	27.24	96.24	98	4.33	48.34	47.28	0.05	1
1-3-04V7-SFD	TS2-1-3-A-2	26.58	97.11	25	3.01	60.01	26.98	0.03	1
1-3-04MC-SFD	TS2-1-3-0-2	26.58	97.11	25	13.13	64.50	22.36	0.15	1
2-3-04Y7-SFD	TS2-2-3-A-2	26.58	96.48	65	0.65	55.41	43.43	0.01	1
2-3-04YC-SFD	TS2-2-3-0-2	26.58	96.48	65	1.62	42.08	56.30	0.02	1
3-3-04TA-SFD	TS2-3-3-A-2	26.58	96.33	106	1.46	47.06	51.47	0.02	1
2-3-04TA-SFD	TS2-3-3-0-2	26.58	96.33	106	0.70	45.03	54.27	0.01	1
4-3-04B7-SFD	TS2-4-3-A-2	26.58	97.20	15	82.44	11.20	6.37	4.69	1
4-3-04TC-SFD	TS2-4-3-0-2	26.58	97.20	15	84.40	9.42	6.18	5.41	1
5-3-04D3-SFD	TS2-5-3-A-2	26.58	97.02	40	2.84	50.46	46.70	0.03	1
5-3-04DH-SFD	TS2-5-3-0-2	26.58	97.02	40	1.38	50.40	48.22	0.01	1
6-3-04TE-SFD	TS2-6-3-A-2	26.58	96.30	125	1.47	49.81	48.72	0.02	1
6-3-04TE-SFD	TS2-6-3-0-2	26.58	96.30	125	0.97	35.96	63.07	0.01	1

	11	12	13	14	15	16	17	18
5-1-04FH-SFD	TS2-5-1-0-2	1.51	6.37	2.44	0.11	-1.22		2
6-1-04GC-SFD	TS2-6-1-1-2	1.78	6.75	2.22	0.05	-1.00		2
6-1-04GE-SFD	TS2-6-1-0-2	2.12	6.36	2.21	0.15	-0.96		2
1-2-04HY-SFD	TS2-1-2-A-2	1.69	6.89	2.15	0.07	-1.14		2
1-2-04IA-SFD	TS2-1-2-E-2	1.39	6.41	2.41	0.12	-1.33		2
1-2-04IU-SFD	TS2-1-2-C-2	1.12	7.16	2.23	-0.06	-1.22		2
2-2-04KQ-SFD	TS2-2-2-A-2	2.03	6.10	2.29	0.26	-0.98		2
2-2-04KO-SFD	TS2-2-2-0-2	1.12	7.39	2.18	-0.06	-1.25		2
2-2-04KI-SFD	TS2-2-2-C-2	1.32	7.02	2.22	0.03	-1.35		2
3-2-04MF-SFD	TS2-3-2-A-2	0.86	7.07	1.97	-0.22	-0.52		2
3-2-04MT-SFD	TS2-3-2-E-2	0.26	7.85	1.39	-0.14	-0.92		2
3-2-04MC-SFD	TS2-3-2-C-2	0.88	7.80	1.37	-0.20	-0.66		2
4-2-04PQ-SFD	TS2-4-2-A-2	2.15	6.62	2.13	0.19	-1.00		2
4-2-04PI-SFD	TS2-4-2-0-2	2.53	5.80	2.15	0.35	-0.64		2
5-2-04PV-SFD	TS2-5-2-A-2	0.84	7.63	2.18	-0.19	-0.98		2
5-2-04PY-SFD	TS2-5-2-0-2	1.17	7.48	2.06	-0.07	-1.02		2
6-2-04T7-SFD	TS2-6-2-A-2	1.23	7.38	2.12	-0.05	-1.12		2
6-2-04UC-SFD	TS2-6-2-0-2	1.02	7.65	2.02	-0.12	-0.98		2
1-3-04V7-SFD	TS2-1-3-A-2	1.62	7.29	1.97	0.02	-1.07		2
1-3-04MC-SFD	TS2-1-3-0-2	2.98	6.15	2.00	0.35	-0.65		2
2-3-04Y7-SFD	TS2-2-3-A-2	1.20	7.56	1.92	0.02	-1.27		2
2-3-04YC-SFD	TS2-2-3-0-2	0.75	8.14	1.41	-0.19	-0.84		2
3-3-04JQ-SFD	TS2-3-3-A-2	0.91	7.96	1.91	-0.12	-1.08		2
3-3-04JE-SFD	TS2-3-3-0-2	0.83	8.08	1.72	-0.12	-0.98		2
4-3-04P7-SFD	TS2-4-3-A-2	1.76	4.10	1.64	1.26	5.57		2
4-3-04IC-SFD	TS2-4-3-0-2	1.52	4.06	1.50	1.36	6.58		2
5-3-04ID-SFD	TS2-5-3-A-2	1.08	7.63	1.49	-0.10	-1.03		2
5-3-04ID-SFD	TS2-5-3-0-2	1.05	7.82	1.84	-0.07	-1.03		2
6-3-04IF-SFD	TS2-6-3-A-2	1.02	7.84	1.80	-0.12	-0.77		2
6-3-04IF-SFD	TS2-6-3-0-2	0.57	8.38	1.72	-0.30	-0.51		2

1	2	3	4	5	6	7	8	9	10
1-4-RTG7-SFD	TS2-1-4-A-2	26.10	97.01	27	55.67	18.82	25.51	1.26	1
1-4-RTHC-SFD	TS2-1-4-B-2	26.10	97.01	27	41.55	21.45	37.00	0.71	1
2-4-RTJ7-SFD	TS2-2-4-A-2	26.10	96.39	47	8.89	53.77	37.34	0.10	1
2-4-RTJC-SFD	TS2-2-4-B-2	26.10	96.39	47	4.14	53.60	42.26	0.04	1
2-4-RTJH-SFD	TS2-2-4-C-2	26.10	96.39	47	4.00	41.45	54.54	0.04	1
2-4-RTIC-SFD	TS2-2-4-A-2	26.10	96.24	91	44.73	29.95	25.32	0.81	1
2-4-RTIE-SFD	TS2-2-4-B-2	26.10	96.24	91	35.27	38.76	25.97	0.55	1
4-4-RTMA-SFD	TS2-4-4-A-2	26.10	97.08	15	84.47	10.25	5.27	5.44	1
4-4-RTMD-SFD	TS2-4-4-B-2	26.10	97.08	15	76.04	11.88	11.17	3.34	1
5-4-RTOD-SFD	TS2-5-4-A-2	26.10	96.54	37	79.60	12.32	8.07	3.90	1
5-4-RTOH-SFD	TS2-5-4-B-2	26.10	96.54	37	69.69	18.52	11.79	2.30	1
6-4-RTOF-SFD	TS2-6-4-A-2	26.10	96.31	65	47.73	23.33	28.95	0.91	1
6-4-RTOT-SFD	TS2-6-4-B-2	26.10	96.31	65	55.51	23.38	21.11	1.25	1
7-4-RTOW-SFD	TS2-7-4-A-2	26.10	96.20	130	0.85	49.08	50.07	0.01	1
7-4-RTOZ-SFD	TS2-7-4-B-2	26.10	96.20	130	0.70	39.58	59.71	0.01	1
1-1-ROD1-SFD	TS2-1-1-A-3	27.12	96.27	18	53.75	26.66	19.60	1.16	1
1-1-ROD4-SFD	TS2-1-1-B-3	27.12	96.27	18	54.04	24.30	21.66	1.18	1
2-1-ROD1-SFD	TS2-2-1-A-3	27.55	96.20	42	24.04	50.32	25.64	0.32	1
2-1-ROD1-SFD	TS2-2-1-B-3	27.55	96.20	42	22.90	54.66	22.75	0.30	1
3-1-ROFH-SFD	TS2-3-1-A-3	27.34	96.07	134	5.68	39.07	55.26	0.06	1
3-1-ROFK-SFD	TS2-3-1-B-3	27.34	96.07	134	4.08	47.74	48.17	0.04	1
4-1-ROHF-SFD	TS2-4-1-A-3	27.14	96.29	10	55.98	20.67	23.36	1.27	1
4-1-ROHH-SFD	TS2-4-1-B-3	27.14	96.29	10	49.17	31.33	19.50	0.97	1
5-1-ROTH-SFD	TS2-5-1-A-3	27.44	96.14	82	8.27	49.63	42.99	0.09	1
5-1-ROTY-SFD	TS2-5-1-B-3	27.44	96.14	82	6.08	46.25	47.67	0.06	1
6-1-ROPK-SFD	TS2-6-1-A-3	27.39	96.12	100	10.07	57.13	32.80	0.11	1
6-1-ROPN-SFD	TS2-6-1-B-3	27.39	96.12	100	13.73	55.45	30.82	0.15	1
1-2-RODM-SFD	TS2-1-2-A-3	27.40	96.59	22	13.45	56.42	30.13	0.15	1

	11	12	13	14	15	16	17	18
1-4-PTG7-SFD	TS2-1-4-1-2	0.74	4.07	3.06	-0.30	-1.25		?
1-4-PTHC-SFD	TS2-1-4-0-2	0.58	5.00	3.13	-0.01	-1.42		?
2-4-PTI7-SFD	TS2-2-4-A-2	1.64	7.11	2.24	-0.10	-0.51		?
2-4-PTIC-SFD	TS2-2-4-B-2	1.27	7.47	2.02	-0.18	-0.24		?
2-4-PTIH-SFD	TS2-2-4-C-2	0.76	7.03	1.94	-0.36	0.31		?
3-4-PTIC-SFD	TS2-3-4-A-2	1.18	5.45	2.80	0.18	-1.32		?
3-4-PTIF-SFD	TS2-3-4-B-2	1.40	5.77	2.76	0.02	-1.29		?
4-4-PTIA-SFD	TS2-4-4-A-2	1.94	3.36	1.82	1.14	4.07		?
4-4-PTID-SFD	TS2-4-4-C-2	1.06	3.04	2.30	0.83	1.38		?
5-4-PTID-SFD	TS2-5-4-A-2	1.53	3.42	2.21	0.94	2.26		?
5-4-PTIH-SFD	TS2-5-4-B-2	1.57	3.85	2.51	0.60	0.56		?
6-4-PTIC-SFD	TS2-6-4-A-2	1.01	5.34	3.12	0.15	-1.48		?
6-4-PTIT-SFD	TS2-6-4-B-2	1.11	5.12	2.60	0.38	-0.89		?
7-4-PTIP-SFD	TS2-7-4-A-2	0.98	7.04	1.77	-0.08	-1.03		?
7-4-PTIP-SFD	TS2-7-4-B-2	0.66	8.30	1.60	-0.20	-0.80		?
1-1-PPBI-SFD	TS2-1-1-A-3	1.36	5.19	2.54	0.36	-0.88		?
1-1-PPBI-SFD	TS2-1-1-B-3	1.12	5.22	2.62	0.36	-0.92		?
2-1-PPBI-SFD	TS2-2-1-A-3	1.96	6.31	2.22	0.14	-1.00		?
2-1-PPBI-SFD	TS2-2-1-B-3	2.39	6.03	2.22	0.25	-0.87		?
3-1-PPFH-SFD	TS2-3-1-A-3	0.71	7.04	2.00	-0.40	0.24		?
3-1-PPFK-SFD	TS2-3-1-B-3	0.90	7.71	1.95	-0.21	-0.47		?
4-1-PPHF-SFD	TS2-4-1-A-3	0.88	5.16	2.90	0.30	-1.16		?
4-1-PPHH-SFD	TS2-4-1-B-3	1.61	5.22	2.56	0.31	-0.95		?
5-1-PPIH-SFD	TS2-5-1-A-3	1.18	7.30	2.08	-0.14	-0.81		?
5-1-PPIX-SFD	TS2-5-1-B-3	0.97	7.47	2.14	-0.17	-0.98		?
6-1-PPKK-SFD	TS2-6-1-A-3	1.74	6.85	2.12	0.03	-0.98		?
6-1-PPKN-SFD	TS2-6-1-B-3	1.90	6.56	2.26	0.09	-1.08		?
1-2-PPOV-SFD	TS2-1-2-A-3	1.87	6.55	2.21	0.11	-1.12		?

1	2	3	4	5	6	7	8	9	10
1-2-000M-SFD	TS2-1-2-A-3	27.40	06.50	22	0.20	50.17	31.63	0.10	1
2-2-005M-SFD	TS2-2-2-A-3	27.30	06.45	40	6.28	67.49	26.23	0.07	1
2-2-005M-SFD	TS2-2-2-B-3	27.30	06.45	40	11.84	63.69	24.49	0.13	1
3-2-00V6-SFD	TS2-3-2-A-3	27.18	06.23	131	2.44	43.21	54.35	0.02	1
3-2-00V1-SFD	TS2-3-2-B-3	27.18	06.23	131	2.55	39.76	57.60	0.03	1
4-2-00Y4-SFD	TS2-4-2-A-3	27.34	06.50	34	3.86	68.12	28.02	0.04	1
4-2-00Y0-SFD	TS2-4-2-B-3	27.34	06.50	34	3.20	73.91	22.80	0.03	1
5-2-0071-SFD	TS2-5-2-A-3	27.24	06.36	78	2.21	55.95	41.84	0.02	1
5-2-0070-SFD	TS2-5-2-B-3	27.24	06.36	78	3.63	61.37	35.00	0.04	1
6-2-00RK-SFD	TS2-6-2-A-3	27.24	06.20	98	1.72	41.34	56.94	0.02	1
6-2-000M-SFD	TS2-6-2-B-3	27.24	06.20	98	0.00	39.02	60.98	0.00	1
1-3-00SU-SFD	TS2-1-3-A-3	26.58	07.11	25	2.10	72.98	24.84	0.02	1
1-3-0001-SFD	TS2-1-3-B-3	26.58	07.11	25	2.82	71.27	25.91	0.03	1
1-3-0000-SFD	TS2-1-3-C-3	26.58	07.11	25	1.56	66.70	31.74	0.02	1
2-3-00SV-SFD	TS2-2-3-A-3	26.58	06.48	65	1.55	65.70	32.76	0.02	1
2-3-0050-SFD	TS2-2-3-B-3	26.58	06.48	65	2.40	62.41	35.19	0.02	1
2-3-0050-SFD	TS2-2-3-C-3	26.58	06.48	65	1.26	72.38	26.36	0.01	1
2-3-0050-SFD	TS2-2-3-D-3	26.58	06.48	65	0.71	52.02	47.27	0.01	1
3-3-0061-SFD	TS2-3-3-A-3	26.58	06.33	106	0.44	56.99	42.57	0.00	1
3-3-00HV-SFD	TS2-3-3-B-3	26.58	06.33	106	0.80	48.74	50.46	0.01	1
3-3-00HY-SFD	TS2-3-3-C-3	26.58	06.33	106	0.00	48.29	51.71	0.00	1
4-3-00IX-SFD	TS2-4-3-A-3	26.58	07.20	15	73.10	15.63	11.18	2.73	1
4-3-00KA-SFD	TS2-4-3-B-3	26.58	07.20	15	76.00	13.14	9.06	3.33	1
5-3-00IM-SFD	TS2-5-3-A-3	26.58	07.02	40	2.85	60.70	36.45	0.03	1
5-3-00IO-SFD	TS2-5-3-B-3	26.58	07.02	40	1.77	41.96	56.27	0.02	1
6-3-00MD-SFD	TS2-6-3-A-3	26.58	06.30	125	0.90	48.83	50.37	0.01	1
6-3-00MC-SFD	TS2-6-3-B-3	26.58	06.30	125	1.33	41.27	57.39	0.01	1
1-4-0001-SFD	TS2-1-4-A-3	26.10	07.01	27	52.34	26.74	20.91	1.10	1
1-4-000Y-SFD	TS2-1-4-B-3	26.10	07.01	27	61.30	21.85	16.76	1.59	1
2-4-000X-SFD	TS2-2-4-A-3	26.10	06.39	47	2.30	51.74	45.96	0.02	1

	11	12	13	14	15	16	17	18
1-2-0000-SFD	TS2-1-2-0-3	1.87	6.66	2.10	0.11	-1.10		?
2-2-0050-SFD	TS2-2-2-A-3	2.57	6.47	2.07	0.25	-0.94		?
2-2-0050-SFD	TS2-2-2-0-3	2.60	6.23	2.14	0.20	-0.90		?
3-2-0050-SFD	TS2-3-2-A-3	0.90	7.00	1.70	-0.28	-0.14		?
3-2-0050-SFD	TS2-3-2-0-3	0.69	8.06	1.85	-0.33	-0.14		?
4-2-0050-SFD	TS2-4-2-A-3	2.43	6.55	2.00	0.23	-1.02		?
4-2-0050-SFD	TS2-4-2-0-3	2.24	6.23	2.00	0.37	-0.66		?
5-2-0071-SFD	TS2-5-2-A-3	1.34	7.48	1.38	-0.04	-0.90		?
5-2-0070-SFD	TS2-5-2-0-3	1.75	6.05	2.06	0.08	-1.18		?
6-2-0000-SFD	TS2-6-2-A-3	0.73	8.12	1.75	-0.26	-0.45		?
6-2-0000-SFD	TS2-6-2-0-3	0.64	8.40	1.28	-0.13	-0.90		?
1-3-0000-SFD	TS2-1-3-A-3	2.04	6.30	1.97	0.28	-0.74		?
1-3-0000-SFD	TS2-1-3-0-3	2.75	6.45	2.04	0.28	-0.89		?
1-3-0000-SFD	TS2-1-3-0-3	2.10	6.00	2.01	0.15	-1.08		?
2-3-0050-SFD	TS2-2-3-A-3	2.01	6.01	1.96	0.12	-1.00		?
2-3-0050-SFD	TS2-2-3-0-3	1.77	6.05	2.07	0.10	-1.25		?
2-3-0050-SFD	TS2-2-3-0-3	2.75	6.53	1.99	0.28	-0.92		?
2-3-0050-SFD	TS2-2-3-0-3	1.10	7.50	1.92	-0.09	-1.14		?
3-3-0050-SFD	TS2-3-3-A-3	1.34	7.63	1.73	0.01	-1.01		?
3-3-0050-SFD	TS2-3-3-0-3	0.07	7.90	1.31	-0.09	-1.07		?
3-3-0050-SFD	TS2-3-3-0-3	0.93	8.06	1.60	-0.06	-1.10		?
4-3-0050-SFD	TS2-4-3-A-3	1.40	4.55	2.04	0.82	1.37		?
4-3-0050-SFD	TS2-4-3-0-3	1.32	4.35	1.97	0.03	2.28		?
5-3-0050-SFD	TS2-5-3-A-3	1.67	7.05	2.07	0.06	-1.18		?
5-3-0050-SFD	TS2-5-3-0-3	0.75	7.06	1.98	-0.24	-0.88		?
6-3-0050-SFD	TS2-6-3-A-3	0.97	7.04	1.74	-0.10	-0.87		?
6-3-0050-SFD	TS2-6-3-0-3	0.72	8.14	1.70	-0.25	-0.50		?
1-4-0000-SFD	TS2-1-4-A-3	1.28	4.90	2.98	0.28	-1.08		?
1-4-0000-SFD	TS2-1-4-0-3	1.30	4.41	2.74	0.46	-0.58		?
2-4-0000-SFD	TS2-2-4-A-3	1.13	7.57	1.96	-0.16	-0.67		?

1	2	3	4	5	6	7	8	9	10
2-4-BODA-SFD	TSP-2-4-D-3	26.10	06.39	47	3.09	48.74	47.27	0.04	1
3-4-BSCY-SFD	TSP-3-4-A-3	26.10	06.24	91	48.02	26.64	25.34	0.92	1
3-4-BOTA-SFD	TSP-3-4-D-3	26.10	06.24	91	49.40	27.40	23.11	0.99	1
3-4-BOTH-SFD	TSP-3-4-C-3	26.10	06.24	91	60.97	19.36	19.66	1.56	1
3-4-BOTY-SFD	TSP-3-4-D-3	26.10	06.24	91	64.00	17.78	18.21	1.78	1
4-4-BOME-SFD	TSP-4-4-A-3	26.10	07.08	15	84.13	8.76	7.11	5.30	1
4-4-BOMH-SFD	TSP-4-4-D-3	26.10	07.08	15	79.80	12.69	8.43	3.74	1
5-4-BOMH-SFD	TSP-5-4-A-3	26.10	06.54	37	50.40	31.60	17.92	1.02	1
5-4-BOMY-SFD	TSP-5-4-D-3	26.10	06.54	37	37.01	35.00	27.98	0.59	1
6-4-BQYK-SFD	TSP-6-4-A-3	26.10	06.31	65	42.35	35.37	22.28	0.74	1
6-4-BQYN-SFD	TSP-6-4-D-3	26.10	06.31	65	49.46	27.79	31.76	0.68	1
7-4-BPAA-SFD	TSP-7-4-A-3	26.10	06.20	130	0.00	46.17	53.83	0.00	1
7-4-BPAD-SFD	TSP-7-4-E-3	26.10	06.20	130	0.00	46.23	50.77	0.00	1

	11	12	13	14	15	16	17	18
2-4-RADA-SEP	TS2-2-4-E-3	1.03	7.61	2.01	-0.24	-0.33		2
3-4-RSCX-SEP	TS2-3-4-A-3	1.05	5.26	2.99	0.16	-1.41		2
3-4-R TA-SEP	TS2-3-4-F-3	1.10	5.14	2.05	0.22	-1.31		2
3-4-RATD-SEP	TS2-3-4-C-3	0.99	4.62	2.90	0.39	-0.94		2
3-4-RQTY-SEP	TS2-3-4-F-3	0.98	4.41	2.35	0.43	-0.60		2
4-4-ROVE-SEP	TS2-4-4-I-3	1.23	3.40	1.98	1.04	3.76		2
4-4-ROVH-SEP	TS2-4-4-C-3	1.51	3.63	2.16	0.88	2.10		2
5-4-ROVH-SEP	TS2-5-4-A-3	1.76	4.70	2.72	0.35	-0.90		2
5-4-ROVY-SEP	TS2-5-4-F-3	1.25	5.57	2.94	0.10	-1.34		2
6-4-ROVK-SEP	TS2-6-4-A-3	1.50	5.30	2.76	0.10	-1.23		2
6-4-ROYN-SEP	TS2-6-4-D-3	0.88	5.01	3.01	0.05	-1.54		2
7-4-ROAA-SEP	TS2-7-4-A-3	0.86	8.00	1.70	-0.11	-1.04		2
7-4-ROAD-SEP	TS2-7-4-P-3	0.97	8.01	1.66	-0.05	-1.08		2

EXPLANATION FOR APPENDIX 6:

Trace Metals Content, Seasonal Benthic Sediment Samples

Column 1 - Sample number (U.T. Marine Science Institute numbering system)

Column 2 - Barium (ppm)

Column 3 - Cadmium (ppm)

Column 4 - Chromium (ppm)

Column 5 - Copper (ppm)

Column 6 - Iron (ppm)

Column 7 - Manganese (ppm)

Column 8 - Nickel (ppm)

Column 9 - Lead (ppm)

Column 10 - Vanadium (ppm)

Column 11 - Zinc (ppm)

Season I

		1	2	3	4	5	6	7	8	9	10	11
1/TTT	0017	145.5	0.08	26.2	6.5	10700	342	20.4	17.3	12.7	58.8	
1/TTT	0018	136.0	0.09	24.0	6.5	21100	353	19.7	15.4	19.1	65.8	
1/TTT	0019	142.0	0.09	29.7	6.0	21500	353	21.0	20.0	16.2	67.1	
1/TTT	0021	151.5	0.11	31.5	8.0	23200	392	25.6	21.3	23.0	74.8	
1/TTT	0022	128.2	0.08	25.0	7.5	22600	361	20.6	18.5	14.5	68.0	
2/TTT	0023	148.0	0.06	24.6	7.0	24000	465	20.9	23.5	23.0	74.8	
2/TTT	0024	60.0	0.07	24.9	6.8	22000	350	20.0	19.1	19.5	68.9	
2/TTT	0025	121.5	0.06	26.1	6.5	20500	400	22.0	22.0	17.0	70.2	
2/TTT	0026	70.2	0.05	22.6	5.7	19000	336	20.6	17.5	17.5	64.5	
2/TTT	0027	116.7	0.06	21.6	6.1	20500	375	20.2	19.5	18.1	64.3	
1/TV	0010	67.6	0.05	10.5	2.8	8100	151	6.7	10.0	6.4	26.3	
1/TV	0011	87.0	0.06	11.0	2.0	8900	186	9.0	7.3	7.2	26.7	
1/TV	0012	52.2	0.04	6.4	2.1	6900	147	5.3	7.3	8.1	19.1	
1/TV	0013	110.0	0.04	11.3	2.0	7000	162	7.0	9.8	6.5	26.7	
1/TV	0014	63.9	0.05	12.0	2.8	8000	149	7.3	8.2	6.2	22.4	
2/TV	0015	52.7	0.03	15.5	4.1	12100	317	11.3	12.7	9.2	26.7	
2/TV	0016	49.6	0.02	15.0	3.7	11900	246	12.6	10.0	12.4	33.1	
2/TV	0017	69.0	0.03	17.7	4.3	14200	382	14.6	13.7	11.8	39.2	
2/TV	0018	57.4	0.03	18.7	2.9	13100	448	12.5	11.3	11.7	36.3	
2/TV	0019	42.4	0.03	16.5	4.3	12400	366	11.7	13.3	13.0	38.1	
3/TV	0020	60.3	0.06	21.3	5.0	15800	245	15.6	15.6	20.7	47.3	
3/TV	0021	65.2	0.04	22.5	5.5	16900	329	19.0	16.8	16.3	46.8	
3/TV	0022	45.2	0.05	19.7	4.1	13500	445	14.5	12.3	13.1	37.4	
3/TV	0023	44.7	0.04	22.6	5.0	15900	303	17.8	8.9	20.4	48.6	
3/TV	0024	82.4	0.05	21.0	4.5	14200	324	17.9	12.4	14.6	44.7	

Season I

		1	2	3	4	5	6	7	8	9	10	11
4/TV	BCAN	85.3	0.04	10.7	2.5	9100	222	6.3	4.0	10.7	26.3	
4/TV	BCAN	25.6	0.02	5.7	1.2	4000	135	2.0	2.8	6.0	20.7	
4/TV	BCAY	42.2	0.03	7.2	1.9	5500	146	2.8	5.4	7.0	14.1	
4/TV	BCBA	63.0	0.03	6.6	2.0	4700	150	3.2	2.3	6.4	13.0	
4/TV	BCBC	57.0	0.02	8.9	1.7	5200	147	3.3	5.0	7.2	15.3	
5/TV	BCCI	77.1	0.05	24.5	5.6	17300	282	17.8	10.1	14.1	56.8	
5/TV	BCCO	90.7	0.05	21.5	5.3	16200	285	10.4	10.8	12.4	51.2	
5/TV	BCCP	81.0	0.04	21.5	5.4	16200	271	17.0	9.5	12.0	52.3	
5/TV	BCCU	84.0	0.09	26.2	6.1	18700	321	20.2	10.9	12.0	57.0	
5/TV	BCCT	89.4	0.07	25.0	6.3	18100	301	19.0	10.3	14.0	56.5	
6/TV	BCFH	35.5	0.05	15.4	3.7	11700	248	12.2	7.8	10.1	36.7	
6/TV	BCFY	44.2	0.04	14.1	3.6	11800	400	12.2	9.8	10.0	35.6	
6/TV	BCFN	39.1	0.04	16.9	3.5	11300	196	12.0	6.3	10.0	33.2	
6/TV	BCFO	29.7	0.03	15.3	3.5	10200	160	14.4	7.5	9.1	34.0	
6/TV	BCFK	42.5	0.04	17.4	3.7	11600	251	12.3	8.3	12.7	35.0	
7/TV	BCGD	46.0	0.07	31.1	7.0	22000	550	31.7	17.7	21.2	74.0	
7/TV	BCGG	45.6	0.07	29.3	7.3	23500	580	20.4	21.4	24.2	79.1	
7/TV	BCGI	42.9	0.07	32.8	8.4	24200	452	34.2	23.4	25.0	82.0	
7/TV	BCGV	67.0	0.07	32.0	7.6	23800	470	32.3	23.7	21.4	80.1	
7/TV	BCGK	64.0	0.06	31.3	7.8	25400	520	33.8	19.1	26.9	83.1	

Season II

		1	2	3	4	5	6	7	8	9	10	11
1/T	BQUB	27.5	0.05	10.6	4.2	16200	220	7.4	5.4	16.0	54.2	
1/T	BQUC	29.3	0.03	10.6	4.2	15200	202	7.1	4.4	14.4	47.3	
1/T	BQUT	110.7	0.03	21.0	4.4	17400	200	10.0	6.6	16.1	54.1	
2/T	BQYC	65.1	0.03	20.1	4.2	19500	222	0.1	6.0	14.7	55.6	
2/T	BQYE	63.0	0.04	26.3	4.4	19000	270	10.0	6.2	15.0	56.3	
2/T	BQYT	85.6	0.03	24.1	4.5	12800	262	10.9	5.0	14.4	52.6	
3/T	BQYU	45.4	0.00	31.6	4.2	22600	320	12.4	4.2	22.2	71.4	
3/T	BQYV	40.4	0.06	25.6	5.0	23300	400	12.4	5.4	22.7	75.0	
3/T	BQYW	52.5	0.00	31.5	5.4	23200	342	12.5	6.4	22.2	84.2	
4/T	BQYX	22.7	0.14	2.2	1.5	6420	144	2.7	2.0	6.2	20.0	
4/T	BQYH	70.5	0.07	17.0	4.1	13000	200	2.4	3.7	11.1	39.2	
4/T	BQYI	22.0	0.05	14.0	2.2	11500	234	5.2	2.7	10.0	33.5	
5/T	BQYJ	22.2	0.04	24.7	5.0	24000	325	14.1	6.0	17.6	72.0	
5/T	BQYK	56.2	0.04	25.2	5.7	24000	307	11.7	0.2	16.0	79.5	
5/T	BQYL	101.4	0.03	41.4	6.0	26000	306	12.0	9.6	19.2	72.7	
6/T	BQYM	44.2	0.03	22.0	4.5	16000	201	2.5	4.0	16.6	49.0	
6/T	BQYN	44.2	0.03	24.4	4.3	17100	217	2.6	5.6	14.1	51.1	
6/T	BQYO	52.4	0.10	22.6	4.0	16500	200	2.0	5.6	15.2	49.0	

Season II

		1	2	3	4	5	6	7	8	9	10	11
1/11	0401	80.2	0.03	25.4	4.0	10500	370	0.4	6.8	15.1	50.3	
1/11	0402	84.2	0.03	25.0	4.7	18700	350	0.7	6.7	14.4	51.2	
1/11	0403	84.4	0.04	25.2	5.6	10100	320	10.1	6.8	15.4	60.9	
2/11	0404	75.1	0.05	20.0	4.0	22300	347	0.6	7.6	17.1	61.3	
2/11	0405	75.0	0.04	24.9	5.1	10700	320	8.2	6.0	14.7	54.0	
2/11	0406	71.5	0.02	20.2	5.1	10700	306	10.7	5.8	15.1	65.1	
3/11	0407	44.4	0.06	36.2	6.1	26200	370	12.8	6.8	21.1	76.0	
3/11	0408	52.0	0.10	30.2	5.7	26700	360	13.2	9.0	24.7	75.6	
3/11	0409	40.1	0.04	30.5	6.5	25100	354	13.6	8.2	22.0	75.5	
4/11	0410	76.1	0.06	33.5	6.0	20100	365	10.8	9.5	17.1	62.5	
4/11	0411	73.2	0.05	32.1	5.7	19800	337	10.7	9.6	18.0	63.5	
4/11	0412	70.2	0.04	25.2	5.4	21100	336	11.4	7.8	15.8	68.4	
5/11	0413	62.5	0.05	30.4	5.0	23300	462	11.5	11.0	10.0	81.1	
5/11	0414	62.0	0.07	30.6	6.5	23100	375	12.5	12.0	23.0	78.5	
5/11	0415	65.1	0.05	36.2	5.8	26000	400	13.8	11.1	25.8	82.7	
6/11	0416	51.3	0.05	36.5	5.1	21500	354	12.2	7.1	10.0	66.1	
6/11	0417	51.8	0.04	40.4	6.2	22500	462	12.0	9.2	24.3	69.6	
6/11	0418	51.3	0.04	32.2	4.0	22100	400	12.4	7.8	19.6	65.5	

Season II

		1	2	3	4	5	6	7	8	9	10	11
1/111	LBVY	93.8	0.06	40.0	5.0	23100	303	11.6	10.0	10.0	67.6	
1/111	2454	81.4	0.04	23.9	5.8	21600	367	11.9	7.4	16.1	59.4	
1/111	2450	89.1	0.06	28.0	5.6	22000	360	11.6	9.1	15.9	80.8	
2/111	2454	77.1	0.04	31.8	5.0	22300	340	13.4	9.7	18.7	72.7	
2/111	2450	102.4	0.05	35.4	7.4	22900	445	12.4	9.2	20.6	67.9	
2/111	2450	87.2	0.09	24.0	5.4	22100	414	12.2	6.0	15.0	69.6	
2/111	PTAA	62.7	0.06	38.3	7.0	27300	713	14.6	13.1	24.0	83.4	
2/111	PTAB	51.0	0.05	37.3	6.2	23000	410	14.4	8.6	21.4	75.3	
2/111	PTAF	55.6	0.06	37.2	7.8	26400	566	13.2	9.0	20.9	84.3	
4/111	PTBY	61.7	0.04	12.5	2.5	2400	206	3.0	4.4	10.9	29.3	
4/111	PTC2	32.3	0.02	6.0	0.0	6000	205	2.8	2.4	4.4	24.3	
4/111	PTC4	35.3	0.02	0.4	2.0	8200	247	4.9	4.4	8.0	25.0	
5/111	PTD2	72.3	0.07	36.6	6.7	23300	420	13.3	9.4	10.8	76.8	
5/111	PTD1	70.2	0.07	34.4	6.5	23000	430	14.8	9.2	19.3	80.7	
5/111	PTD4	72.1	0.08	32.9	6.5	25900	424	13.3	11.8	18.2	82.2	
6/111	PTF1	44.4	0.07	30.5	6.9	26600	414	14.4	8.0	26.5	83.6	
6/111	PTF2	51.0	0.09	30.0	6.8	26100	466	14.6	8.0	25.9	85.8	
6/111	PTF4	48.2	0.07	37.6	7.2	27400	415	15.8	10.3	23.7	84.2	

Season II

		1	2	3	4	5	6	7	8	9	10	11
1/TV	BTGV	41.2	0.04	10.4	1.0	8100	200	4.7	2.7	9.2	19.0	
1/TV	BTWR	22.2	0.00	11.7	2.1	8900	152	4.4	3.0	7.7	22.2	
1/TV	BTWB	44.7	0.02	11.0	1.0	8300	179	3.5	2.5	8.4	23.1	
2/TV	BTIV	54.4	0.05	21.2	5.4	22200	454	12.6	7.0	15.8	64.7	
2/TV	BTJQ	34.8	0.05	22.0	6.0	22700	375	12.0	8.4	15.8	65.8	
2/TV	BTJQ	49.1	0.03	22.1	5.7	24200	425	11.0	6.8	16.3	81.4	
3/TV	BTJZ	32.5	0.04	22.4	4.1	15500	344	8.4	4.7	15.4	42.0	
3/TV	BTJE	31.5	0.03	22.8	3.8	15300	240	8.4	4.7	16.6	42.0	
3/TV	BTJG	24.0	0.05	26.2	3.0	16500	320	8.1	4.0	17.5	44.4	
4/TV	BTJZ	20.2	0.03	6.2	1.1	5100	141	1.1	2.1	0.1	12.4	
4/TV	BTJG	24.2	0.03	7.5	1.1	5800	173	1.8	2.1	9.8	14.1	
4/TV	BTJE	21.2	0.03	6.9	0.7	5800	166	1.7	1.6	7.3	15.5	
5/TV	BTJQ	45.4	0.04	16.6	3.4	11900	276	6.1	5.3	11.8	32.4	
5/TV	BTJG	42.0	0.03	15.5	2.4	10300	183	4.0	3.5	11.4	27.8	
5/TV	BTJQ	47.5	0.02	18.1	3.2	12000	226	7.3	3.2	11.2	31.0	
6/TV	BTJG	28.4	0.03	21.0	3.2	13700	226	6.7	4.4	12.8	37.4	
6/TV	BTJH	32.0	0.03	24.4	4.2	15800	203	7.8	4.8	15.0	41.6	
6/TV	BTJG	29.2	0.05	22.6	4.0	15800	283	4.3	4.0	14.1	47.2	
7/TV	BTJW	51.1	0.05	27.5	5.6	26400	410	12.0	8.8	17.9	73.8	
7/TV	BTJY	51.0	0.05	30.2	5.0	24700	460	12.5	9.0	17.5	71.6	
7/TV	BTJA	61.1	0.05	32.4	6.5	27200	540	15.6	8.4	18.7	82.8	

Season III

1/11	8001	74.2	0.03	23.5	4.0	17800	351	13.9	9.5	10.7	53.0
1/11	8000	52.0	0.03	16.2	3.7	14600	250	10.8	5.5	4.1	51.8
1/11	8000	90.4	0.08	23.7	4.6	17400	320	17.0	4.0	10.3	54.3
2/11	8050	52.6	0.03	35.2	4.0	20300	275	16.8	9.6	16.3	58.1
2/11	8050	30.5	0.02	34.5	4.8	19100	258	15.0	5.3	15.0	55.1
2/11	8052	65.6	0.04	20.4	3.0	16700	273	15.7	8.1	9.6	54.4
3/11	8056	24.4	0.05	34.0	4.0	21300	354	21.4	11.1	16.3	72.7
3/11	8057	20.7	0.05	32.1	6.1	19500	312	21.7	10.3	14.2	70.9
3/11	8058	36.2	0.11	28.1	6.3	22800	352	24.7	10.5	14.7	73.7
4/11	8051	52.1	0.03	25.2	5.0	19000	270	10.7	10.8	14.4	57.1
4/11	8050	70.9	0.04	33.9	5.7	19100	285	10.7	10.7	13.9	73.7
5/11	8050	71.1	0.08	21.2	4.8	19800	298	21.0	9.7	13.5	64.1
5/11	8078	42.2	0.04	40.7	6.8	21400	370	21.4	13.0	14.6	69.4
5/11	8078	26.4	0.04	29.7	6.0	19600	200	10.3	9.7	14.8	79.9
5/11	8070	51.9	0.09	28.3	5.0	24700	316	23.8	11.5	17.3	79.3
6/11	8041	39.8	0.05	37.3	6.1	23300	327	24.7	13.3	17.7	79.4
6/11	8052	42.0	0.05	33.4	6.6	20500	337	23.6	13.4	15.9	72.5
6/11	8000	27.3	0.12	39.5	6.6	27200	313	30.3	12.5	19.8	87.2

Season III

		1	2	3	4	5	6	7	8	9	10	11
1/III	B0DK	74.1	0.05	24.2	6.1	20200	313	17.6	6.9	11.4	72.6	
1/III	B0DN	61.0	0.07	36.0	6.5	22500	332	18.2	9.5	12.1	67.3	
1/III	B0DD	70.4	0.11	30.7	5.9	19700	302	21.2	10.1	14.1	66.5	
2/III	B0EO	57.7	0.04	40.7	6.5	23700	293	10.6	6.6	12.0	67.2	
2/III	B0EU	45.6	0.05	36.8	5.1	22300	285	10.1	7.9	14.0	76.3	
2/III	B0ET	30.2	0.13	42.0	5.8	20700	270	23.4	10.2	15.4	68.0	
3/III	B0HU	42.7	0.06	47.0	6.0	26600	308	23.0	11.1	15.3	76.1	
3/III	B0HT	20.7	0.06	51.5	6.6	26600	330	22.6	8.0	20.4	72.8	
3/III	B0H7	30.3	0.00	55.1	6.8	25600	351	27.0	11.6	10.9	78.4	
4/III	B0L4	21.7	0.01	0.7	1.4	5000	145	2.1	1.0	5.2	26.2	
4/III	B0L7	22.3	0.01	0.5	1.7	6200	192	2.3	2.2	3.9	31.0	
4/III	B0K0	20.4	0.07	0.2	1.4	5900	178	3.0	2.0	6.3	26.8	
5/III	B0L4	42.5	0.07	41.2	7.4	22200	330	21.1	10.5	13.2	73.5	
5/III	B0L8	50.1	0.05	46.1	7.9	24500	403	21.6	11.0	13.7	73.3	
5/III	B0L9	62.0	0.13	45.1	6.5	22600	366	26.0	10.8	13.3	70.6	
6/III	B0M0	24.0	0.06	48.4	6.8	25000	365	23.0	7.6	17.1	79.3	
6/III	B0NE	36.6	0.06	40.2	7.3	26200	418	22.2	9.8	18.4	77.1	
6/III	B0M4	47.4	0.00	51.0	6.7	25100	362	28.5	11.6	19.8	75.4	

1/III B0DK 74.1 0.05 24.2 6.1 20200 313 17.6 6.9 11.4 72.6
 1/III B0DN 61.0 0.07 36.0 6.5 22500 332 18.2 9.5 12.1 67.3
 1/III B0DD 70.4 0.11 30.7 5.9 19700 302 21.2 10.1 14.1 66.5
 2/III B0EO 57.7 0.04 40.7 6.5 23700 293 10.6 6.6 12.0 67.2
 2/III B0EU 45.6 0.05 36.8 5.1 22300 285 10.1 7.9 14.0 76.3
 2/III B0ET 30.2 0.13 42.0 5.8 20700 270 23.4 10.2 15.4 68.0
 3/III B0HU 42.7 0.06 47.0 6.0 26600 308 23.0 11.1 15.3 76.1
 3/III B0HT 20.7 0.06 51.5 6.6 26600 330 22.6 8.0 20.4 72.8
 3/III B0H7 30.3 0.00 55.1 6.8 25600 351 27.0 11.6 10.9 78.4
 4/III B0L4 21.7 0.01 0.7 1.4 5000 145 2.1 1.0 5.2 26.2
 4/III B0L7 22.3 0.01 0.5 1.7 6200 192 2.3 2.2 3.9 31.0
 4/III B0K0 20.4 0.07 0.2 1.4 5900 178 3.0 2.0 6.3 26.8
 5/III B0L4 42.5 0.07 41.2 7.4 22200 330 21.1 10.5 13.2 73.5
 5/III B0L8 50.1 0.05 46.1 7.9 24500 403 21.6 11.0 13.7 73.3
 5/III B0L9 62.0 0.13 45.1 6.5 22600 366 26.0 10.8 13.3 70.6
 6/III B0M0 24.0 0.06 48.4 6.8 25000 365 23.0 7.6 17.1 79.3
 6/III B0NE 36.6 0.06 40.2 7.3 26200 418 22.2 9.8 18.4 77.1
 6/III B0M4 47.4 0.00 51.0 6.7 25100 362 28.5 11.6 19.8 75.4

Season III

		1	2	3	4	5	6	7	8	9	10	11
1/TV	240T	26.0	0.01	13.4	2.5	6200	112	2.3	3.0	7.2	34.0	
1/TV	4000	24.5	0.02	0.7	2.4	7400	112	3.3	3.7	7.0	34.3	
1/TV	500V	54.2	0.08	14.1	2.1	8100	120	5.9	3.7	8.4	29.4	
2/TV	000W	30.0	0.04	41.0	5.5	21100	280	10.4	9.5	13.4	70.1	
2/TV	000Z	47.6	0.04	20.0	5.6	10000	1011	17.6	13.3	13.8	67.0	
2/TV	40000	45.7	0.00	30.1	5.0	20500	200	10.9	10.4	14.6	68.3	
2/TV	005Z	20.7	0.04	24.4	5.0	16600	253	14.5	7.9	14.8	54.3	
2/TV	00TC	10.2	0.04	20.7	4.4	14900	232	11.8	6.8	11.4	49.3	
2/TV	00TE	27.0	0.05	24.2	4.2	16200	243	16.0	8.6	15.3	53.5	
4/TV	00V0	12.4	0.02	6.1	1.4	4700	112	1.2	1.0	7.4	15.5	
4/TV	00V6	10.7	0.02	5.3	1.6	5200	113	1.6	2.6	5.5	19.8	
4/TV	00VT	25.0	0.03	4.8	1.0	4400	102	1.7	2.7	7.4	14.9	
5/TV	00WT	39.0	0.04	23.2	4.5	13000	104	12.5	5.2	0.3	45.4	
5/TV	00WY	40.7	0.06	26.0	5.3	10700	265	15.8	7.6	15.3	56.1	
5/TV	00WV	45.6	0.06	24.0	4.4	14900	214	16.5	8.1	8.7	47.7	
6/TV	00Y1	23.5	0.03	31.3	3.8	14100	212	12.7	5.5	12.9	44.1	
6/TV	00Y4	17.5	0.03	27.7	4.0	13900	183	10.6	5.2	11.4	43.0	
6/TV	00Y0	20.4	0.04	22.4	3.4	12500	103	12.5	6.8	11.7	41.8	
7/TV	00Z7	37.7	0.05	42.9	7.0	28000	305	26.0	10.9	22.7	76.0	
7/TV	00AC	30.8	0.05	37.1	8.0	27400	406	26.3	10.4	20.0	74.3	
7/TV	00AF	41.5	0.08	33.7	6.0	24000	301	27.0	12.7	16.4	68.6	

EXPLANATION FOR APPENDIX 7:

Rates of Sedimentation (1976 Study)

10
11
12
13
14
15
16
17
18
19
20
21
22
23
24
25
26
27
28
29
30
31
32
33
34
35
36
37
38
39
40
41
42
43
44
45
46
47
48
49
50
51
52
53
54
55
56
57
58
59
60
61
62
63
64
65
66
67
68
69
70
71
72
73
74
75
76
77
78
79
80
81
82
83
84
85
86
87
88
89
90
91
92
93
94
95
96
97
98
99
100

RATES OF SEDIMENTATION

CORE	LAT	LONG	TYPE	RIC	RATE	REMARKS
5	29 10	96 02	20X		.45	
9	29 10	96 23	20C	10	1.92	
10	29 10	96 23	20Y	NA	0.00	
16	27 59	96 05	G	95	1.94	
21	23 00	96 20	20C	97	4.41	
23A	26 04	97 05	G	NA	1.88	TOP 30CM APPEARS TO HAVE CONSTANT PH-210
27	27 55	96 44	20Y	00	.97	TOP 5CM SAND LAYER
32	27 56	96 20	20Y	10	1.42	
42	27 50	96 25	20Y	7	1.93	
45	27 50	96 53	20X	00	0.00	
57	27 46	96 00	G	NA	1.90	
60	27 49	96 12	20Y	2	.99	
62	27 41	96 17	G	NA	3.32	
64	27 49	96 29	20C	NA	7.39	
70	27 35	96 52	20Y	NA	2.91	
75	27 46	96 47	G	NA	3.73	
87	27 33	96 57	G	NA	0.14	
106	27 24	96 44	20X	NA	3.45	S&P TOOTH PATTERN DUE TO SAND LAYERS
115	27 19	96 24	20Y	NA	0.02	
120	27 18	96 47	20Y	NA	1.39	TOP SAND LAYER
127	27 13	97 05	20Y	NA	0.00	
137	27 09	96 24	20C	NA	.56	

283

RATES OF SEDIMENTATION

CORE LAT LONG TYPE RIO RATE REMARKS

137A	27 08 96	24	G	NA	.50	
151	27 03 96	43	G	13	1.42	
155	26 57 96	27	HOX	NA	.03	
156	26 57 96	33	HOX	NA	0.00	- disturbed
157	26 57 96	39	HOX	NA	0.03	
160	26 58 96	47	HOX	NA	0.00	- disturbed
164	26 58 97	02	G	NA	2.40	
171	26 52 96	48	HOX	NA	0.00	- disturbed
174	26 52 96	36	HOX	NA	0.54	
176	26 47 96	27	HOX	NA	.03	
179	26 46 96	41	HOX	NA	.03	
185	26 47 97	08	HOX	NA	0.00	
191	26 42 96	39	HOX	NA	0.03	
193	26 41 96	27	HOX	NA	0.00	
199	26 37 96	51	G	NA	1.12	
203	26 32 97	05	G	NA	0.00	
206	26 31 96	54	G	4	1.37	
217	26 26 96	31	G	2	2.04	
235	26 16 96	21	G	5	3.61	
238	26 15 96	34	G	3	2.66	
243	26 16 96	51	HOX	NA	0.00	
249	26 10 96	48	G	NA	2.71	

EXPLANATION FOR APPENDIX 8:

27^c Geochemical Anomaly

Column 1 - Sample number (at one cm intervals below the top 2 cm)

Column 2 - Copper, in ppm

Column 3 - Manganese, in ppm

Column 4 - Nickel, in ppm

Column 5 - Zinc, in ppm

Column 6 - Values for excess ²¹⁰Po in dpm/g

SAMPLE NUMBER	DDM CU	DDM FN	DDM NT	DDM 7N	²¹⁰ Po
SC1					
0-2	0.0	261	10.2	75.5	4.12
2-3	0.0	257	10.7	75.5	3.42
3-4	0.3	260	17.7	79.4	3.03
4-5	0.0	205	10.1	73.1	3.63
5-6	0.6	270	18.0	73.1	3.68
6-7	0.3	242	18.7	77.0	3.82
7-8	0.1	201	10.0	76.9	3.44
8-9	0.6	202	10.6	78.9	1.37
9-10	0.6	288	20.6	80.2	3.56
10-11	0.2	276	18.0	77.8	3.15
11-12	0.4	275	10.2	79.0	2.66
12-13	0.8	266	18.0	77.7	2.67
13-14	6.0	265	17.0	73.4	2.22
14-15	6.7	231	17.7	68.5	2.02
15-16	6.3	231	10.6	68.2	1.78
16-17	6.3	224	14.6	63.2	1.78
17-18	6.1	237	15.5	64.1	2.15
18-19	6.0	210	15.0	60.6	2.18
19-20	5.3	213	13.4	57.5	2.00

SAMPLE NUMBER	DDM CM	DDM 4M	DDM M1	DDM 7N	²¹⁰ Po
SC2					
0-2	0.0	375	22.4	93.4	4.27
2-2	0.2	350	22.2	93.2	4.44
3-4	1.1	350	21.0	95.8	5.00
4-5	0.6	370	22.2	96.4	5.08
5-6	7.0	371	20.2	85.5	4.21
6-7	1.6	304	15.4	96.2	3.14
7-8	0.5	340	27.1	83.6	4.07
8-9	1.4	306	20.1	92.0	4.14
9-10	0.2	322	22.2	93.5	4.76
10-11	0.1	360	20.4	80.5	5.24
11-12	0.2	317	21.0	75.0	5.20
12-13	10.0	320	16.7	77.1	5.11
13-14	7.0	310	20.8	71.8	4.20
14-15	1.2	313	10.3	70.1	3.26
15-16	0.2	326	25.1	78.0	2.79
16-17	0.6	324	18.0	92.1	2.37
17-18	1.6	320	14.4	81.4	2.20
19-20	7.4	325	22.3	41.6	1.01
10-20	0.1	326	27.2	48.1	1.41

SAMPLE NUMBER	PPM CU	PPM ZN	PPM NI	PPM 7N	²¹⁰ Po
SC6					
0-2	10.6	321	25.7	84.7	6.00
2-2	0.0	327	22.7	90.1	5.63
3-4	10.6	335	20.5	46.9	6.01
4-5	11.2	326	22.5	93.7	6.84
5-6	10.7	357	21.3	99.2	4.80
6-7	11.5	323	20.4	47.7	4.56
7-8	11.6	313	22.3	90.6	3.67
8-9	12.0	296	22.0	94.6	4.25
9-10	11.0	305	22.6	95.6	4.81
10-11	12.1	306	22.5	92.6	2.88
11-12	11.6	288	21.1	89.6	2.94
12-13	12.2	295	22.6	91.4	4.15
13-14	11.2	343	23.2	95.6	5.07
14-15	11.0	352	20.8	93.4	4.53
15-16	10.6	501	21.4	87.5	6.16
16-17	10.7	526	20.8	27.1	8.82
17-18	10.3	492	22.0	86.9	5.51
18-19	10.4	476	21.4	95.5	7.41
19-20	10.2	515	22.4	100.1	6.52

SAMPLE NUMBERS	DDM CU	DDM LM	DDM MT	DDM 7W	210 Po
0-2	0.6	347	22.5	20.1	3.14
2-3	0.5	352	22.9	20.7	3.30
3-4	10.1	351	22.7	23.5	2.09
4-5	0.4	347	27.1	24.5	2.10
5-6	0.1	313	20.7	22.1	1.88
6-7	4.2	324	10.2	26.6	1.46
7-8	7.6	324	22.2	24.1	.71
8-9	4.6	341	20.5	21.0	.71
9-10	0.0	337	21.5	22.2	.32
10-11	2.4	356	21.2	24.4	.02
11-12	4.5	360	22.5	25.0	.10
12-13	4.4	372	24.2	26.6	.21
13-14	0.0	351	20.1	22.0	.00
14-15	4.1	352	22.0	20.6	.00
15-16	7.5	360	22.5	20.5	.00
16-17	2.1	377	24.2	21.9	.00
17-18	4.0	372	22.8	22.5	.00
18-19	4.7	372	19.0	22.6	.00
19-20	7.9	381	21.6	20.2	.00

SAMPLE NUMBER	DDM CU	DDM ME	DDM MT	DDM 7N	^{210}Po
SC6					
1-2	9.6	322	21.4	96.0	2.87
2-3	8.7	405	21.0	70.4	2.53
3-4	7.7	415	21.7	44.7	4.30
4-5	8.1	404	23.1	84.0	4.18
5-6	8.4	393	21.0	70.5	4.67
6-7	8.6	396	20.7	84.1	5.09
7-8	7.5	386	18.0	72.7	4.57
8-9	8.0	340	21.7	70.0	5.14
9-10	8.3	401	22.7	82.8	4.00
10-11	8.3	300	24.5	86.2	4.42
11-12	8.6	410	21.0	84.0	2.39
12-13	8.6	402	23.1	82.8	2.40
13-14	8.0	393	27.3	80.6	4.09
14-15	8.1	428	23.1	80.5	2.93
15-16	8.3	460	20.0	90.3	4.48
16-17	7.3	424	25.1	75.5	4.70
17-18	8.0	422	23.4	83.2	6.13
18-19	8.5	407	23.5	82.7	5.84
19-20	8.1	411	24.3	84.7	4.84

SAMPLE NUMBER	DDM CU	DDM MM	DDM MI	DDM 7N	210Po
CC7					
0-2	8.2	407	21.2	91.1	6.47
2-3	8.0	360	19.7	82.6	5.89
3-4	9.7	428	19.7	83.0	4.44
4-5	9.2	421	19.0	81.5	5.24
5-6	4.6	452	19.1	78.8	3.69
6-7	7.9	403	20.0	83.6	3.08
7-8	8.2	500	20.7	77.6	2.82
8-9	4.8	512	18.6	82.6	1.14
9-10	7.0	432	13.1	76.0	1.37
10-11	0.1	478	22.7	43.2	1.32
11-12	0.5	407	19.0	82.0	1.54
12-13	0.1	430	20.6	94.7	1.00
13-14	7.0	487	22.1	91.9	1.86
14-15	0.3	440	22.4	86.3	.37
15-16	8.0	447	22.4	81.4	.38
16-17	8.5	425	24.7	80.9	1.57
17-18	8.8	432	23.6	78.4	.77
18-19	8.6	419	20.9	81.6	.51
19-20	0.1	400	22.4	42.7	.00

SAMPLE NUMBER	DDM CI	DDM MIN	DPM MI	DDM IN	210Po
5-2	0.0	354	22.0	74.6	.00
2-3	0.3	364	20.2	85.4	3.28
3-4	0.6	365	19.4	74.8	2.00
4-5	0.8	342	19.7	76.0	2.54
5-6	0.9	305	21.3	82.9	2.73
6-7	0.4	174	10.6	40.2	2.45
7-8	10.0	300	21.0	84.0	2.25
8-9	0.1	342	22.3	70.0	1.09
9-10	0.6	304	21.6	74.4	1.50
10-11	0.5	347	25.1	82.0	1.07
11-12	0.6	370	21.0	81.7	.80
12-13	0.0	347	22.5	70.0	.29
13-14	0.1	321	20.5	84.4	.17
14-15	0.2	322	21.7	80.2	.00
15-16	0.7	345	21.4	81.1	.00
16-17	0.6	305	22.0	82.5	.00
17-18	0.4	347	21.3	76.0	.00
18-19	0.6	300	22.5	81.5	.00
19-20	0.7	407	26.9	80.0	.00

CAMMIE NUMBER	DDM CU	DDM DN	DDM MT	DDM ZN	210Po
0-0					
0-2	8.5	222	25.3	126.7	7.59
2-2	7.3	250	20.6	78.7	6.36
3-4	7.7	276	20.0	97.7	6.40
4-5	6.0	262	22.7	75.1	6.51
4-6	7.5	240	23.9	90.2	5.70
6-7	7.4	242	23.1	112.3	5.50
7-4	8.0	254	22.5	91.4	5.33
8-3	8.1	203	24.7	117.5	4.43
8-10	8.3	273	28.0	113.9	3.00
10-11	7.4	250	26.0	90.7	3.53
11-12	4.0	277	22.5	80.0	2.86
12-13	7.5	276	26.2	42.8	1.63
13-16	8.7	277	25.5	40.5	1.62
14-15	7.7	279	22.2	132.2	1.63
15-16	7.4	244	26.6	86.9	.70
16-17	7.2	407	20.3	124.8	.58
17-18	8.0	206	22.7	98.2	.72
18-19	4.5	270	34.5	24.5	.00
19-20	7.7	225	28.2	85.9	1.22

SAMPLE NUMBER	DDM CU	DDM MN	DDM HT	DDM 7N	²¹⁰ Po
SC11					
0-2	7.6	308	21.0	73.6	6.65
2-3	7.8	413	10.2	40.2	.00
3-4	7.1	352	18.5	60.7	5.70
4-5	7.7	458	21.2	76.0	6.02
5-6	7.2	344	20.2	48.6	4.86
6-7	8.1	342	20.6	77.7	5.72
7-8	8.6	357	21.8	70.6	2.60
7-9	7.1	359	20.8	73.4	1.18
9-10	6.6	361	10.8	67.2	1.44
10-11	7.0	306	10.4	75.8	1.05
11-12	7.7	401	21.5	70.6	.70
12-13	7.6	423	26.2	78.6	.00
13-14	7.2	406	17.0	72.6	.00
14-15	7.1	400	20.1	106.4	.00
15-16	8.0	450	24.3	77.1	.00
16-17	7.8	424	21.6	78.2	.00
17-18	6.3	425	20.5	73.4	.00
18-19	6.6	431	20.0	73.0	.00
19-20	7.0	423	23.7	80.2	.00

SAMPLE NUMBER	DDM	DDV	DDM	DDM	210Po
	CU	PN	NI	7N	
SC12					
0-2	8.7	333	17.1	68.0	1.80
2-3	6.6	265	11.0	54.0	.01
3-4	6.5	266	11.5	55.0	.43
4-5	0.2	304	15.4	64.2	1.50
5-6	0.5	326	17.6	72.2	1.65
6-7	10.3	295	15.8	74.0	1.62
7-8	0.7	325	16.0	60.6	.70
8-9	0.2	345	10.5	68.5	.63
9-10	10.6	356	18.4	74.0	.53
10-11	0.6	355	20.6	82.2	.34
11-12	8.7	317	14.1	58.4	.08
12-13	5.6	300	14.8	70.0	.00
13-14	7.6	360	16.9	71.7	.00
14-15	7.3	321	10.2	62.0	.00
15-16	7.1	312	13.7	61.0	.00
16-17	7.4	284	13.1	68.4	.00
17-18	7.5	317	15.7	60.1	.00
18-19	8.0	263	17.8	64.3	.00
19-20	7.1	295	14.1	62.8	.00

SAMPLE NUMBER	DDM CU	DDM LN	DDM MT	DDM 7N	²¹⁰ Po
0010					
0-2	8.0	362	17.5	63.1	2.70
2-3	4.4	351	17.0	63.1	2.01
3-4	11.5	336	24.5	55.6	1.82
4-5	5.0	324	15.4	55.0	2.00
5-6	9.0	320	15.4	54.2	1.91
6-7	8.0	320	16.0	54.3	1.19
7-8	0.7	342	18.7	70.0	1.07
8-9	0.3	314	19.4	70.2	.82
9-10	0.6	346	20.9	64.7	.53
10-11	0.6	345	19.6	67.0	.97
11-12	8.6	348	19.4	64.7	.97
12-13	8.4	360	20.0	65.2	.80
13-14	21.7	352	26.9	62.4	1.03
14-15	8.4	347	15.4	65.4	.63
15-16	8.4	345	17.4	60.4	.40
16-17	7.8	311	16.4	63.1	.25
17-18	7.6	332	16.7	61.6	.00
18-19	7.4	329	16.8	62.0	.00
19-20	7.2	334	16.6	66.0	.00

SAMPLE NUMBER	DDM CII	DDM MIN	DDM NT	DDM 7NI	²¹⁰ Po
SC14					
0-2	11.0	246	22.0	70.0	1.30
2-2	0.1	242	20.2	65.6	.05
3-4	7.7	224	15.3	60.4	.00
4-5	5.2	171	12.7	45.7	.37
5-6	7.5	217	15.9	57.1	1.53
6-7	7.5	212	20.6	60.7	1.57
7-8	8.1	213	17.6	65.2	.50
8-9	0.5	222	22.6	60.3	1.00
9-10	0.6	232	20.7	74.2	.51
10-11	0.7	240	24.2	78.2	.67
11-12	10.0	243	23.8	78.8	.35
12-13	11.3	246	26.3	78.0	.14
13-14	0.8	241	22.6	73.5	.22
14-15	0.2	242	19.7	73.4	.12
15-16	8.2	246	20.6	67.1	.00
16-17	8.1	240	18.0	63.3	.00
17-18	6.6	210	15.9	53.4	.00
18-19	6.0	215	15.1	55.8	.00
19-20	5.0	213	12.6	55.7	.00

SAMPLE NUMBER	DDM CU	DDM IN	DDM NI	DDM ZN	210 _{PO}
SC15					
0-2	0.0	301	10.0	75.3	2.80
2-3	8.7	376	10.2	67.4	2.75
3-4	10.1	376	10.0	70.8	2.06
4-5	10.0	373	10.1	76.0	1.65
5-6	0.2	350	10.1	68.3	1.71
6-7	8.6	340	10.6	64.0	1.27
7-8	0.2	310	10.1	50.7	1.26
9-0	7.5	316	15.6	61.0	1.35
0-10	10.9	320	17.8	65.7	1.24
10-11	11.6	312	17.5	66.8	1.17
11-12	8.6	309	20.2	65.8	1.12
12-13	0.3	305	10.4	68.4	1.47
13-14	8.7	303	10.8	70.4	1.28
14-15	0.0	312	17.9	60.5	1.24
15-16	8.3	326	16.7	63.2	1.31
16-17	0.5	322	17.0	70.9	1.18
17-18	0.1	323	10.1	66.2	.85
18-19	0.0	319	10.8	70.4	.54
19-20	0.3	272	10.5	68.4	.58

SAMUI F MUMACO	DDM CI	DDM MN	DDM NI	DDM 7N	210Po
SC16					
1-2	7.1	351	20.4	77.6	1.42
2-3	6.0	334	22.4	127.1	1.35
3-4	6.5	315	21.5	87.6	1.40
4-5	7.4	308	23.6	95.5	1.66
5-6	6.0	273	19.4	77.5	1.45
6-7	0.1	308	21.7	73.0	1.56
7-8	7.0	304	22.5	75.0	1.53
8-9	7.5	300	18.1	92.0	1.86
9-10	8.3	306	20.5	88.0	.00
10-11	6.0	286	22.3	125.0	.55
11-12	6.6	282	19.5	64.4	.37
12-13	5.1	260	19.0	64.2	.01
13-14	4.5	266	17.8	58.5	.00
14-15	5.3	287	16.5	61.8	.00
15-16	5.8	304	18.0	80.3	.00
16-17	5.0	282	18.2	72.3	.00
17-18	5.0	289	19.7	98.1	.00
18-19	4.4	288	15.3	60.5	.00
19-20	5.2	284	20.3	103.1	.00
20-21	5.4	282	14.5	64.4	.00

CANDLE NUMBER	DDM CI	DDM 7N	DDM NT	DDM 7N	210Po
SC17					
1-2	0.6	370	19.4	76.7	2.72
2-3	2.5	370	14.3	78.5	2.42
3-4	7.6	360	14.8	79.7	2.20
4-5	8.4	373	15.2	70.6	2.08
5-6	8.6	370	15.2	72.6	1.51
6-7	0.5	361	15.6	74.2	1.04
7-8	0.2	331	18.9	79.4	1.61
8-9	8.4	312	15.4	83.1	1.71
9-10	10.3	294	18.0	82.0	1.57
10-11	6.0	291	18.0	76.4	.80
11-12	7.5	295	16.3	73.9	1.40
12-13	8.4	297	16.4	78.0	1.14
13-14	6.0	282	14.0	55.7	.86
14-15	4.8	236	12.4	52.6	.15
15-16	7.8	296	16.1	60.5	.17
16-17	7.4	284	12.6	67.2	.17
17-18	7.6	301	17.2	69.4	.62
18-19	8.4	306	17.3	74.0	.72
19-20	8.4	296	22.8	69.8	.52

SAMPLE NUMBER	DDC CIN	DDM MIN	DDH HT	DDH ZN	²¹⁰ Po
SC27					
0-2	0.4	241	10.3	77.5	4.20
2-3	0.0	260	21.3	93.1	4.30
3-4	7.7	263	10.4	82.5	2.50
4-5	6.0	258	17.0	73.1	2.60
5-6	6.3	240	16.0	73.3	1.67
6-7	7.6	272	20.7	73.8	1.58
7-8	7.2	205	17.0	74.8	2.45
9-9	7.0	202	10.2	83.7	2.04
9-10	7.0	207	22.6	92.4	1.80
10-11	0.7	310	20.0	84.0	1.67
11-12	0.7	320	23.1	97.4	.72
12-13	0.2	326	23.7	70.2	1.11
13-14	0.1	325	22.6	84.7	.26
14-15	0.4	345	22.0	86.1	.53
15-16	7.7	359	21.8	83.2	.63
16-17	0.5	352	25.8	86.6	.57
17-18	7.7	361	10.8	82.9	.34
18-19	0.6	353	30.0	87.9	.79
19-20	7.5	373	20.3	80.6	.26

SAMPLE NUMBER	DDM CM	DDM IN	DDM MT	DDM 7M	²¹⁰ Po
SC2R					
0-2	8.0	346	19.5	73.6	.00
2-3	7.7	367	19.5	67.8	.00
3-4	7.9	318	17.7	67.2	.00
4-5	6.0	204	17.0	61.3	.00
5-6	7.7	317	17.7	66.2	.00
6-7	8.2	324	20.8	78.5	.00
7-8	8.5	362	20.9	73.9	.00
8-9	8.2	335	18.4	76.7	.00
9-10	8.2	334	21.7	74.5	.00
10-11	7.9	311	17.7	72.5	.00
11-12	9.0	308	19.9	86.2	.00
12-13	8.6	302	21.5	86.6	.00
13-15	9.3	290	20.6	87.2	.00
15-16	8.6	289	23.0	85.3	.00
16-17	9.1	290	22.7	84.1	.00
17-18	8.7	283	20.6	80.9	.00
18-19	9.0	249	23.8	83.6	.00
19-20	9.3	293	23.6	83.1	.00

SAMPLE NUMBER	DDM CM	DDM MM	DDM NT	DDM 7N	²¹⁰ Po
SC24					
0-2	6.8	327	14.6	62.8	.00
2-3	6.2	335	15.3	63.6	.00
3-4	6.5	320	14.0	59.5	.00
4-5	7.0	338	25.7	50.4	.00
5-6	7.2	341	19.4	68.5	.00
6-7	6.9	348	17.4	67.1	.00
7-8	6.3	342	18.1	63.7	.00
8-9	7.4	400	17.5	70.3	.00
9-10	6.6	374	22.6	67.9	.00
10-11	6.0	365	18.4	70.4	.00
11-12	6.2	351	17.1	63.4	.00
12-13	6.2	323	16.3	57.8	.00
13-14	6.0	304	16.3	60.6	.00
14-15	6.1	215	17.4	64.7	.00
15-16	6.3	314	16.7	68.3	.00
16-17	6.5	308	18.3	59.7	.00
17-18	6.5	302	22.6	61.2	.00
18-19	6.0	304	15.9	63.5	.00
19-20	6.7	318	17.7	64.5	.00

SC30 core lost.

CAMPUS ATTACHED	DDM CU	DDM UM	DDM MT	DDM ZN	²¹⁰ Po
0031					
0-2	7.8	316	10.8	68.7	2.02
2-3	8.4	320	17.6	69.0	2.61
3-4	6.5	327	10.4	67.5	1.82
4-5	7.0	331	17.7	66.2	.06
5-6	7.3	323	17.3	70.7	.74
6-7	7.8	350	17.3	60.0	1.23
7-8	8.2	363	22.3	70.7	1.14
8-9	8.2	354	23.0	73.7	.61
9-10	8.6	358	18.9	75.0	.86
10-11	7.4	366	18.6	68.8	.40
11-12	8.7	348	20.1	72.1	.28
12-13	8.2	354	10.3	72.2	.00
13-14	7.1	361	10.3	72.5	.14
14-15	8.1	353	18.8	74.2	.14
15-16	6.0	361	18.8	71.8	.25
16-17	7.0	360	18.2	72.1	.21
17-18	6.8	353	18.2	60.4	.23
18-19	6.1	366	18.2	71.7	.10
19-20	7.5	348	17.2	68.5	.00

CAMP F NUMBER	DOB CII	UPA MIN	DDM MIF	DDM ZNI	²¹⁰ Po
SC32					
0-2	4.5	363	19.6	69.8	.00
2-3	4.0	301	18.8	75.3	.00
3-4	4.1	367	18.1	70.9	.00
4-5	7.4	361	20.4	72.9	.00
5-6	4.0	340	17.7	70.6	.00
6-7	4.2	376	21.2	76.3	.00
7-8	4.5	3011	21.5	78.4	.00
8-9	4.7	389	20.9	78.7	.00
9-10	7.0	305	20.1	73.2	.00
10-11	4.1	348	19.9	72.6	.00
11-12	4.1	370	19.0	72.2	.00
12-13	7.2	383	19.0	67.0	.00
13-14	4.0	307	20.2	70.1	.00
14-15	4.6	408	20.8	78.4	.00
15-16	0.0	439	24.0	70.1	.00
16-17	4.5	402	24.4	76.6	.00
17-18	4.8	477	22.8	90.3	.00
18-19	4.8	400	21.6	75.7	.00
19-20	4.9	464	22.7	86.4	.00



The Department of the Interior Mission

As the Nation's principal conservation agency, the Department of the Interior has responsibility for most of our nationally owned public lands and natural resources. This includes fostering sound use of our land and water resources; protecting our fish, wildlife, and biological diversity; preserving the environmental and cultural values of our national parks and historical places; and providing for the enjoyment of life through outdoor recreation. The Department assesses our energy and mineral resources and works to ensure that their development is in the best interests of all our people by encouraging stewardship and citizen participation in their care. The Department also has a major responsibility for American Indian reservation communities and for people who live in island territories under U.S. administration.



The Minerals Management Service Mission

As a bureau of the Department of the Interior, the Minerals Management Service's (MMS) primary responsibilities are to manage the mineral resources located on the Nation's Outer Continental Shelf (OCS), collect revenue from the Federal OCS and onshore Federal and Indian lands, and distribute those revenues.

Moreover, in working to meet its responsibilities, the **Offshore Minerals Management Program** administers the OCS competitive leasing program and oversees the safe and environmentally sound exploration and production of our Nation's offshore natural gas, oil and other mineral resources. The MMS **Minerals Revenue Management** meets its responsibilities by ensuring the efficient, timely and accurate collection and disbursement of revenue from mineral leasing and production due to Indian tribes and allottees, States and the U.S. Treasury.

The MMS strives to fulfill its responsibilities through the general guiding principles of: (1) being responsive to the public's concerns and interests by maintaining a dialogue with all potentially affected parties and (2) carrying out its programs with an emphasis on working to enhance the quality of life for all Americans by lending MMS assistance and expertise to economic development and environmental protection.